이학박사학위논문

Holographic approach to quantum black holes

양자 블랙홀에 대한 홀로그래피 연구

2021 년 2 월

서울대학교 대학원

물리천문학부

최 선 진

이학박사학위논문

Holographic approach to quantum black holes

양자 블랙홀에 대한 홀로그래피 연구

2021 년 2 월

서울대학교 대학원

물리천문학부

최 선 진

Holographic approach to quantum black holes

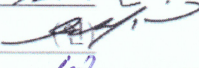양자 블랙홀에 대한 홀로그래피 연구
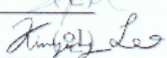
지도교수 김 석

이 논문을 이학박사 학위논문으로 제출함

2020 년 12 월

서울대학교 대학원

물리천문학부 물리학전공

최 선 진

최선진의 이학박사 학위논문을 인준함

2021 년 1 월

위 원 장	이 상 민	
부위원장	김 석	
위 원	이 원 종	
위 원	김 지 훈	(인)
위 원	이 기 명	

Abstract

Holographic approach to quantum black holes

Sunjin Choi

Department of Physics and Astronomy

The Graduate School

Seoul National University

This thesis aims to holographically study the black holes in anti-de Sitter spacetime from the dual conformal field theories. We show that the Cardy limit of the indices of superconformal field theories in $d = 3, 4, 5, 6$ exhibit the deconfined degrees of freedom in the large N limit. They precisely agree with the Bekenstein-Hawking entropies of supersymmetric black holes in $\mathrm{AdS}_{4,5,6,7}$, thus accounting for their microstates as dual deconfined quark-gluon plasma.

We also clarify that the $N^{3/2}$ deconfined degrees of freedom of M2-brane superconformal field theory (SCFT) arises from the magnetic monopole condensation. We further study the $N^{5/2}$ deconfined degrees of freedom of 5d SCFTs and subtle roles of the instanton solitons realizing such exotic deconfinement.

Moreover, we numerically study the index of 4d $\mathcal{N} = 4$ supersymmetric-Yang-Mills theory and show how the rapid oscillation of the index can be realized by the complex chemical potential saddle points of the Legendre transformation. Finally, we comment on the deconfinement transition from the index.

Keywords: Holography, Black holes, Conformal Field Theory, Deconfinement

Student Number: 2016-20321

Contents

Chapter 1

Introduction

One of the most important and challenging problems in theoretical physics is to establish the quantum theory of gravity. A complete formulation of the quantum gravity is aimed at the consistent unification of two major subjects of the modern physics: general relativity and quantum mechanics. Black holes, which are both strong gravitational objects with event horizon and thermodynamic objects with macroscopic number of quantum states, provide a theoretical probe to understand the major properties of such yet unknown quantum gravity. The goal of this thesis is to deepen our understanding of quantum gravity through the holographic approach to quantum black holes.

In this chapter, we briefly review on the developments of viewpoints on the quantum gravity, with great emphasis on the quantum black holes as a key to reveal the mysteries of quantum gravity.

1.1 Why black holes?

Whereas the other three fundamental interactions of nature; electromagnetic interaction, weak interaction, and strong interaction, are successfully elucidated by the quantum field theory (QFT) and now unified as the Standard Model, the gravitational interaction defies such quantum field theoretical description. Why is it so? What makes the gravity so special?

General relativity, a classical field theory of gravity, is non-renormalizable as a quantum field theory viewpoint. There is nothing wrong about this. It just means that the general relativity is the effective field theory (EFT) of quantum gravity at low energy. Then, let us recall what we have done when we have such non-renormalizable EFT at low energy in particle physics. One of the well-known examples is the Fermi theory of beta decay. It has a dimensionful coupling $G_F \sim 1/(293\,\text{GeV})^2$, so it was supposed to be break down at energies below 293 GeV. Below this energy scale, the physics changes drastically and new particles are produced. That is the W and Z bosons of the electroweak theory. Similar things happen when we approach to other characteristic energy scale of the EFT, such as the QCD scale; new physics appears and new particle are produced.

One may try to use the above approach to the EFT of quantum gravity, the general relativity. Its characteristic energy scale is the Planck energy $E_p = \sqrt{\hbar c^3/G} \sim 10^{19}\,\text{GeV}$. The problem is that when we go beyond that energy scale, the black holes are created. No new particles appear and we cannot learn any new physics. Adding more energy just results in larger black holes, which is even more classical. So naive reductionist experiment with colliders comes to an end.

In fact, there are some deeper reasons why we cannot study the naive UV completion of general relativity. When we say about the quantum gravity, it means that a quantum theory of the dynamical metric. From the linearized equation of motion for general relativity, we can get a propagating mode of the metric, which can be viewed as a massless spin-2 particle called a graviton. Thus, if there is an UV completion of general relativity, this massless spin-2 graviton would be described as a bound state of two massless spin-1 particles. However, there is a powerful no-go theorem that forbids it. According to the Weinberg-Witten theorem [1], a QFT with a Poincaré invariant non-zero conserved stress-energy tensor does not admit massless particles with spin $s > 1$. (General relativity is still OK as an EFT since the stress-energy tensor vanishes due to the equation of motion.)

Of course, this does not mean that we have to give up to find a quantum theory of gravity. It signals that we are heading in the wrong direction. A good example is the Coleman-Mandula theorem [2], which classifies all possible symmetries of the S-matrix. One natural assumption of this theorem was that the symmetry generators are bosonic, and it was a loophole. It missed the possibility of the supersymmetry whose generator is fermionic.

So the lesson of the no-go theorem is to violate its assumption. But in order to do so, we should understand the major property of quantum gravity. Our Gedanken experiment somehow seems to indicate that lots of information about quantum gravity is hidden inside the black holes. Indeed, we will see that the black holes are not just the classical solutions of gravity, but thermodynamic objects with macroscopic number of quantum states, which should be understood statistically through the quantum gravity.

1.2 Black hole thermodynamics

Black holes are the classical solutions of the general relativity, with an event horizon in which the gravitational interaction is so strong that not even light can escape from it. In 1970's, it was known that the black holes satisfy several universal laws under very basic assumptions such as "the energy should be positive." They are called the laws of black hole mechanics [3]. In the geometrized units, i.e. $c = G = 1$, they are stated as following.

The 1st law For perturbations of stationary black holes, the change of its energy E is given by

$$dE = \frac{\kappa}{8\pi} dA + \Omega dJ + \Phi dQ \; , \qquad (1.2.1)$$

where κ is the surface gravity, A is the horizon area, Ω is the angular velocity, J is the angular momentum, Φ is the electrostatic potential, and Q is the electric charge of the black holes.

The 2nd law Under the null energy condition, $T_{\alpha\beta} k^\alpha k^\beta \geq 0$ for every future-pointing null vector field k^α, the horizon area of black holes does not decrease over time t:

$$\frac{dA}{dt} \geq 0 \; . \qquad (1.2.2)$$

This is also known as the Hawking's area theorem [4].

These laws are very universal in a sense that they do not assume any kind of matter or additional interaction between them, but just the gravitational interaction according to the Einstein's equivalence principle. They even hold regardless of the spacetime dimension. This universality is reminiscent of the laws of thermodynamics, and suggests that one should identify the surface gravity and the horizon area with temperature and entropy of black holes [5]. Nonetheless,

at the classical level, black holes do not emit any particles, thus they have zero temperature. Hence, these laws seem to be just the analogous thermodynamic laws, classically. However, if one carefully analyzes the quantum field theory near the event horizon, one will find that the black holes do emit thermal radiation at a temperature

$$T_{\mathrm{H}} = \frac{\hbar}{ck_B}\frac{\kappa}{2\pi} \ , \qquad (1.2.3)$$

which is the celebrated Hawking radiation [6]. Then, from the 1st law of black hole mechanics, we can read off the entropy of the black holes given by

$$S_{\mathrm{BH}} = \frac{c^3 k_B}{G\hbar}\frac{A}{4} \ , \qquad (1.2.4)$$

which is called the Bekenstein-Hawking entropy. Now, the 1st law of black hole mechanics is indeed the 1st law of thermodynamics. The first term in (1.2.1) is nothing but $T_{\mathrm{H}}\, dS_{\mathrm{BH}}$. Reflecting that the horizon area equals the black hole entropy, the 2nd law should be generalized as $\frac{d}{dt}(S + S_{BH}) \geq 0$, where S is the entropy outside the black hole horizon, which states that the total entropy of the universe does not decrease over time, i.e. the 2nd law of thermodynamics [7]. Note that these laws of black hole thermodynamics turn out to hold even in generalized gravity theories [8], such as Lovelock gravity [9], which take into account the higher curvature corrections, in any spacetime dimensions.

Understanding the black holes as thermodynamic objects, a direct question is whether we can statistically account for the Bekenstein-Hawking entropy of black holes. Namely, can we derive the Bekenstein-Hawking entropy formula by counting microstates of black holes as $S_{\mathrm{BH}} = k_B \log \Omega$? This question is hard to answer since it basically asks about the spectrum of quantum gravity. Moreover, the Bekenstein-Hawking entropy formula gives rise to central issues of black holes, which are connected to the mysterious properties of quantum gravity. One prime example is the black hole information paradox [10]. If basically

occurs since the Hawking radiation is purely thermal and does not keep any information about the matters formed black holes. If this is true, then the information is lost in the black holes and the unitarity of quantum mechanics breaks down. We believe this is not the case in the consistent quantum theory of gravity.

In order to resolve various puzzles of black holes, we should first understand the Bekenstein-Hawking entropy of black holes microscopically. The rest of this chapter will focus on the microstates of black holes.

1.3   Black holes in string theory

It is known that the string theory gives a consistent quantum gravity theory. In the low energy spectrum of the string theory, there exists the massless spin-2 particles, i.e. gravitons. Note that the string theory is nothing to do with the Weinberg-Witten theorem since it is not a quantum field theory. The next question will be whether the string theory can provide a microscopic picture to understand black holes.

In the pioneered work of [11], the authors derived the Bekenstein-Hawking entropy of certain five-dimensional supersymmetric black holes by counting the degeneracy of BPS bound states of strings and branes in the string compactification model. They considered the type IIB string theory compactified on $K3 \times S^1$. The low energy effective theory can be described by the five-dimensional supergravity. It admits a supersymmetric black hole solution with three electric charges Q_1, Q_5, P and its Bekenstein-Hawking entropy is given by $S_{BH} = 2\pi\sqrt{Q_1 Q_5 P}$. On the other hand, this black hole can be formed by the BPS bound states of fundamental strings with Q_1 D1-branes wrapped on S^1 and Q_5 D5-branes wrapped on $K3 \times S^1$. Degeneracy of such bound states

can be computed from the world-volume theory of branes. When the size of $K3$ is much smaller than S^1, the world volume theory of branes can be effectively described by two-dimensional superconformal field theory (SCFT), which is a supersymmetric sigma model whose target manifold is a symmetric product orbifold $(K3)^{Q_1 Q_5 + 1}/S_{Q_1 Q_5 + 1}$, where S_N is the permutation group of order N. When the S^1 size becomes small, the momentum P along S^1 becomes large and the partition function of the 2d conformal field theory (CFT), using the modular invariance, is given by

$$Z = \text{Tr}[e^{2\pi i \tau P}] \sim \exp\left[\frac{\pi i c}{12\tau}\right] \quad (\tau \to i\,0^+) \,, \tag{1.3.1}$$

where the central charge $c = 6Q_1 Q_5$ for our CFT. Then, the Legendre transformation gives the asymptotic degeneracy, which is the Cardy formula [12]:

$$S = 2\pi\sqrt{Q_1 Q_5 P} \,, \tag{1.3.2}$$

which precisely agrees with the Bekenstein-Hawking entropy of black holes.

Soon after, the rotating version of the above black holes were analyzed in [13]. While the general five-dimensional black holes can have two independent angular momenta, the supersymmetric black holes can have only one. In microscopic point of view, this angular momentum corresponds to one of two R-charges of the BPS states in 2d SCFT living on the D1-D5 system. Slight modification of the Cardy formula gives the entropy $S = 2\pi\sqrt{Q_1 Q_5 P - J^2}$ and this coincides with the Bekenstein-Hawking entropy of rotating BPS black holes. Similarly, four-dimensional supersymmetric black holes with four electric charges are studied in the context of the type IIA string theory compactified on T^6 [14, 15]. The relevant BPS bound states forming black holes correspond to the BPS states of the world-volume theory of Q_2 D2-branes, Q_6 D6-branes, and m NS5-branes. With large momentum P along $S^1 \subset T^6$, the entropy reads

$S = 2\pi\sqrt{Q_2 Q_6 nP}$, which exactly equals to the Bekenstein-Hawking entropy of the black holes.

The above approach based on string theory provides a powerful tool for microscopic understanding of black holes. However, it has a disadvantage due to our lack of understanding about the string theory itself. In order to account for certain black holes, one should assume certain bound states of branes and strings, which form the black holes. Then, one should study the effective theory describing such bound states. This will only give us an effective description for that certain black holes. For other types of black holes, one should design other effective descriptions. The famous example is the black rings in five-dimensional spacetime whose horizon topology is given by $S^2 \times S^1$ [16–22]. The microscopic accounting for the entropy of black rings [23] comes from not the D1-D5 CFT we discussed above, but the wrapped M5-brane CFT [24].

All these things happen because we do not use the full description of quantum gravity but just an effective one for the black holes of our interest. In fact, the quantum gravity in flat spacetime is not fully defined due to our lack of knowledge about the full non-perturbative definition of the string theory. In other words, in order to systematically study the black holes and various phases of quantum gravity, it is desired to have a set-up with a full description of quantum gravity. It turns out to be a holographic description.

1.4 Holographic approach to quantum black holes

1.4.1 AdS/CFT correspondence

Let us go back to the Bekenstein-Hawking entropy formula of black holes. It has a peculiar property that the entropy is not proportional to the volume but the

surface area of black holes, which implies that the information inside the event horizon is encoded on the event horizon. This is the largest possible entropy for a system with given surface area, which is called the Bekenstein bound [25–27]. Note that this formula or bound is very universal in a sense that it does not depend on the matter inside the event horizon. This suggests that it is not just a peculiar property of the black holes but the fundamental property of quantum gravity. This idea leads to the holographic principle, which states that the quantum gravity in any volume of space is described by the quantum field theory on its boundary [26, 27]. This violates the hidden assumption of the Weinberg-Witten theorem: the graviton bound state as the gauge boson constituents moves in one additional spacetime dimension.

In order to realize the holographic principle, one should first decide where to place the holographic screen. The holographic screen should be non-penetrable since we want an unitarily evolving quantum gravity system. The anti-de Sitter(AdS) spacetime provides such a setting. The AdS spacetime is the maximally symmetric spacetime with negative curvature and a vacuum solution to the Einstein's equation with a negative cosmological constant. In the global patch, the metric tensor of AdS_{d+1} is given by

$$ds^2 = \frac{1}{\cos^2\left(\frac{r}{\ell}\right)} \left(-dt^2 + dr^2 + \sin^2\left(\frac{r}{\ell}\right) d\Omega_{d-1}^2\right) , \qquad (1.4.1)$$

where the radial coordinate $r \in \left[0, \frac{\pi}{2}\right)$, and time $t \in (-\infty, \infty)$, and the angular coordinates Ω cover S^{d-1}. ℓ is called the AdS radius. Note that although the AdS is non-compact, the radial coordinate r runs only over a finite range. There is the conformal boundary at the spatial infinity $r \to \frac{\pi}{2}$, which is the Lorentzian cylinder $S^{d-1} \times \mathbb{R}$. Thus, we can think of AdS as the interior of the cylinder. Furthermore, due to the warp or Weyl factor $1/\cos^2(r/\ell)$ of the metric, the particles in AdS feels a strong gravitational force pushing towards

the center and cannot reach the boundary cylinder. In fact, they move along the periodic orbits passing through the center with the same period. This fact makes AdS spacetime like a 'periodic box' and suggests the interpretation of the AdS spacetime as the IR regulated version of the flat Minkowski spacetime. Therefore, the AdS spacetime gives an ideal setting for the holography. We can safely place the holographic screen at the conformal boundary. (One should demand proper reflective boundary conditions for the null geodesics [28–31].)

Note that one can get the conformal boundary manifolds other than the cylinder by taking other limits approaching the boundary of AdS. For example, one will naturally find a Minkowski spacetime as the conformal boundary of AdS in the Poincaré patch. In fact, we can obtain any conformally flat manifold as the boundary of AdS. However, in this thesis, we shall mostly focus on the case when the conformal boundary is given by the cylinder. This is because the black holes in AdS have the natural boundary as the cylinder.

The next task is to design the QFT living on the boundary, which holographically describes the quantum gravity on AdS. In fact, there are already some hints on AdS. The isometry of AdS_{d+1} is $SO(d,2)$ and this should be realized as the symmetry of the boundary QFT_d. This is the conformal group in d-dimensions. Furthermore, the fact that all particles in AdS have the same period means that the energy level for the free particles in AdS are integer quantized with a lower bound. Quantum mechanically, this fact implies that the particle states in AdS can be described by the language of the $so(d,2)$ conformal algebra such as the primary and descendant states. Therefore, we can now say that the boundary QFT should be the conformal field theory (CFT), that is the RG fixed point of the QFT, which is scale-invariant due to the conformal symmetry. One can further relates the radial coordinates in AdS to the

energy scale in the CFT, which is called the holographic renormalization group (RG) [32, 33].

Now, we need two more ingredients to finish our heuristic 'derivation' of the duality. In order that the bulk gravity emerges, we should impose two nontrivial conditions to CFT. We want that the boundary CFT has large number of degrees of freedom so that it can take into account the macroscopic degrees of freedom of black holes in AdS. Additionally, we want the gauge boson bound state behaves like a graviton and not like a gauge boson pair, so the CFT should be very strongly coupled. Thus, the strongly coupled CFT with large number of degrees of freedom is needed to holographically describe the bulk gravity. In fact, in the large N limit, or the 't Hooft limit, of the gauge theory, where N is the gauge group rank, the correlation functions factorize and the quantum fluctuations are highly suppressed [34]. Thus, the large N gauge theory really behaves like a "free, classical" theory, similar to the classical gravity, or the string theory [35].

Note that as we shall focus on the case with the conformal boundary of AdS is given by the Lorentzian cylinder $S^{d-1} \times \mathbb{R}$, we should understand how to put the CFT on $S^{d-1} \times \mathbb{R}$. This can be achieved by the so-called radial quantization. Consider the CFT on the plane $\mathbb{R}^d$. Using a Weyl transformation, we can comformally map the plane to the cylinder. That is to regard the radial coordinate in $\mathbb{R}^d$ as the time coordinate. Then, we will quantize the theory in the slices with equal radius, i.e. S^{d-1}, which we interpret as the equal time slices. Basically, this is the radial quantization. In addition, there is one more intriguing fact: the operator-state correspondence. We can insert an local operator at the origin of $\mathbb{R}^d$ and then path-integrate inside S^{d-1} under this insertion. Then, this will naturally define the quantum state on S^{d-1} and vice-versa. Thus, the local

operators of CFT on $\mathbb{R}^d$ are in one-to-one correspondence with the quantum states of CFT on $S^{d-1} \times \mathbb{R}$. This can be also argued using the conformal algebra. Note that this is only true for the CFT, where we can map the cylinder to plane. In general non-conformal theories, the local operator creates many different states.

We have now arrived at the celebrated proposal, the AdS/CFT correspondence [36–38]. This is the most successful realization of the holographic principle. There are many more motivations and evidences for the AdS/CFT correspondence. (For pedagogical review, refer to [35, 39–43].) In fact, the string/M-theory gives many explicit examples for the AdS/CFT correspondence and most of the concrete evidences are found in these examples [35]. These examples can be 'derived' from the string/M-theory studying two equivalent descriptions of the low energy physics of a stack of multiple branes in the decoupling limit: gravity on the near horizon AdS geometry of (black) branes and the SCFT living on the branes. The most famous example comes for the stack of N D3-branes, which gives rise to the equivalence between the 4d $\mathcal{N} = 4$ $U(N)$ supersymmetric Yang-Mills theory (SYM) and the type IIB string theory on $\mathrm{AdS}_5 \times S^5$. The parameters; N, the gauge group rank, and g_{YM}, the coupling constant, of SYM determines the quantum corrections to the classical type IIB supergravity on $\mathrm{AdS}_5 \times S^5$ as following:

$$\frac{1}{Ng_{\mathrm{YM}}^2} = \frac{\ell_s^4}{\ell^4} \,, \quad \frac{\pi^4}{2N^2} = \frac{\ell_p^8}{\ell^8} \,, \tag{1.4.2}$$

where ℓ_s is the string scale, and ℓ_P is the 10d Planck scale. The first factor is about the stringy correction and the second one is about the gravity loop correction to the classical supergravity. Hence, the classical gravity description is valid when the gauge group rank N and the 't Hooft coupling $\lambda = Ng_{\mathrm{YM}}^2$ is very large, as expected.

There are lots of other examples in other spacetime dimensions from string/M-theory. From the decoupling limit of M2-branes, we get the equivalence between the 3d $U(N)_1 \times U(N)_{-1}$ ABJM SCFT, which is the $\mathcal{N} = 8$ supersymmetric Chern-Simons-matter theory, and the M-theory on $\text{AdS}_4 \times S^7$ [44]. Similarly, from M5-brane stacks, we get the correspondence between the 6d A_N type $(2, 0)$-SCFT [45, 46] and the M-theory on $\text{AdS}_7 \times S^4$. Of course, there are $\text{AdS}_6/\text{CFT}_5$ examples states that certain 5d $\mathcal{N} = 1$ SCFTs [47, 48] are equivalent to the massive type IIA string theory on $\text{AdS}_6 \times S^4/\mathbb{Z}_2$ [49–51]. These are the prime examples we will cover in this thesis. We will study the black holes in $\text{AdS}_{4,5,6,7}$ from the above $\text{SCFT}_{3,4,5,6}$ duals in the large N limit. In addition, the example discussed in Strominger-Vafa's work [11], in fact, can also be understood as the $\text{AdS}_3/\text{CFT}_2$ correspondence. In the decoupling limit, the D1-D5 system gives the equivalence between the type IIB string theory on $\text{AdS}_3 \times S^3 \times T^4$ and the 2d $\mathcal{N} = (4, 4)$ SCFT whose target space is the symmetric product orbifold of T^4, which we discussed. $\text{AdS}_3 \times S^3 \times T^4$ is nothing but the near horizon geometry in the decoupling limit of the type IIB string theory on $T^4 \times S^1$.

Note that the AdS/CFT correspondence is not limited to the string/M-theory. There is a prominent example states that the Vassiliev's higher spin gravity in AdS_4 and the 3d CFT called the critical $O(N)$ vector model are equivalent [52, 53]. Thus, we should regard the AdS/CFT correspondence as the basic principle describing the full quantum gravity, whatever it is, in AdS. At least, there are lots of evidences supporting it and many physicists believe that it is true. Some people even believe that it gives the definition of quantum gravity on AdS as the CFT dual. Nevertheless, one can ask, under what conditions on the boundary CFT, the classical Einstein gravity emerges in the bulk AdS, just like the string/M-theory example. The answer is believed to be when the CFT has a large central charge with a low-lying sparse spectrum [54].

1.4.2 Black holes as deconfined quark-gluon plasma

Now, we have the systematic and ideal setting to study the black holes: the AdS/CFT correspondence. Then, what will be the CFT dual states of AdS black holes? Let us first consider the thermodynamic behavior of the AdS in the canonical ensemble. At low temperature, there will be just a thermal gas of gravitons in AdS. Due to the gravitational potential in AdS, these particles will mostly move around the center. Then, as we increase the temperature, more and more energy will be put into the region nearby the center of AdS. Eventually, at the critical temperature T_{HP}, this hot gas with large energy density will collapse and form a black hole in AdS. This is the famous Hawking-Page phase transition [55], which is the 1st order phase transition between the thermal gas of gravitons and black holes in AdS. These two solutions, graviton gas and black holes, should be understood as the classical saddle points of the quantum gravity in AdS.

Before we move our discussion to the dual CFT side, let us study the thermodynamic behavior of AdS black holes in more detail. Our concrete example is the AdS$_5$-Schwarzschild black holes. They have mass (energy) M, conjugate to the temperature T. The relations of M, T and the horizon radius r_+ is given by

$$T = \frac{r_+}{\pi \ell^2} + \frac{1}{2\pi r_+} \quad , \quad r_+^2 = -\frac{\ell^2}{2} + \ell \sqrt{\frac{\ell^2}{4} + \omega M} \, , \qquad (1.4.3)$$

where ℓ is the radius of AdS$_5$, and $\omega \equiv \frac{16\pi G_N}{3\text{vol}(S^3)}$ with 5d Newton constant G_N, and $\text{vol}(S^3)$ is the volume of unit 3-sphere. For instance, see [56] for its summary. r_+ is a monotonically increasing function of M, and thus labels the energy to certain extent. From the expression of T, one finds that the black holes exist only at $T \geq T_0 \equiv \frac{\sqrt{2}}{\pi \ell}$. At given temperature $T > T_0$, two black hole solutions exist, solving the first equation of (1.4.3). The one with smaller

r_+ is called small black holes and has negative specific heat, $\frac{\partial r_+(T)}{\partial T} < 0$ and thus $\frac{\partial M}{\partial T} < 0$, irrelevant for discussing canonical ensemble. However, we can consider the small black holes in the microcanonical ensemble and this gives the IR regulated version of the black holes in flat spacetime, which also have the negative specific heat. Thus, studying the small black hole limit of the AdS black holes, we can also study the physics of the black holes in asymptotically flat spacetime. The solution with larger r_+ is called large black holes, having positive specific heat.

The thermodynamics in the canonical ensemble with two saddle points: large black holes and thermal gravitons in AdS_5, is what we have discussed before. The thermal graviton phase is dominant at $T < T_{\mathrm{HP}}$ with $T_{\mathrm{HP}} = \frac{3}{2\pi\ell}$, while the large black hole is dominant at $T > T_{\mathrm{HP}}$ [55–57]. Since the free energy of thermal gravitons is of order $\mathcal{O}(G_N^0)$, as they are free gas, while that of the black hole is $\mathcal{O}(G_N^{-1})$, due to the $1/G_N$ factor in the Einstein-Hilbert action, the dominant saddle point is determined by the sign of the black hole free energy. The transition is known to be of first order, called Hawking-Page transition.

Now, let us consider the dual CFT side. Our concrete example is the 4d $\mathcal{N} = 4$ $U(N)$ SYM, which is dual to $\mathrm{AdS}_5 \times S^5$. The CFT dual picture of the Hawking-Page transition is the confinement-deconfinement phase transition at strong coupling [56, 57]. One can ask how does the phase transition exist and what is the confinement in the CFT, which is scale-invariant. These all come from the fact that we put our CFT on the compact space $S^{d-1} \times S^1$, where S^1 is the Euclidean time circle. When the temperature is lower than the energy scale given by the sphere radius, we can only see the gauge singlet composite particles, the hadrons, on the sphere due to the Gauss' law. However, when the temperature becomes high enough, we can see the small constituents

of the hadrons on the sphere, which is the quark-gluon plasma. This is the confinement-deconfinement phase transition of the CFT on compact manifold [56, 57]. The confined hadrons are dual to the thermal gas of gravitons in AdS and the deconfined quark-gluon plasma is dual to the large black holes in AdS. Hence, the quark-gluon plasma of CFT will be the main target of this thesis to holographically study black holes in AdS. Also note that this sharp phase transition on the compact manifold is only possible in the large N limit, where there is infinite number of degrees of freedom in the theory [58].

One important properties of the confined phase is the Hagedorn behavior [59], which means that the density of states $d(E)$ grows exponentially at large E, i.e. $d(E) \sim e^{E/T_H}$. This Hagedorn behavior implies that the confined phase is ill-defined in the canonical ensemble above the Hagedorn temperature T_H. This is because the canonical partition function diverges when we approach to the Hagedorn temperature. Accordingly, it takes infinite amount of energy to reach the Hagedorn temperature, and the Hagedorn temperature sets the maximum temperature of the confined phase. These confined hadrons, which are the gauge singlets, are dual to the closed strings in AdS, which serves as the gravitons at low energy and exhibits the Hagedorn behavior at high energy [60]. The breakdown of the canonical ensemble at the Hagedorn temperature T_H implies the existence of the phase transition below T_H. That is the deconfinement transition we discussed above. The quarks and gluons, which are gauge non-singlet, are liberated from the hadrons before the Hagedorn temperature and the growth of the density of states is tamed down. In dual AdS, the strings are deconfined to the string bits, which are dual to the gauge non-singlets such as the quarks and gluons. Although we do not know how to describe the string bits, at least in the classical level this implies the black hole formation since deconfinement transition is dual to the Hawking-Page transition.

When there is a phase transition, there should be the corresponding order parameter. The conventional order parameter for the deconfinement transition is the Polyakov loop $P = \text{tr}\left[\mathcal{T}\exp\left(i\oint_{S_\beta^1} A\right)\right]$, where S_β^1 is the temporal circle [61,62]. The Polyakov loop $<P> = e^{-\beta F}$ represents the free energy cost F of the quark-anti-quark pair creation and annihilation along the temporal circle. In the confined phase, this costs the infinite energy, so $<P> = 0$. In the deconfined phase, the energy cost will be finite, so $<P> \neq 0$. Note that while the local operators are not charged under the center symmetry of the gauge group, this loop operator is charged. So, one can understand $<P> \neq 0$ as the spontaneous symmetry breaking of the center symmetry [56,63].

As we are dealing with the large N gauge theory, there is another more useful order parameter for the deconfinement transition. That is $f = \lim_{N\to\infty} F/N^2$ [57]. In the confined phase, the hadrons cannot see N since they are gauge singlets and thus, $F \sim \mathcal{O}(N^0)$ and $f = 0$. In the deconfined phase, the quark-gluon plasma have matrix degrees of freedom, so $F \sim \mathcal{O}(N^2)$ and $f \neq 0$. This is consistent with the fact that the thermal graviton gas has free energy of order $\mathcal{O}(G_N^0)$, while that of black holes are of order $\mathcal{O}(G_N^{-1})$ in the AdS gravity dual.

So far, we have discussed with the $\text{AdS}_5/\text{CFT}_4$ example: 4d $\mathcal{N} = 4$ SYM and the gravity on $\text{AdS}_5 \times S^5$. However, most of the argument in this subsection can be generalized to the other spacetime dimensions except for the N^2 scaling in the deconfined phase of CFT. It is known that the degrees of freedom of 3d SCFT living on M2-branes scales like $N^{3/2}$. For the 6d SCFT living on M5-branes, we get N^3 scaling and the 5d SCFTs exhibit $N^{5/2}$ scaling. These were studied from the black brane geometry [64] or the sphere partition function [65–67]. One goal of this thesis is to explain such exotic behavior of SCFTs from counting states in the deconfined phase.

1.5   Overview of thesis

This thesis is devoted to holographically study black holes in AdS from the CFT dual. In this thesis, we will focus on the solvable sector: the supersymmetric black holes with electric charges and angular momenta. One will concern that the supersymmetric black holes exhibit no interesting thermodynamics as its Hawking temperature is 0. However, in chapter 2, we shall see that the supersymmetric black holes exhibit interesting thermodynamics analogous to the AdS-Schwarzschild black holes such as the Hawking-Page phase transition.

In the dual CFT side, we will mostly analyze the superconformal indices [68–70], which count the excited states of the radially quantized SCFT on $S^{d-1} \times \mathbb{R}$ satisfying the BPS condition with $(-1)^F$. Like the Witten indices [71], this quantity is invariant under the RG flow due to the supersymmetry, which makes it exactly calculable by the supersymmetric localization [72]. However, one will concern that, due to the $(-1)^F$ factor, the macroscopic degrees of freedom of black holes is invisible in the index, and this was the standard lore [69, 73]. We will see that this is not the case. Introducing the phase of the fugacity, the index does capture deconfined degrees of freedom of SCFT, as we shall see through chapters 3,4,5,6. Furthermore, we will show that in chapter 8, this phase precisely shows the boson-fermion oscillating behavior of the index.

The rest of the thesis is orgranized as follows. In chapter 2, we will study the thermodynamics of the supersymmetric AdS black holes in terms of the entropy functions. These entropy functions are simple but encode the apparently complicated properties of the supersymmetric AdS black holes. Utilizing these functions, we will see that they exhibit nontrivial thermodynamic behaviors analogous to the AdS-Schwarzschild black holes.

In chapter 3, we study the index of 4d $\mathcal{N} = 4$ SYM on $S^3 \times \mathbb{R}$ at large angular momenta. We show that introducing the phases of the fugacities, the index exhibits the deconfined N^2 degrees of freedom. This precisely captures the Bekenstein-Hawking entropy of the BPS black holes in $AdS_5 \times S^5$.

In chapter 4, we study the indices of 5d SCFT on $S^4 \times \mathbb{R}$ at large angular momenta and large N. The large N free energy scales like $N^{5/2}$, statistically accounting for the entropy of the large supersymmetric AdS_6 black holes. Instanton solitons play subtle roles to realize these deconfined degrees of freedom

In chapter 5, we study the index on $S^2 \times \mathbb{R}$ at large angular momenta and large N, in gauge theories describing N M2-branes. Monopole condensation confines most of the N^2 degrees of freedom except $N^{3/2}$ of them, even in the high temperature deconfined phase. The resulting large N free energy statistically accounts for the Bekenstein-Hawking entropy of large BPS black holes in $AdS_4 \times S^7$.

In chapter 6, we discuss the large angular momentum limit of 3d supersymmetric partition functions, which allow the factorization into the hemisphere indices: the generalized superconformal index, the refined topologically twisted index and the squashed sphere partition function. Our result provides the microscopic derivation of the universal relations among entropic quantities of the gravity theory in AdS_4.

In chapter 7, we use a background field method on S^3 and S^5 and 't Hooft anomalies to analyze the asymptotic free energies of the indices on $S^3 \times S^1$ and $S^5 \times S^1$ at large angular momenta. The resulting free energies exactly agree with the entropy functions of the BPS black holes in $AdS_5 \times S^5$ and $AdS_7 \times S^4$ respectively, thus statistically accounting for their microstates.

In chapter 8, we study the index of 4d $\mathcal{N} = 4$ SYM numerically. We shall

explicitly see the oscillating behavior of the index and how it is realized by the complex chemical potential saddle points of the Legendre transformation.

In chapter 9, we will study how the deconfinement transition can be captured from the index of 4d $\mathcal{N} = 4$ SYM introducing the phases of the fugacities.

This thesis is based on the author's papers [74–80].

Chapter 2

Entropy functions of supersymmetric AdS black holes

In this chapter, we introduce the entropy functions of supersymmetric AdS black holes with electric charges and angular momenta in four, five, six, and seven spacetime dimensions. Extremizing these functions, one obtains the entropies and the chemical potentials of known analytic black hole solutions.

These entropy functions can be regarded as the free energies of the supersymmetric black holes. Analyzing them, we show that the supersymmetric AdS black holes exhibit interesting thermodynamic properties analogous to the AdS-Schwarzschild black holes, such as the Hawking-Page phase transition and the small/large black hole branches.

2.1   Introduction

Understanding black holes [55–57] is an important subject in AdS/CFT [36]. In models with supersymmetry, one expects that quantitative analysis at strong coupling would be easier in the BPS sectors of SCFTs. Supersymmetric AdS black holes correspond to thermal ensembles of BPS states, carrying angular momenta and also internal charges (electric charges in AdS). In AdS_d with $d > 3$, supersymmetric black holes have very complicated structures. First of all, it is known that there are no BPS black holes with electric charges only, at zero angular momenta. This is because in the dual field theory, the local BPS operators will reduce to chiral rings which do not have enough numbers of microstates to form black holes: e.g. see [69] for the case with $d = 5$. With nonzero angular momenta, the solutions appear very involved. See, e.g. [81, 82] for $d = 4$, [83–86] for $d = 5$, [87] for $d = 6$, and [88, 89] for $d = 7$.

Recently, it was discovered that the apparently complicated properties of supersymmetric AdS black holes can be encoded by extremely simple formulae, so called the entropy functions: e.g. see [90] for the AdS_5 case, [91] for AdS_7, and [74] for the AdS_4 and AdS_6 cases. These simple functions provided very useful inspirations for microscopic studies based on CFT duals. We will discuss some of these works aiming at microscopic accounts for the BPS black holes in the following chapters.

In the rest of this chapter, we will summarize the properties of known supersymmetric black holes in $AdS_{4,5,6,7}$, and show that the entropy functions we suggest encode these properties. These functions can be interpreted as the free energies of the BPS black holes. Analyzing these free energies, we shall see that the supersymmetric AdS black holes have small/large black hole branches, and undergo the Hawking-Page phase transition in terms of the BPS chemical po-

tentials. These properties are analogous to the AdS-Schwarzschild black holes, which have non-zero Hawking temperature. Further note that these entropy functions or the free energies can be obtained from the (regularized) Euclidean on-shell actions of the supersymmetric AdS black holes [92, 93].

2.2 AdS$_4$ black holes

2.2.1 Black hole solutions

We study the supersymmetric black holes in AdS$_4 \times S^7$ of [82]. These are obtained by taking supersymmetric limits of [94], also demanding the existence of smooth horizons.

Black holes in AdS$_4 \times S^7$ can carry six kinds of conserved quantities: mass (or energy) E, angular momentum J on S^2 of global AdS$_4$, and four Cartan charges Q_I ($I = 1, 2, 3, 4$) of $SO(8)$ symmetry on S^7. The last four conserved quantities Q_I appear in 4d gravity as $U(1)^4$ electric charges. The convention of [82] for Q_I is to take four angular momenta acting on the orthogonal 2-planes of $\mathbb{R}^8$ related to S^7. The most general black holes known to date have pairwise equal electric charges, $Q_1 = Q_3$, $Q_2 = Q_4$. With the last charge restrictions, the four conserved quantities E, J, Q_1, Q_2 are labeled by four parameters m, a, δ_1, δ_2 as [82]

$$E = \frac{m}{2G\Xi^2}(\cosh 2\delta_1 + \cosh 2\delta_2) \ , \quad J = \frac{ma}{2G\Xi^2}(\cosh 2\delta_1 + \cosh 2\delta_2) \ ,$$
$$Q_1 = Q_3 = \frac{m}{4G\Xi}\sinh 2\delta_1 \ , \quad Q_2 = Q_4 = \frac{m}{4G\Xi}\sinh 2\delta_2 \ , \qquad (2.2.1)$$

where $\Xi = 1 - a^2 g^2$. The entropy is given by

$$S = \frac{\pi(r_1 r_2 + a^2)}{G\Xi} \ , \qquad (2.2.2)$$

where $r_i = r_+ + 2m\sinh^2 \delta_i$. $r = r_+$ is the location of the event horizon. G is the

4d Newton constant, which will be replaced by microscopic parameters later. (In [82], all charges and entropy are computed omitting the overall $\frac{1}{G}$ factor, or at $G = 1$. E.g. the entropy is computed by dividing the horizon area by 4, rather than $S = \frac{A}{4G}$.) g is a parameter of the 4d gauged supergravity, and is related to the radius ℓ of AdS$_4$ as $g = \ell^{-1}$.

The BPS limit of these black holes is given by

$$e^{2\delta_1 + 2\delta_2} = 1 + \frac{2}{ag} \; , \tag{2.2.3}$$

which corrects a typo of [82]. Only after this correction, the BPS relation

$$E = gJ + \sum_{I=1}^{4} Q_I = gJ + 2Q_1 + 2Q_2 \tag{2.2.4}$$

is met. A further condition to have a regular horizon is $\Delta_r = 0$ having a double root at $r = r_+$. (See [82] for the definition of the function Δ_r.) This happens only after a further tuning of m. After the tuning, the horizon location $r = r_+$ is given by

$$r_+ = \frac{2m \sinh \delta_1 \sinh \delta_2}{\cosh(\delta_1 + \delta_2)} \; , \tag{2.2.5}$$

when m satisfies

$$(mg)^2 = \frac{\cosh^2(\delta_1 + \delta_2)}{e^{\delta_1 + \delta_2} \sinh^3(\delta_1 + \delta_2) \sinh(2\delta_1) \sinh(2\delta_2)} \; . \tag{2.2.6}$$

This again corrects the formula $mg = \frac{\cosh(\delta_1 + \delta_2)}{e^{\frac{\delta_1 + \delta_2}{2}} \sinh^2(\delta_1 + \delta_2) \sinh(2\delta_1) \sinh(2\delta_2)}$ of [82]. The typos found in this paragraph are also reported in [95].

Taking the BPS limit, the entropy of the supersymmetric black hole is given by

$$S = \frac{2\pi}{g^2 G (e^{2\delta_1 + 2\delta_2} - 3)} \; . \tag{2.2.7}$$

The two conditions (2.2.3), (2.2.6) leave two independent parameters among m, a, δ_1, δ_2. Even after restricting E as (2.2.4) due to the BPS condition, the

remaining charges Q_1, Q_2, J satisfy a relation. Together with S, we find the following two relations after taking the BPS limit:

$$\left(\frac{2Q_1}{g} + \frac{2Q_2}{g}\right) S = \frac{\pi}{g^2 G} J,$$
$$S^2 + \frac{\pi}{g^2 G} S - 4\pi^2 \frac{2Q_1}{g} \frac{2Q_2}{g} = 0. \qquad (2.2.8)$$

Since these equations determine S twice, one will get a charge relation between Q_1, Q_2, J from the compatibility of two equations. Explicitly, we insert the solution of the first equation to the second equation, demanding two equations have the same solution for S. Then, taking the unique positive solution assuming $Q_1, Q_2, J > 0$, one obtains

$$S = \frac{\pi}{g^2 G} \frac{J}{\left(\frac{2Q_1}{g} + \frac{2Q_2}{g}\right)} \ ,$$
$$J = \frac{1}{2}\left(\frac{2Q_1}{g} + \frac{2Q_2}{g}\right)\left(-1 + \sqrt{1 + 16g^4 G^2 \frac{2Q_1}{g} \frac{2Q_2}{g}}\right) \ . \qquad (2.2.9)$$

Thus, we have explicitly found the charge relation between Q_1, Q_2, J.

The black hole chemical potentials and the free energy F satisfy

$$S = -T^{-1} F(T) + T^{-1} E - T^{-1} \Omega J - T^{-1} \sum_{I=1}^{4} \Phi_I Q_I \ , \qquad (2.2.10)$$

where T is the temperature, Ω is the angular velocity, and Φ_i's are the electrostatic potentials. The chemical potentials are evaluated on the horizon. In the BPS limit we are interested in,

$$T = \frac{\Delta_r'}{4\pi(r_1 r_2 + a^2)} \to 0 \qquad (2.2.11)$$

because Δ_r has a double root at the horizon. On the other hand, as one inserts the value of the variables in the BPS limit, $a = \frac{2}{g(e^{2\delta_1 + 2\delta_2} - 1)}$, mg given by (2.2.6), and then the horizon location $r \to r_+$ (2.2.5), one finds

$$\Omega = \frac{a(1 + g^2 r_1 r_2)}{r_1 r_2 + a^2} \to g \ , \quad \Phi_1 = \frac{m r_2 \sinh(2\delta_1)}{r_1 r_2 + a^2} \to 1 \ , \quad \Phi_2 = \frac{m r_1 \sinh(2\delta_2)}{r_1 r_2 + a^2} \to 1 \ . \qquad (2.2.12)$$

Defining ΔE by $E = \Delta E + 2Q_1 + 2Q_2 + gJ$, one finds that

$$S = -T^{-1}F(T) + T^{-1}\Delta E - T^{-1}(\Omega - g)J - T^{-1}\sum_{I=1}^{4}(\Phi_I - 1)Q_I . \quad (2.2.13)$$

The BPS limit satisfies $T \to 0$, $\Delta E \to 0$. One first finds that

$$\omega = -\lim_{T\to 0}\left(T^{-1}(\Omega - g)\right) , \quad \Delta_I = -\lim_{T\to 0}\left(T^{-1}(\Phi_I - 1)\right) \quad (2.2.14)$$

are well defined in the BPS limit, by explicitly computing them (although the expressions are very complicated). Since S is also finite in this limit, the 'BPS free energy' $F_{\mathrm{BPS}} \equiv \lim_{T\to 0}(T^{-1}(F - \Delta E))$ should also be well defined. So one finds

$$S = -F_{\mathrm{BPS}} + \omega J + \sum_{I=1}^{4}\Delta_I Q_I \quad (2.2.15)$$

in the BPS limit. $-F_{\mathrm{BPS}}$ is to be interpreted as $\log Z$, where Z is the BPS partition function of this system. We again stress that the BPS limit is taken by first inserting $ag \to \frac{2}{e^{2\delta_1 + 2\delta_2} - 1}$, $mg \to \sqrt{\frac{(\coth(\delta_1+\delta_2)-1)\coth^2(\delta_1+\delta_2)}{\sinh(2\delta_1)\sinh(2\delta_2)}}$ and then $r \to \frac{2m\sinh\delta_1\sinh\delta_2}{\cosh(\delta_1+\delta_2)}$. This results in quite complicated expressions for ω, Δ_i. After taking the BPS limit, one can show that they satisfy

$$\Delta_1 + \Delta_2 = \frac{1}{g}\omega \quad \Rightarrow \quad \sum_{I=1}^{4}\frac{g}{2}\Delta_I - \omega = 0 . \quad (2.2.16)$$

This is an alternative statement of the charge relation between Q_1, Q_2, J.

2.2.2 Entropy function

We now present an entropy function, whose suitable Legendre transformation in Δ_I, ω yields the entropy $S(Q_I, J)$ and the BPS chemical potentials of the supersymmetric black holes. Our entropy function $S(\Delta_I, \omega; Q_I, J)$ is given by

$$S(\Delta_I, \omega; Q_I, J) = -i\frac{4\sqrt{2}N^{\frac{3}{2}}}{3}\frac{\sqrt{\Delta_1\Delta_2\Delta_3\Delta_4}}{\omega} + \omega J + \sum_{I=1}^{4}\Delta_I Q_I . \quad (2.2.17)$$

We extremize S in Δ_I, ω with the constraint

$$\Delta_1 + \Delta_2 + \Delta_3 + \Delta_4 - \omega = 2\pi i . \tag{2.2.18}$$

A microscopic derivation of the entropy function (2.2.17) from the CFT$_3$ dual was studied in [79] in the Cardy limit $\omega \to 0$, and we will discuss it in chapter 5. Just like AdS$_5$, AdS$_7$ black holes analyzed in [75], discussed in chapter 3, 7, the constraint (2.2.18) is given an interpretation in [79]. Here the number of M2-branes N is related to the 4d Newton constant G as follows:

$$G_{11} = 16\pi^7 \ell_{\mathrm{P}}{}^9, \ \ell_{S^7} = 2\ell = \ell_{\mathrm{P}}(2^5 \pi^2 N)^{1/6} \ \Rightarrow \ \frac{1}{g^2 G} = \frac{\mathrm{vol}(S^7)}{g^2 G_{11}} = \frac{2\sqrt{2}}{3} \frac{N^{3/2}}{g^2 \ell^2} = \frac{2\sqrt{2}}{3} N^{3/2} .$$
$$\tag{2.2.19}$$

ℓ_{P} is the 11d Planck scale, ℓ_{S^7} is the radius of S^7, and ℓ is the AdS$_4$ radius as defined in the previous subsection. We claim that the resulting extremal value of $\mathrm{Re}(S)$ is the entropy of supersymmetric black holes. We shall check this against the known solutions summarized in the previous subsection, at $Q_1 = Q_3$, $Q_2 = Q_4$ (which is equivalent to $\Delta_1 = \Delta_3$, $\Delta_2 = \Delta_4$). Here, note that the chemical potentials Δ_I, ω are all complexified. With complex Δ_I, the square root $\sqrt{\Delta_1 \Delta_2 \Delta_3 \Delta_4}$ in (2.2.17) should be understood as to take the argument of $\Delta_1 \Delta_2 \Delta_3 \Delta_4$ in the principal branch $(-\pi, \pi)$ [79].

We show our claim by extremizing S, subject to the constraint (2.2.18). We introduce the Lagrange multiplier λ and extremize

$$S = -i \frac{4\sqrt{2} N^{\frac{3}{2}}}{3} \frac{\sqrt{\Delta_1 \Delta_2 \Delta_3 \Delta_4}}{\omega} + \omega J + \sum_{I=1}^{4} \Delta_I Q_I + \lambda \left(\sum_{I=1}^{4} \Delta_I - \omega - 2\pi i \right) .$$
$$\tag{2.2.20}$$

The extremum conditions are given by

$$\lambda + Q_I = i \frac{4\sqrt{2} N^{\frac{3}{2}}}{3\omega} \frac{\sqrt{\Delta_1 \Delta_2 \Delta_3 \Delta_4}}{2\Delta_I} \quad (I = 1, \cdots, 4) , \tag{2.2.21}$$

$$\lambda - J = i \frac{4\sqrt{2} N^{\frac{3}{2}}}{3\omega^2} \sqrt{\Delta_1 \Delta_2 \Delta_3 \Delta_4} .$$

Inserting these charges into (2.2.20), to eliminate the appearances of Q_I, J, one obtains

$$S = -2\pi i\lambda .$$
(2.2.22)

Multiplying the four equations on the first line of (2.2.21), one finds

$$(\lambda + Q_1)(\lambda + Q_2)(\lambda + Q_3)(\lambda + Q_4) = \frac{64N^6}{81\omega^4}\Delta_1\Delta_2\Delta_3\Delta_4 = -\frac{2N^3}{9}(\lambda - J)^2 .$$
(2.2.23)

So one obtains a very useful expression,

$$\left(\frac{S}{2\pi i} - Q_1\right)\left(\frac{S}{2\pi i} - Q_2\right)\left(\frac{S}{2\pi i} - Q_3\right)\left(\frac{S}{2\pi i} - Q_4\right) = -\frac{2N^3}{9}\left(\frac{S}{2\pi i} + J\right)^2 .$$
(2.2.24)

One needs care to treat the above expression. While the above is the quartic equation in S, only the half of them are the true solutions to (2.2.21) satisfying the constraint (2.2.18). The other halves are the extraneous solutions. Hence, after solving the above equation, one should check whether the resulting solution is a true one.

After extremizing the entropy function, one would generally obtain complex solutions for S by solving (2.2.24). Along the spirit of [75], we shall generally regard $\mathrm{Re}(S)$ as the entropy at the extremum. See [75, 79, 80, 96] for the interpretation of the imaginary part. We shall revisit this problem in chapter 8 in a more concrete set-up of [80]. There, the imaginary part of the entropy will be given a clear interpretation. (See also [96].) However, in this chapter, we are primarily interested in comparing our results against the known black hole solutions of section 2.2.1. Therefore, we impose the charge relation of these black holes and compare the thermodynamic quantities on that surface only. Somewhat remarkably, the charge relation of known black holes will turn out to be $\mathrm{Im}(S) = 0$ at the extremum of our entropy function. So from now on, we demand the existence of a real solution for S in (2.2.24), and compare the results with

the known black holes. Demanding real S for real charges Q_1, Q_2, Q_3, Q_4, J, the complex equation (2.2.24) is separated into two real equations as follows:

$$\frac{1}{16\pi^4}S^4 - \frac{\sum_{I<J}Q_IQ_J}{4\pi^2}S^2 + Q_1Q_2Q_3Q_4 = \frac{N^3}{18\pi^2}S^2 - \frac{2N^3J^2}{9} ,$$

$$-\frac{\sum_I Q_I}{8\pi^3}S^3 + \frac{\sum_{I<J<K}Q_IQ_JQ_K}{2\pi}S = \frac{2N^3J}{9\pi}S . \qquad (2.2.25)$$

These equations determine S twice as functions of charges. From the compatibility of two equations, one will get a relation of Q_I, J. Explicitly, one may take the unique positive solution of the second equation and insert it to the first equation, to obtain the charge relation. One can check that this solution is a true solution satisfying (2.2.21) and (2.2.18).

To compare with known black holes summarized in section 2.2.1, we set $Q_1 = Q_3$, $Q_2 = Q_4$. Then, taking the unique positive solution assuming $Q_1, Q_2, J > 0$, one obtains

$$S = \frac{2\pi}{3}\sqrt{\frac{9Q_1Q_2(Q_1+Q_2)-2N^3J}{Q_1+Q_2}},$$

$$0 = 2N^3J^2 + 2N^3(Q_1+Q_2)J - 9Q_1Q_2(Q_1+Q_2)^2 . \qquad (2.2.26)$$

These can be rearranged as

$$S = \frac{2\sqrt{2}\pi N^{\frac{3}{2}}}{3}\frac{J}{Q_1+Q_2} = \frac{\pi}{g^2G}\frac{J}{Q_1+Q_2} , \qquad (2.2.27)$$

$$J = \frac{1}{2}(Q_1+Q_2)\left(-1+\sqrt{1+\frac{18}{N^3}Q_1Q_2}\right) = \frac{1}{2}(Q_1+Q_2)\left(-1+\sqrt{1+16g^4G^2Q_1Q_2}\right) .$$

One can easily check that this solution indeed satisfies (2.2.21) and (2.2.18), i.e. it is not an extraneous solution. The above expressions are exactly the same as (2.2.9), which we obtained from the supersymmetric black holes. Note that the charges and chemical potentials of the entropy function (2.2.20) are related to

those of supersymmetric black holes as

$$S_{\mathrm{BH}} = S, \ J_{\mathrm{BH}} = J, \ \frac{2}{g} Q_{I,\mathrm{BH}} = Q_I \ ,$$

$$\omega_{\mathrm{BH}} = \mathrm{Re}(\omega), \ \frac{g}{2} \Delta_{I,\mathrm{BH}} = \mathrm{Re}(\Delta_I).$$

(2.2.28)

Here, the subscripts 'BH' denote the black hole quantities, while the others are the quantities used in the entropy function. The second line can be shown by a rather straightforward but tedious calculus. One also finds that the relation between the chemical potentials in the entropy function (2.2.18) is equivalent to that of the supersymmetric black holes (2.2.16).

To summarize, our entropy function (2.2.20) indeed reproduces the Bekenstein-Hawking entropy of the supersymmetric AdS$_4$ black holes (2.2.7) and the corresponding charge/chemical potential relations (2.2.9), (2.2.16), at $Q_1 = Q_3$, $Q_2 = Q_4$ where solutions are known. Recently, 4 parameter BPS black hole solutions with all different Q_I's were discovered in [97], whose physics is successfully described by our entropy function (2.2.20).

Our entropy function (2.2.20) can be regarded as the free energy of the BPS black holes in the grand canonical ensemble since its Legendre transformation to the microcanonical ensemble gives the entropy. Accordingly, it can obtained from the Euclidean on-shell action of the BPS black holes in AdS$_4$ [93]. Analyzing the free energy, we can investigate interesting thermodynamic properties of the BPS black holes. As these properties are similar regardless of the spacetime dimensions of the black holes, we simply omit to study them in this section. We shall study thermodynamic properties of the supersymmetric AdS$_5$ black holes in the next section, and most of them can be applied to the supersymmetric AdS$_4$ black holes treated in this section.

One may think of generalizations of our results on AdS$_4 \times S^7$, to more general 4d $\mathcal{N} = 2$ gauged supergravity models arising from string or M-theory. To see a

natural possibility of generalization, note that the numerator $\sim \sqrt{\Delta_1 \Delta_2 \Delta_3 \Delta_4}$ of our entropy function (2.2.17) is the homogeneous degree 2 prepotential of the $U(1)^4$ supergravity [98]. The prepotential is the square root of a degree 4 polynomial. See, e.g. [99, 100] for such structures in other backgrounds. We conjecture that, for BPS black holes in 4d $\mathcal{N} = 2$ gauged supergravity, an entropy function like (2.2.17) can be constructed by replacing the numerator by the prepotential of the theory. Recently, such an entropy function was found in [97], and also microscopically studied in [77] from the indices of SCFT$_3$ duals in the Cardy limit $\omega \to 0$.

2.3 AdS$_5$ black holes

In this section, we study the supersymmetric black holes in AdS$_5 \times S^5$ of [82–86]. The entropy function of these black holes was introduced in [90]. Later, it was extended in section 2.3 of [75] by checking the agreements of chemical potentials as in the former section. This allows us to regard the real part of the entropy function as the free energy of known BPS black holes. We will not cover the detailed computations for the extremization of the entropy function in this section. The procedures are essentially the same as the former section. For details, refer to [90] and section 2.3 of [75].

Instead, we shall view the entropy function as the free energy of the BPS black holes in the grand canonical ensemble, and focus on their thermodynamic properties. Here, the grand canonical ensemble should be understood as the restricted ensemble on the zero-temperature BPS sector. However, even in the BPS sector, the BPS chemical potentials forming thermal ensemble exhibit nontrivial thermodynamic structures such as the phase transition.

The entropy function of supersymmetric AdS$_5$ black holes is given by [90]

$$S(\Delta_I, \omega_i; Q_I, J_i) = \frac{N^2}{2} \frac{\Delta_1 \Delta_2 \Delta_3}{\omega_1 \omega_2} + \sum_{I=1}^{3} Q_I \Delta_I + \sum_{i=1}^{2} J_i \omega_i \ , \qquad (2.3.1)$$

where

$$\Delta_1 + \Delta_2 + \Delta_3 - \omega_1 - \omega_2 = 2\pi i \ , \qquad (2.3.2)$$

Extremizing this function, one obtains the entropies and the chemical potentials of known analytic black hole solutions as in the former section. A microscopic derivation of the entropy function (2.3.1) from the CFT$_4$ dual was studied in [75] in the Cardy limit $\omega_{1,2} \to 0$, and we will discuss it in chapter 3. Here the number of D3-branes N is related to the 5d Newton constant G as follows:

$$N^2 = \frac{\pi \ell^3}{2G} \ , \qquad (2.3.3)$$

where ℓ is the AdS$_5$ radius. In addition, Q_I and J_i are $U(1)^3 \subset SO(6)$ electric charges and $U(1)^2 \subset SO(4)$ angular momenta, respectively. The Bekenstein-Hawking entropy of the black hole is the extremal value of $\text{Re}(S)$, at one of the extremum solutions for Δ_I, ω_i [90]. The black hole chemical potentials are the extremal values of $\text{Re}(\Delta_I)$, $\text{Re}(\omega_i)$ [75]. This entropy function was later obtained from the Euclidean on-shell action of the BPS black holes in AdS$_5$ [92, 93].

Now, for simplicity, let us consider the case with equal electric charges, $Q_1 = Q_2 = Q_3 \equiv Q$, and equal angular momenta $J_1 = J_2 \equiv J$. Then, we also set the corresponding chemical potentials to be equal, $\Delta_1 = \Delta_2 = \Delta_3 \equiv \Delta$, $\omega_1 = \omega_2 \equiv \omega$. The constraint on chemical potentials is $3\Delta = 2\pi i + 2\omega$. Inserting this, the entropy function is given by

$$S = \frac{N^2}{2} \frac{\left(\frac{2\pi i + 2\omega}{3}\right)^3}{\omega^2} + 2\omega(J + Q) + 2\pi i Q \ . \qquad (2.3.4)$$

We ignore the last constant term $2\pi i Q$, as this will not contribute to $\text{Re}(S)$. (In fact, $e^{2\pi i Q} = \pm 1$ from charge quatization.) The saddle point equation $\frac{\partial S}{\partial \omega} = 0$

yields

$$J + Q = \frac{N^2}{54} \left(\frac{(2\pi i + 2\omega)^3}{\omega^3} - 3\frac{(2\pi i + 2\omega)^2}{\omega^2} \right) . \qquad (2.3.5)$$

ω will be complex, but since the left hand side of (2.3.5) is real, it is helpful to write $\omega = \omega_R + i\omega_I$ with real $\omega_{I,R}$. Then (2.3.5) can be separated to real and imaginary parts. Setting the imaginary part to zero, one obtains three solutions for ω_R at given ω_I:

$$\omega_R = \begin{cases} 0 & \text{for } \omega_I \in (-\infty, \infty) \\ \pm\omega_I\sqrt{\frac{3\pi+3\omega_I}{\pi-3\omega_I}} & \text{for } \omega_I \in (-\pi, \frac{\pi}{3}) \end{cases} . \qquad (2.3.6)$$

If one inserts (2.3.6) to (2.3.5), the real part of this equation becomes

$$J + Q = \begin{cases} \frac{2N^2}{27} \frac{(2\pi-\omega_I)(\pi+\omega_I)^2}{\omega_I^3} & \text{if } \omega_R = 0 \\ -\frac{N^2}{54} \frac{(\pi-2\omega_I)^2(\pi+\omega_I)}{\omega_I^3} & \text{if } \omega_R = \pm\omega_I\sqrt{\frac{3\pi+3\omega_I}{\pi-3\omega_I}} \end{cases} . \qquad (2.3.7)$$

Also, $\log Z = \frac{N^2}{2}\frac{\Delta^3}{\omega^2}$ becomes

$$\log Z = \begin{cases} i\frac{4N^2}{27}\frac{(\pi+\omega_I)^3}{\omega_I^2} & \text{if } \omega_R = 0 \\ \mp\frac{N^2}{18}\frac{\pi^3-9\pi\omega_I^2-8\omega_I^3}{\omega_I^2}\sqrt{\frac{\pi+\omega_I}{3\pi-9\omega_I}} - i\frac{N^2}{54}\frac{(\pi-8\omega_I)(\pi+\omega_I)^2}{\omega_I^2} & \text{if } \omega_R = \pm\omega_I\sqrt{\frac{3\pi+3\omega_I}{\pi-3\omega_I}} \end{cases} . \qquad (2.3.8)$$

The solution with $\omega_R = 0$ will yield imaginary $\log Z$ and therefore $\text{Re}(S) = 0$, making it an irrelevant solution. In the remaining two solution, the free parameter ω_I is related to the unique charge combination $J + Q$ captured by the index, which can be used to express $\log Z$ and S.

We further discuss which of the remaining solutions corresponds to black holes. Since ω_R should be positive, one should choose the upper sign for $0 < \omega_I < \frac{\pi}{3}$, and lower sign for $-\pi < \omega_I < 0$. Also, since $J+Q$ has to be positive, one obtains $\omega_I < 0$ from the second line of (2.3.7). Therefore the physical solution is $\omega_R = -\omega_I\sqrt{\frac{3\pi+3\omega_I}{\pi-3\omega_I}}$ for $-\pi < \omega_I < 0$. Various quantities labeled by ω_I are
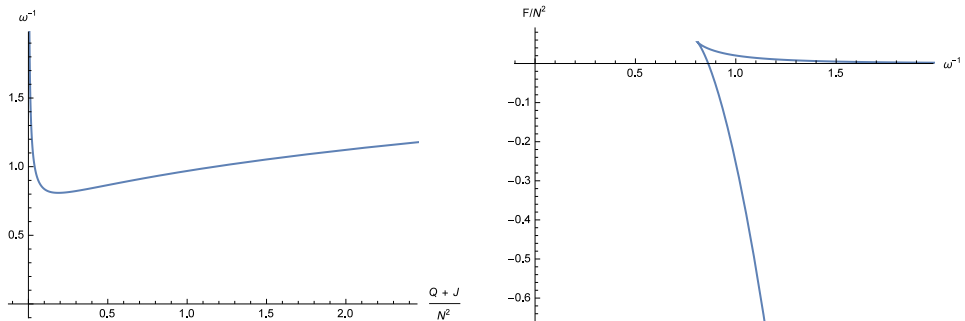
Figure 2.1: [left] Charge vs. temperature. There are small and large black hole branches, with negative/positive specific heat, respectively. [right] Temperature vs. free energy. The upper curve for is small black holes with positive free energy, always losing against thermal AdS gravitons. The lower curve is for large black holes, dominating for $\omega < \omega_{\mathrm{HP}}^{\mathrm{known}}$ with $F < 0$.

summarized as

$$\omega = -\omega_I \sqrt{\frac{3\pi + 3\omega_I}{\pi - 3\omega_I}} + i\omega_I, \quad -\pi < \omega_I < 0$$

$$J + Q = -\frac{N^2}{54} \frac{(\pi - 2\omega_I)^2(\pi + \omega_I)}{\omega_I^3}$$

$$\log Z = \frac{N^2}{18} \frac{\pi^3 - 9\pi\omega_I^2 - 8\omega_I^3}{\omega_I^2} \sqrt{\frac{\pi + \omega_I}{3\pi - 9\omega_I}} - i\frac{N^2}{54} \frac{(\pi - 8\omega_I)(\pi + \omega_I)^2}{\omega_I^2} . \quad (2.3.9)$$

The plots for the 'temperature' ω^{-1}, the 'free energy' $\frac{F}{N^2} = -\frac{\mathrm{Re}(\log Z)}{N^2}$, charge $\frac{Q+J}{N^2}$ are shown in Fig. 2.1. Let us call $T \equiv \omega^{-1}$ the 'temperature' as this plays this role, conjugate to $Q + J$. From the left figure, one finds that there are two branches of black holes for $T > T_0 \equiv \left[\pi\sqrt{\frac{2}{\sqrt{3}} - 1}\right]^{-1} \approx 1.24^{-1}$, similar to the AdS-Schwarzschild black holes, which we discussed in the introduction. In the small black hole branch, the specific heat (the slope) is negative. So we do not consider this saddle point if we are in the grand canonical ensemble. The large black hole branch is to compete with the thermal BPS graviton phase, at

$\frac{F}{N^2} \approx 0$, and the Hawking-Page like first order phase transition will occur at this point. From the graph on the right side of Fig. 2.1, one finds that the large black hole dominates over thermal BPS gravitons for

$$T^{-1} = \omega < \omega_{\text{HP}}^{\text{known}} \equiv \frac{\pi}{16} \sqrt{414 - 66\sqrt{33}} \approx 1.16 \ , \qquad (2.3.10)$$

which corresponds to $Q + J > \frac{3+\sqrt{33}}{18} N^2 \approx 0.486 N^2$.

As said, these interesting thermodynamic properties are analogous to those of the AdS-Schwarzschild black holes, which have non-zero Hawking temperature. Namely, even if the BPS black holes have zero Hawking temperature, they exhibit nontrivial thermodynamics in terms of the BPS chemical potentials. Thus, studying the BPS black holes, we may further semi-quantitatively study the physics of finite temperature Schwarzschild black holes. These thermodynamic structures are not unique properties of the BPS black holes in AdS_5. One can easily check that the BPS black holes in $\text{AdS}_{4,5,6,7}$ all exhibit similar properties although we will not explicitly show that in this chapter.

2.4 AdS_6 black holes

2.4.1 Black hole solutions

In this section, we study the supersymmetric AdS_6 black holes, and find an entropy function which accounts for their physics. We construct an entropy function for the solution of [87]. The solution may be regarded as describing BPS states of any large N 5d SCFT dual. For instance, as our favorite example, results in this section may be understood in the context of massive type IIA string theory on warped $\text{AdS}_6 \times S^4/\mathbb{Z}_2$ product background. This system is dual to 5d $\mathcal{N} = 1$ SCFT living on N D4-branes probing the O8-D8 system [47]. The 5d SCFT dual has a gauge theory description, with $Sp(N)$ gauge group, rank

2 antisymmetric hypermultiplet, and $N_f \leq 7$ fundamental hypermultiplets. However, we expect that our general analysis can be embedded to AdS$_6$ black holes in the backgrounds of [101–105].

The 6d $\mathcal{N} = (1, 0)$ $SU(2)$ gauged supergravity was obtained by a consistent Kaluza-Klein truncation of massive type IIA supergravity on $S^4/\mathbb{Z}_2$ [106]. In [87], the charged rotating AdS$_6$ black hole solution in this gauged supergravity was obtained. It has four kinds of conserved quantities: mass E, two angular momenta J_1, J_2, which describe the orthogonal 2-plane rotations on S^4 in global AdS$_6$, and one $U(1) \subset SU(2)$ electric charge Q. They are given in terms of four parameters m, a, b, δ of the solution as [87]

$$
E = \frac{2\pi m}{3G\Xi_a\Xi_b} \left[\frac{1}{\Xi_a} + \frac{1}{\Xi_b} + \sinh^2\delta \left(1 + \frac{\Xi_a}{\Xi_b} + \frac{\Xi_b}{\Xi_a} \right) \right] \ , \quad Q = \frac{\pi m}{G\Xi_a\Xi_b} \sinh 2\delta \ ,
$$
$$
J_1 = \frac{2\pi ma}{3G\Xi_a^2\Xi_b}(1 + \Xi_b \sinh^2\delta) \ , \quad J_2 = \frac{2\pi mb}{3G\Xi_a\Xi_b^2}(1 + \Xi_a \sinh^2\delta) \ ,
$$

$$(2.4.1)$$

where $\Xi_a = 1 - a^2g^2$ and $\Xi_b = 1 - b^2g^2$. The entropy is given by

$$
S = \frac{2\pi^2 \left[(r_+^2 + a^2)(r_+^2 + b^2) + 2mr_+ \sinh^2\delta \right]}{3G\Xi_a\Xi_b} \ .
$$

$$(2.4.2)$$

The event horizon is located at $r = r_+$. Here, G is the 6d Newton constant. (In [87], the unit $G = 1$ is used.) g is a gauge coupling constant in 6d gravity, setting the inverse-radius of AdS$_6$.

This black hole solution admits the supersymmetric limit without naked closed timelike curves. The BPS condition

$$
E = gJ_1 + gJ_2 + Q
$$

$$(2.4.3)$$

is satisfied if

$$
e^{2\delta} = 1 + \frac{2}{(a + b)g} \ .
$$

$$(2.4.4)$$

In addition, a smooth horizon exists only if

$$m = \frac{(a+b)^2(1+ag)(1+bg)(2+ag+bg)}{2(1+ag+bg)}\sqrt{\frac{ab}{1+ag+bg}} \qquad (2.4.5)$$

is satisfied. The horizon is located at

$$r_+ = \sqrt{\frac{ab}{1+ag+bg}} \ . \qquad (2.4.6)$$

Taking the BPS limit, the entropy of the supersymmetric black hole is given by

$$S = \frac{2\pi^2 ab(a+b)}{3gG(1-ag)(1-bg)(1+ag+bg)} \ . \qquad (2.4.7)$$

The two conditions (2.4.4), (2.4.5) leave two independent parameters among m, a, b, δ. Even after restricting E as (2.4.3) from the BPS condition, the remaining charges J_1, J_2, Q carried by the supersymmetric black holes will satisfy a charge relation. Equivalently, together with S, we find the following two relations:

$$S^3 - \frac{2\pi^2}{3g^4G}S^2 - 12\pi^2\left(\frac{Q}{3g}\right)^2 S + \frac{8\pi^4}{3g^4G}J_1 J_2 = 0 \ ,$$
$$\frac{Q}{3g}S^2 + \frac{2\pi^2}{9g^4G}(J_1+J_2)S - \frac{4\pi^2}{3}\left(\frac{Q}{3g}\right)^3 = 0 \ . \qquad (2.4.8)$$

Since these equations determine S twice, one will get a charge relation between J_1, J_2, Q from the compatibility of two equations. Explicitly, one may take the unique positive solution of the second equation and insert it to the first equation, to get the charge relation.

The black hole chemical potentials and the free energy F satisfy

$$S = -T^{-1}F + T^{-1}E - T^{-1}\Omega_1 J_1 - T^{-1}\Omega_2 J_2 - T^{-1}\Phi Q \ , \qquad (2.4.9)$$

where T is the temperature, Ω_1, Ω_2 are the angular velocities, and Φ is the electrostatic potential. The temperature of the supersymmetric black hole is

zero in the BPS smooth horizon limit,

$$T = \frac{2r_+^2(1+g^2r_+^2)(2r_+^2+a^2+b^2)-(1-g^2r_+^2)(r_+^2+a^2)(r_+^2+b^2)+8mg^2r_+^3\sinh^2\delta-4m^2g^2\sinh^4\delta}{4\pi r_+[(r_+^2+a^2)(r_+^2+b^2)+2mr_+\sinh^2\delta]}$$

$$(2.4.10)$$

The other chemical potentials in the BPS limit are given by

$$\Omega_1 = a\frac{(1+g^2r_+^2)(r_+^2+b^2)+2mg^2r_+\sinh^2\delta}{(r_+^2+a^2)(r_+^2+b^2)+2mr_+\sinh^2\delta} \to g \ ,$$

$$\Omega_2 = b\frac{(1+g^2r_+^2)(r_+^2+a^2)+2mg^2r_+\sinh^2\delta}{(r_+^2+a^2)(r_+^2+b^2)+2mr_+\sinh^2\delta} \to g \ , \qquad (2.4.11)$$

$$\Phi = \frac{mr_+\sinh 2\delta}{(r_+^2+a^2)(r_+^2+b^2)+2mr_+\sinh^2\delta} \to 1 \ .$$

Similar to the analysis in section 2.2.1, the following limits exist,

$$F_{\text{BPS}} = \lim_{T\to 0}\left(T^{-1}(F-\Delta E)\right), \ \omega_i = -\lim_{T\to 0}\left(T^{-1}(\Omega_i - g)\right) \ , \ \Delta = -\lim_{T\to 0}\left(T^{-1}(\Phi - 1)\right) \ ,$$

$$(2.4.12)$$

where $\Delta E \equiv E - Q - gJ_1 - gJ_2$. Then, in the zero temperature BPS limit, one obtains

$$S = -F_{\text{BPS}} + \omega_1 J_1 + \omega_2 J_2 + \Delta Q \ . \qquad (2.4.13)$$

Using the computed expressions for ω_i, Δ, one finds that

$$\omega_1 + \omega_2 = 3g\Delta \ . \qquad (2.4.14)$$

Again, this is the alternative statement of the charge relation of J_1, J_2, Q.

2.4.2 Entropy function

We now present an entropy function which encodes the physics of the BPS black holes presented in the previous subsection. The entropy function is given by

$$S = -i\frac{\pi}{81g^4G}\frac{\Delta^3}{\omega_1\omega_2} + \Delta Q + \omega_1 J_1 + \omega_2 J_2 + \lambda\left(\Delta - \omega_1 - \omega_2 - 2\pi i\right) \ , \quad (2.4.15)$$

where G is the 6d Newton constant as before. Having in mind the concrete example of massive IIA supergravity on warped $AdS_6 \times S^4/\mathbb{Z}_2$ background, one would find $\frac{1}{g^4 G} = \frac{27\sqrt{2}}{5\pi} \frac{N^{\frac{5}{2}}}{\sqrt{8-N_f}}$ [78]. In that case, a microscopic derivation of the entropy function (2.4.15) from the CFT_5 dual was studied in [78] in the Cardy limit $\omega_{1,2} \to 0$, and we will discuss it in chapter 4. Here, we introduced the Lagrange multiplier λ to extremize S in $\Delta, \omega_1, \omega_2$ subject to the constraint

$$\Delta - \omega_1 - \omega_2 = 2\pi i . \tag{2.4.16}$$

Differentiating with respect to the chemical potentials, one obtains

$$\lambda + Q = i\frac{\pi}{27g^4 G}\frac{\Delta^2}{\omega_1 \omega_2} \quad , \quad \lambda - J_1 = i\frac{\pi}{81g^4 G}\frac{\Delta^3}{\omega_1^2 \omega_2} \quad , \quad \lambda - J_2 = i\frac{\pi}{81g^4 G}\frac{\Delta^3}{\omega_1 \omega_2^2} . \tag{2.4.17}$$

Inserting these back to the original entropy function formula, one obtains

$$S = -2\pi i \lambda. \tag{2.4.18}$$

Multiplying the last two equations of (2.4.17), one obtains

$$(\lambda - J_1)(\lambda - J_2) = -\left(\frac{\pi}{81g^4 G}\right)^2 \frac{\Delta^6}{\omega_1^3 \omega_2^3} = -i\frac{3g^4 G}{\pi}(\lambda + Q)^3 . \tag{2.4.19}$$

Hence, one obtains

$$\left(\frac{S}{2\pi i} + J_1\right)\left(\frac{S}{2\pi i} + J_2\right) = i\frac{3g^4 G}{\pi}\left(\frac{S}{2\pi i} - Q\right)^3 . \tag{2.4.20}$$

As in our section 2.2 and [75], we dismiss $\mathrm{Im}(S)$, focussing on $\mathrm{Re}(S)$ as our entropy. However, again note that all known supersymmetric AdS_6 black holes have a charge relation. This charge relation will coincide with the condition $\mathrm{Im}(S) = 0$ at the saddle point. So we demand real S for real charges Q, J_1, J_2. Then, (2.4.20) is separated into two real equations as follows:

$$S^3 - \frac{2\pi^2}{3g^4 G}S^2 - 12\pi^2 Q^2 S + \frac{8\pi^4}{3g^4 G}J_1 J_2 = 0 ,$$

$$QS^2 + \frac{2\pi^2}{9g^4 G}(J_1 + J_2)S - \frac{4\pi^2}{3}Q^3 = 0 . \tag{2.4.21}$$

These equations determine S twice as functions of charges. Therefore, from the compatibility of two equations, one obtains a charge relation of Q, J_1, J_2. These two equations of S, Q, J_1, J_2 (2.4.21), derived from the entropy function (2.4.15), are exactly the same as those from the supersymmetric black holes (2.4.8). Note that the charges and chemical potentials of the entropy function (2.4.15) are related to those of the black holes as

$$S_{\text{BH}} = S, \ J_{i,\text{BH}} = J_i, \ \frac{1}{3g}Q_{\text{BH}} = Q \ ,$$

$$\omega_{i,\text{BH}} = \text{Re}(\omega_i), \ 3g\,\Delta_{\text{BH}} = \text{Re}(\Delta) \ . \tag{2.4.22}$$

The subscripts 'BH' denote the black hole quantities, while the others are the quantities used in the entropy function. One can also realize that the relation between the chemical potentials in the entropy function (2.4.16) is equivalent to that of the supersymmetric black holes (2.4.14).

Thus, our entropy function (2.4.15) indeed reproduces the Bekenstein-Hawking entropy of the supersymmetric AdS_6 black holes (2.4.7), and also their chemical potentials. Later, this entropy function was obtained from the Euclidean on-shell action of the BPS black holes in AdS_6 [93].

While AdS_6 black hole solution known to date has only one electric charge dual to R-charge of 5d SCFT dual, [78] obtained a more general form of the entropy function, which describes AdS_6 black holes carrying various electric charges, dual to R-charge, mesonic charge and baryonic charges, yet to be discovered. For example, when the black hole has one more electric charge dual to the mesonic charge, the numerator $\sim \Delta^3$ of our entropy function (2.4.15) is refined to $[(\Delta + \hat{m})(\Delta - \hat{m})]^{\frac{3}{2}}$, where $m \equiv \hat{m} + 2\pi i$ is the chemical potential conjugate to the mesonic charge.

2.5 AdS$_7$ black holes

The entropy function of the BPS black holes in AdS$_7 \times S^4$ of [88, 89] is given by [91]

$$S(\Delta_I, \omega_i; Q_I, J_i) = -\frac{N^3}{24}\frac{\Delta_1^2 \Delta_2^2}{\omega_1 \omega_2 \omega_3} + \sum_{I=1}^{2} Q_I \Delta_I + \sum_{i=1}^{3} J_i \omega_i \ , \qquad (2.5.1)$$

where

$$\Delta_1 + \Delta_2 - \omega_1 - \omega_2 - \omega_3 = 2\pi i \ . \qquad (2.5.2)$$

Here, Q_I and J_i are $U(1)^2 \subset SO(5)$ electric charges and $U(1)^3 \subset SO(6)$ angular momenta. Extremizing this function, one obtains the entropies [91] and the chemical potentials [75] of known analytic black hole solutions as in the former sections. A derivation of the entropy function (2.5.1) from the CFT$_6$ dual was studied in [75] in the Cardy limit $\omega_{1,2,3} \to 0$, and we will discuss it in chapter 7. Here the number of M5-branes N is related to the 7d Newton constant G as follows:

$$N^3 = \frac{3\pi^2 \ell^5}{16G} \ , \qquad (2.5.3)$$

where ℓ is the AdS$_7$ radius. This entropy function was later obtained from the Euclidean on-shell action of the BPS black holes in AdS$_7$ [93].

We will not cover the detailed computations for the extremization of the entropy function. The procedures are essentially the same as the former sections. For details, refer to [91] and section 4 of [75].

Chapter 3

Large AdS$_5$ black holes from 4d $\mathcal{N} = 4$ SYM

In this chapter, we study the index of $\mathcal{N} = 4$ Yang-Mills theory on $S^3 \times \mathbb{R}$ at large angular momenta. A generalized Cardy limit exhibits macroscopic entropy at large N. Our result is derived using free QFT analysis but is valid even in the strong coupling regime. The index sets a lower bound on the entropy. It saturates the Bekenstein-Hawking entropy of known supersymmetric AdS$_5$ black holes, thus accounting for their microstates. We further analyze the so-called Macdonald index, exploring small black holes and possibly new black holes reminiscent of hairy black holes.

3.1   Introduction and summary

It has been believed that the BPS black holes in AdS$_5$ defied quantitative understandings from indices of SCFTs on $S^3 \times \mathbb{R}$ [68,69]. There have been many

speculations on why the index fails to capture black holes. A possible reason is that bosonic/fermionic states undergo big cancelation. For instance, the index cannot see the deconfinement phase transition at an order 1 temperature in the unit of AdS$_5$ radius [69], which is the QFT dual of the Hawking-Page transition of AdS black holes [55]. So the index cannot capture all the physics of generic supersymmetric AdS$_5$ black holes. Direct studies of BPS operators at weak coupling did not discover enough microstates for such black holes either [107–110], at least so far.

In this chapter, we show that the index of 4d $\mathcal{N} = 4$ Yang-Mills theory _does_ capture large supersymmetric AdS$_5$ black holes [82–86] in an asymptotic Cardy-like limit. Our Cardy limit is more refined than [73], in that the imaginary parts of chemical potentials are tuned to optimally obstruct boson/fermion cancelations. The entropy of our asymptotic index is macroscopic, meaning that it is proportional to N^2 when all the charges are at this order. This sets a lower bound on the true microscopic entropy of BPS states, assuring the existence of BPS black holes in $AdS_5 \times S^5$. In particular, when a charge relation is met, our asymptotic free energy agrees with the Bekenstein-Hawking entropy of known supersymmetric AdS$_5$ black holes [83, 84, 86], thereby microscopically counting them. The asymptotic free energy of our index is the recently suggested entropy function for supersymmetric AdS$_5$ black holes [90], in our large black hole limit. At general values of charges, perhaps our findings may have implications to possible supersymmetric hairy black holes in $AdS_5 \times S^5$ [111, 112]. The last suggestion is indirectly supported by studying the asymptotic free energy of the so-called Macdonald index [113]. Here, depending on charge regime, the Cardy-like free energy differs from the entropy function of [90], showing properties reminiscent of hairy black holes in $AdS_5 \times S^5$.

In the rest of this chapter, we will derive the asymptotic free energy of the index of 4d $\mathcal{N} = 4$ Yang-Mills theory, in a generalized Cardy-like limit. This free energy counts known supersymmetric AdS$_5$ black holes. In addition, we study similar asymptotic free energy of the index in the Macdonald limit, suggesting rich structures such as small black holes and new saddle points reminiscent of hairy black holes.

3.2 Large supersymmetric AdS$_5$ black holes

We study the the partition function of $\mathcal{N} = 4$ Yang-Mills theory on $S^3 \times \mathbb{R}$, focussing on the index limit [69]. The partition function counts states carrying six charges. The first one is the energy E, made dimensionless by multiplying the S^3 radius. Three charges Q_1, Q_2, Q_3 are for the Cartans of $SO(6)$ R-symmetry, defined to be the angular momenta on three orthogonal 2-planes on $\mathbb{R}^6$, being $\pm\frac{1}{2}$ for spinors. The final two are the angular momenta J_1, J_2 on S^3, being $\pm\frac{1}{2}$ for spinors. The BPS states of our interest saturate the bound $E \geq Q_1 + Q_2 + Q_3 + J_1 + J_2$, but we shall impose the BPS limit at a later stage to see more universal features. Consider the general partition function:

$$Z(\beta, \Delta_I, \omega_i) = \text{Tr} \left[e^{-\beta E} e^{-\sum_{I=1}^{3} \Delta_I Q_I} e^{-\sum_{i=1}^{2} \omega_i J_i} \right] . \qquad (3.2.1)$$

The complex chemical potentials Δ_I, ω_i satisfy five periodicity conditions $\Delta_I \sim \Delta_I + 4\pi i$, $\omega_i \sim \omega_i + 4\pi i$. The 16 supercharges are $\mathcal{Q}_{J_1,J_2}^{Q_1,Q_2,Q_3}$. 16 possible values of Q_I, J_i carried by $\mathcal{Q}$ are $\pm\frac{1}{2}$, where the product of all 5 $\pm$ signs is $+$. The conformal supercharges are $\mathcal{S}_{J_1,J_2}^{Q_1,Q_2,Q_3}$ with five charges being $\pm\frac{1}{2}$, where the product of signs is $-$. Taking the trace without $(-1)^F$, the fermionic fields are anti-periodic along temporal circle, twisted by Δ_I, ω_i. So the SUSY connecting periodic bosons and anti-periodic fermions are generally broken. In a sense,

the supercharges are anti-periodic which has no zero modes on temporal S^1. However, if

$$\sum_{I=1}^{3} s_I \Delta_I - \sum_{i=1}^{2} t_i \omega_i = 2\pi i \,(\text{mod } 4\pi i) \ , \quad s_I, t_i = \pm 1 \ \text{ satisfying } \ s_1 s_2 s_3 t_1 t_2 = +1 \ ,$$

$$(3.2.2)$$

(3.2.1) becomes an index if one takes $\beta \to 0^+$. This is because

$$e^{-\Delta \cdot Q - \omega \cdot J} \mathcal{Q}_{-t_1,-t_2}^{s_1,s_2,s_3} = e^{-\frac{s \cdot \Delta - t \cdot J}{2}} \mathcal{Q}_{-t_1,-t_2}^{s_1,s_2,s_3} e^{-\Delta \cdot Q - \omega \cdot J} = -\mathcal{Q}_{-t_1,-t_2}^{s_1,s_2,s_3} e^{-\Delta \cdot Q - \omega \cdot J} \ ,$$

$$(3.2.3)$$

so that translating $\mathcal{Q}_{-t_1,-t_2}^{s_1,s_2,s_3}$ along the trace will cause extra -1 sign, creating a zero mode of this supercharge. So restricting Z to this hypersurface of Δ_I, ω_i, it becomes an index which counts $\frac{1}{16}$-BPS states annihilated by $\mathcal{Q} \equiv \mathcal{Q}_{-t_1,-t_2}^{s_1,s_2,s_3}$ and $\mathcal{S} \equiv \mathcal{S}_{t_1,t_2}^{-s_1,-s_2,-s_3}$. From the algebra

$$\{\mathcal{Q}, \mathcal{S}\} = E - \sum_{I=1}^{3} s_I Q_I - \sum_{i=1}^{2} t_i J_i \ , \qquad (3.2.4)$$

one finds $E = s_I Q_I + t_i J_i$. Therefore, having in mind that we shall eventually live on one of the hyperspaces (3.2.2), we study Z in the 'formal high temperature limit' $\beta \to 0^+$.

We shall analyze $\log Z$ in an asymptotic Cardy-like limit $|\omega_i| \ll 1$. In our limit, Δ_I is kept complex, $\mathcal{O}(1)$, and generic. Our computation is based on the free QFT analysis, which is reliable because Z will be independent of the coupling constant at the hyperspace (3.2.2).

The partition function (3.2.1) of weakly-coupled $\mathcal{N} = 4$ Yang-Mills theory is given by [57]

$$\begin{aligned} Z \ = \ & \frac{1}{N!} \oint \prod_{a=1}^{N} \frac{d\alpha_a}{2\pi} \cdot \prod_{a<b} \left(2\sin\frac{\alpha_{ab}}{2} \right)^2 \exp\Big[\sum_{a,b=1}^{N} \sum_{n=1}^{\infty} \frac{1}{n} \Big(f_B^{\text{v}}(n\beta, n\omega_i) + (-1)^{n-1} f_F^{\text{v}}(n\beta, n\omega_i) \\ & + \chi_{\mathbf{3}}(n\Delta_I)(f_B^{\text{c}}(n\beta, n\omega_i) + (-1)^{n-1} f_F^{\text{c}}(n\beta, n\omega_i)) \\ & + \chi_{\bar{\mathbf{3}}}(n\Delta_I)(f_B^{\text{a}}(n\beta, n\omega_i) + (-1)^{n-1} f_F^{\text{a}}(n\beta, n\omega_i)) \Big) e^{in\alpha_{ab}} \Big] \end{aligned}$$

$$(3.2.5)$$

where $\alpha_{ab} \equiv \alpha_a - \alpha_b$, $\chi_{\mathbf{3}} = \sum_{I=1}^3 e^{\Delta_I}$, $\chi_{\bar{\mathbf{3}}} = \sum_{I=1}^3 e^{-\Delta_I}$, and

$$f_B^{\mathrm{v}} = \frac{e^{-\beta}(1-e^{-2\beta})(e^{\omega_1}+e^{\omega_2}+e^{-\omega_1}+e^{-\omega_2})-1+e^{-4\beta}}{(1-e^{-\beta+\omega_1})(1-e^{-\beta+\omega_2})(1-e^{-\beta-\omega_1})(1-e^{-\beta-\omega_2})}+1 \qquad (3.2.6)$$

$$f_F^{\mathrm{v}} = \frac{e^{-\frac{3}{2}\beta}(e^{\Delta}-e^{-\Delta}e^{-\beta})(e^{\omega_+}+e^{-\omega_+})+e^{-\frac{3}{2}\beta}(e^{-\Delta}-e^{\Delta}e^{-\beta})(e^{\omega_-}+e^{-\omega_-})}{(1-e^{-\beta+\omega_1})(1-e^{-\beta+\omega_2})(1-e^{-\beta-\omega_1})(1-e^{-\beta-\omega_2})}$$

$$f_B^{\mathrm{c}} = f_B^{\mathrm{a}} = \frac{e^{-\beta}(1-e^{-2\beta})}{(1-e^{-\beta+\omega_1})(1-e^{-\beta+\omega_2})(1-e^{-\beta-\omega_1})(1-e^{-\beta-\omega_2})}$$

$$f_F^{\mathrm{c}} = \frac{e^{-\frac{3}{2}\beta-\Delta}\left((e^{\omega_+}+e^{-\omega_+})-e^{-\beta}((e^{\omega_-}+e^{-\omega_-}))\right)}{(1-e^{-\beta+\omega_1})(1-e^{-\beta+\omega_2})(1-e^{-\beta-\omega_1})(1-e^{-\beta-\omega_2})}$$

$$f_F^{\mathrm{a}} = \frac{e^{-\frac{3}{2}\beta+\Delta}\left((e^{\omega_-}+e^{-\omega_-})-e^{-\beta}((e^{\omega_+}+e^{-\omega_+}))\right)}{(1-e^{-\beta+\omega_1})(1-e^{-\beta+\omega_2})(1-e^{-\beta-\omega_1})(1-e^{-\beta-\omega_2})}\ ,$$

with $\Delta \equiv \frac{\Delta_1+\Delta_2+\Delta_3}{2}$, $\omega_\pm \equiv \frac{\omega_1\pm\omega_2}{2}$. The superscripts v, c, a refers to $\mathcal{N}=1$ vector, chiral, anti-chiral multiplets, respectively, with the chiral supercharges $\mathcal{Q}_\alpha \equiv \mathcal{Q}_\alpha^{+,+,+}$ (at $(t_1,t_2)=(+,+),(-,-)$).

With the understanding that one of the BPS index conditions (3.2.2) will be taken, we study the $\beta \to 0^+$ limit of this partition function. One might worry that, before reaching $\beta \to 0$, the factors $1-e^{-\beta+\omega_{1,2}}$ in the denominators will hit zeros or make the sum divergent if $\mathrm{Re}(\omega_{1,2})>0$ (for BPS states with $t_1 = t_2 = +1$). These are divergences caused by two non-BPS derivatives, losing fugacity factors smaller than 1. In general partition function, going beyond this point will probably have no meaning, analogous to going beyond infinite temperature. However, having in mind imposing (3.2.2) at $t_1 = t_2 = 1$, these poles are canceled between bosons/fermions, so that one can reduce β below $\omega_{1,2}$. Anyway, later in this subsection, we shall present a complementary derivation manifestly within the index. (However, we think the analysis presented now has a conceptual advantage.) In this limit, one finds $f_B^{\mathrm{c;a}} \to 0$ due to the vanishing of the equation of motion factor $1-e^{-2\beta} \to 0$ on the numerators. Also, one finds

$f_B^{\mathrm{v}} \to 1$ for the same reason. The fermionic letter partition functions reduce to

$$f_F^{\mathrm{v}} \;\to\; \frac{(e^\Delta - e^{-\Delta})(e^{\omega_+} + e^{-\omega_+} - e^{\omega_-} - e^{-\omega_-})}{(1 - e^{\omega_1})(1 - e^{\omega_2})(1 - e^{-\omega_1})(1 - e^{-\omega_2})} = \frac{e^\Delta - e^{-\Delta}}{2\sinh\frac{\omega_1}{2} \cdot 2\sinh\frac{\omega_2}{2}}$$

$$f_F^{\mathrm{c,a}} \;\to\; \pm\frac{e^{\mp\Delta}}{2\sinh\frac{\omega_1}{2} \cdot 2\sinh\frac{\omega_2}{2}} \;. \tag{3.2.7}$$

Z then becomes

$$Z \to \frac{1}{N!} \oint \prod_{a=1}^{N} \frac{d\alpha_a}{2\pi} \cdot \prod_{a<b} \left(2\sin\frac{\alpha_{ab}}{2}\right)^2 \exp\left[\sum_{a,b=1}^{N} \sum_{n=1}^{\infty} \frac{1}{n} \left(1 + \sum_{s_1,s_2,s_3=\pm1} \frac{s_1 s_2 s_3 (-1)^{n-1} e^{\frac{n s_I \Delta_I}{2}}}{2\sinh\frac{n\omega_1}{2} \cdot 2\sinh\frac{n\omega_2}{2}}\right) e^{in\alpha_{ab}}\right] \;. \tag{3.2.8}$$

Note that the sum over n in the exponent is convergent with nonzero real parts of $\omega_{1,2}$. For instance, let us have in mind imposing $\sum_I \Delta_I = \sum_i \omega_i + 2\pi i$ for an index, with all chemical potentials having positive real part. For the terms with given s_1, s_2, s_3, the sum over n is separately convergent if $(s_1, s_2, s_3) \neq (+, +, +)$. This is because, for large n, one finds

$$\sim \sum_n \frac{(-1)^{n-1}}{n} e^{-\frac{n}{2}(\omega_1 + \omega_2)} e^{in\alpha_{ab}} e^{\frac{ns\cdot\Delta}{2}} = -\sum_n \frac{1}{n} e^{-\frac{n}{2}\sum_I (1 - s_I)\Delta_I} e^{in\alpha_{ab}} \;. \tag{3.2.9}$$

If some s_I is -1, this sum is convergent at large n, due to an exponential damping. On the other hand, the remaining terms in the exponent are the first term '1' and the term with $(s_1, s_2, s_3) = (+, +, +)$. The sum over each term over n may be divergent, for instance at $\alpha_{ab} = 0$. For $a \neq b$, divergence at $\alpha_{ab} = 0$ is fine because there is a suppression factor given by the Haar measure $\left(2\sinh\frac{\alpha_{ab}}{2}\right)^2$. For the Cartans, $a = b$, one has to study the possible convergence of the sum of these two terms without resorting to the phase factor $e^{i\alpha_{ab}}$ or the Haar measure. The sum of these two terms at large n behaves as

$$\sum_n \frac{1}{n}\left(1 + \frac{(-1)^{n-1} e^{\frac{\Delta_1 + \Delta_2 + \Delta_3}{2}}}{2\sinh\frac{n\omega_1}{2} \cdot 2\sinh\frac{n\omega_2}{2}}\right) e^{i\alpha_{ab}} \;=\; \sum_n \frac{1}{n}\left(1 + \frac{(-1)^{n-1} e^{\frac{\omega_1 + \omega_2 + 2\pi i}{2}}}{2\sinh\frac{n\omega_1}{2} \cdot 2\sinh\frac{n\omega_2}{2}}\right) e^{i\alpha_{ab}}$$

$$\sim \sum_n \frac{1}{n}\left[1 - \left(1 - \mathcal{O}(e^{-n\omega})\right)\right] e^{i\alpha_{ab}} \tag{3.2.10}$$

So even at $\alpha_{ab} = 0$, or $a = b$, the sum over n converges.

Having realized that the sum converges at $\sum_I \Delta_I = \omega_1 + \omega_2 + 2\pi i$, we also note here that it will be useful later to consider this sum slightly away from this surface. Namely, we shall consider the approximation of the index in the 'Cardy limit' $|\omega_i| \ll 1$. Imposing the relation $\sum_I \Delta_I = \omega_1 + \omega_2 + 2\pi i$, Δ_I's will share the $\mathcal{O}(1)$ imaginary part $2\pi i$, and furthermore will have small real parts to match $\mathrm{Re}(\omega_1 + \omega_2)$. However, for convenient intermediate manipulations, we shall take Δ_I's slightly away from this surface by temporarily demanding them to be of order 1 and purely imaginary. This parameter deformation clearly does not affect the convergence analysis of (3.2.9) for $(s_I) \neq (+,+,+)$. So as for this part, the function is well defined even after slight deformations. However, for (3.2.10), the convergence issue becomes tricky after the deformation. Just working with the left hand side of (3.2.10) with $\Delta_1 + \Delta_2 + \Delta_3$ being imaginary, the second term containing Δ_I, ω_i will be convergent by itself, for any a, b, while the first term '1' will remain divergent at $a = b$. Therefore, in the analysis below, we shall separate the Cartan parts at $a = b$ and the off-diagonal parts at $a \neq b$. The former has an exponent proportional to N, and it can be taken out of the α_a integral. The latter part has $N^2 - N$ terms, and only for these terms we shall make a deformation to purely imaginary Δ_I's. Ignoring the former contribution to the free energy $\sim \mathcal{O}(N^1)$ will be justified if one obtains a free energy and entropy of order N^2 from the latter part only. So with this understanding, we shall often ignore the exponents at $a = b$ in the discussions below. Note also that, for the off-diagonal parts, the term '1' in the exponent completely cancels the Haar measure part, so we can ignore this term together with the Haar measure.[1]

---

[1] Probably, using asymptotic properties of special functions in the integrand carefully, one can do the approximation below without using our small deformations of Δ_I. We just regard it as a short-cut derivation, similar to familiar '$i\epsilon$' prescriptions which often makes many calculus

Now we consider the Cardy limit $|\omega_i| \ll 1$, keeping Δ_I order 1 and purely imaginary. The sum over n can be divided into two parts: the 'dominant part' till $n \ll |\omega_i|$, and the 'suppressed part' from $n \gtrsim |\omega_i|$. As for the 'dominant' part, we can approximate $2 \sinh \frac{n\omega_i}{2} \approx n\omega_i$. The terms in the exponent of (3.2.8) from these n's is given by

$$\frac{s_1 s_2 s_3}{\omega_1 \omega_2} \sum_{n < n_0} \frac{(-1)^{n-1}}{n^3} e^{n\left(\frac{s \cdot \Delta}{2} + i\alpha_{ab}\right)} \tag{3.2.11}$$

where $n_0 \ll |\omega|^{-1}$ is a 'cut-off' which defines the 'dominant part.' (Note again that we considser the terms at $a \neq b$ only, and we ignored the term 1 which cancels the Haar measure.) The summation over n is now independent of the cut-off value n_0, as the summand is independent of ω_i and converges when $e^{\frac{s \cdot \Delta}{2} + i\alpha_{ab}}$ is a pure phase. So one obtains the dominant part given by

$$\frac{s_1 s_2 s_3}{\omega_1 \omega_2} \sum_{n < n_0} \frac{(-1)^{n-1}}{n^3} e^{n\left(\frac{s \cdot \Delta}{2} + i\alpha_{ab}\right)} \overset{n_0 \to \infty}{\longrightarrow} -\frac{s_1 s_2 s_3}{\omega_1 \omega_2} \text{Li}_3\left(-e^{\frac{s \cdot \Delta}{2} + i\alpha_{ab}}\right) . \tag{3.2.12}$$

Before proceeding, we note that if one wishes, one can take the cut-off n_0 to be as big as $|\omega|^{-1}$. This is because at $n \sim |\omega|^{-1}$, both summands $\frac{e^{n\left(\frac{s \cdot \Delta}{2} + i\alpha_{ab}\right)}}{n^3 \omega_1 \omega_2}$ and $\frac{1}{n} \frac{e^{n\left(\frac{s \cdot \Delta}{2} + i\alpha_{ab}\right)}}{2\sinh\frac{n\omega_1}{2} \cdot 2\sinh\frac{n\omega_2}{2}}$ are very small, much smaller than the final asserted result (3.2.12) which is $\frac{\mathcal{O}(1)}{\omega_1 \omega_2}$. So we proceed with assuming $n_0 \sim |\omega|^{-1}$ below. Now we discuss the 'suppressed' part. It is easy to see that it is indeed suppressed at $|\omega_i| \ll 1$. This is because

$$\left| \sum_{n \gtrsim |\omega|^{-1}} \frac{s_1 s_2 s_3}{n} \frac{(-1)^{n-1} e^{n\left(\frac{s \cdot \Delta}{2} + i\alpha_{ab}\right)}}{2\sinh\frac{n\omega_1}{2} \cdot 2\sinh\frac{n\omega_2}{2}} \right| \lesssim \sum_{n \gtrsim |\omega|^{-1}} \frac{1}{n \cdot 2\sinh\frac{n\omega_1}{2} \cdot 2\sinh\frac{n\omega_2}{2}} \lesssim |\omega| \sum_{n \gtrsim |\omega|^{-1}} \left(2\sinh\frac{n\omega}{2}\right)^{-2} \tag{3.2.13}$$

which is indeed much smaller than $\frac{1}{\omega^2}$. With these approximations, one then

_____

more straightforward.

obtains

$$Z \sim \frac{1}{N!} \oint \prod_{a=1}^{N} \frac{d\alpha_a}{2\pi} \exp\left[-\frac{1}{\omega_1\omega_2} \sum_{a \neq b} \sum_{s_1,s_2,s_3=\pm 1} s_1 s_2 s_3 \text{Li}_3\left(-e^{\frac{s_I \Delta_I}{2}} e^{i\alpha_{ab}} \right) \right]$$
(3.2.14)

where we used the series definition $\text{Li}_3(x) = \sum_{n=1}^{\infty} \frac{x^n}{n^3}$ when $|x| \leq 1$. The summations over $a \neq b$, (s_1, s_2, s_3) can be arranged so that

$$Z \sim \frac{1}{N!} \oint \prod_{a=1}^{N} \frac{d\alpha_a}{2\pi} \cdot \exp\left[-\frac{1}{\omega_1\omega_2} \sum_{a \neq b} \sum_{s_1 s_2 s_3=+1} \left(\text{Li}_3\left(-e^{\frac{s \cdot \Delta}{2} + i\alpha_{ab}} \right) - \text{Li}_3\left(-e^{-\frac{s \cdot \Delta}{2} - i\alpha_{ab}} \right) \right) \right] .$$
(3.2.15)

Here, we note an identity

$$\text{Li}_3(-e^x) - \text{Li}_3(-e^{-x}) = -\frac{x^3}{6} - \frac{\pi^2 x}{6} , \qquad (3.2.16)$$

valid for $-\pi < \text{Im}(x) < \pi$, taking $-e^x = e^{x+\pi i}$, $-e^{-x} = e^{-(x+\pi i)}$, respectively. When $(2p-1)\pi < \text{Im}(x) < (2p+1)\pi$ for $p \in \mathbb{Z}$, similar identity holds with $x \to x - 2\pi i p$ on the right hand side. This identity can be continued to include either positive or negative real parts of x.

Now we treat the integrals over α_a's by a saddle point approximation at $|\omega_1\omega_2| \ll 1$. Considering a pair of terms $\text{Li}_3(-e^{\frac{s_I \Delta_I}{2} + i\alpha_{ab}}) + \text{Li}_3(-e^{\frac{s_I \Delta_I}{2} - i\alpha_{ab}})$ at given s_I, one finds that α_a derivative of these are all zero at $\alpha_1 = \alpha_2 = \cdots = \alpha_N$. In fact, one can analytically prove the dominance of this $U(N)$ saddle point in our generalized Cardy limit. Moreover, it will reproduce the physics of known large black holes. As a very basic check, one can confirm at $N = 2$ that $\alpha_1 = \alpha_2$ is the global maximum of $\log Z$, making its real part maximal and imaginary part stationary, along the line of [114]. Since our free energy will depend on various complex parameters Δ_I, ω_i, it will be convenient to test it self-consistently at the extremal values of Δ_I, ω_i found in section 2.3, at $Q_1 = Q_2 = Q_3$, $J_1 = J_2$. The dominance of such a saddle point was assumed in

the Cardy limit of [73]. But it may fail to be dominant in certain models, e.g. for other gauge groups than $U(N)$, with fields in certain representations [114]. More conceptually, [114] discussed the relation between other possible saddle points and the behaviors of the S^3 partition function of 4d QFT reduced on small S^1. Depending on how bad the IR divergence of this partition function is [73,114], one may either expect more nontrivial saddle points to be dominant, or otherwise zero modes like α_a to cause subleading $N^1 \log \omega$ corrections. As we shall discuss further in section 1 of chapter 7, our reduced QFT on S^3 is maximal SYM, belonging to the latter class [73,114]. The expected log correction at N^1 order should come from the Cartan terms that we have ignored. So mostly in this chapter, we shall proceed with the fact that the above 'maximally deconfining' saddle point is dominant. (In only section 3, we discuss a different saddle point in a non-Cardy scaling limit.)

Perhaps as a related issue, one may worry from the Haar measure factor $\sim \left(2 \sin \frac{\alpha_a - \alpha_b}{2}\right)^2$ that there is a net factor of 0 when all α_a are the same, making this saddle point suppressed. Indeed, in the usual large N saddle point analysis (see e.g. [57]), the Haar measure provides relative repulsions between pairs of α_a's, forbidding them to be on top of each other. However, in our Cardy saddle point, log of Haar measure is sub-dominant $\mathcal{O}(\omega^0)$. So $\alpha_1 = \cdots = \alpha_N$ should make sense only as the asymptotic Cardy saddle point at $\omega \ll 1$.

So assuming this saddle point, one finds

$$\log Z \sim -\frac{N^2}{\omega_1 \omega_2} \sum_{s_1 s_2 s_3 = +1} \left[\mathrm{Li}_3 \left(-e^{\frac{s_I \Delta_I}{2}} \right) - \mathrm{Li}_3 \left(-e^{-\frac{s_I \Delta_I}{2}} \right) \right] \qquad (3.2.17)$$

where we used $N^2 - N \sim N^2$. Now using the identity (3.2.16), one obtains

$$\log Z \sim \frac{N^2}{6 \omega_1 \omega_2} \sum_{s_1 s_2 s_3 = +1} \left[\left(\frac{s \cdot \Delta}{2} - 2\pi p_s \right)^3 + \pi^2 \left(\frac{s \cdot \Delta}{2} - 2\pi p_s \right) \right] \quad (3.2.18)$$

in the chamber defined by

$$(2p_s - 1) < \pi \sum_{I=1}^{3} \text{Im}\left(\frac{s_I \Delta_I}{2}\right) < (2p_s + 1)\pi \ , \ p_s \in \mathbb{Z} \ , \ s_1 s_2 s_3 = +1 \ . \ (3.2.19)$$

Let us consider the 'canonical chamber,' with all four $p_s = 0$. This chamber is an octahedron in the space of $\text{Im}(\Delta_I)$. In this chamber, summing over 4 values of s, one obtains

$$\log Z \sim \frac{N^2 \Delta_1 \Delta_2 \Delta_3}{2\omega_1 \omega_2} \ . \tag{3.2.20}$$

This is the final form of our free energy in the generalized Cardy-like limit. Now we can continue Δ_I's to have (small) real parts, to go back to one of the surfaces (3.2.2). This formula is reliable at strong coupling on any hypersurface (3.2.2). Note that in our notation, it appears that [73] restricted their interest to $\omega_1 = \omega_2 \equiv \omega \ll 1$, one of Δ_I's $2\pi i + \mathcal{O}(\omega)$, and the remaining two of Δ_I's at $\mathcal{O}(\omega)$. The partition function is trivial in this setting. However, as we shall explain in section 2.3, complex $\Delta_I \sim \mathcal{O}(1)$ are required for all $I = 1, 2, 3$ to see the black hole saddle points, with minimally obstructed boson/fermion cancelation by the phases of fugacities.

We discussed the asymptotic free energy in the octahedral 'canonical chamber,' defined by

$$-2\pi < \text{Im}(\Delta_1 + \Delta_2 + \Delta_3) < 2\pi \ , \ \ -2\pi < \text{Im}(\Delta_1 - \Delta_2 - \Delta_3) < 2\pi \tag{3.2.21}$$
$$-2\pi < \text{Im}(-\Delta_1 + \Delta_2 - \Delta_3) < 2\pi \ , \ \ -2\pi < \text{Im}(-\Delta_1 - \Delta_2 + \Delta_3) < 2\pi \ .$$

Here, note that we should seek for an expression on one of the surfaces (3.2.2). For instance, let us consider $\Delta_1 + \Delta_2 + \Delta_3 - \omega_1 - \omega_2 = 2\pi i$. Since $\omega_{1,2}$ are very small in our scaling limit, our hypersurface is very close to the right boundary of the first inequality, $\text{Im}(\Delta_1 + \Delta_2 + \Delta_3) = 2\pi$. Whether one is within the octahedral chamber or not will depend on the small imaginary parts of ω_i's. So

one may wonder if the expression (3.2.20) can be used or not. This issue does not matter, as (3.2.18) is continuous across $\Delta_1 + \Delta_2 + \Delta_3 = 2\pi i$. To see this, note that one uses

$$\mathrm{Li}_3(-e^x) - \mathrm{Li}_3(-e^{-x}) = -\frac{(x - 2\pi i)^3}{6} - \frac{\pi^2(x - 2\pi i)}{6} \; , \qquad (3.2.22)$$

outside the boundary, instead of (3.2.16), where $x = \frac{\Delta_1 + \Delta_2 + \Delta_3}{2}$. However, the differences between the right hand sides of (3.2.22) and (3.2.16) is $\pi i (x - \pi i)^2$, being continuous and differentiable at $x = \pi i$. We shall therefore use (3.2.20) at the surface (3.2.2).

Note that we used large N limit very trivially so far, just to ignore the Cartans. We basically relied on $|\omega_i| \ll 1$ to approximate the calculations. This is similar to the Cardy limit of 2d QFT's describing black holes or strings. There, central charge c is kept fixed while the chemical potential τ conjugate to the left Hamiltonian is taken small. However, the entropy in the Cardy limit is useful to study black holes with large c [11], sometimes beyond the Cardy regime. To derive the true large N free energy in the non-Cardy regime, one should consider the large N saddle point approximation of α_a integrals, at finite Δ_I, ω_i. As we explained above, we expect a more complicated saddle point. Also, we are not sure how the graviton phase will get converted to the black hole phase as we change chemical potentials. In section 3, in the Macdonald limit, we find that (3.2.20) may _not_ be true in general. However, still there might be other regime in which (3.2.20) is true, which we shall partly probe in the Macdonald limit. With this in mind, in section 2.3, we shall also explore the 'thermodynamics phenomenology' of (3.2.20) beyond Cardy limit, especially pointing out the existence of a Hawking-Page transition of this free energy.

So far, we took the limit $\beta \to 0$ first, having in mind imposing the index condition (3.2.2) later. We think this is completely fine, but some people might

think that this way of thinking is dangerous. Appreciating possible worries, we start from the index given by [69] and rederive (3.2.20) at (3.2.2). A direct consideration of the index will also give interesting lessons beyond the Cardy limit, in the Macdonald limit [113]. Let us insert the following shifted values to the chemical potentials in (3.2.1),

$$\Delta_I \to \Delta_I - \beta , \quad \omega_i \to \omega_i - \beta , \qquad (3.2.23)$$

after which the partition function is given by

$$Z(\beta, \Delta_I, \omega_i) = \mathrm{Tr} \left[e^{-\beta(E - \sum_I Q_I - \sum_i J_i)} e^{-\Delta_I Q_I - \omega_i J_i} \right] . \qquad (3.2.24)$$

Now imposing the condition $\Delta_1 + \Delta_2 + \Delta_3 - \omega_1 - \omega_2 = 2\pi i$, the measure in the trace commutes with the supercharge $\mathcal{Q}_{--}^{+++}$, $\mathcal{S}_{++}^{---}$, at any value of β. We take $\beta \to \infty$ to suppress the contributions from all non-BPS letters. Let us redefine one of the chemical potentials, say $\Delta_1 - 2\pi i$ as the new Δ_1, so that the index condition becomes

$$\Delta_1 + \Delta_2 + \Delta_3 = \omega_1 + \omega_2 . \qquad (3.2.25)$$

Then, the shift by $2\pi i$ generates extra $e^{-2\pi i Q_1} = (-1)^F$ in the trace formula (3.2.24), making it a manifest index. (This redefinition can be made with any one of the five chemical potentials.) After this redefinition, and taking $\beta \to \infty$ in (3.2.5), one obtains [69]

$$Z = \frac{1}{N!} \int \prod_{a=1}^{N} \frac{d\alpha_a}{2\pi} \prod_{a<b} \left(2\sin \frac{\alpha_{ab}}{2} \right)^2 PE \left[\left(1 - \frac{\prod_{I=1}^{3}(1 - t^2 v_I)}{(1 - t^3 y)(1 - t^3/y)} \right) \sum_{a,b=1}^{N} e^{in\alpha_{ab}} \right] ,$$
$$(3.2.26)$$

where v_i's satisfying $v_1 v_2 v_3 = 1$ are the fugacities for $SU(3) \subset SO(6)$ part of R-symmetry. The parameters t, v_i, y are related to our parameters in (3.2.5) by $(e^{-\omega_1}, e^{-\omega_2}, e^{-\Delta_I}) = (t^3 y, t^3/y, t^2 v_I)$, manifestly satisfying (3.2.25). This is

rewritten as

$$Z = \frac{1}{N!} \int \prod_{a=1}^{N} \frac{d\alpha_a}{2\pi} \prod_{a<b} \left(2\sin\frac{\alpha_{ab}}{2}\right)^2 \exp\left[\sum_{n=1}^{\infty} \frac{1}{n}\left(1 - \frac{\prod_{I=1}^{3} 2\sinh\frac{n\Delta_I}{2}}{2\sinh\frac{n\omega_1}{2} \cdot 2\sinh\frac{n\omega_2}{2}}\right) \sum_{a,b=1}^{N} e^{in\alpha_{ab}}\right] .$$
$$(3.2.27)$$

We again take $|\omega_i| \ll 1$, keeping them complex with $\mathrm{Re}(\omega_{1,2}) > 0$. Had we been taking this limit with real positive Δ_i's, which is the canonical range for the chemical potentials, Δ_i's should also vanish at order $\mathcal{O}(\omega_{1,2})$ due to the relation (3.2.25). This will make the free energy to be small, $\sim \frac{\Delta^3}{\omega^2} \ll 1$, making the index uninteresting. However, we keep finite imaginary parts of Δ_i's while taking the limit $\omega_{1,2} \to 0$. Physically, we take advantage of the possibility of tuning the phases of bosonic/fermionic terms to maximally obstruct their cancelations. The asymptotic limit of (3.2.25) is $\Delta_1 + \Delta_2 + \Delta_3 \approx 0$, so we take all Δ_I's to be purely imaginary whose sum is zero, and continue back to complex numbers later. The details of the approximation is the same as we presented above. Following very similar procedures, again taking out the Cartan parts and ignoring them, one obtains

$$Z \sim \frac{1}{N!} \int \prod_{a=1}^{N} \frac{d\alpha_a}{2\pi} \exp\left[-\frac{1}{\omega_1\omega_2} \sum_{s_1s_2s_3=+1} \sum_{a\neq b} \left(\mathrm{Li}_3\left(e^{\frac{s\cdot\Delta}{2}+i\alpha_{ab}}\right) - \mathrm{Li}_3\left(e^{-\frac{s\cdot\Delta}{2}-i\alpha_{ab}}\right)\right)\right] .$$
$$(3.2.28)$$

Here, note that $\mathrm{Li}_3(e^x) - \mathrm{Li}_3(e^{-x}) = -\frac{(2\pi i)^3}{6}B_3(\frac{x}{2\pi i})$ for $\mathrm{Re}(x) \geq 0$ and $0 < \mathrm{Im}(x) < 2\pi$, with $B_3(x) = x^3 - \frac{3}{2}x^2 + \frac{1}{2}x$. After some computations using this formula similar to the above, one can obtain

$$\log Z \sim \frac{N^2}{2\omega_1\omega_2} \prod_{I=1}^{3}(\Delta_I + 2\pi i n_I) , \qquad (3.2.29)$$

where $2\pi p_I < -i\Delta_I < 2\pi(p_I+1) \quad (p_I \in \mathbb{Z})$, and $n_1 \equiv 1+p_2+p_3$, $n_2 \equiv 1+p_3+p_1$, $n_3 \equiv 1+p_1+p_2$, satisfying $\sum_{I=1}^{3} n_I = \pm 1$. (For detailed computations, refer to [75].) This agrees with the previous analysis, supposing that $\Delta_1 + \Delta_2 + \Delta_3$ there and here are related by a shift of $2\pi i \pmod{4\pi i}$.

Now, let us consider a Legendre transformation of the free energy (3.2.20) to the microcanonical ensemble, as the macroscopic saddle point approximation of the inverse Laplace transformation. One should extremize the following entropy function

$$S(\Delta_I, \omega_i; Q_I, J_i) = \frac{N^2}{2} \frac{\Delta_1 \Delta_2 \Delta_3}{\omega_1 \omega_2} + \sum_{I=1}^{3} Q_I \Delta_I + \sum_{i=1}^{2} J_i \omega_i \ . \qquad (3.2.30)$$

Since this free energy is reliable only at one of the surfaces (3.2.2), we make variation with 4 independent variables, which couples to four combinations of 5 charges. This is our ignorance due to restricting considerations to the index. We consider the surface

$$\Delta_1 + \Delta_2 + \Delta_3 - \omega_1 - \omega_2 = 2\pi i \ , \qquad (3.2.31)$$

for BPS states saturating $E \geq Q_1 + Q_2 + Q_3 + J_1 + J_2$. The above is nothing but the entropy function of the BPS black holes in $AdS_5 \times S^5$, which we considered in section 2.3. Thus, assuming the charge relation, the lower bound of entropy given by our index saturates the black hole entropy. Namely, we have microscopically accounted for the microstates of large BPS black holes in $AdS_5 \times S^5$.

Even though we managed to derive the free energy (3.2.30) only in our Cardy limit, it is correct one describing the known black holes. However, beyond the Cardy regime $|\omega_i| \ll 1$, it is not guaranteed that there are no more black hole saddle points, so that the true free energy of large N $\mathcal{N} = 4$ Yang-Mills may be more complicated. Indeed, in the next section, we find that the true free energy may be more complicated than (3.2.30), by studying another special limit. Now focussing on our Cardy limit, it demands that the four combinations of charges $Q_I + J_1$, $J_2 - J_1$ are much larger than N^2. This is all one can say intrinsically from the index. However, we can discuss the implication of the Cardy limit on

the known black hole solutions that we have just counted. Their charge relation in the Cardy limit becomes

$$(Q_1 + Q_2 + Q_3)(Q_1 Q_2 + Q_2 Q_3 + Q_3 Q_1) - Q_1 Q_2 Q_3 \approx \frac{N^2}{2} J_1 J_2 . \quad (3.2.32)$$

When all charges are equal, $\equiv Q$, and also when all angular momenta are equal $\equiv J$, it becomes $(J/N^2)^2 \approx 16(Q/N^2)^3$. So our Cardy limit on known solutions demands $J/N^2 \gg Q/N^2 \gg 1$.

As emphasized, (3.2.30) is the free energy of known black hole saddle points. Our microscopic analysis assures that this is the dominant one for large black holes in the Cardy limit. But for not-so-large or small black holes, the situation is unclear. In particular, numerical studies are made recently on hairy BPS black holes [111], predicting more general black holes as one approaches the zero temperature BPS limit. In particular, as far as we see from the reported charge regimes in [111], evidences for new black holes are found for small angular momenta, at around $\frac{J}{N^2} \lesssim 0.05$. If we take these results seriously, the true free energy may deviate from (3.2.20) for small black holes. Of course, there could be a possibility that the intrinsic prediction from the index has its own ambiguity, in that the physical charges Q, J cannot be separately be specified.

Before end this section, let us make a basic consideration on what the extremization of (3.2.30) does. Although the entropy function (3.2.30) has real coefficients only, it should have complex solutions for Δ_I, ω_i due to the constraint (3.2.31). During the extremization, we will be led to distribute $2\pi i$ on the right hand side suitably to the 5 chemical potentials. We assert that one should pay attention to nontrivial distribution of this phase to the fugacities. Allowing nontrivial imaginary parts of Δ_I, ω_i (mod $2\pi i$) satisfying (3.2.31), one can hope to reduce unnecessary boson/fermion cancelations in the index. Namely, we insert $(-1)^F$ in the index because we want pairs of bosonic/fermionic states related

by $\mathcal{Q}, \mathcal{S}$ to cancel. If the index does not acquire contributions from such states, it can be computed at any coupling constant. However, inserting -1 factor to all fermions, it may cause unnecessary cancelations between bosonic/fermionic states which are not superpartners of each other. So as long as it is allowed by (3.2.31), we attempt to insert extra phase factor $e^{-i\varphi}$ for each state, defined by $e^{-i\mathrm{Im}(\Delta_I Q_I + \omega_i J_i)} \equiv (-1)^F e^{-i\varphi}$, trying to maximally obstruct cancelations. Converting to microscopic ensemble at definite charges, the 'entropy' is counted with such phase factor inserted for each state:

$$e^{S(Q_I, J_i)} \sim \sum_B e^{-i\varphi_B} - \sum_F e^{-i\varphi_F} = \sum_B e^{-i\varphi_B} + \sum_F e^{-i(\varphi_F + \pi)} \ . \qquad (3.2.33)$$

Morally, the real parts of chemical potentials are extremized to tune the system to definite charges in the microscopic ensemble, while imaginary parts are tuned to make (3.2.33) maximally unobstructed. However, the two extremizations are intertwined, so that both real and imaginary parts participate in both processes. If one is lucky so that all phases $\varphi_B, \varphi_F + \pi$ at a saddle point are same (mod 2π) for all microstates, then $\mathrm{Re}(S)$ of the index would be the true BPS entropy. In the unlucky case that one cannot make all these phases collinear, $\mathrm{Re}(S)$ would be smaller than the entropy. In any case, $\mathrm{Re}(S)$ computed from our index sets a lower bound on the true entropy, and there is no a priori way of knowing when this bound saturates the true entropy. In particular, there seems to be no a priori reason to care about $\mathrm{Im}(S)$, as the saturation may happen or not irrespective of whether $\mathrm{Im}(S)$ assumes a specific value.

3.3   The $\frac{1}{8}$-BPS Macdonald sector

In this section, we investigate the Cardy-like and non-Cardy-like free energy of the index in the so-called Macdonald limit [113]. We first explain the Macdonald

index in the context of $\mathcal{N} = 4$ Yang-Mills theory. Consider the index

$$Z = \text{Tr}\left[(-1)^F e^{-\Delta_I Q_I - \omega_i J_i}\right] \tag{3.3.1}$$

at $\Delta_1 + \Delta_2 + \Delta_3 = \omega_1 + \omega_2$, which is obtained from (3.2.24) by shifting a chemical potential by $2\pi i$, and by sending $\beta \to \infty$. This is an index counting $\frac{1}{16}$-BPS states preserving $\mathcal{Q}_{--}^{+++}$ and $\mathcal{S}_{++}^{---}$. Eliminating $\omega_2 = \Delta_1 + \Delta_2 + \Delta_3 - \omega_1$, one obtains

$$Z = \text{Tr}\left[(-1)^F e^{-\Delta_1(Q_1+J_2)-\Delta_2(Q_2+J_2)-\Delta_3(Q_3+J_2)-\omega_1(J_1-J_2)}\right] \tag{3.3.2}$$

in terms of four independent variables Δ_I, ω_i with positive real parts. Now we take the limit $\Delta_3 \to \infty$, projecting to states satisfying $Q_3 + J_2 = 0$. One can show that this projection demands the BPS states to be annihilated by an extra pair of supercharges, $\mathcal{Q}_{-+}^{++-}, \mathcal{S}_{+-}^{--+}$. A quick way to see this is that the new pair demands the BPS energy relation $E = Q_1 + Q_2 - Q_3 + J_1 - J_2$, which is satisfied by imposing the original BPS bound $E = Q_1 + Q_2 + Q_3 + J_1 + J_2$ and the new projection condition $Q_3 + J_2 = 0$. This is a limit which takes $\Delta_3, \omega_2 \to \infty$, with $\frac{\Delta_3}{\omega_2} \to 1$. One also has to keep $\Delta_3 - \omega_2$ ($= \omega_1 - \Delta_1 - \Delta_2$) finite. This way, one obtains the Macdonald index for $\frac{1}{8}$-BPS states depending on $\Delta_1, \Delta_2, \omega_1$.

In the weakly interacting theory, $\frac{1}{16}$-BPS operators are made of: 3 anti-chiral scalars $\overline{\Phi}^{Q_I}$ with $(Q_I) = (1,0,0), (0,1,0), (0,0,1)$; three chiralinos $\Psi^{Q_I}_{+\frac{1}{2},+\frac{1}{2}}$ with $(Q_I) = (-\frac{1}{2},\frac{1}{2},\frac{1}{2}), (\frac{1}{2},-\frac{1}{2},\frac{1}{2}), (\frac{1}{2},\frac{1}{2},-\frac{1}{2})$; two gauginos $\Psi^{\frac{1}{2},\frac{1}{2},\frac{1}{2}}_{\pm\frac{1}{2},\mp\frac{1}{2}}$; one self-dual component of field strength $f_{+1,+1}$; two covariant derivatives $D_{1,0}, D_{0,1}$. In the Macdonald limit, $\frac{1}{8}$-BPS operators are made of: two complex scalars $\overline{\Phi}^{1,0,0}, \overline{\Phi}^{0,1,0}$; two fermions $\Psi^{+\frac{1}{2},+\frac{1}{2},\pm\frac{1}{2}}_{+\frac{1}{2},\mp\frac{1}{2}}$; one derivative $D_{1,0}$. Despite preserving enhanced SUSY, the full spectrum of this sector is not completely solved yet even at weak coupling, to the best of our knowledge. This is in contrast to other $\frac{1}{8}$-BPS sectors of $\mathcal{N} = 4$ Yang-Mills theory. There are two more inequivalent

$\frac{1}{8}$-BPS subsectors of the above canonical $\frac{1}{16}$-BPS sector, specified by either $J_1 + J_2 = 0$ or $Q_1 + Q_2 = 0$. The former is the well-known chiral ring sector, completely solved in, e.g. [69]. The solution in the second sector can be found, e.g. in [109]. It might be surprising that the last $\frac{1}{8}$-BPS sector given by the Macdonald limit is still unsolved. As we shall see below, perhaps the reason is that this sector is too rich to admit a simple exact solution.[2]

We shall study a new Cardy-like limit and a non-Cardy-like limit of the Macdonald index at $|\omega_1| \ll 1$. Although we also call the former a Cardy limit, it is different from the one in section 2 in that ω_2 is sent large. In a way, the previous one is a 4d Cardy limit, acquiring large contributions from two BPS derivatives. Here, it is more like a 2d Cardy limit.

In the Macdonald limit $\Delta_3, \omega_2 \to \infty$, $\Delta_3/\omega_2 \to 1$, the index (3.2.27) reduces to

$$Z = \frac{1}{N!} \int \prod_{a=1}^{N} \frac{d\alpha_a}{2\pi} \prod_{a<b} \left(2\sin\frac{\alpha_{ab}}{2}\right)^2 \exp\left[\sum_{n=1}^{\infty} \frac{1}{n}\left(1 - \frac{(1-e^{-n\Delta_1})(1-e^{-n\Delta_2})}{1-e^{-n\omega_1}}\right) \sum_{a,b=1}^{N} e^{in\alpha_{ab}}\right] .$$
$$(3.3.3)$$

As before, we ignore the exponents for the Cartans, $a = b$, which will give $\mathcal{O}(N^1)$ contribution to the free energy. Then, for $a \neq b$, the term '1' in the exponent will cancel with the Haar measure. Taking $\omega_1 \ll 1$ with the remaining non-Abelian terms, with $\Delta_{1,2}$ kept fixed, and again assuming the maximally deconfining saddle point $\alpha_1 \approx \cdots \approx \alpha_N$, one obtains

$$\log Z \sim -\frac{N^2}{\omega_1}\left[\text{Li}_2(1) - \text{Li}_2(e^{-\Delta_1}) - \text{Li}_2(e^{-\Delta_2}) + \text{Li}_2(e^{-\Delta_1-\Delta_2})\right] \quad (3.3.4)$$

with unconstrained $\Delta_1, \Delta_2, \omega_1$. This is the Macdonald-Cardy limit of the index.

---

[2]However, [115] solved the Schur index problem, which is an unrefined version of the Macdonald index. The Schur limit of the general $\frac{1}{16}$-BPS index (3.2.27) is defined as $\Delta_3 = \omega_2$. In the Macdonald index, to be studied shortly, one further unrefines as $\Delta_1 + \Delta_2 = \omega_1$ to get the Schur index.

On the other hand, had (3.2.20) or the result of [90] been exact for general $\omega_{1,2}$, one would have obtained a very different result from (3.3.4). Namely, taking the Macdonald limit of (3.2.20) assuming its validity at general $\omega_{1,2}$, $\Delta_3, \omega_2 \to +\infty$ with $\Delta_3/\omega_2 \to 1$, one would have obtained

$$\log Z \sim \frac{N^2 \Delta_1 \Delta_2}{2\omega_1} \tag{3.3.5}$$

without any constraint on $\Delta_1, \Delta_2, \omega_1$. But keeping $\omega_1 \ll 1$ and $\Delta_{1,2}$ finite, we derive (3.3.4) instead of (3.3.5) (assuming maximally deconfining saddle points). So the true phase structure of black holes may be richer than simply the known black holes, or [90], even in the $\frac{1}{8}$-BPS Macdonald sector.

However, before proceeding, we explain that there appears to be a scaling limit of the Macdonald index which yields (3.3.5). To see this, let us scale $\omega_1 \ll 1$, but also take $\Delta_1, \Delta_2 \ll 1$ keeping $\frac{\Delta_1 \Delta_2}{\omega_1}$ finite. In this case, we take large N and disregard the integrand factors for the Cartans, $a = b$, assuming that this $\mathcal{O}(N^1)$ term will not affect our scaling free energy at $\mathcal{O}(N^2)$. In fact, as we shall see later, the last assumption will fail, with an interesting implication: however, let us proceed for now to derive (3.3.5) first. With the summation in the exponent restricted to $a \neq b$, (3.3.3) can be written as

$$Z \sim \frac{1}{N!} \int \prod_{a=1}^{N} \frac{d\alpha_a}{2\pi} \exp\left[-\frac{\Delta_1 \Delta_2}{\omega_1} \sum_{n=1}^{\infty} \sum_{a \neq b} e^{in\alpha_{ab}} \right] . \tag{3.3.6}$$

Since

$$\sum_{n=1}^{\infty} \sum_{a \neq b} e^{in\alpha_{ab}} = \sum_{n \neq 0} \sum_{a < b} e^{in\alpha_{ab}} = \sum_{a < b} \left(2\pi \delta(\alpha_a - \alpha_b) - 1 \right) , \tag{3.3.7}$$

one obtains

$$Z \sim \frac{1}{N!} \int \prod_{a=1}^{N} \frac{d\alpha_a}{2\pi} \exp\left[-\sum_{a < b} V_{\text{eff}}(\alpha_a - \alpha_b) \right] , \quad V_{\text{eff}}(\theta) \equiv \frac{\Delta_1 \Delta_2}{\omega_1} \left[2\pi\delta(\theta) - 1 \right] , \tag{3.3.8}$$

where $\delta(\theta)$ is the delta function on a circle, with $\theta \sim \theta + 2\pi$. Therefore, by keeping $\text{Re}(\frac{\Delta_1 \Delta_2}{\omega_1}) > 0$, one finds an effective potential with very small repulsive core. Whether this is satisfied or not will be controversial at the end, for a reason to be explained shortly. In any case, let us assume this and proceed. In this case, if α_a's are not equal, the potential is at its flat minimum, with constant negative energy. Since the repulsive core is scaling to zero size in our scaling limit, one can take $V_{\text{eff}} = -\frac{\Delta_1 \Delta_2}{\omega_1}$ for most values of α_a. It makes real part of $\log Z$ maximal, and imaginary part stationary. Therefore, one approximates

$$\log Z \sim \frac{(N^2 - N)\Delta_1 \Delta_2}{2\omega_1} \approx \frac{N^2 \Delta_1 \Delta_2}{2\omega_1} \ . \tag{3.3.9}$$

In fact, as we will show below, the assumption that $\mathcal{O}(N^1)$ terms are ignorable will fail, by the free energy (3.3.5) failing to have nontrivial large N saddle point with $\log Z \sim N^2$. But we shall use this free energy as a probe of small black holes.

We shall now discuss the thermodynamic aspects of two free energies (3.3.4) and (3.3.5).

It is first illustrative to see what is the consequence of (3.3.5). As we emphasized in section 2.3, we can regard (3.2.20) as describing known black holes, even beyond the Cardy limit. Firstly, from the known black hole solutions, one can show that the horizon area vanishes as one takes limit $Q_3 + J_2 \to 0^+$. To see this, we start from the charge relation of known black holes. Setting $J_2 = -Q_3$, and rearranging, one obtains

$$0 = \left(Q_1 + Q_2 + \frac{N^2}{2} \right) \left(Q_1 Q_2 + Q_2 Q_3 + Q_3 Q_1 - \frac{N^2}{2}(J_1 + J_2) + Q_3^2 \right) \ , \tag{3.3.10}$$

where we suitably inserted back $Q_3 \to -J_2$ on the second factor. The first factor is positive since $Q_1 + Q_2 \geq 0$ in the BPS sector. On the second factor, $Q_3^2 \geq 0$ for the last term. The remaining terms in the second factor are simply square

of the black hole entropy $\left(\frac{S}{2\pi}\right)^2$. So the solution becomes meaningless if this is negative. So from the vanishing of (3.3.10) on the solutions without naked singularities, one finds

$$Q_3 \to 0 \ , \quad Q_1 Q_2 + Q_2 Q_3 + Q_3 Q_1 - \frac{N^2}{2}(J_1 + J_2) = \left(\frac{S}{2\pi}\right)^2 \to 0 \ . \quad (3.3.11)$$

We conclude that the known black solutions become 'small black holes' in the Macdonald limit. Here 'small' and 'large' is an entropic notion, different from those used in the other part of this chapter: the above configuration has small entropy at large charges. Collecting all the conditions, the charges carried by these small black holes satisfy

$$Q_1 Q_2 = \frac{N^2}{2} J_1 \ , \quad Q_3 = J_2 = 0 \ , \quad (3.3.12)$$

where the first relation is the vanishing condition of the horizon area when $Q_3 = J_2 = 0$.

Similar conclusion can be obtained from (3.3.5), in a rather curious manner. Note that

$$\frac{N^2 \Delta_1 \Delta_2}{2\omega_1} + (Q_1 + J_2)\Delta_1 + (Q_2 + J_2)\Delta_2 + (J_1 - J_2)\omega_1 \quad (3.3.13)$$

is homogeneous degree 1 in three independenet $\Delta_1, \Delta_2, \omega_1$. Therefore, the overall scaling mode of them plays the role of Lagrange multiplier, making the extremized entropy to vanish. Since the remaining two ratios of the chemical potentials determine three charges $Q_1 + J_2, Q_2 + J_2, J_1 - J_2$, the charges satisfy a relation. The relation is

$$(Q_1 + J_2)(Q_2 + J_2) = \frac{N^2}{2}(J_1 - J_2) \ . \quad (3.3.14)$$

We find it as closest as one can get to (3.3.12) from the index, without extra input on the charges that the index cannot see (such as '$Q_3 = J_2 = 0$'). However,

we emphasize that both approaches predict small black holes $S \to 0$ in the $\frac{1}{8}$-BPS Macdonald limit. And coming back to the derivation of (3.3.5) ignoring $\mathcal{O}(N^1)$ terms, we simply arrive at the conclusion that we may have to include them to obtain the leading entropy. In any case, both known black hole solutions and the QFT analysis in the non-Cardy scaling limit predicts small black holes. As an additional comment, we cannot determine in this framework whether $\mathrm{Re}\left(\frac{\Delta_1 \Delta_2}{\omega_1}\right)$ is positive or not, because an overall scaling mode is a Lagrange multiplier which cannot be determined. The sign of this quantity was important above, when we want to regard (3.3.13) as derived from the Macdonald index in a scaling limit. Perhaps it is related to the degenerate nature of this saddle point, which one may resolve clearly by going slightly beyond the Macdonald limit and doing a more careful calculation. We leave a more detailed study to the future.

Now we study the free energy (3.3.4). We study the associated entropy function:

$$
\begin{aligned}
S &= \log Z + Q_1 \Delta_1 + Q_2 \Delta_2 + Q_3 \Delta_3 + J_1 \omega_1 + J_2 \omega_2 \\
&= -\frac{N^2}{\omega_1} \left[\mathrm{Li}_2\left(1\right) - \mathrm{Li}_2\left(e^{-\Delta_1}\right) - \mathrm{Li}_2\left(e^{-\Delta_2}\right) + \mathrm{Li}_2\left(e^{-\Delta_1 - \Delta_2}\right) \right] \qquad (3.3.15) \\
&\qquad + (Q_1 + J_2)\Delta_1 + (Q_2 + J_2)\Delta_2 + (J_1 - J_2)\omega_1 \ .
\end{aligned}
$$

Extremizing, one obtains

$$
\begin{aligned}
Q_1 + J_2 &= \frac{N^2}{\omega_1} \left[-\log\left(1 - e^{-\Delta_1}\right) + \log\left(1 - e^{-\Delta_1 - \Delta_2}\right) \right] , \\
Q_2 + J_2 &= \frac{N^2}{\omega_1} \left[-\log\left(1 - e^{-\Delta_2}\right) + \log\left(1 - e^{-\Delta_1 - \Delta_2}\right) \right] , \\
J_1 - J_2 &= -\frac{N^2}{\omega_1^2} \left[\mathrm{Li}_2\left(1\right) - \mathrm{Li}_2\left(e^{-\Delta_1}\right) - \mathrm{Li}_2\left(e^{-\Delta_2}\right) + \mathrm{Li}_2\left(e^{-\Delta_1 - \Delta_2}\right) \right] .
\end{aligned}
$$

$$(3.3.16)$$

From now on, we shall use some identities of Li_2 to make a semi-analytic study. However, all solutions below are cross-checked numerically against (3.3.16).

Using the following identity (W. Schaeffer, 1846)

$$\text{Li}_2\left(xy\right)-\text{Li}_2\left(x\right)-\text{Li}_2\left(y\right)+\text{Li}_2\left(1\right) = \text{Li}_2\left(\frac{1-x}{1-xy}\right)-\text{Li}_2\left(y\frac{1-x}{1-xy}\right)+\log(x)\log\left(\frac{1-x}{1-xy}\right),$$
(3.3.17)

the extremized entropy becomes

$$S = \frac{N^2}{\omega_1}\left[-\text{Li}_2\left(\frac{1-e^{-\Delta_1}}{1-e^{-\Delta_1-\Delta_2}}\right) - \text{Li}_2\left(\frac{1-e^{-\Delta_2}}{1-e^{-\Delta_1-\Delta_2}}\right)\right.$$
$$\left. + \text{Li}_2\left(e^{-\Delta_2}\frac{1-e^{-\Delta_1}}{1-e^{-\Delta_1-\Delta_2}}\right) + \text{Li}_2\left(e^{-\Delta_1}\frac{1-e^{-\Delta_2}}{1-e^{-\Delta_1-\Delta_2}}\right)\right].$$
(3.3.18)

From this formula, one finds $S < 0$ if $\Delta_1, \Delta_2, \omega_1$ are strictly real and positive. This is because $\text{Li}_2(x)$ is an increasing function of $x > 0$, so that first plus third terms are negative, and second plus fourth terms are also negative. Hence, in order to get black holes with $\text{Re}(S) > 0$ at positive chemical potential, we should turn on the imaginary part of chemical potentials. Physically, this again implies that one should turn on phases of fugacities to obstruct boson/femrion cancelation in the index to see black holes.

Now, for simplicity, we consider the case with equal charge: $Q_1 = Q_2$. Below, we will frequently use (3.3.17) at $x = y$ and the Euler's reflection formula:

$$\text{Li}_2\left(x^2\right) - 2\text{Li}_2\left(x\right) + \text{Li}_2\left(1\right) = \text{Li}_2\left(\frac{1}{1+x}\right) - \text{Li}_2\left(\frac{x}{1+x}\right) - \log(x)\log\left(1+x\right),$$

$$\text{Li}_2(x) + \text{Li}_2(1-x) = \text{Li}_2(1) - \log(x)\log(1-x).$$
(3.3.19)

Then, setting $\Delta \equiv \Delta_1 = \Delta_2$, one obtains

$$q \equiv \frac{Q_1 + J_2}{N^2} = \frac{Q_2 + J_2}{N^2} = \frac{1}{\omega_1}\log\left(1 + e^{-\Delta}\right),$$
(3.3.20)

$$j \equiv \frac{J_1 - J_2}{N^2} = -\frac{1}{\omega_1^2}\left[\text{Li}_2\left(1\right) - 2\text{Li}_2\left(e^{-\Delta}\right) + \text{Li}_2\left(e^{-2\Delta}\right)\right]$$
$$= -\frac{1}{\omega_1^2}\left[\text{Li}_2\left(1\right) - 2\text{Li}_2\left(\frac{1}{1+e^\Delta}\right) - \left(\log\left(1+e^{-\Delta}\right)\right)^2\right]$$

(a) $\mathrm{Re}[f(r)]$: Green line denotes real parts of both yellow and green lines in Fig. 3(b).

(b) $(\mathrm{Re}[f(r)], \mathrm{Im}[f(r)])$: Arrows denote an increase of r. Yellow and green lines are complex conjugate to each other.
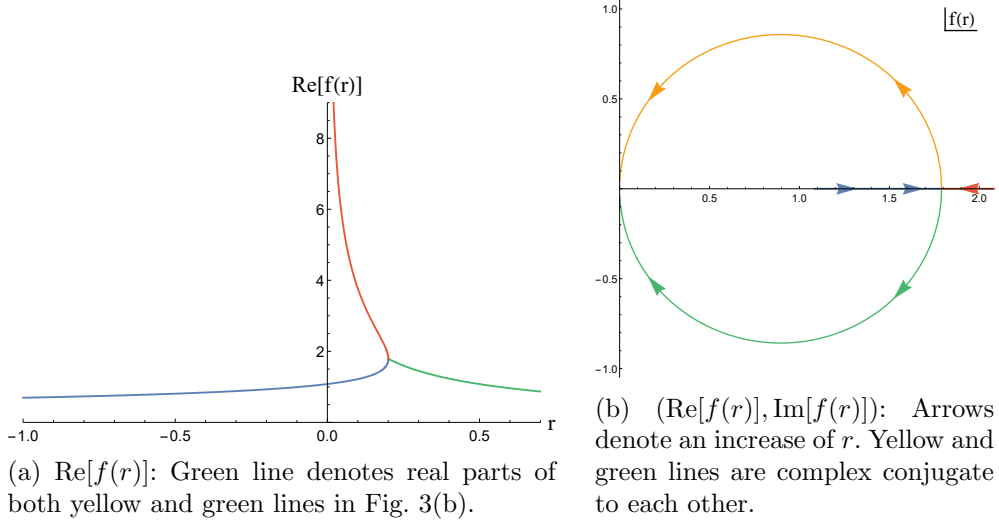
Figure 3.1: Various solutions $f(r)$ of (3.3.21)

$$= q^2 - \frac{1}{\omega_1^2} \left[\mathrm{Li}_2\,(1) - 2\mathrm{Li}_2\left(1 - e^{-q\omega_1}\right) \right] ,$$

$$s \equiv \frac{S}{N^2} = 2(q\Delta + j\omega_1) = \frac{2}{\omega_1} \left[\mathrm{Li}_2\left(\frac{1}{1+e^\Delta}\right) - \mathrm{Li}_2\left(\frac{1}{1+e^{-\Delta}}\right) \right]$$

$$= \frac{2}{\omega_1} \left[\mathrm{Li}_2\left(1 - e^{-q\omega_1}\right) - \mathrm{Li}_2\left(e^{-q\omega_1}\right) \right] = 2\omega_1(j - q^2) - 2q\log(1 - e^{-q\omega_1})$$

$$\equiv 2q \left[rf\,(r) - \log\left(1 - e^{-f(r)}\right) \right] ,$$

where $r \equiv \frac{j}{q^2} - 1$, $f\left(\frac{j}{q^2} - 1\right) \equiv q\omega_1$, and $f(r)$ is defined implicitly by the following equation:

$$f(r)^2 r = 2\,\mathrm{Li}_2(1 - e^{-f(r)}) - \mathrm{Li}_2(1). \qquad (3.3.21)$$

Note that $\mathrm{Li}_2(1) = \frac{\pi^2}{6}$. We expect macroscopic physical solutions only when $q > 0$ and $j > 0$. Indeed, with some efforts, one can check this fact explicitly from the above formulae.

Due to the complexity of these equations, we numerically/graphically solve this problem. For $r = \frac{j}{q^2} - 1 > 0$, one finds that $f(r)$ is a double-valued,

(a) ω_1 as a function of q at $j = 300$ (b) Δ as a function of q at $j = 300$
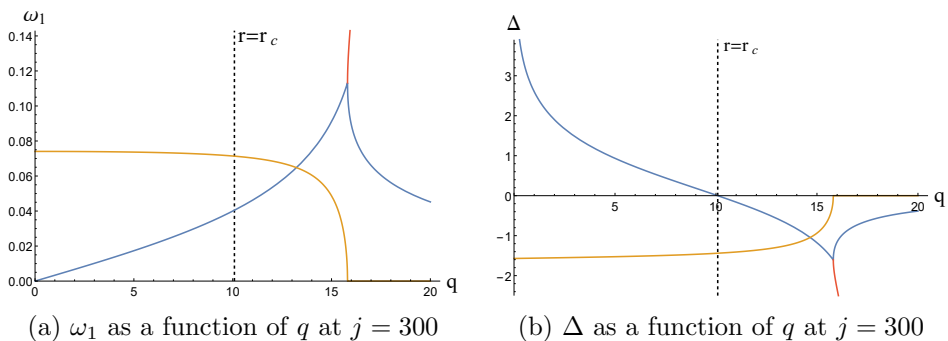
Figure 3.2: Blue/yellow line denotes the real/imaginary part of (a) ω_1, (b) Δ. Red line denotes ω_1, Δ corresponding to $f(r)$ described as the red line in Fig. 3.1 (a), which we dismiss.

while for $-1 < r < 0$, it is single-valued. See Fig. 3.1. We find that only when $r > r_0 \equiv 0.2003559478...$, $\mathrm{Im}(f(r)) \neq 0$. If r is smaller than this critical value r_0, $f(r)$ is strictly real. Then, one finds that ω_1, Δ are also real, from the definition of f and the first equation of (3.3.20), since $f = q\omega_1 > 0$. Namely, only when $j > (1 + r_0)q^2$, $\mathrm{Im}(\omega_1), \mathrm{Im}(\Delta) \neq 0$, and we may expect a solution with macroscopic entropy and positive chemical potentials. One can see that we have two distinct solutions $f(r) = x(r) \pm iy(r)$ when $r > r_0$. In fact, one can analytically show that if $f(r) = x(r) + iy(r)$ is one solution of its defining equation (3.3.21) at certain r, then $(f(r))^* = x(r) - iy(r)$ becomes another solution. Correspondingly, for given j, q, one will find the following form of two distinct solutions for the chemical potentials and entropy: $\omega_1 = \omega_1^R \pm i\omega_1^I$, $\Delta = \Delta^R \pm i\Delta^I$, and $S = S^R \pm iS^I$. So the directly observable physical quantities, given by the real parts $\omega_1^R, \Delta^R, S^R$, are uniquely determined in terms of j, q. As commented below (3.3.18), the region $r < r_0$ does not yield sensible saddle points.

For $r > r_0$, we study whether $\mathrm{Re}(\Delta), \mathrm{Re}(\omega_1)$ are actually positive. In Fig. 3.2, ω_1, Δ are plotted with respect to q, at fixed j. Note that among two solutions

(a) $s(q)$ at $j = 300$ (b) $s(j)$ at $q = 10$
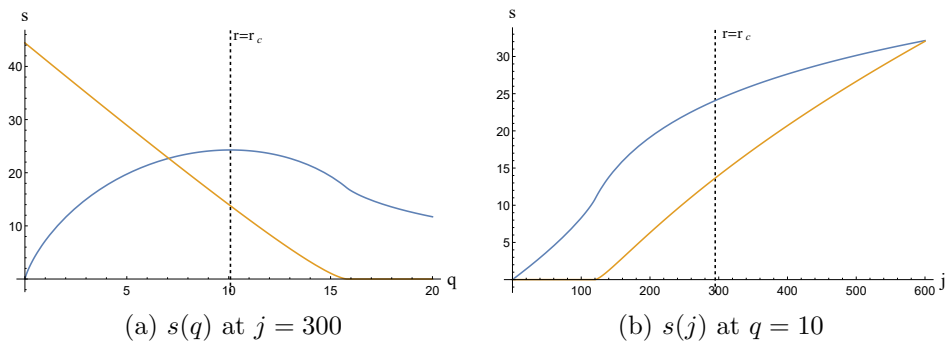
Figure 3.3: $s(q, j)$ at particular slices: blue/yellow line denotes its real/imaginary part.

of $f(r)$, we chose the blue one and the yellow one in Fig. 3.1. From Fig. 3.2(b), $\mathrm{Re}(\Delta)$ decreases to zero as q increase to a finite quantity, $q_{\mathrm{max}}(j)$. We find that only for $r > r_{\mathrm{c}} \approx 1.9488532...$, i.e. $j > (1 + r_{\mathrm{c}})q^2 \approx 2.9488532q^2$, $\mathrm{Re}(\Delta) > 0$. So at given angular momentum j, a sensible saddle point at $\mathrm{Re}(\Delta) > 0$ exists only when the electric charge q is smaller than a maximal value $q_{\mathrm{max}}(j) = \sqrt{\frac{j}{1+r_{\mathrm{c}}}} \approx 0.582336 j^{\frac{1}{2}}$. If r is smaller than this critical value r_c, $\mathrm{Re}(\Delta) < 0$. Note that in the BPS partition function, $\mathrm{Re}(\Delta) \to 0^+$ is analogous to infinite temperature limit, since its dual charge is positive. It is curious to find such an 'infinite temperature limit' at finite $q_{\mathrm{max}}(j)$. See a related comment below. In Fig. 3.3, s is plotted with respect to j, q. As before, we chose the blue and yellow solution of $f(r)$. One can see that $\mathrm{Re}(s) > 0$ for arbitrary $j, q > 0$. Also, when $j > (1 + r_c)q^2$, the entropy S increases as the charges j, q increases, as expected.

One may want to find explicit forms of chemical potentials and entropy, in terms of charges, at least in certain asymptotic regime. This amounts to knowing the function $f(r)$. An explicit asymptotic form of $f(r)$ can be deduced at very large r. When $r \gg 1$, $f(r) \to 0$. Hence, we can approximate the equation

(3.3.21) as

$$(f(r))^2 r \sim 2\text{Li}_2(f(r)) - \text{Li}_2(1) \sim 2f(r) - \text{Li}_2(1) \to f(r) \sim \frac{1}{r}\left(1 \pm i\pi\sqrt{\frac{r}{6}}\right).$$
(3.3.22)

So when $r \gg 1$, i.e. $j \gg q^2$, one obtains the asymptotic formula of the chemical potentials and the entropy in terms of j, q as follows:

$$\omega_1 = \frac{f(r)}{q} \sim \frac{1}{qr}\left(1 \pm i\pi\sqrt{\frac{r}{6}}\right) \sim \frac{1}{j}\left(q \pm i\pi\sqrt{\frac{j}{6}}\right),$$

$$\Delta = -\log(e^{q\omega_1} - 1) = -\log(e^{f(r)} - 1) \sim -\log f(r) \sim \log r - \log\left(1 \pm i\pi\sqrt{\frac{r}{6}}\right)$$

$$\sim \frac{1}{2}\log r - \frac{1}{2}\log\frac{\pi^2}{6} \mp \log i \sim \frac{1}{2}\log\frac{j}{q^2} - \frac{1}{2}\log\frac{\pi^2}{6} \mp \log i,$$

$$s = 2(q\Delta + j\omega_1) \sim q\log\frac{j}{q^2} + \left(2 - \log\frac{\pi^2}{6} \mp 2\log i\right)q \pm i\pi\sqrt{\frac{2j}{3}}.$$
(3.3.23)

One finds that the Cardy-like condition $|\omega_1| \ll 1$ is met in this regime, since $\text{Re}(\omega_1) \sim \frac{q}{j} \ll 1$ and $\text{Im}(\omega_1) \sim j^{-\frac{1}{2}} \ll 1$. In fact, just as a side comment, the above approximate entropy formula is very well-fitted even from $r \gtrsim r_c$. At, $r = r_c$, $\left|\frac{S - S_{\text{approx}}}{S}\right| \sim 0.07$.

We study the validity of our Cardy approximation $\omega_1 \ll 1$ for more general q, j's, at $r > r_c$. This can be easily seen in Fig. 3.4, where we showed the lines with constant $|\omega_1|$ on the q-j space. We can highly trust our approximation when $|\omega_1| \ll 1$. When $r > r_c$, one can see that if $j \gtrsim 200$, then $|\omega_1| < 0.1$. Therefore, we can say that when $r > r_c$ and $j \gtrsim 200$, our results are within the Cardy regime.

In summary, only when $j > (1 + r_c)q^2$, or $q < q_{\max}(j) = \sqrt{\frac{j}{1+r_c}} \approx 0.582532 j^{\frac{1}{2}}$, all chemical potentials ω_1, Δ and the macroscopic entropy S have positive chemical potentials. Otherwise, we find solutions with $\text{Re}(\Delta) < 0$, which we disregard.
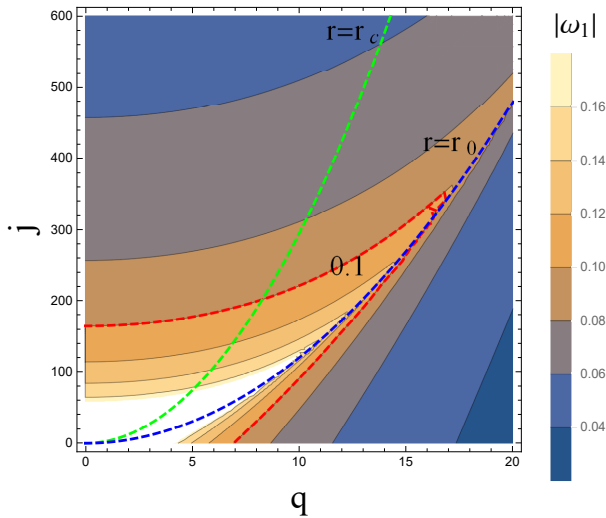
Figure 3.4: $|\omega_1| > 0.1$ in the region encircled by the red dashed line.

So far, we presented a semi-analytical analysis, using some identities of Li_2 functions to simplify the structures. However, to be absolutely sure, we plugged in our numerical saddle points back to the original extremization conditions (3.3.16) without any analytic treatement, to numerically reconfirm the correctness of our results, at least when $\mathrm{Re}(\Delta) > 0$ in which case $\mathrm{Li}_2(e^{-\Delta})$, $\mathrm{Li}_2(e^{-2\Delta})$ are very safely well defined.

We also note that, in the regime $q < q_{\max}(j)$, we numerically analyzed the Hessian

$$H_{ij} \equiv -\frac{\partial^2 \mathrm{Re}(S(Q))}{\partial Q_i \partial Q_j} \ , \quad (Q_1 = q, \ Q_2 = j) \tag{3.3.24}$$

for S at the saddle point, to study the local thermodynamic stability. At least for $q < q_{\max}(j)$, we find that both eigenvalues of H_{ij} are positive, implying that all susceptibility parameters are positive. Also, we find that $\log Z$ at the saddle point is always positive in our Cardy regime with large charges, making it more dominant than the gravitons.

Now we turn to discuss some aspects of our results. First of all, it is in-

teresting to see where the small black holes satisfying $Q^2 = \frac{N^2}{2}J_1$ are located. Since $J_2 = 0$ on the known solutions, this charge condition translates to $q = \frac{j^{\frac{1}{2}}}{\sqrt{2}} \approx 0.707 j^{\frac{1}{2}}$. This is the charge region where our new predicted saddle points cannot exist, since its q is larger than $q_{\max}(j)$. So to conclude, our free energy predicted new $\frac{1}{8}$-BPS black hole-like saddle points with macroscopic entropy, when $q < q_{\max}(j) = \sqrt{\frac{j}{1+r_c}} \approx 0.582532 j^{\frac{1}{2}}$, in the Cardy regime. Since no such black holes are known so far in this sector, including the small black hole limits of [83, 84, 86], one may ask where to seek for such objects in the gravity dual.

Here we note that there has been some endeavors to construct black holes beyond those known in the literature, based on allowing condensations of matters outside the event horizon. These black holes are called hairy black holes. In the context of global $AdS_5 \times S^5$, [116, 117] made studies of hairy black holes with one electric charge $Q \equiv Q_1 = Q_2 = Q_3$ at $J_1 = J_2 = 0$. At zero angular momentum, one finds that the hairy black hole horizon disappears as one reduces the energy to its BPS bound $E \searrow 3Q$, with fixed Q. The end point is either a smooth AdS soliton when Q is smaller than a critical value Q_c, or a singular horizonless solution if $Q > Q_c$. Studying the temperature as $E \searrow 3Q$, the subcritical solutions have zero temperature $T = 0$, while the supercritical solutions have $T = \infty$. As for hairy black holes with nonzero angular momenta, [111, 112] studied those at nonzero $Q \equiv Q_1 = Q_2 = Q_3$ and $J \equiv J_1 = J_2$. In this case, as E is reduced to its BPS bound $M \searrow 3Q + 2J$ at fixed Q, J, one still finds black holes with nonzero entropy. Again here, one finds a signal of two different types of endpoints. In the subcritical region $Q < Q_{\max}(J)$, the temperature of the limiting hairy black hole goes to 0. In the supercritical region, $Q > Q_{\max}(J)$, the temperature blows up to ∞. The critical charge depends on J. It seems that due to numerical limitations, the precise value of $Q_{\max}(J)$ could not be

determined [111].

Even if the hairy black holes explained above are in a different charge sector, we find some qualitative similarities with the new saddle points that we find in the Macdonald-Cardy limit. This is because our new saddle points also exist only in a subcritical region $q < q_{\max}(j) \approx 0.582532 j^{\frac{1}{2}}$. The reason why this gets spoiled at $q = q_{\max}(j)$ is because the chemical potential $\text{Re}(\Delta)$ approaches zero, which is analogous to the high temperature limit in the BPS sector. It will be interesting to see if this more than just an analogy.

3.4 Discussions and future directions

We first discuss possible subtleties of our results. We also try to suggest conservative interpretations of our results, in case some readers might be worrying about subtleties.

- Throughout this chapter, we mostly took (with one exception) Cardy-like limits which suppress the fluctuations relying on large J. However, general black holes are semi-classical saddle points at large N, rather than large charges. So we are assuming an interpolation, which connects large N saddle points given by black holes and large J saddle points of our QFT. This often turned out to provide the correct quantitative results, starting from the seminal work [11]. The fact that our Cardy free energy successfully captures known black holes of [83–86] makes us to hope that a similar situation is happening here.

- In our Cardy limit, we took the $U(N)$ gauge holonomies α_a to be at the maximally deconfining point. One cannot imagine such saddle points at finite charges (or finite ω), because the Haar measure repulsion forbids α_a's to be on top of another [57,69]. We expect our maximally deconfining

saddle point to actually mean that the distances of α_a's are suppressed by small ω. It is easy to check that this is the local saddle point in the Cardy limit, but one may ask if this is the global minimum of free energy. There are examples of 4d $\mathcal{N} = 1$ QFTs in which this fails to be true [114]. Considering the empirical relation between more nontrivial saddle points and the behaviors of $Z[S^3]$ [114], it seems that our model should be safe of this issue. Indeed, one can analytically prove that the maximally deconfining saddle point is the global minimum in our model.

- The fact that BPS black holes exist only with a charge relation might be somewhat puzzling from the QFT dual side, especially after we claimed that we have counted them (at large charges). We have little to comment on it, especially in our Cardy regime in which other solutions seem to be unknown so far [111,112]. Especially, intertwined with the ignorance of the index on one of the 5 charges, the possibility of more general black holes seems not easy to address within our results. However, technically from the gravity side, such charge relations of BPS black holes are ubiquitous. Familiar examples are single-centered 4d black holes [118] at zero angular momentum, or 5d BMPV black holes [13] with self-dual angular momenta. By now we know much richer families of BPS black solutions, such as 4d multi-centered black holes [119] or 5d black rings [20–22, 120, 121], which violate such charge relations. In AdS, one can naturally seek for hairy black holes. The BPS version of such black holes were recently reported [111,112], even though it appears not in our large rotation regime (at least from the data presented there).

- We studied Cardy-like and non-Cardy-like scaling limits of the $\frac{1}{8}$-BPS Macdonald index. In the latter, we have identified the small black hole

limit of the known BPS solutions (third reference of [83, 84, 86]). In the former, our Cardy free energy is quite nontrivial, and exhibits rich saddle points. These saddle points exhibit properties very reminiscent of hairy black holes [111, 116]. If one can again trust the smooth interpolation between our Cardy saddle point and the large N saddle point, we can claim that we have predicted new (hairy) black holes in the Macdonald sector. Since no solutions are actually constructed yet, we are much less confident about the issues raised above in this section. Perhaps actual constructions of such gravity solutions can clear the uncertainty.

We think there are many interesting future directions to pursue. We finish this chapter by briefly mentioning some of them.

- Having seen macroscopic entropies from the index, one should expect an explicit construction of such operators at weak-coupling. At 1-loop level, the BPS states are mapped to cohomologies of the supercharge $\mathcal{Q}$. [69, 107–110]. Considering the free QFT analysis of section 2.1, (3.2.7) and comments above it, fermionic fields may be responsible for our asymptotic free energy. [107, 108] considered a class of such operators called 'Fermi liquid operators.' Unfortunately, the operators discussed there were shown to be (weakly) renormalized, even at weak coupling. As already mentioned in [108] as a possible scenario, dressing these operators with other fermion fields might yield large number of new BPS states. Perhaps a clever 'ansatz' for such operators using all four fermions should be discovered, generalizing [107]. [110] performed a systematic analysis of this cohomology at $N = 2, 3$, up to certain energy order, without using an ansatz. However, it is not completely clear to us whether the energy orders covered in [110] are definitely well above N^2. For instance, our Cardy

limit demands ω to be small. Its conjugate J is given by $J \sim \frac{1}{\omega^3}$. So even if one generously accepts $\omega \sim 0.1$ to be small, the associated charge will be $J \sim 10^3$, definitely out of reach in [110].

- On the other hand, the roles of fermions seen around (3.2.7) might be an 'emergent' one. This is because, if we study the Cardy limit honestly from the index, (3.2.28) is obtained by both bosons and fermions. Here, note that there is a known toy model in which a fermion picture emerges. This is the half-BPS sector of 4d $\mathcal{N} = 4$ Yang-Mills theory, exhibiting a Fermi droplet picture [122, 123]. It may be interesting to clarify the true nature of the 'fermion picture' we think we see around (3.2.7).

- As also commented at various places earlier, it will be interesting to see what one obtains by going beyond the Cardy limit, seeking for large N saddle points of N integral variables, again carefully tuning the imaginary parts of the chemical potentials. The analysis of [69] already seems to set some limitation of this approach, but it would be interesting (if possible) to see how their results at order 1 chemical potentials get connected to our results in the Cardy-like limit. However, at least at the moment, this appears to be a very challenging calculus.

- In the $\frac{1}{8}$-BPS Macdonald sector, our studies 'predict' that there should be black holes, in case one believes that our Cardy saddle points will transmute to large N saddle points. Known black holes reduce to small black holes with vanishing entropy in this limit. Considering some qualitative aspects similar to the recently explored hairy black holes, we speculate that they might be hairy $\frac{1}{8}$-BPS black holes. Since one is now equipped with 4 real Killing spinors, perhaps combining the general SUSY analysis with a clever ansatz may shed lights on such solutions.

Chapter 4

Large AdS$_6$ black holes from CFT$_5$

In this chapter, we study supersymmetric AdS$_6$ black holes at large angular momenta, from the index of 5d SCFTs on $S^4 \times \mathbb{R}$ in the large N and Cardy limit. Our examples are the strong coupling limits of 5d gauge theories on the D4-D8-O8 system. The large N free energy scales like $N^{5/2}$, statistically accounting for the entropy of large black holes in AdS$_6$. Instanton solitons play subtle roles to realize these deconfined degrees of freedom.

4.1 Introduction

Superconformal field theories (SCFTs) in spacetime dimensions $d > 4$ were discovered indirectly from string theory. First examples are [45] in 6d, and [47] in 5d. These QFTs defy microscopic descriptions from traditional Lagrangian methods so far. One interesting aspect is that they have much larger numbers of degrees of freedom than conventional gauge theories, at given gauge group 'rank.' For instance, if the QFTs are engineered by N ($\gg 1$) branes, the 6d/5d

QFTs of [45] and [47,48] exhibit N^3 and $N^{5/2}$ degrees of freedom respectively. This is much larger than N^2 for gauge theories on D-branes at weak coupling.

Recently, formulae for certain supersymmetric partition functions for these SCFTs have been suggested and explored. We shall be interested in the index of 5d SCFTs on $S^4 \times \mathbb{R}$ [70]. Its matrix integral formula has been obtained in [124]. This formula has been providing new channels to quantitatively study 5d SCFTs. In this chapter, we shall add one more intriguing finding, by exploring novel deconfinements of large N 5d SCFTs and the holographically dual black holes in AdS_6 spacetime. We study 5d SCFTs engineered on D4-D8-O8 systems [47, 48]. In this setting, the large N deconfined degrees of freedom would be visible in the high temperature phase. The gravity dual of deconfinement is the nucleation of black holes after the Hawking-Page phase transition [55, 56]. Our deconfined index successfully counts the microstates of the supersymmetric AdS_6 black holes of [87], in the framework of [74].

We study a Cardy limit of the 5d SCFT index in this chapter. We shall take large N limit, and also take the chemical potentials $\omega_{1,2}$ conjugate to the two rotations on S^4 to be small. The last limit partly defines our Cardy limit. See section 2 for the precise definition. Apparently, the large N calculation in the Cardy limit turns out to be rather simple. The index on $S^4 \times S^1$ is given by an integral over the $U(1)^r \subset G$ holonomies α_a on S^1 which are all periodic variables on a circle, where G is the 5d gauge group of rank r [124]. The integrand consists of a pair of instanton partition functions [125], or more abstractly the Omega-deformed partition functions of 5d SCFTs in the Coulomb phase. We seek for the large N saddle points of α_a, also taking the Cardy limit $|\omega_{1,2}| \ll 1$. To get the relevant saddle point, it turns out that one has to complexify α_a to variables living on cylinders, and spread them over a large

interval of length $\sim N^{\frac{1}{2}}$. This is similar to the partition functions of 5d SCFTs on S^5 [67], and especially to the topologically twisted indices on suitable spatial manifolds [126, 127] which counted certain black holes in AdS_6. It seems that the physical implications of such novel large N saddle points were not fully discussed in the literature. We find this especially novel, having in mind the deconfinement phase transition to $N^{\frac{5}{2}}$ degrees of freedom. The novelty partly has to do with the rather mysterious instanton solitons in higher dimensional gauge theories, concerning their noncompact internal zero modes and infinite towers of bound states. We shall comment on these aspects briefly.

The rest of this chapter is organized as follows. In section 2, we study the large N Cardy limit of the index for 5d gauge theories having AdS_6 gravity duals in massive IIA string theory. These Cardy free energies precisely account for the large BPS black holes in AdS_6, using the recently discovered entropy functions [74] for these black holes. We also comment on subtle aspects of our free energy, especially concerning the physics of instantons. In section 3, we conclude and discuss some open questions.

4.2   Cardy limit of large N 5d SCFTs and black holes

We first briefly review the large N 5d SCFT models that we shall discuss in sections 2.1 and 2.2. 5d $\mathcal{N} = 1$ SCFTs of our interest live on N D4-branes probing an O8-plane and $N_f \leq 7$ D8-branes on $\mathbb{C}^2/\mathbb{Z}_n$ [47, 48, 50, 51]. Note that $\mathbb{Z}_n$ orbifold is transverse to D4 branes, while O8, D8's are parallel to them. So in the probe limit, the net spacetime is given by $\mathbb{R}^{4,1} \times \mathbb{R}^+ \times \mathbb{C}^2/\mathbb{Z}_n$, where $\mathbb{R}^+ = \mathbb{R}/\mathbb{Z}_2$ is the direction transverse to the O8-plane.

When $n = 1$, the low energy dynamics on D4-branes is described by an $Sp(N)$ gauge theory with one rank 2 antisymmetric hypermultiplet and $N_f \leq 7$

orbifold	gauge group	matter	flavor symmetries
$\mathbb{Z}_{2k}^-$	$Sp(N) \times SU(2N)^{k-1} \times Sp(N)$	$\sum_{i=1}^{k}(\mathbf{2N}_i, \overline{\mathbf{2N}}_{i+1})$	$U(1)_M \times U(1)_B^{k-1} \times U(1)_I^{k+1}$
$\mathbb{Z}_{2k}^+$	$SU(2N)^k$	$\overline{\mathbf{A}}_1 + \sum_{i=1}^{k-1}(\mathbf{2N}_i, \overline{\mathbf{2N}}_{i+1}) + \mathbf{A}_k$	$U(1)_M \times U(1)_B^{k} \times U(1)_I^{k}$
$\mathbb{Z}_{2k+1}$	$Sp(N) \times SU(2N)^k$	$\sum_{i=1}^{k}(\mathbf{2N}_i, \overline{\mathbf{2N}}_{i+1}) + \mathbf{A}_{k+1}$	$U(1)_M \times U(1)_B^{k} \times U(1)_I^{k+1}$

Table 4.1: Properties of the quiver gauge theories. $\mathbf{A}_i$ denotes rank 2 anti-symmetric hypermultiplet of the i'th node, and fundamental matters are not shown.

fundamental hypermultiplets [47, 48]. When $n = 2$, there is a $\mathbb{Z}_2$ orbifold. If it is the orbifold without vector structure, the worldvolume theory on D4-branes is $SU(2N)$ gauge theory with two rank 2 antisymmetric hypermultiplets and $N_f \leq 7$ fundamental hypermultiplets [50, 51]. The other orbifold theories for $n \geq 2$ are quiver gauge theories [50, 51]. Gauge groups, matter contents, and flavor symmetries of these quivers are shown in Table 4.1. In all these models, the q'th gauge node of the quiver may have $N_f^{(q)}$ fundamental matters, which should satisfy $\sum_q N_f^{(q)} = N_f$. In the table, $\mathbb{Z}_{2k}^{\pm}$ denotes the orbifold without/with vector structure, respectively. They are associated with two choices for the orientifold projection in k-th twisted sector. $\mathbb{Z}_{2k}^+$ projects onto even states, i.e. this is the 'ordinary' orbifold [50].

Bifundamental and antisymmetric fields in these quiver gauge theories can form various gauge invariant operators: a meson, n_I di-baryons of the bifundamental fields, and n_A Pfaffian baryons of antisymmetric fields. Numbers of the baryon operators (n_I, n_A) in each quiver gauge theories are given by $(k, 0)$, $(k - 1, 2)$, $(k, 1)$, respectively. These baryon operators are not all independent since a product of them is related to the meson operator. The mesonic $U(1)_M$ symmetry rotates all the antisymmetric and bifundamental fields of the quiver, with charge 1 and 2, respectively. We shall introduce a mesonic charge Q_M, $n_A + n_I$ baryonic charges Q_{B_A}, Q_{B_I} and their conjugate chemical potentials

m, b_A, b_I. Then we impose a constraint

$$\sum_{A=1}^{n_A} b_A + 2 \sum_{I=1}^{n_I} b_I = 0 \ , \tag{4.2.1}$$

which reduces the number of independent baryonic charges by one. See [50] for more details.

The strong coupling limits of these gauge theories are 5d SCFTs. In the large N limit, these SCFTs are dual to the massive IIA string theory in the warped $AdS_6 \times (S^4/\mathbb{Z}_2)/\mathbb{Z}_n$ product background [49–51]. The $SU(2)_R$ R-symmetry of the SCFT corresponds to the $SU(2)$ part of $SU(2) \times U(1)$ isometry of $(S^4/\mathbb{Z}_2)/\mathbb{Z}_n$. The overall $U(1)_M$ mesonic symmetry, acting on all the antisymmetric and bifundamental matters, corresponds to the remaining $U(1)$ part of $SU(2) \times U(1)$ isometry. When $n = 1, 2$, the $U(1)_M$ mesonic symmetry is enhanced to $SU(2)_M$. This corresponds to the fact that the isometry of $S^4/\mathbb{Z}_2$ or $(S^4/\mathbb{Z}_2)/\mathbb{Z}_2$ is $SU(2) \times SU(2)$.

The gravity duals of other global symmetries – $U(1)_B^{n_I+n_A-1}$ baryonic symmetries, $U(1)_I$ instanton symmetries for every gauge nodes, and flavor symmetries acting on the fundamental matters – are also well understood [47,48,50,51]. In particular, when $n = 1$, $U(1)_I \times SO(2N_f)$ is enhanced to E_{N_f+1} [47,48,128–132] . In the dual gravity, the states charged under E_{N_f+1} are localized at D8-O8, the boundary of $S^4/\mathbb{Z}_2$ [49,50]. The $SO(2N_f)$ part comes from perturbative open strings on O8-D8. The $U(1)_I$ charge at $n = 1$ is carried by D0-branes in the gravity dual [49,50]. Since the inverse-dilaton field diverges at the boundary of $S^4/\mathbb{Z}_2$ (i.e. at the 8-brane), the D0-branes are attracted to the 8-branes and nonperturbatively render E_{N_f+1} enhancement.

When $n \geq 2$, there can be more $U(1)_I$ instanton symmetries if there are more than one gauge nodes, and there are $U(1)_B$ baryonic symmetries as well [50,51]. The bulk duals of these symmetries are given as follows [50]. These symmetries

basically come from the $\mathbb{Z}_n$ orbifold. $\mathbb{Z}_n$ acts freely on the S^3 base of $S^4/\mathbb{Z}_2$, yielding the Lens space $S^3/\mathbb{Z}_n$. The full compact internal space $(S^4/\mathbb{Z}_2)/\mathbb{Z}_n$ has an A_{n-1} singularity at the pole. There are $n-1$ vanishing 2-cycles at the pole, and also $n-1$ dual finite 2-cycles since the internal space is compact. These cycles should be identified pairwise by the O8-orientifold. When n is odd, the O8 action leaves $\frac{n-1}{2}$ vanishing 2-cycles and $\frac{n-1}{2}$ finite 2-cycles. When n is even, we should be careful about the $\frac{n}{2}$-th unpaired 2-cycles. If the $\mathbb{Z}_n$ orbifold is without vector structure, $\frac{n}{2}$-th vanishing 2-cycle is projected out, while $\frac{n}{2}$-th finite 2-cycle is mapped to itself. So there are $\frac{n-2}{2}$ vanishing 2-cycles and $\frac{n}{2}$ finite 2-cycles after the O8 projection. On the contrary, when $\mathbb{Z}_n$ is the orbifold with vector structure, $\frac{n}{2}$-th vanishing 2-cycle is mapped to itself, while $\frac{n}{2}$-th finite cycle is projected out, leaving $\frac{n}{2}$ vanishing 2-cycles and $\frac{n-2}{2}$ finite 2-cycles after O8-projection. Baryons are described by D2-branes wrapping the finite 2-cycles. Instantons are dual to D0-brane and D2-branes wrapping the vanishing 2-cycles, i.e. fractional D0-branes. These explain all the symmetries listed in Table 4.1.

4.2.1 $Sp(N)$ theories

In this subsection, we study the large N index for the 5d $\mathcal{N}=1$ gauge theories with $Sp(N)$ gauge group, one rank 2 antisymmetric hypermultiplet, and $N_f \leq 7$ fundamental hypermultiplets [124]. We shall consider the radially quantized theory on $S^4 \times \mathbb{R}$. We choose a supercharge Q to define the index, so that we count $\frac{1}{8}$-BPS states annihilated by the supercharge Q and its conjugate conformal supercharge $S = Q^\dagger$. We will denote by j_1, j_2 the Cartan generators of $SU(2)_1 \times SU(2)_2 \subset Sp(2) \cong SO(5)$ rotation symmetry, and by R the Cartan generator of $SU(2)_R$ R-symmetry. We introduce the fugacities $e^{-\beta}$, x, y for $\{Q, S\}$, $j_1 + R$, j_2 in $F(4)$ superconformal symmetry, which commute with the

supercharges Q and S. Since the antisymmetric representation of $Sp(N)$ group is real, the antisymmetric hypermultiplet splits into two half-hypermultiplets, which transform as a doublet under $Sp(1)_M \cong SU(2)_M$ global symmetry. We call its Cartan generator h. This system also has $SO(2N_f)$ flavor symmetry rotating the fundamental quarks. We call their Cartan generators H_l, with $l = 1, \cdots, N_f$. Finally, there is a $U(1)_I$ topological symmetry related to the current $j_\mu \sim \star_5 \mathrm{tr}(F \wedge F)_\mu$. The corresponding conserved charge is the instanton number k. We introduce the fugacities e^{-m}, e^{-M_l}'s, and q for h, H_l, k. The index is defined as [70, 124]

$$Z(x, y, m, M_l, q) = \mathrm{Tr}\left[(-1)^F e^{-\beta\{Q, S\}} x^{2(j_1 + R)} y^{2j_2} e^{-mh} e^{-\sum_l M_l H_l} q^k \right] \ , \quad (4.2.2)$$

where F is the fermion number operator. The trace is taken over the Hilbert space of the QFT on $S^4 \times \mathbb{R}$. This index counts BPS states, for which the eigenvalue of $\{Q, S\}$ is 0. So the index does not depend on β. For the $Sp(N)$ theory with one rank 2 antisymmetric hypermultiplet and N_f fundamental hypermultiplets, this index is given by [124]

$$\begin{aligned}
Z(x, y, m, M_l, q) &= \oint [d\alpha] \, \mathrm{PE}\left[f_{vec}(x, y, e^{i\alpha_a}) + f_{mat}^{asym}(x, y, e^{i\alpha_a}, e^m) + f_{mat}^{fund}(x, y, e^{i\alpha_a}, e^{M_l}) \right] \\
&\quad \times \prod_{\pm} Z_{\mathrm{inst}}(x^{\pm 1}, y^{\pm 1}, e^{\pm i\alpha_a}, e^{\pm m}, e^{\pm M_l}, q^{\pm 1}) \ , \quad (4.2.3)
\end{aligned}$$

where $[d\alpha]$ including the Haar measure is given by

$$[d\alpha] = \frac{1}{2^N N!} \left[\prod_{a=1}^{N} \frac{d\alpha_a}{2\pi} \left(2\sin\alpha_a \right)^2 \right] \prod_{a<b} \left[2\sin\left(\frac{\alpha_a - \alpha_b}{2} \right) \right]^2 \left[2\sin\left(\frac{\alpha_a + \alpha_b}{2} \right) \right]^2 \ . \quad (4.2.4)$$

f_{vec}, f^{asym}_{mat}, f^{fund}_{mat} are the letter indices for the vector, antisymmetric, and fundamental hypermultiplets, given by

$$f_{vec} = -\frac{x(y+1/y)}{(1-xy)(1-x/y)} \left[\sum_{a<b}^{N} e^{i(\pm\alpha_a \pm \alpha_b)} + \sum_{a=1}^{N} \left(e^{-2i\alpha_a} + e^{2i\alpha_a} \right) + N \right] \quad (4.2.5)$$

$$f^{asym}_{mat} = \frac{x}{(1-xy)(1-x/y)} (e^{m/2} + e^{-m/2}) \left[\sum_{a<b}^{N} e^{i(\pm\alpha_a \pm \alpha_b)} + N \right] ,$$

$$f^{fund}_{mat} = \frac{x}{(1-xy)(1-x/y)} \sum_{a=1}^{N} \sum_{l=1}^{N_f} \left(e^{-i\alpha_a - M_l} + e^{i\alpha_a - M_l} + e^{-i\alpha_a + M_l} + e^{i\alpha_a + M_l} \right) .$$

Our notation is that the terms with $\pm$ are all summed over: for instance, $e^{i(\pm\alpha_a \pm \alpha_b)} \equiv e^{-i\alpha_a - i\alpha_b} + e^{-i\alpha_a + i\alpha_b} + e^{i\alpha_a - i\alpha_b} + e^{i\alpha_a + i\alpha_b}$. Z_{inst} is the Coulomb branch instanton partition function [125], taking the form of

$$Z_{\text{inst}} = \sum_{k=0}^{\infty} q^k Z_k(x, y, e^{i\alpha_a}, e^m, e^{M_l}) , \quad Z_{k=0} = 1 , \quad (4.2.6)$$

where Z_k is the k-instanton contribution. Z_k can be computed using the methods of [132–134]. PE in (4.2.3) is the Plethystic exponential defined as

$$\text{PE}\left[f(\{t\}) \right] = \exp\left[\sum_{n=1}^{\infty} \frac{1}{n} f(\{t^n\}) \right] , \quad (4.2.7)$$

where $\{t\}$ collectively denotes all fugacities for gauge and global symmetries appearing in f.

For later convenience, we redefine the fugacities as $e^{-\omega_1}$, $e^{-\omega_2}$ for the angular momenta $J_1 \equiv j_1 + j_2$, $J_2 \equiv j_1 - j_2$, which act on the orthogonal 2-planes of $\mathbb{R}^5$ which contains S^4. We also define $e^{-\tilde{\Delta}} \equiv e^{-(\Delta - 2\pi i)}$ for R. They are related to the original fugacities as

$$e^{-\omega_1} = xy, \ e^{-\omega_2} = x/y, \ e^{-\tilde{\Delta}} = x^2 . \quad (4.2.8)$$

The new chemical potentials satisfy $\Delta - \omega_1 - \omega_2 = 2\pi i \pmod{4\pi i}$. Since R, J_1, J_2 are normalized to be half-integers, all chemical potentials have $4\pi i$ periods. This

is the reason for the mod $4\pi i$ in the last equation. Below, we shall always take

$$\Delta - \omega_1 - \omega_2 = 2\pi i \ . \tag{4.2.9}$$

The Haar measure can be rewritten as

$$[d\alpha] = \frac{1}{2^N N!} \prod_{a=1}^{N} \frac{d\alpha_a}{2\pi} \ \mathrm{PE}\left[-\sum_{a<b}^{N} e^{i(\pm\alpha_a\pm\alpha_b)} - \sum_{a=1}^{N} \left(e^{-2i\alpha_a} + e^{2i\alpha_a} \right) \right] \ . \tag{4.2.10}$$

Combining this exponent of PE from the Haar measure to f_{vec}, one obtains

$$\tilde{f}_{vec} = -\frac{1+x^2}{(1-xy)(1-x/y)}\left[\sum_{a<b}^{N} e^{i(\pm\alpha_a\pm\alpha_b)} + \sum_{a=1}^{N} \left(e^{-2i\alpha_a} + e^{2i\alpha_a} \right) \right] + \left(1 - \frac{1+x^2}{(1-xy)(1-x/y)} \right) N$$

$$-\frac{1+e^{-\tilde{\Delta}}}{(1-e^{-\tilde{\omega}_1})(1-e^{-\omega_2})}\left[\sum_{a<b}^{N} e^{i(\pm\alpha_a\pm\alpha_b)} + \sum_{a=1}^{N} \left(e^{-2i\alpha_a} + e^{2i\alpha_a} \right) \right] + \left(1 - \frac{1+e^{-\tilde{\Delta}}}{(1-e^{-\omega_1})(1-e^{-\omega_2})} \right) N$$

$$-\frac{2\cosh\frac{\tilde{\Delta}}{2}}{2\sinh\frac{\tilde{\omega}_1}{2}\cdot 2\sinh\frac{\omega_2}{2}}\left[\sum_{a<b}^{N} e^{i(\pm\alpha_a\pm\alpha_b)} + \sum_{a=1}^{N} \left(e^{-2i\alpha_a} + e^{2i\alpha_a} \right) \right] + \left(1 - \frac{2\cosh\frac{\tilde{\Delta}}{2}}{2\sinh\frac{\omega_1}{2}\cdot 2\sinh\frac{\omega_2}{2}} \right) N \ . \tag{4.2.11}$$

We used (4.2.9) on the last line. Other letter indices are given by

$$f_{mat}^{asym} = \frac{2\cosh\frac{m}{2}}{2\sinh\frac{\omega_1}{2}\cdot 2\sinh\frac{\omega_2}{2}}\left[\sum_{a<b}^{N} e^{i(\pm\alpha_a\pm\alpha_b)} + N \right] \ , \ f_{mat}^{fund} = \frac{\sum_{l=1}^{N_f} 2\cosh M_l}{2\sinh\frac{\omega_1}{2}\cdot 2\sinh\frac{\omega_2}{2}} \sum_{a=1}^{N} \left(e^{i\alpha_a} + e^{-i\alpha_a} \right) \ . \tag{4.2.12}$$

Now we consider a Cardy-like limit $|\omega_i| \ll 1$ [75]. We will keep ω_i's complex with $\mathrm{Re}(\omega_i) > 0$. Due to (4.2.9), Δ will be close to $2\pi i$. Namely, its imaginary part is $\mathcal{O}(1)$ and close to $2\pi i$, while its real part is small at order $|\omega_i|$. However, as in [75], for convenient intermediate manipulations, we shall temporarily take Δ to be pure imaginary, and continue back to a complex number with small real part later. The other chemical potentials m, M_l's are kept purely imaginary (which may be continued back to suitable complex numbers later, if one wishes). Then following the similar procedures used in [75], ignoring the Cartan parts of $Sp(N)$ at large N, the PE of the letter indices are approximated as

$$\mathrm{PE}\left[\tilde{f}_{vec}\right] \sim \exp\left[-\frac{1}{\omega_1\omega_2} \sum_{n=1}^{\infty} \frac{e^{\frac{n(\Delta-2\pi i)}{2}} + e^{-\frac{n(\Delta-2\pi i)}{2}}}{n^3} \left(\sum_{a=1}^{N} \left(e^{-2in\alpha_a} + e^{2in\alpha_a} \right) + \sum_{a<b}^{N} e^{i(\pm\alpha_a\pm\alpha_b)} \right) \right]$$

$$= \exp\left[-\frac{1}{\omega_1\omega_2} \sum_{n=1}^{\infty} \frac{(-e^{\frac{\Delta}{2}})^n + (-e^{-\frac{\Delta}{2}})^n}{n^3} \left(\sum_{a=1}^{N} \left(e^{-2in\alpha_a} + e^{2in\alpha_a} \right) + \sum_{a<b}^{N} e^{i(\pm\alpha_a\pm\alpha_b)} \right) \right]$$

$$= \exp\left[-\frac{1}{\omega_1\omega_2} \left(\sum_{a=1}^{N} \mathrm{Li}_3(-e^{\pm\frac{\Delta}{2}\pm2i\alpha_a}) + \sum_{a<b}^{N} \mathrm{Li}_3(-e^{\pm\frac{\Delta}{2}\pm i\alpha_a\pm i\alpha_b}) \right) \right] \equiv \exp\left[-\frac{\mathcal{F}_{vec}(\alpha_a, \Delta)}{\omega_1\omega_2} \right] ,$$

$$(4.2.13)$$

$$\mathrm{PE}\left[f_{mat}^{asym}\right] \sim \exp\left[\frac{1}{\omega_1\omega_2} \sum_{n=1}^{\infty} \frac{1}{n^3}(e^{\frac{nm}{2}} + e^{-\frac{nm}{2}}) \sum_{a<b}^{N} e^{i(\pm\alpha_a\pm\alpha_b)} \right]$$

$$= \exp\left[\frac{1}{\omega_1\omega_2} \sum_{a<b}^{N} \mathrm{Li}_3(e^{\pm\frac{m}{2}\pm i\alpha_a\pm i\alpha_b}) \right] \equiv \exp\left[-\frac{\mathcal{F}_{mat}^{asym}(\alpha_a, m)}{\omega_1\omega_2} \right] , \qquad (4.2.14)$$

$$\mathrm{PE}\left[f_{mat}^{fund}\right] \sim \exp\left[\frac{1}{\omega_1\omega_2} \sum_{n=1}^{\infty} \frac{1}{n^3} \sum_{l=1}^{N_f}(e^{nM_l} + e^{-nM_l}) \sum_{a=1}^{N} \left(e^{in\alpha_a} + e^{-in\alpha_a} \right) \right]$$

$$= \exp\left[\frac{1}{\omega_1\omega_2} \sum_{l=1}^{N_f}\sum_{a=1}^{N}\sum_{\pm} \left(\mathrm{Li}_3(e^{\pm M_l+i\alpha_a}) + \mathrm{Li}_3(e^{\pm M_l-i\alpha_a}) \right) \right] \equiv \exp\left[-\frac{\mathcal{F}_{mat}^{fund}(\alpha_a, M_l)}{\omega_1\omega_2} \right] .$$

$$(4.2.15)$$

Here, we used the power series definition of the trilogarithm function in appendix A. Δ here can be taken back to be the one satisfying (4.2.9). It is important to remember that the imaginary parts of chemical potentials may be kept nonzero and $\mathcal{O}(1)$, to obstruct boson/fermion cancelations as in [74, 75]. (Especially, those of Δ and m will play important roles later.) On the other hand, the real parts in the Cardy limit are either kept small (for Δ) or just set to 0 (for m, M_l, since we are uninterested in such continuations). The integral contours for the variables $e^{i\alpha_a}$'s are all along the unit circle, $|e^{i\alpha_a}| = 1$.

The instanton part Z_{inst} is subtler, and needs a more careful study. So far, Z_{inst} is understood only as a series expansion in certain fugacity. Canonically, the fugacity q for the $U(1)_I$ flavor symmetry is the expansion parameter of Z_{inst}. As we shall consider dual AdS_6 black holes which do not carry flavor charges, we set $q = 1$ (or to a generic order 1 value so that it does not provide an expansion

parameter). This qualitatively corresponds to taking the 5d gauge coupling to infinity. So apparently, the series which sums over the instanton number k is unsuppressed. The proper way of understanding (4.2.2), (4.2.3) was explained in [124], as a series expansion in the fugacity x. However, in our Cardy limit, we take $|x| \to 1^-$, so that it is unclear how to understand Z_{inst} part. Here, we quote an idea explored in [67], which is to focus on a particular large N saddle point of N integral variables. The integral variables of [67] are N real scalars ϕ, while the analogous N variables in our problem will be analytically continued α_a's in their imaginary directions. (Namely, $-i\alpha_a > 0$ with purely imaginary α_a's will play the role of ϕ of [67].) [67] considered a saddle point in which the N scalars are spread with a wide width $N^{\frac{1}{2}}$ (which is assumed to be the dominant one), and self-consistently showed that the instanton parts can be approximated to $Z_{\text{inst}} \approx 1$. A simple argument for ignoring the instanton part was presented in [67], based on the renormalized gauge coupling in the Coulomb branch of 5d SCFT. In the next paragraph and in appendix B of [78], we shall correct some naive 1-loop arguments in [67] made for this conclusion. However, this will not spoil their final conclusion that $Z_{\text{inst}} \approx 1$.

The idea of [67] is that, if the scalar VEV ϕ is nonzero, there is a nonzero 1-loop contribution to the 5d gauge coupling in the Coulomb branch. The 1-loop effective coupling which depends on the scalar schematically takes the form of

$$\frac{1}{g_{\text{eff}}^2(\phi)} \sim (8 - N_f)|\phi| \qquad (4.2.16)$$

at infinite bare coupling (corresponding to $q = 1$ in our setting). This expression is in fact slightly imprecise. This is because $\frac{1}{g_{\text{eff}}^2(\phi)}$ is the coefficient of the kinetic term of the Coulomb branch fields, so should be an $N \times N$ matrix in our $Sp(N)$ theory. The above expression should be understood as a schematic expression for the eigenvalues, where ϕ denotes a component of the N Coulomb VEVs.

The key argument of [67] is that the mass of instantons is basically the inverse-square of the gauge coupling, so in the Coulomb branch it should also acquire a contribution of the form (4.2.16). If this is the case, and if the saddle point values of ϕ's are large, the k instanton correction would come with a suppression factor of $\sim e^{-k(8-N_f)|\phi|}$, with $|\phi| \sim N^{\frac{1}{2}}$. This was the argument for self-consistently approximating $Z_{\text{inst}} \approx 1$. However, we find that such a 1-loop argument is incomplete, for the following reason. In the brane setting, $\frac{1}{g_{\text{eff}}^2(\phi)}$ is given by the running dilaton field sourced by O8-D8, where ϕ is the coordinate for the transverse direction to the 8-branes. If a D4-brane is at the location ϕ, the D0-brane ($\sim$ instanton) bound to it will find $\frac{1}{g_{\text{eff}}^2(\phi)}$ is its mass. However, if one studies the detailed structures of Z_{inst} for this system, D0-branes can be stuck not only to N separated D4-branes. They can also be bound to the O8-plane at $\phi = 0$, still contributing to the 5d QFT spectrum. Details are explained in appendix B of [78]. Therefore, the 1-loop argument of regarding $\frac{1}{g_{\text{eff}}^2(\phi)}$ as the instanton mass and the suppression factor is incorrect. Had such a claim been true, one would have expected the suppression factor of $e^{-k(8-N_f)|\phi|}$ at k instanton sector, with real $\phi \equiv -i\alpha \sim N^{\frac{1}{2}}$. However, as explained in appendix B of [78], the D0-branes bound to O8 turns out to have lighter quantum masses, so that the true suppression factor for k instantons turns out to be

$$
\begin{aligned}
N_f \neq 0 &: \quad \sim e^{-k|\phi|} \\
N_f = 0 &: \quad \sim e^{-2k|\phi|} \ .
\end{aligned}
\tag{4.2.17}
$$

For most values of N_f, this is larger than the naively estimated suppression factors.[1] In any case, although the detailed estimates in the literature are incorrect, the final conclusion $Z_{\text{inst}} \approx 1$ will not change. Among the N eigenvalues

---

[1]More fundamentally, such exotic masses are allowed since the instanton masses cannot be determined just from the 5d effective action in the Coulomb branch. For instance, the argument above for D0-D4 bounds uses string theory.

α_a, most of them will take large imaginary values $\propto N^{\frac{1}{2}}$, so that the above suppression factors are indeed small. α_a will not be large for some eigenvalues, but their number is much smaller than N so that the leading large N free energy will not be affected [67].

In our problem, we shall consider the large N and Cardy limit $\omega_{1,2} \to 0$ together, seeking for a similar saddle point. Our large N saddle point will complexify the angle variables α_a, into cylinders. The complexified α_a's will be spread at order $\mathcal{O}(\sqrt{N})$ in their imaginary directions. This is very similar to the studies made with the 5d topological indices [126]. Therefore, with such spreadings of eigenvalues assumed (to be shown later in this section), the instanton contribution to the free energy is exponentially suppressed at large N. So we shall ignore the instanton contribution to $\log Z$ from now. More comments on these large N saddle point, and the subtle roles of Z_{inst}, will be postponed to section 2.4. With these understood, approximately setting $Z_{\text{inst}} \approx 1$, one obtains the following expression for the large N Cardy index at $|\omega_i| \ll 1$:

$$
\begin{aligned}
Z(\omega_1,\,\omega_2,\,\Delta,\,m,\,M_l) &\sim \frac{1}{2^N N!} \oint \prod_{a=1}^{N} \frac{d\alpha_a}{2\pi} \exp\left[-\frac{\mathcal{F}^{pert}(\alpha_a,\,\Delta,\,m,\,M_l)}{\omega_1 \omega_2} \right] \\
&\equiv \frac{1}{2^N N!} \oint \prod_{a=1}^{N} \frac{d\alpha_a}{2\pi} \exp\left[-\frac{\mathcal{F}_{vec} + \mathcal{F}_{mat}^{asym} + \mathcal{F}_{mat}^{fund}}{\omega_1 \omega_2} \right],
\end{aligned}
$$

(4.2.18)

where $\mathcal{F}^{pert}$ is the perturbative part of the effective action.

At $|\omega_{1,2}| \to 0$ and $N \gg 1$, one can evaluate (4.2.18) by a saddle point method. We assume that the eigenvalues are spread at order $\mathcal{O}(N^\alpha)$, with $0 < \alpha < 1$, in the imaginary direction at large N [67, 126]. The ansatz for the eigenvalue distribution is given by

$$
\alpha_a = i N^\alpha x_a \quad (0 < x_a < x_*) .
$$

(4.2.19)

Here, x_a's are of order $\mathcal{O}(N^0)$, and the value of α will be determined later.

We restricted $\text{Im}(\alpha_a) > 0$ and also ordered x_a's to be increasing, using the Weyl symmetry of $Sp(N)$, setting $0 < x_1 < x_2 < \cdots < x_N$. Since we assume $0 < \alpha < 1$, the N eigenvalues will be densely distributed on an interval of length $\sim N^\alpha$. The range $(0, x_*)$ will be determined later. We take the continuum limit by defining the continuous variable $x \in (0, x_*)$ and introducing the density function of eigenvalues $\rho(x) = \frac{1}{N}\frac{da}{dx}$ normalized as $\int \rho(x) dx = 1$. Then we replace the sum over a by an integral of the form

$$\sum_{a=1}^{N} \rightarrow N \int_0^{x_*} dx \rho(x) \,, \tag{4.2.20}$$

in the $N \rightarrow \infty$ continuum limit.

Before proceeding, we note again that the chemical potentials m, M_l all have $4\pi i$ periodicity. We shall assume that all parameters m, M_l are purely imaginary, and put them in the 'canonical chamber' $(0, 4\pi i)$. The expressions of the free energy in different chambers can be found by periodic shifts of the variables. Applying the ansatz (4.2.19) and taking the continuum limit (4.2.20), the contribution of the antisymmetric hypermultiplet is given by

$$\mathcal{F}_{mat}^{asym} = -N^2 \int_0^{x_*} dx \rho(x) \int_x^{x_*} dx' \rho(x') \sum_{\pm} \left[\text{Li}_3(e^{-N^\alpha(x+x')\pm\frac{m}{2}}) + \text{Li}_3(e^{-N^\alpha(-x+x')\pm\frac{m}{2}}) \right. \tag{4.2.21}$$

$$\left. + \text{Li}_3(e^{N^\alpha(x+x')\pm\frac{m}{2}}) + \text{Li}_3(e^{N^\alpha(-x+x')\pm\frac{m}{2}}) \right]$$

$$\sim \frac{2}{3} N^{2+\alpha} \int_0^{x_*} dx \rho(x) \int_x^{x_*} dx' \rho(x') \left[\left(3\frac{m}{2}\left(\frac{m}{2} - 2\pi i\right) - 2\pi^2 \right) x' + N^{2\alpha}(x'^3 + 3x^2 x') \right] \,,$$

where m is in the range $(0, 4\pi i)$, as explained above. Here, we used the trilogarithm formulae in appendix A at $N \rightarrow \infty$. Similarly, the fundamental hypermultiplet contribution is given by

$$\mathcal{F}_{mat}^{fund} = -N \sum_{l=1}^{N_f} \int_0^{x_*} dx \rho(x) \sum_{\pm} \left[\text{Li}_3(e^{-N^\alpha x \pm M_l}) + \text{Li}_3(e^{N^\alpha x \pm M_l}) \right]$$

$$\sim \frac{1}{3} N^{1+3\alpha} \sum_{l=1}^{N_f} \int_0^{x_*} dx \rho(x) x^3 = \frac{N_f}{3} N^{1+3\alpha} \int_0^{x_*} dx \rho(x) x^3 \tag{4.2.22}$$

Finally, the vector multiplet contribution is given by

$$\mathcal{F}_{vec} = N \int_0^{x_*} dx \rho(x) \sum_{\pm} \left[\mathrm{Li}_3(-e^{-2N^\alpha x \pm \frac{\Delta}{2}}) + \mathrm{Li}_3(-e^{2N^\alpha x \pm \frac{\Delta}{2}}) \right] \tag{4.2.23}$$

$$+ N^2 \int_0^{x_*} dx \rho(x) \int_x^{x_*} dx' \rho(x') \sum_{\pm} \left[\mathrm{Li}_3(-e^{-N^\alpha(x+x') \pm \frac{\Delta}{2}}) + \mathrm{Li}_3(-e^{-N^\alpha(-x+x') \pm \frac{\Delta}{2}}) \right.$$

$$\left. + \mathrm{Li}_3(-e^{N^\alpha(x+x') \pm \frac{\Delta}{2}}) + \mathrm{Li}_3(-e^{N^\alpha(-x+x') \pm \frac{\Delta}{2}}) \right]$$

$$\sim \quad -\frac{8}{3} N^{1+3\alpha} \int_0^{x_*} dx \rho(x) x^3$$

$$+ N^2 \int_0^{x_*} dx \rho(x) \int_x^{x_*} dx' \rho(x') \sum_{\pm} \left[\mathrm{Li}_3(e^{N^\alpha(x+x') \pm \frac{\omega_1+\omega_2}{2}}) + \mathrm{Li}_3(e^{N^\alpha(-x+x') \pm \frac{\omega_1+\omega_2}{2}}) \right]$$

$$\sim -\frac{8}{3} N^{1+3\alpha} \int_0^{x_*} dx \rho(x) x^3$$

$$- \frac{2}{3} N^{2+\alpha} \int_0^{x_*} dx \rho(x) \int_x^{x_*} dx' \rho(x') \left[\left(3 \left(\frac{\Delta}{2} + \pi i \right) \left(\frac{\Delta}{2} - \pi i \right) - 2\pi^2 \right) x' + N^{2\alpha}(x'^3 + 3x^2 x') \right] ,$$

where $\Delta \approx 2\pi i$, and we also used (4.2.9).[2] Note that in the final expressions of $\mathcal{F}_{mat}^{asum}$, $\mathcal{F}_{vec}$, the last terms $\sim N^{2\alpha}(x'^3 + 3x^2 x')$ in the integrand look more dominant than the remaining terms. We keep the apparently subdominant terms in foresight, as they will be dominant after a partial cancelation at the saddle point.

Collecting all, one obtains

$$\mathcal{F}^{pert} \sim -\frac{8 - N_f}{3} N^{1+3\alpha} \int_0^{x_*} dx \rho(x) x^3 + 2\gamma N^{2+\alpha} \int_0^{x_*} dx \rho(x) \int_x^{x_*} dx' \rho(x') x' , \tag{4.2.24}$$

$$\gamma \equiv \frac{m}{2} \left(\frac{m}{2} - 2\pi i \right) - \left(\frac{\Delta}{2} + \pi i \right) \left(\frac{\Delta}{2} - \pi i \right) > 0 \quad \text{with } 0 < -im < 4\pi , \ \Delta \approx 2\pi i .$$

For later convenience, we will use the following alternative expression for the

---

[2]Here we applied a trilogarithm formula in appendix A valid for $-2\pi < -i\Delta < 2\pi$. The value $\Delta \approx 2\pi i$ constrained by (4.2.9) is actually close to the edge of this interval, so one might wonder if using this formula is valid. We performed a similar calculus for $2\pi < -i\Delta < 6\pi$ and confirmed the continuity of $\mathcal{F}_{vec}$ at $\Delta = 2\pi i$, so that using (4.2.23) near $\Delta = 2\pi i$ is fine.

last integral:

$$\int_0^{x_*} dx\rho(x) \int_x^{x_*} dx'\rho(x')x' = \int_0^{x_*} dx' \int_0^{x'} dx\,\rho(x)\rho(x')x' = \int_0^{x_*} dx \int_0^{x} dx'\,\rho(x')\rho(x)x$$

$$= \frac{1}{2}\left[\int_0^{x_*} dx \int_0^{x} dx'\,\rho(x)\rho(x')x + \int_0^{x_*} dx \int_x^{x_*} dx'\,\rho(x)\rho(x')x'\right]$$

$$= \frac{1}{2}\int_0^{x_*}\int_0^{x_*} dx\,dx'\rho(x)\rho(x')\frac{x+x'+|x-x'|}{2}\ . \qquad (4.2.25)$$

We extremize (4.2.24) in $\rho(x)$, where $\rho(x)$ is nonzero only in $0 < x < x_*$, and satisfies $\int_0^{x_*}\rho(x)dx = 1$, $\rho(x) \geq 0$. To find a nontrivial saddle point at $N \to \infty$, all terms should be of the same order in N. So we set

$$N^{1+3\alpha} = N^{2+\alpha} \ \to \ \alpha = \frac{1}{2}\ , \qquad (4.2.26)$$

which implies $\mathcal{F} \propto N^{\frac{5}{2}}$. Also note that this setting justifies ignoring the instanton corrections, as explained earlier in this section. Introducing the Lagrange multiplier λ for the constraint $\int_0^{x_*}\rho(x)dx = 1$, one should extremize

$$\mathcal{F} = N^{\frac{5}{2}}\left[-\lambda\left(\int_0^{x_*}\rho(x)dx - 1\right) - \frac{8-N_f}{3}\int_0^{x_*}dx\rho(x)x^3 + \gamma\int_0^{x_*}\int_0^{x_*} dx\,dx'\rho(x)\rho(x')\frac{x+x'+|x-x'|}{2}\right]\ .$$

$$(4.2.27)$$

The other constraint $\rho(x) \geq 0$ is to be confirmed later, after obtaining the extremal solution. Extremizing this functional with $\rho(x)$, one obtains

$$\lambda + \frac{8-N_f}{3}x^3 = \gamma\int_0^{x_*} dx'\rho(x')\left(x+x'+|x-x'|\right) = 2\gamma\left[x\int_0^{x} dx'\rho(x') + \int_x^{x_*} dx'\rho(x')x'\right]\ .$$

$$(4.2.28)$$

Differentiating this equation with x, one obtains

$$(8-N_f)x^2 = 2\gamma\left[\int_0^{x} dx'\rho(x') + x\rho(x) - \rho(x)x\right] = 2\gamma\int_0^{x} dx'\rho(x')\ . \quad (4.2.29)$$

Differentiating once more with x, one obtains

$$\rho(x) = \frac{8-N_f}{\gamma}x \geq 0 \quad (x \in [0, x_*])\ . \qquad (4.2.30)$$

$\rho(x)$ is always positive for $x > 0$, since $\gamma > 0$ and $N_f \leq 7$. From $\int_0^{x_*} \rho(x)dx = 1$, one obtains

$$x_* = \sqrt{\frac{2\gamma}{8 - N_f}} \ . \tag{4.2.31}$$

λ is determined by (4.2.28), whose solution is $\lambda = \frac{2(8-N_f)}{3}x_*^3$. Inserting these solutions (4.2.30), (4.2.31) into (4.2.27), one obtains

$$\mathcal{F} \sim \frac{8\sqrt{2}}{15}\frac{N^{\frac{5}{2}}}{\sqrt{8 - N_f}}\gamma^{\frac{3}{2}} \ . \tag{4.2.32}$$

So the large N and Cardy free energy is given by

$$\log Z \sim -\frac{8\sqrt{2}}{15}\frac{N^{\frac{5}{2}}}{\sqrt{8 - N_f}}\frac{\gamma^{\frac{3}{2}}}{\omega_1\omega_2} \ , \tag{4.2.33}$$

where

$$\gamma = \frac{m}{2}\left(\frac{m}{2} - 2\pi i\right) - \left(\frac{\Delta}{2} + \pi i\right)\left(\frac{\Delta}{2} - \pi i\right) = -\frac{(\Delta + \hat{m})(\Delta - \hat{m})}{4} > 0 \ , \tag{4.2.34}$$

where we defined $\hat{m} = m - 2\pi i$.

To summarize, the large N and Cardy free energy of the index (4.2.33) is given by

$$\log Z \sim -i\frac{\sqrt{2}}{15}\frac{N^{\frac{5}{2}}}{\sqrt{8 - N_f}}\frac{[(\Delta + \hat{m})(\Delta - \hat{m})]^{\frac{3}{2}}}{\omega_1\omega_2} \ , \tag{4.2.35}$$

subject to the constraint

$$\Delta - \omega_1 - \omega_2 = 2\pi i \ , \tag{4.2.36}$$

in the Cardy-like limit $|\omega_i| \ll 1$. $\Delta^2 - \hat{m}^2$ appearing in the square-root is negative in our canonical chamber. The expression (4.2.35) and similar expressions at the end of section 2.2 are obtained with the convention $(-1)^{\frac{3}{2}} = -i$. In section 2.3, we shall explain that this free energy counts the dual BPS black holes in the background of warped $AdS_6 \times S^4/\mathbb{Z}_2$ product. Here we simply note that

the leading large N free energy $\propto N^{\frac{5}{2}}$ does not see the flavor symmetries, e.g. M_l's and q for $SO(2N_f) \times U(1)_I \subset E_{N_f+1}$. This is natural in the bulk dual because the states charged under E_{N_f+1} are localized on a codimension 1 wall, $S^3 \sim \partial(S^4/\mathbb{Z}_2)$, so that the leading large N bulk physics does not see them. However, the value of N_f itself is visible in the leading free energy. This is because the number of D8-branes affects the bulk dilaton field.

4.2.2 $SU(2N)$ theories

Similar to the studies of section 4.2.1, we analyze the large N and Cardy free energy of the index for 5d $\mathcal{N} = 1$ gauge theory with $SU(2N)$ gauge group, two rank 2 antisymmetric hypermultiplets, and N_f fundamental hypermultiplets. The related geometric settings are explained at the beginning of this section. The index is defined as [124]

$$Z(\omega_1, \omega_2, \Delta, m, M, q) = \text{Tr}\left[(-1)^F e^{-\beta\{Q,S\}} e^{-\omega_1 J_1} e^{-\omega_2 J_2} e^{-(\Delta - 2\pi i)R} e^{-mh_M - bh_B} e^{-\sum_l M_l H_l} q^k \right].$$
(4.2.37)

We introduced the fugacities e^{-m}, e^{-b} for the Cartans h_M, h_B of $SU(2)_M \times U(1)_B \cong U(2)$ acting on two antisymmetric matters, and the fugacities e^{-M_l} for the Cartans H_l of $U(N_f)$ acting on fundamental matters. As before, the parameters should meet the constraint $\Delta - \omega_1 - \omega_2 = 2\pi i$ for Z to be an index. Again, the index is given by [51, 124]

$$Z(\omega_{1,2}, \Delta, m, b, M_l, q) = \oint [d\alpha] \text{PE}\big[f_{vec}(\omega_{1,2}, \Delta, \alpha_a) + f_{mat}^{asym}(\omega_{1,2}, m, b, \alpha_a) + f_{mat}^{fund}(\omega_{1,2}, M_l, \alpha_a) \big]$$
$$\times \prod_{\pm} Z_{\text{inst}}(\pm\omega_1, \pm\omega_2, \pm\Delta, \pm m, \pm b, \pm M_l, \pm\alpha_a, q^{\pm 1}) .$$
(4.2.38)

The Haar measure is given by $[d\alpha] = \frac{1}{(2N)!} \left[\prod_a \frac{d\alpha_a}{2\pi} \right] \prod_{a<b} \left[2\sin\left(\frac{\alpha_a - \alpha_b}{2} \right) \right]^2$, with $\sum_{a=1}^{2N} \alpha_a = 0$. Sum of all α_a's vanishes because the gauge group is $SU(2N)$. The

letter indices are given by

$$
\begin{aligned}
\tilde{f}_{vec} &= -\frac{2\cosh\frac{\tilde{\Delta}}{2}}{2\sinh\frac{\omega_1}{2}\cdot 2\sinh\frac{\omega_2}{2}}\left[\sum_{a<b}^{2N}\left(e^{-i\alpha_a+i\alpha_b}+e^{i\alpha_a-i\alpha_b}\right)\right]+\left(1-\frac{2\cosh\frac{\tilde{\Delta}}{2}}{2\sinh\frac{\omega_1}{2}\cdot 2\sinh\frac{\omega_1}{2}}\right)(2N-1)\ , \\
f_{mat}^{asym} &= \frac{2\cosh\frac{m}{2}}{2\sinh\frac{\omega_1}{2}\cdot 2\sinh\frac{\omega_2}{2}}\sum_{a<b}^{2N}\left(e^{\frac{b}{2}+i\alpha_a+i\alpha_b}+e^{-\frac{b}{2}-i\alpha_a-i\alpha_b}\right)\ , \\
f_{mat}^{fund} &= \frac{1}{2\sinh\frac{\omega_1}{2}\cdot 2\sinh\frac{\omega_2}{2}}\sum_{l=1}^{N_f}\sum_{a=1}^{2N}\left(e^{M_l+i\alpha_a}+e^{-M_l-i\alpha_a}\right)\ ,
\end{aligned}
\tag{4.2.39}
$$

where $\tilde{\Delta}=\Delta-2\pi i$. As in section 2.1, the Haar measure contribution is absorbed into $\tilde{f}_{vec}$. The instanton part Z_{inst} can be computed from the ADHM construction of multi-instantons [132]. We assume $Z_{\text{inst}}\approx 1$ at the large N saddle point that we shall present below. We believe this can be shown using the methods of [132]. With this assumed, and following the steps similar to section 4.2.1, PE of the letter indices in the Cardy limit $|\omega_i|\ll 1$ are given by

$$
\begin{aligned}
\mathrm{PE}\left[\tilde{f}_{vec}\right] &\sim \exp\left[-\frac{1}{\omega_1\omega_2}\sum_{a<b}^{2N}\sum_{\pm,\pm}\mathrm{Li}_3(-e^{\pm\frac{\Delta}{2}\pm i(\alpha_a-\alpha_b)})\right]\equiv\exp\left[-\frac{\mathcal{F}_{vec}(\alpha_a,\,\Delta)}{\omega_1\omega_2}\right]\ , \\
\mathrm{PE}\left[f_{mat}^{asym}\right] &\sim \exp\left[\frac{1}{\omega_1\omega_2}\sum_{a<b}^{2N}\sum_{\pm,\pm}\mathrm{Li}_3(e^{\pm\frac{m}{2}\pm(\frac{b}{2}+i\alpha_a+i\alpha_b)})\right]\equiv\exp\left[-\frac{\mathcal{F}_{mat}^{asym}(\alpha_a,\,m,\,b)}{\omega_1\omega_2}\right]\ , \\
\mathrm{PE}\left[f_{mat}^{fund}\right] &\sim \exp\left[\frac{1}{\omega_1\omega_2}\sum_{l=1}^{N_f}\sum_{a=1}^{2N}\sum_{\pm}\mathrm{Li}_3(e^{\pm(M_l+i\alpha_a)})\right]\equiv\exp\left[-\frac{\mathcal{F}_{mat}^{fund}(\alpha_a,\,M_l)}{\omega_1\omega_2}\right]
\end{aligned}
\tag{4.2.40}
$$

The index is then given by the following expression,

$$
\begin{aligned}
Z(\omega_1,\,\omega_2,\,\Delta,\,m,\,b,\,M_l) &\sim \frac{1}{(2N)!}\oint\prod_{a=1}^{2N}\frac{d\alpha_a}{2\pi}\exp\left[-\frac{\mathcal{F}^{pert}(\alpha_a,\,\Delta,\,m,\,b,\,M_l)}{\omega_1\omega_2}\right] \\
&\equiv \frac{1}{(2N)!}\oint\prod_{a=1}^{2N}\frac{d\alpha_a}{2\pi}\exp\left[-\frac{\mathcal{F}_{vec}+\mathcal{F}_{mat}^{asym}+\mathcal{F}_{mat}^{fund}}{\omega_1\omega_2}\right]\ .
\end{aligned}
\tag{4.2.41}
$$

We study the saddle point in the large N and Cardy limit. We again take

the following ansatz for the eigenvalue distribution:

$$\alpha_a = iN^\alpha \tilde{x}_a \ , \quad \sum_{a=1}^{2N} \tilde{x}_a = 0 \ , \tag{4.2.42}$$

where $\tilde{x}_a$'s are of order $\mathcal{O}(N^0)$, and $0 < \alpha < 1$. We order $\tilde{x}_a$'s to be increasing using the Weyl symmetry of $SU(2N)$, i.e. $\tilde{x}_1 < \tilde{x}_2 < \cdots < \tilde{x}_{2N}$. With the ansatz (4.2.42), $\mathcal{F}_{mat}^{asym}$ is given by

$$\begin{aligned}
\mathcal{F}_{mat}^{asym} &= -\sum_{a<b}^{2N}\sum_{\pm} \left[\mathrm{Li}_3(e^{-N^\alpha(\tilde{x}_a+\tilde{x}_b)\pm\frac{m}{2}+\frac{b}{2}}) + \mathrm{Li}_3(e^{N^\alpha(\tilde{x}_a+\tilde{x}_b)\pm\frac{m}{2}-\frac{b}{2}}) \right] \\
&\sim \frac{1}{3}N^\alpha \sum_{a<b}^{2N} \left[\left\{ \frac{3}{2}\frac{m+b}{2}\left(\frac{m+b}{2}-2\pi i\right) + \frac{3}{2}\frac{m-b}{2}\left(\frac{m-b}{2}-2\pi i\right) - 2\pi^2 \right\} |\tilde{x}_a+\tilde{x}_b| \right. \\
&\qquad\qquad \left. -\frac{3}{2}N^\alpha b\, \mathrm{sgn}(\tilde{x}_a+\tilde{x}_b)|\tilde{x}_a+\tilde{x}_b|^2 + N^{2\alpha}|\tilde{x}_a+\tilde{x}_b|^3 \right] \ , \tag{4.2.43}
\end{aligned}$$

where $m \pm b$ are understood to be in the range $(0, 4\pi i)$. Here, we used the trilogarithm formulae in appendix A at $N \to \infty$. Similarly, $\mathcal{F}_{mat}^{fund}$, $\mathcal{F}_{vec}$ are given by

$$\mathcal{F}_{mat}^{fund} = -\sum_{l=1}^{N_f}\sum_{a=1}^{2N} \left[\mathrm{Li}_3(e^{-N^\alpha\tilde{x}_a+M_l}) + \mathrm{Li}_3(e^{N^\alpha\tilde{x}_a-M_l}) \right] \sim \frac{1}{6}N^{3\alpha}\sum_{l=1}^{N_f}\sum_{a=1}^{2N}|\tilde{x}_a|^3 = \frac{N_f}{6}N^{3\alpha}\sum_{a=1}^{2N}|\tilde{x}_a|^3 \tag{4.2.44}$$

and

$$\begin{aligned}
\mathcal{F}_{vec} &= \sum_{a<b}^{2N}\sum_{\pm} \left[\mathrm{Li}_3(-e^{-N^\alpha(-\tilde{x}_a+\tilde{x}_b)\pm\frac{\Delta}{2}}) + \mathrm{Li}_3(-e^{N^\alpha(-\tilde{x}_a+\tilde{x}_b)\pm\frac{\Delta}{2}}) \right] \\
&\sim \sum_{a<b}^{2N}\sum_{\pm} \mathrm{Li}_3(e^{N^\alpha(-\tilde{x}_a+\tilde{x}_b)\pm\frac{\omega_1+\omega_2}{2}}) \tag{4.2.45} \\
&\sim -\frac{1}{3}N^\alpha \sum_{a<b}^{2N} \left[\left(3\left(\frac{\Delta}{2}+\pi i\right)\left(\frac{\Delta}{2}-\pi i\right) - 2\pi^2\right)(\tilde{x}_b-\tilde{x}_a) + N^{2\alpha}(\tilde{x}_b-\tilde{x}_a)^3 \right] \ ,
\end{aligned}$$

where $\Delta \approx 2\pi i$, and we used $\Delta - \omega_1 - \omega_2 = 2\pi i$. Again, we have shown apparently subleading terms in N^{-1} in foresight, which will turn out to be dominant after

extremization and cancelations. Collecting all, $\mathcal{F}^{pert} = \mathcal{F}_{vec} + \mathcal{F}_{mat}^{asym} + \mathcal{F}_{mat}^{fund}$ is given by

$$\mathcal{F}^{pert} \sim \frac{N_f}{6} N^{3\alpha} \sum_{a=1}^{2N} |\tilde{x}_a|^3 + \frac{1}{2} N^{\alpha} \sum_{a \neq b}^{2N} (\gamma_m |\tilde{x}_b + \tilde{x}_a| - \gamma_\Delta |\tilde{x}_b - \tilde{x}_a|) - \frac{\pi^2}{3} N^{\alpha} \sum_{a \neq b}^{2N} (|\tilde{x}_b + \tilde{x}_a| - |\tilde{x}_b - \tilde{x}_a|)$$

$$-\frac{1}{4} N^{2\alpha} b \sum_{a \neq b}^{2N} \text{sgn}(\tilde{x}_a + \tilde{x}_b)|\tilde{x}_a + \tilde{x}_b|^2 + \frac{1}{6} N^{3\alpha} \sum_{a \neq b}^{2N} \left(|\tilde{x}_b + \tilde{x}_a|^3 - |\tilde{x}_b - \tilde{x}_a|^3 \right) \ ,$$

$$\gamma_m \equiv \frac{1}{2} \sum_{\pm} \frac{m \pm b}{2} \left(\frac{m \pm b}{2} - 2\pi i \right) \ , \quad \gamma_\Delta \equiv \left(\frac{\Delta}{2} + \pi i \right) \left(\frac{\Delta}{2} - \pi i \right) \ . \tag{4.2.46}$$

At this moment, the leading contribution to (4.2.46) at large N comes from the last term which is of order $O(N^{2+3\alpha})$. So we extremize the last term. The analysis is similar to [67]. To find a saddle point of the last term, we define

$$x_{N+1-a} \equiv \frac{\tilde{x}_{2N+1-a} - \tilde{x}_a}{2} \ , \quad y_{N+1-a} \equiv \frac{\tilde{x}_{2N+1-a} + \tilde{x}_a}{2} \quad (1 \leq a \leq N) \ . \tag{4.2.47}$$

Let us first consider the extremization with y_{N+1-a}'s. Differentiating the last term of (4.2.46), one obtains

$$0 = \frac{\partial}{\partial y_{N+1-i}} \sum_{a \neq b}^{2N} \left(|\tilde{x}_b + \tilde{x}_a|^3 - |\tilde{x}_b - \tilde{x}_a|^3 \right) = \left(\frac{\partial}{\partial \tilde{x}_{2N+1-i}} + \frac{\partial}{\partial \tilde{x}_i} \right) \sum_{a \neq b}^{2N} \left(|\tilde{x}_b + \tilde{x}_a|^3 - |\tilde{x}_b - \tilde{x}_a|^3 \right)$$

$$= 6 \sum_{a \neq i}^{2N} \left(\text{sgn}(\tilde{x}_i + \tilde{x}_a)(\tilde{x}_i + \tilde{x}_a)^2 - \text{sgn}(\tilde{x}_i - \tilde{x}_a)(\tilde{x}_i - \tilde{x}_a)^2 \right) \tag{4.2.48}$$

$$+6 \sum_{a \neq 2N+1-i}^{2N} \left(\text{sgn}(\tilde{x}_{2N+1-i} + \tilde{x}_a)(\tilde{x}_{2N+1-i} + \tilde{x}_a)^2 - \text{sgn}(\tilde{x}_{2N+1-i} - \tilde{x}_a)(\tilde{x}_{2N+1-i} - \tilde{x}_a)^2 \right) \ ,$$

where $1 \leq i \leq N$. One can find that a solution is given by [67]

$$- \tilde{x}_a = \tilde{x}_{2N+1-a} = x_{N+1-a} \quad (1 \leq a \leq N) \ . \tag{4.2.49}$$

So on this solution, we can take N variables x_a's as the remaining variables to extremize with. They are ordered as $0 \leq x_1 < x_2 < \cdots < x_N$. Note that this

solution satisfies the condition $\sum_{a=1}^{2N} \tilde{x}_a = 0$. As in [67], we assume that this solution for δy_{N+1-a} variation is the relevant one for our problem. Then, the remaining problem is to extremize with x_a's. Inserting the saddle point solution for y_a's (4.2.49) to the last term of (4.2.46), one finds

$$\frac{N^{3\alpha}}{6} \sum_{a \neq b}^{2N} \left(|\tilde{x}_b + \tilde{x}_a|^3 - |\tilde{x}_b - \tilde{x}_a|^3 \right) \Bigg|_{-\tilde{x}_a = \tilde{x}_{2N+1-a}} = -\frac{8N^{3\alpha}}{3} \sum_{a=1}^{N} x_a^3 = O(N^{1+3\alpha}) \,.$$
(4.2.50)

This is of the same order as the first term of (4.2.46). So from now on, one should also consider all other terms in (4.2.46) at the same order. The possible leading terms in (4.2.46) are of order $O(N^{1+3\alpha})$ and $O(N^{2+2\alpha})$ at large N. However, imposing (4.2.49), one can easily check that the terms at order $O(N^{2+2\alpha})$ vanish because of the $\mathrm{sgn}(\tilde{x}_a + \tilde{x}_b)$ factor in those terms. Then we are finally left with terms at $O(N^{1+3\alpha})$ and $O(N^{2+\alpha})$ orders. These two terms will be balanced and provide leading terms. Note that there are also subleading terms at $O(N^{1+\alpha})$ order after inserting (4.2.49) into (4.2.46), which we ignore.

So inserting (4.2.49) into (4.2.46), one obtains

$$\mathcal{F}^{pert} \sim -\frac{8 - N_f}{3} N^{3\alpha} \sum_{a=1}^{N} x_a^3 + \frac{\gamma}{2} N^{\alpha} \sum_{a \neq b}^{2N} |\tilde{x}_b + \tilde{x}_a| \qquad (4.2.51)$$

$$\sim -\frac{8 - N_f}{3} N^{3\alpha} \sum_{a=1}^{N} x_a^3 + \gamma N^{\alpha} \sum_{a<b}^{N} \left(2(x_b + x_a) + 2(x_b - x_a) \right) = -\frac{8 - N_f}{3} N^{3\alpha} \sum_{a=1}^{N} x_a^3 + 4\gamma N^{\alpha} \sum_{a<b}^{N} x_b$$

$$\sim -\frac{8 - N_f}{3} N^{1+3\alpha} \int_0^{x_*} dx \rho(x) x^3 + 4\gamma N^{2+\alpha} \int_0^{x_*} dx \rho(x) \int_x^{x_*} dx' \rho(x') x' \,,$$

where

$$\gamma \equiv \gamma_m - \gamma_\Delta = \frac{1}{2} \sum_{\pm} \frac{m \pm b}{2} \left(\frac{m \pm b}{2} - 2\pi i \right) - \left(\frac{\Delta}{2} + \pi i \right) \left(\frac{\Delta}{2} - \pi i \right) > 0$$
(4.2.52)

if we take $\Delta \approx 2\pi i$ and $m \pm b$ purely imaginary within the canonical range $(0, 4\pi i)$. The above effective action is essentially the same as that for the $Sp(N)$

gauge theory, (4.2.24). The only difference is that double integral part for the $SU(2N)$ gauge theory is twice that of $Sp(N)$ gauge theory. Thus, the remaining extremization procedures are the same as those presented in section 2.1. The resulting free energy is given by

$$\log Z \sim -i\frac{\sqrt{2}}{15}\frac{N^{\frac{5}{2}}}{\sqrt{8-N_f}}\frac{[(\Delta+(\hat{m}+b))(\Delta-(\hat{m}+b))+(\Delta+(\hat{m}-b))(\Delta-(\hat{m}-b))]^{\frac{3}{2}}}{\omega_1\omega_2},$$

(4.2.53)

where $\Delta - \omega_1 - \omega_2 = 2\pi i$, $\hat{m} \equiv m - 2\pi i$.

It is straightforward to generalize this result to the quivers for the general $\mathbb{Z}_n$ orbifold [50, 51]. Assuming $Z_{\text{inst}} \approx 1$, we simply present the final result for the large N and Cardy free energy:

$$\log Z \quad \sim \quad -i\frac{\sqrt{2}}{15}\frac{N^{\frac{5}{2}}}{\sqrt{8-N_f}}\frac{[\sum_A(\Delta+(\hat{m}+b_A))(\Delta-(\hat{m}+b_A))+2\sum_I(\Delta+(\hat{m}+b_I))(\Delta-(\hat{m}+b_I))]^{\frac{3}{2}}}{\omega_1\omega_2},$$

$$N_f \equiv \sum_q N_f^{(q)} \le 7, \ \hat{m} \equiv m - 2\pi i, \ \sum_A b_A + 2\sum_I b_I = 0, \ \Delta - \omega_1 - \omega_2 = 2\pi i. \quad (4.2.54)$$

4.2.3 AdS$_6$ black holes

In this subsection, we explain that the large N Cardy free energies derived in sections 2.1 and 2.2 account for the BPS black holes in the dual AdS$_6$ backgrounds. A crucial ingredient is the universal entropy function of such black holes found in [74].

In principle, general black holes in AdS$_6$ can carry various electric charges dual to the R-charge, mesonic charge, and baryonic charges. However, BPS black hole solution in AdS$_6$ known to date was found in 6d $\mathcal{N} = (1,0)$ $SU(2)$ gauged supergravity [87]. For instance, this 6d theory can be obtained by a consistent Kaluza-Klein truncation of massive type IIA supergravity on $S^4/\mathbb{Z}_2$ [106]. This black hole solution has only one electric charge, corresponding to the $SU(2)$ R-charge R. So to compare our field theory results with known

AdS$_6$ black holes of [87], we should perform Legendre transformations of the free energies (4.2.35), (4.2.53), (4.2.54) at zero mesonic and baryonic charges. Firstly, at generic $n \geq 2$, one should extremize the following entropy function,

$$S(\Delta, m, b_{A,I}, \omega_i; \ R, Q_M, Q_{B_{A,I}}, J_i) = \log Z + \Delta R + m Q_M + \sum_{A,I} b_{A,I} Q_{B_{A,I}} + \omega_1 J_1 + \omega_2 J_2 \ ,$$

(4.2.55)

subject to the constraints

$$\sum_A b_A + 2 \sum_I b_I = 0 \ , \quad \Delta - \omega_1 - \omega_2 = 2\pi i \ .$$

(4.2.56)

$\log Z$ is given by either (4.2.53) or (4.2.54). To compare with known black holes, we set

$$Q_M = 0 \ , \quad Q_{B_A} = 0 \ , \quad Q_{B_I} = 0 \ .$$

(4.2.57)

Let us first consider the baryonic chemical potentials. For $SU(2N)$ gauge theory at $n = 2$, one should extremize

$$-i \frac{\sqrt{2}}{15} \frac{N^{\frac{5}{2}}}{\sqrt{8 - N_f}} \frac{[(\Delta + (\hat{m} + b))(\Delta - (\hat{m} + b)) + (\Delta + (\hat{m} - b))(\Delta - (\hat{m} - b))]^{\frac{3}{2}}}{\omega_1 \omega_2} + b \, Q_B$$

(4.2.58)

with b at $Q_B = 0$. The extremal solutions are given by $b = 0, \pm\sqrt{\Delta^2 - \hat{m}^2}$. However, for the latter two solutions, one finds that $\log Z = 0$ after inserting these values of b. Making further Legendre transformation of $\log Z = 0$ in $\omega_{1,2}$'s and $\hat{m}$ would yield zero entropy, which means that $b = \pm\sqrt{\Delta^2 - \hat{m}^2}$ will not yield the dominant saddle point. So we take the solution $b = 0$. Similarly, for the most general case with $n \geq 2$, one can easily show that the dominant saddle point at zero baryon charges is given by

$$b_A = 0 \ , \quad b_I = 0 \ .$$

(4.2.59)

Inserting this solution (4.2.59) to (4.2.55), one obtains

$$S(\Delta, m, \omega_i; R, Q_M, J_i) = -i\frac{\sqrt{2}}{15}\frac{n^{\frac{3}{2}}N^{\frac{5}{2}}}{\sqrt{8-N_f}}\frac{[(\Delta+\hat{m})(\Delta-\hat{m})]^{\frac{3}{2}}}{\omega_1\omega_2}+\Delta R+mQ_M+\omega_1 J_1+\omega_2 J_2 \ ,$$

(4.2.60)

where $\hat{m} = m - 2\pi i$. Here, note that for the $Sp(N)$ gauge theory at $n = 1$, the free energy (4.2.35) of section 2.1 agrees with the above formula at $n = 1$. So one can use this entropy function for $\Delta, m, \omega_{1,2}$ as universally describing the 5d SCFTs labelled by $n \geq 1$ at zero baryon charges.

We then Legendre transform in m, at $Q_M = 0$. The saddle points for $\hat{m}$ variation at $Q_M = 0$ are given by

$$\hat{m} = 0 \ , \quad \pm\Delta \ .$$

(4.2.61)

Again, the latter two solutions have $\log Z = 0$, so that further Legendre transformation with $\omega_{1,2}$ will yield zero. So the dominant saddle point is given by

$$\hat{m} = 0 \ \rightarrow \ m = 2\pi i \ .$$

(4.2.62)

Inserting this solution for m, we finally obtain the following entropy function:

$$S = -i\frac{\sqrt{2}}{15}\frac{n^{\frac{3}{2}}N^{\frac{5}{2}}}{\sqrt{8-N_f}}\frac{\Delta^3}{\omega_1\omega_2} + \Delta R + \omega_1 J_1 + \omega_2 J_2 \ ,$$

(4.2.63)

subject to the constraint $\Delta - \omega_1 - \omega_2 = 2\pi i$. This form of entropy function was shown in [74] to precisely account for the entropy and chemical potentials of BPS black holes in AdS$_6$. However, the entropy function there was expressed universally, in terms of the Newton constant G of 6d gauged supergravity instead of the microscopic parameters n, N, N_f of our models. In the remaining part of this subsection, we explain the conversion of these parameters to establish the microscopic account for the BPS black holes.

To find the relation between G and N, N_f, n, we need the explicit metric of AdS$_6 \times (S^4/\mathbb{Z}_2)/\mathbb{Z}_n$ in massive type IIA supergravity. It is a warped product of

AdS$_6$ with radius ℓ and half of $S_4/\mathbb{Z}_n$ with radius $\frac{2\ell}{3}$. The 10d metric in string frame is given by [49]

$$ds_{10}^2 = \frac{1}{(\sin\alpha)^{\frac{1}{3}}} \left[\ell^2 ds^2(AdS_6) + \frac{4\ell^2}{9} \left(d\alpha^2 + \cos^2\alpha \, ds^2(S^3/\mathbb{Z}_n) \right) \right] \,, \quad (4.2.64)$$

where $ds^2(AdS_6)$ is the metric of AdS$_6$ with unit radius, and $ds^2(S^3/\mathbb{Z}_n)$ is the metric for $S^3/\mathbb{Z}_n$, whose volume is $\mathrm{vol}(S^3/\mathbb{Z}_n) = \frac{2\pi^2}{n}$. The range of α is given by $\left(0, \frac{\pi}{2}\right]$. The gauge coupling constant g in 6d gauged supergravity is related to the radius ℓ of AdS$_6$ by $g = \ell^{-1}$ [87, 106]. Also, from the quantization of the 4-form flux, ℓ is related to N by [50, 67]

$$\frac{\ell^4}{\ell_s^4} = \frac{18\pi^2 nN}{8 - N_f} \,, \quad (4.2.65)$$

where ℓ_s is the string scale. We will also need the dilaton field, given by [67]

$$e^{-2\Phi} = \frac{3(8 - N_f)^{\frac{3}{2}}\sqrt{nN}}{2\sqrt{2}\pi}(\sin\alpha)^{\frac{5}{3}} \,. \quad (4.2.66)$$

The 10d Newton constant is given by $2\kappa_{10}^2 = 16\pi G_{10} = (2\pi)^7 \ell_s^8$ [67]. The 6d Newton constant is obtained by reducing the 10d Einstein-Hilbert action on $(S^4/\mathbb{Z}_2)/\mathbb{Z}_n$, down to 6d Einstein-Hilbert action. During this reduction, the 6d metric $g_{\mu\nu}$ is embedded into the 10d metric G_{MN} as

$$ds_{10}^2 = G_{MN}dx^M dx^N = \frac{1}{(\sin\alpha)^{\frac{1}{3}}} \left[g_{\mu\nu}dx^\mu dx^\nu + \frac{4\ell^2}{9} \left(d\alpha^2 + \cos^2\alpha \, ds^2(S^3/\mathbb{Z}_n) \right) \right] \,.$$
$$(4.2.67)$$

The 10d Einstein-Hilbert action reduces to 6d as

$$\frac{1}{G_{10}} \int d^{10}x\sqrt{-G}e^{-2\Phi}G^{MN}R_{MN}(G) \;\longrightarrow\; \frac{1}{G}\int d^6x\sqrt{-g}g^{\mu\nu}R_{\mu\nu}(g) \,. \quad (4.2.68)$$

This leads to the following relation:

$$
\begin{aligned}
\frac{1}{G} &= \frac{1}{G_{10}} \int_{(S^4/\mathbb{Z}_2)/\mathbb{Z}_n} d^4x \sqrt{G/g}\, e^{-2\Phi} \times (\sin\alpha)^{\frac{1}{3}} \\
&= \frac{1}{2^3\pi^6\ell_s^8} \int_0^{\frac{\pi}{2}} d\alpha \sqrt{\left(\frac{4\ell^2}{9}\right)^4 (\cos^2\alpha)^3} \cdot \text{vol}(S^3/\mathbb{Z}_n) \cdot \frac{3(8-N_f)^{\frac{3}{2}}\sqrt{nN}}{2\sqrt{2\pi}} (\sin\alpha)^{\frac{5}{3}} \cdot (\sin\alpha)^{-\frac{4}{3}} \\
&= \frac{\sqrt{2}\ell^4}{3^3\pi^5\ell_s^8}(8-N_f)^{\frac{3}{2}} \sqrt{\frac{N}{n}}\frac{9}{20} = \frac{27\sqrt{2}}{5\pi\ell^4}\frac{n^{\frac{3}{2}}N^{\frac{5}{2}}}{\sqrt{8-N_f}} \ .
\end{aligned} \tag{4.2.69}
$$

Here the factor $(\sin\alpha)^{\frac{1}{3}}$ on the first line comes from the relative factor between G^{MN} and $g^{\mu\nu}$ appearing in (4.2.68). Using (4.2.69), (4.2.63) can be rewritten as

$$
S = -i\frac{\pi}{81g^4 G}\frac{\Delta^3}{\omega_1\omega_2} + \Delta R + \omega_1 J_1 + \omega_2 J_2 \ , \tag{4.2.70}
$$

subject to the constraint $\Delta - \omega_1 - \omega_2 = 2\pi i$. This in fact is the universal formula found in [74] and discussed in chapter 2 for any R-charged BPS black holes in AdS$_6$, irrespective of its string theory embedding. In [74], it has been shown that extremizing the above entropy function, and imposing the characteristic charge relation [87] satisfied by these black holes, one obtains the Bekenstein-Hawking entropy and chemical potentials of such black holes.

Before briefly summarizing the key results of [74], let us comment on the intrinsic studies that can be made from the index. Since $\Delta = 2\pi i + \omega_1 + \omega_2$, S takes the form of

$$
S = -\frac{\pi i}{81g^4 G}\frac{(2\pi i + \omega_1 + \omega_2)^3}{\omega_1\omega_2} + \omega_1(R + J_1) + \omega_2(R + J_2) + 2\pi i R \ . \tag{4.2.71}
$$

Therefore, only the two combinations $R + J_1$, $R + J_2$ of charges appear non-trivially in the Legendre transformation, which is natural since this is the free energy of the index. The saddle point value $S_*(R, J_{1,2})$ after the extremization would be complex. One should really consider the degeneracy rather than

entropy, so we study e^{S_*}. This takes the following form:

$$e^{S_*(R,J_1,J_2)} = e^{2\pi i R + i\mathrm{Im}f(R+J_1,R+J_2)} \cdot e^{\mathrm{Re}f(R+J_1,R+J_2)} \ . \qquad (4.2.72)$$

Here, f is a complex function of $R+J_1$, $R+J_2$ that one obtains after extremizing the first three terms of (4.2.71). The first factor is a phase factor which depends on the macroscopic charges R, J_1, J_2, which rapidly oscillates as one changes these charges. For instance, let us first consider the factor $e^{2\pi i R}$. Although R is macroscopic, we know that R is quantized to be a half-integer. Then by changing R by its minimal quantized unit, $e^{2\pi i R}$ will hop between $+1$ and -1. However, it looks highly unclear in general whether the whole phase factor $e^{i(2\pi R + \mathrm{Im}f)}$ is real and hops between ± 1 as the charges are changed by quantized units. At the dominant saddle with largest $e^{\mathrm{Re}f}$, one may change the logic here and demand that the unitarity of QFT guarantees this phase factor to be either ± 1. It appears meaningless to try to check this with the results at hand. This is because we have made a macroscopic saddle point approximation at large charges, and such quantized properties are generally expected to be visible only after including subleading corrections. Anyway, in this strategy, $\mathrm{Re}f(R+J_1,R+J_2)$ would be the macroscopic entropy that one can extract out intrinsically from the index, dressed by the ± 1 factor which is represented by a phase in our macroscopic calculus. This has been often the attitudes assumed in [75, 76].

Now to summarize some key results of [74], we first note that the known BPS black holes of [87] carry two independent parameters. So the charges R, J_1, J_2 satisfy a relation upon the known solutions. [74] imposed this relation, and showed that $\mathrm{Re}f$ agrees with the Bekenstein-Hawking entropy S_{BH} of these

black holes.[3] The resulting $S_{\text{BH}} = \text{Re} f$ is given by [74]

$$S_{\text{BH}}^3 - \frac{2\pi^2}{3g^4 G} S_{\text{BH}}^2 - 12\pi^2 R^2 S_{\text{BH}} + \frac{8\pi^4}{3g^4 G} J_1 J_2 = 0$$

$$R S_{\text{BH}}^2 + \frac{2\pi^2}{9g^4 G}(J_1 + J_2) S_{\text{BH}} - \frac{4\pi^2}{3} R^3 = 0 . \qquad (4.2.73)$$

This is a result derived from QFT by imposing extra charge relation by hand. Solving these two equations, S_{BH} acquires two apparently different expressions in terms of R, J_1, J_2. The compatibility of the two expressions is the charge relation imposed. It was shown in [74] that the Bekenstein-Hawking entropy of the black holes of [87] satisfies precisely the same equations. This establishes the QFT account for the BPS black holes in AdS_6.

Since we have derived $\log Z$ of the dual SCFTs in the Cardy limit $|\omega_{1,2}| \ll 1$, we have microscopically derived the thermodynamics of corresponding large BPS black holes in AdS_6. The Cardy limit $|\omega_{1,2}| \ll 1$ on the known black hole solutions demands $J_1, J_2 \gg R \gg N^{5/2}$. Similar to the $\text{AdS}_5/\text{CFT}_4$ models studied in the literature [75, 76], we generally expect that there could be more complicated and yet unknown black hole saddle points beyond the Cardy limit. However, as shown by [135] in $\text{AdS}_5/\text{CFT}_4$, the known black holes should still represent local large N saddle points, irrespective of whether they are most dominant or not. Here, we note that the entropy function (4.2.70) was shown to describe known black holes even beyond the Cardy limit [74]. If the instanton corrections Z_{inst} can still be ignored to ≈ 1 in the large N non-Cardy regime, it may be technically doable to search for such saddle points. This is beyond the scope of this chapter.

---

[3]Technically, one finds $\text{Im} S_* = 2\pi R + \text{Im} f = 0$ after imposing the charge relation, so that f on these solutions is actually real and equals S_{BH}. We lack an intrinsic QFT understanding, if any, of this phenomenon.

4.2.4 Comments on instantons and 5d deconfinement

While making the saddle point approximations in sections 2.1 and 2.2, we used the perturbative parts of the index only. Here, one might feel confused about the following point. From large N perturbative Yang-Mills theory, one would not expect more than N^2 degrees of freedom. One expects to capture some interesting SCFT physics from formulae like [124] through the instanton part Z_{inst} in the integrand. But in all the large N analyses in the literature for 5d SCFTs, it naively appears that only the perturbative integrand contributes to the large N free energy, with $Z_{\mathrm{inst}} \approx 1$ suppressed. So one may wonder if there are any roles played by Z_{inst} at all. We would like to comment that it plays a subtle role in 'disallowing' the N^2 scaling of the free energy.

Let us first ask the following question. Had the integrand for the index only consisted of the perturbative part,

$$
Z_{\mathrm{pert}}(x, y, \{m\}) = \oint [d\alpha] \mathrm{PE} \left[f_{vec}(x, y, e^{i\alpha_a}) + \sum_{\mathbf{R}} f_{mat}^{\mathbf{R}}(x, y, e^{i\alpha_a}, e^{m_{\mathbf{R}}}) \right]
\tag{4.2.74}
$$

without factors like Z_{inst}, what would have been the expected Cardy free energy in the limit $|\omega_{1,2}| \ll 1$? (Here, $\mathbf{R}$ runs over representations of the gauge group G for hypermultiplets.) The natural answer is already presented in [75, 136, 137] for 4d $\mathcal{N} = 4$ gauge theory, and is extended to 4d $\mathcal{N} = 1$ theories in [138]. Namely, in 4d SUSY gauge theories whose indices take the form of (4.2.74), the Cardy saddle point for the gauge holonomies α_a is such that G is unbroken at the saddle point. In other words, all $e^{i\alpha_a}$ appearing in f_{vec} and $f_{mat}^{\mathbf{R}}$ can be effectively set to $e^{i\alpha_a} = 1$, so that the system is maximally deconfining in the Cardy limit.[4]

---

[4]In 4d Yang-Mills theories, this has been naturally assumed in the literature, e.g. in [57] inspired by the high temperature limit of the Gross-Witten-Wadia model [58, 139].

Had the 5d index been just (4.2.74), we would naturally expect the same holonomy saddle structure because the letter indices basically take the same forms. Most importantly, the letter indices take the form of $\frac{1}{(1-xy)(1-x/y)} = \frac{1}{(1-e^{-\omega_1})(1-e^{-\omega_2})}$ times finite polynomials of fugacities, both in 4d and 5d. So it is natural to expect the same large N and Cardy saddle point structures for these integrals. At these saddle points, the free energy of the index (4.2.74) would be proportional to N^2, naturally agreeing with the combinatoric interpretation of this formula which counts gauge invariant operators of the free theory. Therefore, although Z_{inst} can be ignored at the final stage of our saddle point analyses in sections 2.1 and 2.2, Z_{inst} should somehow play subtle intermediate roles to disfavor the saddle point $e^{i\alpha_a} \sim 1$, rather preferring the complexified saddle point with $-i\alpha_a \sim N^{\frac{1}{2}} \gg 1$.

In fact, one can see that the possibility of the saddle point $e^{i\alpha_a} \sim 1$ becomes highly unclear with the presence of Z_{inst}, for the following reason. For instance, the 1 instanton part of Z_{inst} in our $Sp(N)$ theory is given by [124, 132]

$$
Z_1 = \frac{1}{2}\left[\frac{\prod_{l=1}^{N_f} 2\sinh\frac{M_l}{2} \prod_{a=1}^{N} 2\sinh\frac{m\pm i\alpha_a}{2}}{2\sinh\frac{\omega_{1,2}}{2} \cdot 2\sinh\frac{m\pm\omega_+}{2} \prod_{a=1}^{N} 2\sinh\frac{\omega_+\pm i\alpha_a}{2}} + \frac{\prod_{l=1}^{N_f} 2\cosh\frac{M_l}{2} \prod_{a=1}^{N} 2\cosh\frac{m\pm i\alpha_a}{2}}{2\sinh\frac{\omega_{1,2}}{2} \cdot 2\sinh\frac{m\pm\omega_+}{2} \prod_{a=1}^{N} 2\cosh\frac{\omega_+\pm i\alpha_a}{2}} \right]
$$
$$
- \frac{1}{2} \frac{\prod_{l=1}^{N_f} 2\sinh\frac{M_l}{2} + \prod_{l=1}^{N_f} 2\cosh\frac{M_l}{2}}{2\sinh\frac{\omega_{1,2}}{2} \cdot 2\sinh\frac{m\pm\omega_+}{2}} ,
\tag{4.2.75}
$$

where $\omega_+ \equiv \frac{\omega_1+\omega_2}{2}$. In the Cardy limit $|\omega_{1,2}| \ll 1$, this becomes

$$
Z_1 \sim \frac{1}{2\omega_1\omega_2}\left[\frac{\prod_{l=1}^{N_f} 2\sinh\frac{M_l}{2}}{2\sinh\frac{m}{2}}\left(\prod_{a=1}^{N} \frac{2\sinh\frac{m\pm i\alpha_a}{2}}{2\sinh\frac{\pm i\alpha_a}{2}} - 1\right) + \frac{\prod_{l=1}^{N_f} 2\cosh\frac{M_l}{2}}{2\sinh\frac{m}{2}}\left(\prod_{a=1}^{N} \frac{2\cosh\frac{m\pm i\alpha_a}{2}}{2\cosh\frac{\pm i\alpha_a}{2}} - 1\right) \right] .
$$
$$
\tag{4.2.76}
$$

This diverges at $\alpha_a = 0$ (and also at $\alpha_a = \pi$). From the physics of instantons, this divergence is due to the non-compact zero mode of instanton size becoming massless. More physically, if one expands Z_1 in the fugacities $e^{i\alpha_a}$'s in the Coulomb branch, at $\text{Im}(\alpha_a) > 0$, one finds infinite towers of BPS bound states

with increasing $U(1)^N \subset Sp(N)$ electric charges, since $2\sinh(\frac{i\alpha_a}{2})$ factors appear in the denominator. So the divergence at $\alpha_a = 0$ comes from these infinite towers of non-perturbative charged states in the Coulomb branch, if one ceases to weight them by fugacity factors $e^{i\alpha_a}$. Since this divergence is caused by replacing $\sinh\frac{\omega_+ \pm i\alpha_a}{2}$ by $\sinh\frac{\pm i\alpha_a}{2}$, the divergence actually represents an extra factor of $\frac{1}{(2\sinh\frac{\omega_+}{2})^{2N}} \sim \frac{1}{\omega_+^{2N}}$ in the naive Cardy limit. As one goes to higher instanton numbers $k > 1$, there appear more infinite towers of charged fields. The extra divergent factor becomes $\frac{1}{\omega^{2Nk}}$. An easy way to see this is to note that there are $2c_2 k = 2(N+1)k$ complex zero modes in the k instanton background, where $c_2 = N+1$ is the dual Coxeter number of $Sp(N)$. Among these, $2k$ comes from the position zero modes of k instantons, so that it only causes $\frac{1}{\omega_1\omega_2}$ divergence in the free energy. The remaining $2Nk$ complex zero modes come from the internal degrees of freedom, yielding extra $\frac{1}{\omega^{2Nk}}$ factor.

Had this been the true saddle point, the Cardy free energy is not behaving like the one for a reasonable 5d CFT, which we expect to be proportional to $\frac{1}{\omega_1\omega_2}$ times a coefficient representing the number of degrees of freedom in this CFT (which is $\sim N^{\frac{5}{2}}$ in our problem). It is not even clear whether the sum over k would make sense.[5] So collecting all, we find that it is highly unclear whether $e^{i\alpha_a} \sim 1$ is a legitimate saddle point in the presence of the Z_{inst} factor.

On the other hand, as we have seen in sections 2.1 and appendix B of [78], the saddle point with $-i\alpha_a \sim \mathcal{O}(N^{\frac{1}{2}})$ has suppressed $Z_{\text{inst}} \approx 1$, and one can self-consistently show that only the 'perturbative integrand' needs to be considered.[6] As a result of such spreading of eigenvalues, it apparently seems that $N^2 \cdot$

---

[5]There is even a signal that this is a divergent series [140]. We thank Antonio Sciarappa for telling this to us.

[6]It may be misleading to simply call it 'perturbative' part, which often refers to the perturbative non-Abelian gauge theory. It should be more precisely stated as the 1-loop Coulomb branch contribution, with both massive instantons and W-bosons integrated out (whose masses are proportional to large Coulomb VEV).

$N^{\frac{1}{2}} \sim N^{\frac{5}{2}}$ enhancement happened, if we just consider it in the context of the partition function (4.2.74). However, with Z_{inst} factor in mind, we think this interpretation is misleading. This is because the instanton part of the free energy at $e^{i\alpha_a} \sim 1$ rapidly grows as $\sim \omega^{-2Nk}$ in k, possibly reflecting an inconsistency of the (grand) canonical ensemble due to the rapid growth of density of states as k is increased. Compared to this, the saddle point with $-i\alpha_a \sim \mathcal{O}(N^{\frac{1}{2}})$ exhibits a sensible growth of free energy in ω^{-1}. The former is perhaps analogous to the Hagedorn-like growth of density of states in the confining phase of 4d free QFT [57], which is made much more extreme in 5d by the additional infinite towers of instanton bound states.

Deconfinement in $\text{AdS}_5/\text{CFT}_4$ implies that the growth of density of states is slowed down after the transition. This is made possible by breaking the infinite towers of 'hadrons' into deconfined quark-gluon partons. It is also associated with absorbing latent heat during the transition, after which extensive quantities show the enhancement $N^0 \to N^2$ in large N. From the gauge theory side, this is achieved by setting $e^{i\alpha_a}$'s closer to 1. In $\text{AdS}_6/\text{CFT}_5$, it seems that there should be more ingredients to achieve the exotic deconfinement in 5d SCFTs. Taking $e^{i\alpha_a} \sim 1$ partly liberates quarks and gluons, from the viewpoint of non-renormalizable perturbative gauge theories. However, the system still has infinite towers of bound states made with instanton solitons. A wild speculation that has been made in the literature is that these instantons are also made of certain partons [141, 142]. The non-compact internal zero modes were interpreted as the position moduli of such hypothetical partons. If such a conjecture is true, liberating the instanton partons should make $N^2 \to N^{\frac{5}{2}}$ enhancement possible, while the rapidly growing density of states in the 'energy' k will be tamed after this deconfinement. From the gauge theory viewpoint, understanding the distinctions between the 4d saddles $e^{i\alpha_a} \sim 1$ and our 5d saddles

$-i\alpha_a \sim N^{\frac{1}{2}}$ should encode some details of such hypothetical deconfinement. In a sense, one can regard the real $i\alpha_a$'s as the 'inverse-temperature' variables for the electric charges. The saddle point $i\alpha_a = 0$ of the 4d Cardy free energy can be understood as such 'temperatures' sent to infinity, to maximally liberate the quark-gluon partons. In our 5d gauge theory analysis, the true saddle point with $i\alpha_a < 0$ may be understood as going beyond this infinite temperature point. This looks like a natural direction in which the remaining instanton-partons can be liberated. We would very much like to make such speculations more precise in the future.

Supplementing the thoughts in the previous paragraph, we finish this subsection by contrasting the differences between apparently similar 4d and 5d indices. Namely, with the nonperturbative completion of (4.2.74) by Z_{inst}, we argued that the saddle point with $e^{i\alpha_a} \sim 1$ is obstructed (or at least its existence is made non-obvious) by nontrivial Z_{inst}. For certain 5d gauge theories, we instead explored alternative large N saddle points in which $-i\alpha_a \sim N^{\frac{1}{2}}$. To make the speculations of previous paragraph more sensible, one would like to make an obvious sanity check that similar saddle points with analytically continued α_a do not exist in 4d indices, which also take the form of (4.2.74). In particular, dimensionally reducing our main 5d examples given by $Sp(N)$ gauge theories, one obtains 4d $\mathcal{N} = 2$ gauge theories. Since the 4d system makes sense as long as $N_f \leq 4$ with very similar field contents, one may technically wonder if similar analytically continued saddle points can exist in its 4d version. However, we have explicitly checked that such analytically continued saddle points do not exist in the 4d $\mathcal{N} = 2$ index, even for precisely the same gauge theories reduced to 4d. Therefore, the analytically continued saddle point which is in charge of $N^{\frac{5}{2}}$ scaling is indeed a 5d phenomenon.

4.3 Conclusions

In this chapter, we studied the index of a class of 5d SCFTs on $S^4 \times \mathbb{R}$, by taking the large N and Cardy limit. Our large N Cardy free energy precisely accounts for the thermodynamic properties of large BPS black holes in global AdS_6.

The basic calculus is very similar to those made in different supersymmetric partition functions [67,126]. In our context, like [126], the gauge holonomies $e^{i\alpha_a}$ have to be analytically continued away from the unit circle to reach the relevant saddle point. At the final stage of calculus, the so-called instanton correction to the partition function is suppressed to $Z_{\text{inst}} \approx 1$ at our saddle point. We have discussed the physical meanings of such a calculus, pointing out the subtle roles of the instanton part and contrasting it to the indices of 4d QFTs. This has close relations to the mysterious deconfinements in 5d SCFTs. Our results should shed concrete lights on getting a better physical picture of such novel deconfinements, and hopefully a better quantitative picture on the instanton partons.

We have focussed on a very small subset of 5d SCFTs, engineered on D4-branes in massive type IIA string theory. Recently, a much broader class of 5d SCFTs have been discovered: e.g. see [143, 144] for geometric engineering, and [145–147] for brane engineering. Also, there have been explorations on the large N AdS_6 duals of 5d SCFTs, engineered by the 5-brane webs [101–105]. In the generic setting in which the numbers of external (p, q) 5-branes are at similar order $\sim N$, various physical quantities are known to scale like N^4 [101–103]. Although we find these examples more difficult to study in our framework, perhaps numerical studies similar to those of [148, 149] could be made.

Chapter 5

Quantum vortices, M2-branes and AdS$_4$ black holes

In this chapter, we study the partition functions of BPS vortices and magnetic monopole operators, in gauge theories describing N M2-branes. In particular, we explore two closely related methods to study the Cardy limit of the index on $S^2 \times \mathbb{R}$. The first method uses the factorization of this index to vortex partition functions, while the second one uses a continuum approximation for the monopole charge sums. Monopole condensation confines most of the N^2 degrees of freedom except $N^{\frac{3}{2}}$ of them, even in the high temperature deconfined phase. The resulting large N free energy statistically accounts for the Bekenstein-Hawking entropy of large BPS black holes in $AdS_4 \times S^7$. Our Cardy free energy also suggests a finite N version of the $N^{\frac{3}{2}}$ degrees of freedom.

5.1 Introduction

M2/M5-branes provide valuable insights to quantum field theories at strong coupling. An intriguing feature is that N M2/M5-branes exhibit $N^{\frac{3}{2}}$ and N^3 degrees of freedom, respectively. These behaviors were first discovered from their black brane solutions [64]. Recent studies from field theory shed more lights on it, e.g. from the partition function on S^3 [65,66] or S^5 [150–155]. However, these studies on $N^{\frac{3}{2}}$, N^3 have been on vacuum properties, such as vacuum entanglement entropy or vacuum energy. For M5-branes, more interesting quantities could be studied using anomalies [156], which see N^3. For instance, certain higher derivative terms proportional to N^3 are studied in [157], and the N^3 scaling of the D0-D4 system at high temperature was studied in [158], which are all related to 6d anomalies. More recently, these anomalies are used to count the microstates of BPS black holes in AdS_7 [75, 159]. For M2-branes, 3d QFTs deformed by topological twisting were studied, in which one finds a macroscopic number of ground states [160]. The entropy of these ground states scales like $N^{\frac{3}{2}}$, which accounts for the magnetic/dyonic black holes in the AdS_4 dual [160, 161].

In this chapter, we study $N^{\frac{3}{2}}$ degrees of freedom of the radially quantized SCFT on M2-branes. We shall find the $N^{\frac{3}{2}}$ scaling of an entropic free energy, by counting excited states of this CFT. This free energy will account for the thermodynamic properties of the electrically charged rotating BPS black holes in $AdS_4 \times S^7$ [82, 97]. From the field theory side, we find the deconfined $N^{\frac{3}{2}}$ degrees of freedom at high 'temperature' (meaning a suitable inverse chemical potential). The physics of magnetic monopoles or vortices makes the structures much richer and subtler than 4d deconfinement, whose details we explore in this chapter.

As an intermediate observable, we first study an index for vortices in the M2-brane QFT deformed by massive parameters. Our QFT lives on N D2-branes and 1 D6-brane. This is a 3d $\mathcal{N} = 4$ Yang-Mills theory with one adjoint and one fundamental hypermultiplet, which flows in IR to the $\mathcal{N} = 8$ SCFT on M2-branes. It has been a useful setting to study M2-branes [162,163]. We shall study its vortices in the Higgs branch, after a deformation by the Fayet-Iliopoulos (FI) parameter. This index is related to our main observable, the index on $S^2 \times \mathbb{R}$ [70,164,165], in two closely related ways. One is by the factorization of the latter into various vortex partition functions. Another relation is obtained by taking the large angular momentum limit on S^2, which we call the Cardy limit. In this limit, we make a continuum approximation of the magnetic monopole's charge sum, finding another asymptotic factorization to vortex partition functions. Using these relations, we compute the asymptotic free energy of the index on $S^2 \times \mathbb{R}$ at large temperature-like parameter, also in the large N limit. This free energy is proportional to $N^{\frac{3}{2}}$, and precisely accounts for the Bekenstein-Hawking entropies of large BPS black holes in $AdS_4 \times S^7$ [82,97]. A crucial role is played by the so-called entropy function of BPS AdS_4 black holes, recently discovered in [74].

The structures of our Cardy and large N saddle points are intriguing. In 4d Cardy formulae studied recently, the Cardy saddle point (or high temperature saddle point) is 'maximally deconfining' in that the gauge symmetry is unbroken by the Polyakov loop operator. This makes the N^2 degrees of freedom fully visible. In 3d gauge theories, one also has to sum over the GNO charges of magnetic monopoles. We argue that this GNO charge sum will forbid the analogous maximally deconfining saddle point for the M2-brane system, following the ideas of [166,167] for the vector-Chern-Simons model. On the other hand, magnetic monopole operators condense at the physical saddle point. The con-

densation effectively breaks the gauge symmetry of the QFTs, confining most of the N^2 degrees of freedom even at high temperature. The number of the remaining light degrees of freedom scales like $N^{\frac{3}{2}}$.

Our Cardy approximation is applicable to the Chern-Simons-matter theories [44, 168–170] such as the ABJM theory, which we explore. Also, one can study the Cardy asymptotic free energy at finite N. We find a finite N version of $N^{\frac{3}{2}}$ in this set-up.

The rest of this chapter is organized as follows. In section 2, we study semi-classical vortices in the Higgs branch, and study their index. We also explain how the index on $S^2 \times \mathbb{R}$ factorizes into vortex partition functions. In section 3, we explain a Cardy approximation of the index on $S^2 \times \mathbb{R}$, based on approximating the GNO charge sum by an integral. We compare it with the vortex factorization formula of section 2. In section 4, we study the large N and Cardy limit of the index on $S^2 \times \mathbb{R}$, which accounts for the entropies of the dual AdS$_4$ black holes. We also comment on the monopole condensation, partial confinement and the behaviors of the Wilson-Polyakov loops. We then study the Cardy limit at finite N, suggesting a finite N version of $N^{\frac{3}{2}}$. Section 5 concludes with remarks.

5.2   Vortices on M2-branes and their indices

We first explain the 3d QFTs that describes M2-branes. Among others, there are Chern-Simons-matter type theories at level 1 [44, 168–170]. We find this approach somewhat tricky for various reasons. The subtle aspects will be commented on below, but we shall also use these QFT approaches in section 4.3.

The gauge theory description that we shall mainly use is a Yang-Mills-matter theory engineered on N D2-branes on top of one D6-brane. The UV

theory has 3d $\mathcal{N} = 4$ SUSY and $U(N)$ gauge symmetry. It consists of the following fields:

$$\begin{aligned} \text{vector multiplet} \quad &: \quad A_\mu \ , \quad \Phi^i \ , \quad \text{fermions} && (5.2.1) \\ \text{adjoint hypermultiplet} \quad &: \quad \phi_A = (\phi, \tilde{\phi}^\dagger) \ , \quad \text{fermions} \\ \text{fundamental hypermultiplet} \quad &: \quad q_A = (q, \tilde{q}^\dagger) \ , \quad \text{fermions} \end{aligned}$$

where $i = 1, 2, 3$ is an $SU(2)_r$ triplet index, and $A = 1, 2$ is an $SU(2)_R$ doublet index. The $\mathcal{N} = 4$ SUSY is associated with $SO(4) \sim SU(2)_r \times SU(2)_R$ R-symmetry. The adjoint hypermultiplet can be decomposed to two half-hypermultiplets, $\phi_A \to \phi_{Aa}$, with $a = 1, 2$ being a doublet index of $SU(2)_L$ flavor symmetry. The $SU(2)_L \times SU(2)_R \sim SO(4)$ acts on $\mathbb{R}^4$ along the D6-brane, transverse to D2's. $SU(2)_r$ acts on $\mathbb{R}^3$ transverse to the D6-brane. Finally, there is a topological $U(1)_T$ symmetry coming from the current $j_\mu \sim \mathrm{tr}(\star F_\mu)$. In string theory, this corresponds to the D0-brane charge, or the momentum charge along the M-theory circle. Here, note that the D6-brane (with transverse direction $\mathbb{R}^3$ spanned by Φ^i) uplifts to a single-centered Taub-NUT (TN) space in M-theory. So the QFT describes N M2-branes probing the transverse space $\mathbb{R}^4 \times TN$. In the asymptotic $\mathbb{R}^3 \times S^1$ region of Taub-NUT, $U(1)_T$ acts as the translation along the circle. The circle is fibered over $\mathbb{R}^3$ to form $\mathbb{R}^4$ near the Taub-NUT center. Near the center, $U(1)_T \times SU(2)_r$ enhances to $SO(4)$ rotation symmetry of $\mathbb{R}^4$. In particular, $U(1)_T$ becomes a Cartan of the rotation symmetry of $SO(8)$ acting on $\mathbb{R}^8$. The strong-coupling limit of 3d QFT corresponds to the large circle limit of M-theory, so the Taub-NUT effectively decompactifies to $\mathbb{R}^4$. So this QFT is expected to flow to the $\mathcal{N} = 8$ SCFT describing N M2-branes on flat spacetime. In particular, $SU(2)_L \times SU(2)_R \times U(1)_T \times SU(2)_r$ symmetry of our gauge theory is expected to enhance to $SO(8)$.

We are interested in the Higgs branch of this system, and the vortex solitons

in this branch. We study the system with nonzero Fayet-Iliopoulos (FI) parameter. One can turn on three FI parameters ζ^I, where $I = 1, 2, 3$ is a triplet index of $SU(2)_R$. We shall only turn on $\zeta \equiv \zeta^3 > 0$, which breaks $SU(2)_R$ to $U(1)$. The Higgs branch vacuum condition is given by the following triplet of D-term conditions:

$$qq^\dagger - \tilde{q}^\dagger\tilde{q} + [\phi, \phi^\dagger] + [\tilde{\phi}, \tilde{\phi}^\dagger] = \zeta , \quad q\tilde{q} + [\phi, \tilde{\phi}] = 0 . \tag{5.2.2}$$

q is an $N \times 1$ matrix, $\tilde{q}$ is a $1 \times N$ matrix, and $\phi, \tilde{\phi}$ are $N \times N$ matrices. These equations describe the moduli space of N $U(1)$ instantons, which is real $4N$ dimensional after modding out by the $U(N)$ gauge orbit. The instanton moduli space appears since the Higgs branch describes N D2-branes dissolved into the $\mathbb{R}^4$ part of D6 world-volume. ζ^I come from NS-NS B-fields on $\mathbb{R}^4$.

We study the vortex solitons on a subspace of the Higgs branch. With $\zeta > 0$, we shall consider the subspace $\tilde{q} = 0$ with nonzero q. The vortex partition functions appearing in the factorization formulae in section 2.2 will all assume $\tilde{q} = 0$. Adjoint scalars $\phi, \tilde{\phi}$ may have very rich possibilities which allow vortices. In most of our discussions in this chapter, we shall consider a simple subspace in which only q, ϕ are nonzero, with $\tilde{q} = 0, \tilde{\phi} = 0$. Only in section 2.2, we shall briefly comment on branches with nonzero $q, \phi, \tilde{\phi}$, and the vortex partition functions in these branches. Setting $\tilde{q} = 0$, $\tilde{\phi} = 0$, the vacuum condition is

$$qq^\dagger + [\phi, \phi^\dagger] = \zeta \mathbf{1}_{N \times N} . \tag{5.2.3}$$

q satisfies $q^\dagger q = N\zeta$. We can set $q^\dagger = (\sqrt{N\zeta}, 0, \cdots, 0)$ using $U(N)$ rotation. Then one obtains

$$[\phi, \phi^\dagger] = \zeta \text{ diag}(-(N-1), 1, \cdots, 1) . \tag{5.2.4}$$

A particular solution to this equation takes the following form:

$$\phi = \sqrt{\zeta} \begin{pmatrix} 0 & \cdots & & & & \\ \sqrt{N-1} & 0 & \cdots & & & \\ 0 & \sqrt{N-2} & 0 & \cdots & & \\ \vdots & & & \ddots & & \\ 0 & \cdots & & \sqrt{2} & 0 & 0 \\ 0 & \cdots & & & 1 & 0 \end{pmatrix}. \tag{5.2.5}$$

This vacuum breaks $U(N)$ gauge symmetry. There are more general solutions labeled by $2N$ real parameters. Below, we discuss the classical vortex solitons only at the point (5.2.5), which will provide enough intuitions to understand our partition function.

In the above vacuum, vortex solitons are semi-classically described as follows. Each $U(1)$ of the spontaneously broken $U(1)^N \subset U(N)$ can host its own vortex charges, i.e. a $U(1)$ flux. On the other hand, vorticities are given by space-dependent VEV's of the N nonzero elements of q and ϕ above, with winding numbers at asymptotic infinity of $\mathbb{R}^2$. Consider the following energy density, involving $\phi_1 \equiv q_1, \phi_i \equiv \phi_{i,i-1}$ $(i = 2, \cdots, N)$, A_μ, where $\mu = 1, 2$:

$$\begin{aligned} \mathcal{E} &= |(\partial_\mu - iA_\mu^1)\phi_1|^2 + \sum_{i=2}^{N} |(\partial_\mu - i(A_\mu^i - A_\mu^{i-1}))\phi_i|^2 + \frac{1}{2g_{YM}^2} \sum_{i=1}^{N} (F_{12}^i)^2 \tag{5.2.6} \\ &\quad + \frac{g_{YM}^2}{2} \left[\mathrm{diag}(|\phi_1|^2 - |\phi_2|^2 - \zeta, |\phi_2|^2 - |\phi_3|^2 - \zeta, \cdots, |\phi_N|^2 - \zeta) \right]^2 \\ &= \sum_{i=1}^{N} |(D_1 + iD_2)\phi_i|^2 + \sum_{i=1}^{N-1} \frac{1}{2g_{YM}^2} \left[F_{12}^i + g_{YM}^2(|\phi_i|^2 - |\phi_{i+1}|^2 - \zeta) \right]^2 \\ &\quad + \frac{1}{2g_{YM}^2} \left[F_{12}^N + g_{YM}^2(|\phi_N|^2 - \zeta) \right]^2 + \zeta \sum_{i=1}^{N} F_{12}^i - i\epsilon^{\mu\nu} \sum_{i=1}^{N} \partial_\mu \left(\phi_i^* D_\nu \phi_i \right). \end{aligned}$$

Here D_μ's are covariantized with $A^1, A^2 - A^1, \cdots, A^N - A^{N-1}$ for $\phi_1, \phi_2, \cdots, \phi_N$, respectively. The last surface term can be ignored if $D_\nu \phi_i$ falls off sufficiently

fast at infinity. One thus obtains the following BPS equations for vortices in this Higgs vacuum:

$$(D_1 + iD_2)\phi_i = 0 \ , \quad F_{12}^i = g_{YM}^2(\zeta - |\phi_i|^2 + |\phi_{i+1}|^2) \ , \quad F_{12}^N = g_{YM}^2(\zeta - |\phi_N|^2) \ .$$
$$(5.2.7)$$

The vorticities $n_i \geq 0$ for ϕ_i are defined by the number of phase rotations made by ϕ_i at spatial infinity. This is related to the fluxes k_i carried by A_μ^i by

$$n_1 = k_1 \ , \quad n_2 = k_2 - k_1 \ , \quad \cdots \ , \quad n_N = k_N - k_{N-1} \ , \qquad (5.2.8)$$

from the ways in which A_μ^i appear in the covariant derivatives. Therefore, from the second term of the last line of (5.2.6), one finds the multi-vortex mass given by

$$M = 2\pi\zeta \sum_{i=1}^{N} k_i \ , \quad k_1 \leq k_2 \leq \cdots \leq k_N \ . \qquad (5.2.9)$$

The vortex masses are proportional to ζ. The masses for elementary particles in the Higgs phase are proportional to $g_{YM} \cdot (\text{VEV}) \sim g_{YM}\zeta^{\frac{1}{2}}$. Therefore, at 'weak coupling' $g_{YM} \ll \zeta^{\frac{1}{2}}$, vortex solitons are non-perturbative and much heavier than elementary particles. At 'strong coupling' $g_{YM} \gg \zeta^{\frac{1}{2}}$, vortices are lighter than elementary particles. We stress that the N vortices are constrained as $k_1 \leq k_2 \leq \cdots \leq k_N$. This is an important aspect which will enable the partition function to have a smooth large N limit. These vorticities are naturally parametrized by Young diagrams with N or less rows, whose lengths are $k_N, k_{N-1}, \cdots, k_1$, respectively.

5.2.1 Indices on $D_2 \times S^1$ and $\mathbb{R}^2 \times S^1$

We study an index which counts the BPS vortices discussed so far. This is a partition function on $\mathbb{R}^2 \times S^1$, where S^1 is for the Euclidean time, in the Higgs

branch. The index is defined by

$$Z(q,t,z,Q) = \text{Tr}\left[(-1)^F q^{R+r+2j} t^{R-r} z^{2L} Q^T\right] \ , \qquad (5.2.10)$$

with suitable boundary conditions for fields assumed at infinity of $\mathbb{R}^2$, to be explained below. r, R, L are the Cartans of $SU(2)_r \times SU(2)_R \times SU(2)_L$, T is the $U(1)_T$ charge (the vorticity), and j is the $SO(2)$ angular momentum on $\mathbb{R}^2$. The factors in the trace are chosen so that they commute with a supercharge within the $\mathcal{N}=4$ SUSY. More concretely, the $\mathcal{N}=4$ supercharges take the form of $Q_\alpha^{\dot{A}B}$, where $\dot{A}$, B and α are doublet indices of $SU(2)_r$, $SU(2)_R$, $SO(2,1)$, respectively. The supercharge $Q_-^{\dot{+}+}$ has charges $r = R = \frac{1}{2}$, $j = -\frac{1}{2}$, $L = 0$, $T = 0$, so it commutes with the whole factor inside the trace. This supercharge and its Hermitian conjugate $Q_+^{\dot{-}-}$ annihilate the BPS states captured by this index. The supercharges $Q_\alpha^{\dot{+}+}$ and their conjugates $Q_\alpha^{\dot{-}-}$ define a 3d $\mathcal{N}=2$ supersymmetry. So the index will be computed below using various techniques developed for 3d $\mathcal{N}=2$ theories. From the $\mathcal{N}=2$ viewpoint, $R+r$ is the $SO(2) \sim U(1)$ R-charge, while $R-r$ is a flavor charge. The index on $\mathbb{R}^2 \times S^1$ can also be regarded as the index on $D_2 \times S^1$, where D_2 is a disk. One should impose suitable boundary conditions at the edge of D_2, which should be chosen to allow the nonzero Higgs VEV for the partition function on $\mathbb{R}^2 \times S^1$. The alternative formulation of this partition function on $D_2 \times S^1$ will have a technical advantage, when one studies the grand partition function summing over all vortex particles. The integral form of the $\mathcal{N}=2$ gauge theory index on $D_2 \times S^1$ was derived in [171]. We summarize the results of [171], focussing on our model. See [171] for more details on SUSY QFTs on $D_2 \times S^1$.

We first explain the boundary conditions on D_2. To realize the boundary conditions which admit nonzero VEV for q and ϕ, we impose Neumann boundary conditions for them: see eqn.(2.18) of [171] for the full boundary conditions

for the corresponding chiral multiplets. As for the $\mathcal{N} = 4$ vector multiplet, we decompose it into $\mathcal{N} = 2$ vector multiplet (containing A_μ, Φ^3) and an adjoint chiral multiplet (containing $\Phi_1 + i\Phi_2$). We impose the boundary condition given by eqn.(2.10) of [171] for the $\mathcal{N} = 2$ vector multiplet. We further need to specify the boundary conditions for: the anti-fundamental chiral multiplet containing $\tilde{q}$, the adjoint chiral multiplet containing $\tilde{\phi}$, and another chiral multiplet containing $\Phi_1 + i\Phi_2$ which originates from the $\mathcal{N} = 4$ vector multiplet. Once the boundary conditions are given for q, ϕ and the $\mathcal{N} = 2$ vector as above, the boundary conditions for the remaining fields can be naturally fixed as in section 6.4 of [171]. Namely, we give Dirichlet boundary conditions for the chiral multiplets $\tilde{q}, \tilde{\phi}$, and Neumann boundary condition for the chiral multiplet $\Phi_1 + i\Phi_2$. This choice naturally guarantees the cancelation of boundary gauge anomaly. We shall assume these boundary conditions below. The partition function with these boundary conditions will also naturally appear as a holomorphic block of the factorized index on $S^2 \times \mathbb{R}$.[1]

The contour integral form of our index on $D_2 \times S^1$ is given by [171]

$$Z = \frac{1}{N!} \oint \prod_{a=1}^{N} \left[\frac{ds_a}{2\pi i s_a} s_a^{-2\pi r \zeta} \right] \prod_{a=1}^{N} \frac{(s_a t^{-\frac{1}{2}} q^{\frac{3}{2}}; q^2)_\infty}{(s_a t^{\frac{1}{2}} q^{\frac{1}{2}}; q^2)_\infty} \cdot \frac{\prod_{a \neq b}(s_a s_b^{-1}; q^2)_\infty}{\prod_{a,b=1}^{N}(s_a s_b^{-1} t^{-1} q; q^2)_\infty} \cdot \prod_{a,b=1}^{N} \frac{(s_a s_b^{-1} z t^{-\frac{1}{2}} q^{\frac{3}{2}}; q^2)_\infty}{(s_a s_b^{-1} z t^{\frac{1}{2}} q^{\frac{1}{2}}; q^2)_\infty}$$

$$(5.2.11)$$

where

$$(a; q)_\infty \equiv \prod_{n=0}^{\infty} (1 - aq^n) \qquad (5.2.12)$$

is the q-Pochhammer symbol. The second/third/fourth product in the integrand come from the fundamental hypermultiplet, $\mathcal{N} = 4$ vector multiplet, adjoint hypermultiplet, respectively. All q-Pochhammer symbols in the denominator come

---

[1]We also tried to define the $D_2 \times S^1$ function of the ABJM theory [44]. However, we were not sure about the natural and simple anomaly-free boundary conditions. However, see section 4.3 for related discussions.

from scalars assuming Neumann boundary conditions, while those in the numerator come from fermions whose superpartner bosons assume Dirichlet boundary conditions. (The argument $t^{-1}q$ in the factor $(s_a s_b^{-1} t^{-1}q; q^2)_\infty$ corrects a typo in [171].) s_a are N holonomy variables of the vector multiplet on S^1. Their integration contours are given by unit circles, $|s_a| = 1$. Here, we note a subtle phenomenon that the FI parameter on $D_2 \times S^1$ is quantized, $2\pi r \zeta \in \mathbb{Z}$, where r is the radius of the hemisphere D_2. This is because the standard FI term is accompanied by a r^{-1} curvature correction given by a 1d Chern-Simons term along the time direction [171], which demands the quantization of ζ. Clearly, the factor $s_a^{-2\pi r \zeta}$ in (5.2.11) makes sense only with this quantization.[2] The extra parameter $2\pi r \zeta > 0$ still admits one to introduce another fugacity-like parameter $Q \equiv q^{4\pi r \zeta}$, which will be the fugacity for the vortex number. The quantization of ζ is an artificial constraint as we regulate our problem on $\mathbb{R}^2 \times S^1$ to that on $D_2 \times S^1$. After all the computation is done for the integral, we can continue ζ back to an arbitrary parameter.

If Q is small enough, one can write the integral as a residue sum by evaluating s_a integrals one by one. For $2\pi r \zeta > 0$, since the factors from $s_a^{-2\pi r \zeta}$ damp to zero at $s_a = \infty$, there is no pole at $s_a = \infty$. We take residues from poles outside the unit circle. We assume $|tq| < 1$, $|t^{-1}q| < 1$, $|z t^{\frac{1}{2}} q^{\frac{1}{2}}| < 1$, $|q| < 1$, for convenience. The poles contributing to the residue sum take the following form, up to $N!$ permutations which cancel the overall $\frac{1}{N!}$ factor of (5.2.11):

$$
\begin{aligned}
s_1 &= t^{-\frac{1}{2}} q^{-\frac{1}{2} - 2n_1} \quad (n_1 \geq 0) , \\
s_a &= s_{a-1} z^{-1} t^{-\frac{1}{2}} q^{-\frac{1}{2} - 2n_a} \quad (a = 2, \cdots, N; n_a \geq 0) .
\end{aligned}
\tag{5.2.13}
$$

---

[2]More precisely, the chemical potential t induces a mixed anomaly with the $U(1) \subset U(N)$ gauge symmetry. To make the system free of gauge anomaly including this effect, one has to quantize ζ after shifting it suitably by the chemical potentials. ζ appearing in (5.2.11) is the shifted FI parameter.

The value of s_1 is determined by the poles from the fundamental hypermultiplet, while other s_a's are determined by the adjoint hypermultiplet. If poles are chosen from other denominators than the above, one can show that the numerator vanishes so that they are actually not poles. Iterating the second line of (5.2.13) to decide s_a's, and defining $k_a \equiv \sum_{i=1}^{a} n_i$, one finds

$$s_a = u^{-1} v^{-a+1} q^{-2k_a} \qquad (5.2.14)$$

for $a = 1, \cdots, N$, where $u \equiv (tq)^{\frac{1}{2}}$, $v \equiv z(tq)^{\frac{1}{2}}$, and $k_1 \leq k_2 \leq \cdots \leq k_N$. k_a's labeling the poles will turn out to be the $U(1)^N$ vortex charges $k_1, \cdots, k_N$ that we introduced in the context of classical solitons. This correspondence can be understood by noting that n_a in the pole (5.2.13) originates from a factor $\frac{1}{(a;q^2)_\infty} \sim \frac{1}{1-aq^{2n_a}}$, which comes from the mode of a bosonic field with winding number n_a. Residue of this pole corresponds to a partition function with vortex defect inserted [172], confirming the vortex interpretation. The residue sum for (5.2.11) is given by

$$Z = \frac{1}{(q^2;q^2)_\infty^N} \sum_{0 \leq k_1 \leq \cdots \leq k_N}^{\infty} \prod_{a=1}^{N} \left(u a^{a-1} q^{2k_a} \right)^{2\pi r \zeta} \frac{(u^{-2} v^{-a+1} q^{2-2k_a};q^2)_\infty}{(v^{-a+1} q^{-2k_a};q^2)'_\infty}$$

$$\times \prod_{a,b=1}^{N} \frac{(v^{-a+b} q^{-2k_a+2k_b};q^2)'_\infty}{(u^{-2} v^{-a+b} q^{2-2k_a+2k_b};q^2)_\infty} \frac{(u^{-2} v^{1-a+b} q^{2-2k_a+2k_b};q^2)_\infty}{(v^{1-a+b} q^{-2k_a+2k_b};q^2)'_\infty} \quad ,(5.2.15)$$

where $(a;q^2)'_\infty$ means $(a;q^2)_\infty$ if $a \neq q^{-2n}$ with any non-negative integer n, and

$$(q^{-2n};q^2)'_\infty = \lim_{a \to q^{-2n}} \frac{(a;q^2)_\infty}{(1 - aq^{2n})} \quad . \qquad (5.2.16)$$

Using

$$(a;q)_n = \frac{(a;q)_\infty}{(aq^n;q)_\infty} \qquad (5.2.17)$$

for $n \geq 0$ and

$$(a;q)_{-n} \equiv \frac{1}{(aq^{-n};q)_n} = \frac{(a;q)_\infty}{(aq^{-n};q)_\infty} \qquad (5.2.18)$$

for $-n < 0$, one finds that (5.2.17) is true for any integer n. Using this, the second line of (5.2.15) can be rearranged as

$$\prod_{a,b=1}^{N} \frac{(v^{-a+b}q^{-2k_a+2k_b};q^2)'_\infty}{(u^{-2}v^{-a+b}q^{2-2k_a+2k_b};q^2)_\infty} \frac{(u^{-2}v^{1-a+b}q^{2-2k_a+2k_b};q^2)_\infty}{(v^{1-a+b}q^{-2k_a+2k_b};q^2)'_\infty} \tag{5.2.19}$$

$$= \prod_{a,b=1}^{N} \frac{(v^{-a+b};q^2)'_\infty}{(u^{-2}v^{-a+b}q^2;q^2)_\infty} \frac{(u^{-2}v^{1-a+b}q^2;q^2)_\infty}{(v^{1-a+b};q^2)'_\infty} \cdot \frac{(u^{-2}v^{b-a}q^2;q^2)_{k_b-k_a}}{(v^{b-a};q^2)_{k_b-k_a}} \cdot \frac{(v^{1-a+b};q^2)_{k_b-k_a}}{(u^{-2}v^{1-a+b}q^2;q^2)_{k_b-k_a}}$$

$$= \prod_{a,b=1}^{N} \frac{(u^{-2}v^{b-a}q^2;q^2)_{k_b-k_a}}{(v^{b-a};q^2)_{k_b-k_a}} \cdot \frac{(v^{1-a+b};q^2)_{k_b-k_a}}{(u^{-2}v^{1-a+b}q^2;q^2)_{k_b-k_a}} \cdot \prod_{a=1}^{N} \frac{(v^{-a+1};q^2)'_\infty}{(v^{-a+N+1};q^2)_\infty} \cdot \frac{(u^{-2}v^{-a+N+1}q^2;q^2)_\infty}{(u^{-2}v^{-a+1}q^2;q^2)_\infty} \ .$$

The product over $a = 1, \cdots, N$ on the first line of (5.2.15) and that on the last line of (5.2.19) combine and get rearranged as

$$\prod_{a=1}^{N} \left(ua^{a-1}q^{2k_a}\right)^{2\pi r\zeta} \frac{(u^{-2}v^{-a+1}q^{2-2k_a};q^2)_\infty}{(v^{-a+1}q^{-2k_a};q^2)'_\infty} \frac{(v^{-a+1};q^2)'_\infty}{(v^{-a+N+1};q^2)_\infty} \cdot \frac{(u^{-2}v^{-a+N+1}q^2;q^2)_\infty}{(u^{-2}v^{-a+1}q^2;q^2)_\infty}$$

$$= \left[u^N v^{\frac{N(N-1)}{2}}\right]^{2\pi r\zeta} Q^{k_1+\cdots+k_N} \prod_{a=1}^{N} \frac{(v^{-a+1};q^2)_{-k_a}}{(u^{-2}v^{-a+1}q^2;q^2)_{-k_a}} \cdot \frac{(u^{-2}v^a q^2;q^2)_\infty}{(v^a;q^2)_\infty} \ , \tag{5.2.20}$$

where $Q \equiv q^{4\pi r\zeta}$. So one obtains

$$Z = \frac{(u^N v^{\frac{N(N-1)}{2}})^{2\pi r\zeta}}{(q^2;q^2)_\infty^N} \prod_{a=1}^{N} \frac{(u^{-2}v^a q^2;q^2)_\infty}{(v^a;q^2)_\infty} \sum_{0 \le k_1 \le \cdots \le k_N} Q^{k_1+\cdots+k_N} \prod_{a=1}^{N} \frac{(v^{-a+1};q^2)_{-k_a}}{(u^{-2}v^{-a+1}q^2;q^2)_{-k_a}}$$

$$\cdot \prod_{a,b=1}^{N} \frac{(v^{-a+b+1};q^2)_{-k_a+k_b}(u^{-2}v^{-a+b}q^2;q^2)_{-k_a+k_b}}{(v^{-a+b};q^2)_{-k_a+k_b}(u^{-2}v^{-a+b+1}q^2;q^2)_{-k_a+k_b}} \ . \tag{5.2.21}$$

In the last expression, one can relax the condition $2\pi r\zeta \in \mathbb{Z}_+$, so we can now regard Q as an independent continuous parameter. Here, let us decompose Z into three factors, $Z = Z_{\text{prefactor}} Z_{\text{pert}} Z_{\text{vortex}}$, where each factor is given as

follows:

$$
Z_{\text{prefactor}} \;=\; \frac{(u^N v^{\frac{N(N-1)}{2}})^{2\pi r \zeta}}{(q^2;q^2)_\infty^N} \;\;,\;\;\;\; Z_{\text{pert}} = \prod_{a=1}^{N} \frac{(u^{-2}v^a q^2;q^2)_\infty}{(v^a;q^2)_\infty}
$$

$$
Z_{\text{vortex}} \;=\; \sum_{0 \le k_1 \le \cdots \le k_N} Q^{k_1 + \cdots + k_N} Z_{k_1,\cdots,k_N} \tag{5.2.22}
$$

$$
Z_{k_1,\cdots,k_N} \;\equiv\; \prod_{a=1}^{N} \frac{(v^{-a+1};q^2)_{-k_a}}{(u^{-2}v^{-a+1};q^2)_{-k_a}} \cdot \prod_{a,b=1}^{N} \frac{(v^{-a+b+1};q^2)_{-k_a+k_b}(u^{-2}v^{-a+b}q^2;q^2)_{-k_a+k_b}}{(v^{-a+b};q^2)_{-k_a+k_b}(u^{-2}v^{-a+b+1}q^2;q^2)_{-k_a+k_b}} \;.
$$

Here, $Z_{0,\cdots,0} = 1$ by definition. In the rational function $Z_{k_1,\cdots,k_N}$ appearing in (5.2.22), one finds further cancelations between denominator and numerator. In fact, since $k_1 \le \cdots \le k_N$ define a Young diagram with k boxes, $Z_{k_1,\cdots,k_N}$ admits a simple expression in terms of this Young diagram $Y = (k_N, k_{N-1}, \cdots, k_1)$ after cancelation. To explain the final result after the cancelation, let us introduce the following 'distance functions' on the Young diagram:

$$
\begin{aligned}
a(s):&\quad \text{arm (horizontal) length} = \text{number of boxes to the right of } s \\
l(s):&\quad \text{leg (vertical) length} = \text{number of the boxes below } s \\
x(s):&\quad \text{horizontal position} = \text{number of boxes to the left of } s \\
y(s):&\quad \text{vertical position} = \text{number of the boxes above } s
\end{aligned} \tag{5.2.23}
$$

Here, s labels the boxes of the Young diagram. For instance, for the two boxes s_1, s_2 of $Y = (6,5,3,2)$ below, they are given by

$$
\longrightarrow \quad
\begin{aligned}
a(s_1) &= 4,\; l(s_1) = 3,\; x(s_1) = 1,\; y(s_1) = 0 \\
a(s_2) &= 2,\; l(s_2) = 1,\; x(s_1) = 2,\; y(s_1) = 1
\end{aligned} \; . \tag{5.2.24}
$$

Using these notations, Z_{vortex} is given by

$$
Z_{\text{vortex}} = \sum_Y Q^{|Y|} \prod_{s \in Y} \frac{(1 - u^{-2}q^{-2a(s)}v^{-l(s)})(1 - u^{-2}vq^2 q^{2a(s)}v^{l(s)})(1 - v^N q^{2x(s)}v^{-y(s)})}{(1 - q^{-2}q^{-2a(s)}v^{-l(s)})(1 - vq^{2a(s)}v^{l(s)})(1 - u^{-2}q^2 v^N q^{2x(s)}v^{-y(s)})} \; . \tag{5.2.25}
$$

We checked this expression up to Q^{11} order, till $N \leq 10$. One can also prove (5.2.25) analytically, which is explained in appendix B of [79].

We also explain other factors, $Z_{\text{prefactor}}$ and Z_{pert}. The factor $(u^N v^{\frac{N(N-1)}{2}})^{2\pi r \zeta}$ in $Z_{\text{prefactor}}$ is the 'zero-point energy' factor, weighting the 'ground state' if one expands Z in fugacities. The factor $(q^2, q^2)_\infty^{-N}$ of $Z_{\text{prefactor}}$ comes from N chiral multiplets containing the N complex scalars, which form the Higgs branch moduli. These scalars are the massless fluctuations from the reference point (5.2.5). This part will not play any important role in the rest of our works. For instance, $Z_{\text{prefactor}}$ will not appear in the factorization formula on $S^2 \times S^1$ later. (More precisely, one can regard it as the two $Z_{\text{prefactor}}$'s canceling in the factorization formula.) So $Z_{\text{prefactor}}$ will be mostly neglected. Z_{pert} comes from 'perturbative' massive particles' contribution in the Higgs branch, which will be important later. Normally, the Higgs branch partition function on $\mathbb{R}^2 \times S^1$ refers to $Z_{\mathbb{R}^2 \times S^1} = Z_{\text{pert}} Z_{\text{vortex}}$.

Now we have two alternative expressions for the index, the integral form (5.2.11) and the residue sum (5.2.21), (5.2.25). The latter expression is a series which is useful for sufficiently small $|Q|$, but (5.2.11) can be used more generally.

Before closing this subsection, we study the case with $N = 1$, for single M2-brane. In this case, the index given by the residue sum becomes simplified. This is because the CFT on one M2-brane is expected to be a free QFT, consisting of four free $\mathcal{N} = 2$ chiral multiplets. In fact, studying (5.2.25) to certain high orders in Q, we find that (5.2.21) can be written as

$$Z_{N=1} = \frac{(tq)^{\pi r \zeta}}{(q^2; q^2)_\infty} \cdot \frac{(zt^{-\frac{1}{2}}q^{\frac{3}{2}}; q^2)_\infty}{(zt^{\frac{1}{2}}q^{\frac{1}{2}}; q^2)_\infty} \cdot \frac{(q^2 Q; q^2)_\infty}{(t^{-1}qQ; q^2)_\infty} = \frac{(tq)^{\pi r \zeta}}{(q^2; q^2)_\infty} \cdot \frac{(zt^{-\frac{1}{2}}q^{\frac{3}{2}}; q^2)_\infty}{(zt^{\frac{1}{2}}q^{\frac{1}{2}}; q^2)_\infty} \cdot \frac{(q^{\frac{3}{2}}t^{\frac{1}{2}}\hat{Q}; q^2)_\infty}{(t^{-\frac{1}{2}}q^{\frac{1}{2}}\hat{Q}; q^2)_\infty}$$
$$(5.2.26)$$

at $N = 1$. This can also be shown analytically by using the infinite q-binomial theorem. Here we defined $\hat{Q} \equiv q^{\frac{1}{2}}t^{-\frac{1}{2}}Q$. The first factor of (5.2.26) is sim-

ply $Z_{\text{prefactor}}$, which we ignore. The second factor $Z_{\text{pert}} = \frac{(zt^{-\frac{1}{2}}q^{\frac{3}{2}};q^2)_\infty}{(zt^{\frac{1}{2}}q^{\frac{1}{2}};q^2)_\infty}$ comes from the adjoint hypermultiplet of the $\mathcal{N} = 4$ theory, which is free at $N = 1$. The factors in the denominator/numerator come from the chiral multiplets with Neumann/Dirichlet boundary conditions, respectively. The last factor $Z_{\text{vortex}} = \frac{(\hat{Q}t^{\frac{1}{2}}q^{\frac{3}{2}};q^2)_\infty}{(\hat{Q}t^{-\frac{1}{2}}q^{\frac{1}{2}};q^2)_\infty}$ makes the contribution from another free hypermultiplet, where two chiral multiplets in it are given Neumann/Dirichlet boundary conditions, respectively. In fact it is well known that the 'vortex field' makes a free hypermultiplet in this case. To see this, first note that with the adjoint hypermultiplet decoupled at $N = 1$, this theory is simply an $\mathcal{N} = 4$ SQED with $N_f = 1$ flavor. In [173], $\mathcal{N} = 4$ $U(N)$ SQCD with $N_f = 2N - 1$ flavors was studied. It was argued that a monopole operator becomes free and decouples in IR. The remaining system in IR was argued to be the $U(N-1)$ SQCD with same number $N_f = 2N - 1$ of $U(N-1)$ fundamental flavors. Since the last theory is void at $N = 1$, SQED at $N_f = 1$ in IR is dual to the free hypermultiplet. Indeed, the vortex partition function of this SQED was shown to be precisely that of a free hypermultiplet [174]. Defining t_I $(I = 1, 2, 3, 4)$ as

$$(t_1, t_2, t_3, t_4) \equiv (t^{\frac{1}{2}}z, t^{\frac{1}{2}}z^{-1}, t^{-\frac{1}{2}}\hat{Q}, t^{-\frac{1}{2}}\hat{Q}^{-1}) , \qquad (5.2.27)$$

satisfying $t_1 t_2 t_3 t_4 = 1$, the Abelian index can be written as

$$Z_{\text{pert}} Z_{\text{vortex}}\Big|_{N=1} = \frac{(t_2^{-1}q^{\frac{3}{2}};q^2)_\infty (t_4^{-1}q^{\frac{3}{2}};q^2)_\infty}{(t_1 q^{\frac{1}{2}};q^2)_\infty (t_3 q^{\frac{1}{2}};q^2)_\infty} . \qquad (5.2.28)$$

In section 4, we shall be interested in the large N free energy of the index, in the limit $\beta \to 0^+$ where $q \equiv e^{-\beta}$. Here, we make such a study at $N = 1$ as a warming up. We shall first study the limit $\beta \to 0$ from the exact expression (5.2.26), and then discuss how to recover the same result from the saddle point analysis of the contour integral expression (5.2.11).

To perform the $\beta \to 0$ approximation, one should understand the $\beta \to 0$ limit of $(a; e^{-2\beta})_\infty$. We are interested in taking $\beta \to 0$ while keeping it complex, with $\text{Re}(\beta) > 0$. Also, other fugacities t_I are kept as pure phases: $|t_I| = 1$, while satisfying $t_1 t_2 t_3 t_4 = 1$. It is important that these phases can be substantially away from 1. This defines our 'Cardy limit' of the index. The importance of these phases was noticed in [75,76], which will be seen again in our later sections. In this set-up, one obtains

$$(a; q^2)_\infty = \prod_{n=0}^{\infty}(1 - aq^{2n}) = \exp\left[-\sum_{n=1}^{\infty}\frac{1}{n}\frac{a^n}{1-q^{2n}}\right] \xrightarrow{\beta \to 0} \exp\left[-\frac{1}{2\beta}\sum_{n=1}^{\infty}\frac{a^n}{n^2}\right] = \exp\left[-\frac{\text{Li}_2(a)}{2\beta}\right]$$

(5.2.29)

when a is a phase, $|a| = 1$. Therefore, in our Cardy limit, the index (5.2.26) is given by

$$\log Z_{N=1} \sim \frac{1}{2\beta}\left[\text{Li}_2(\hat{Q}t^{-\frac{1}{2}}) - \text{Li}_2(\hat{Q}t^{\frac{1}{2}}) + \text{Li}_2(zt^{\frac{1}{2}}) - \text{Li}_2(zt^{-\frac{1}{2}}) + \text{Li}_2(1)\right] + \pi r\zeta \log t .$$

(5.2.30)

Here, we define ξ by $2\pi r\zeta \equiv \frac{\xi}{2\beta}$ ($Q \equiv e^{-\xi}$), and keep ξ fixed as one takes $\beta \to 0$. Then, defining $\mathcal{F}$ by

$$\log Z \sim -\frac{\mathcal{F}}{2\beta}$$

(5.2.31)

in the $\beta \to 0$ limit, one obtains

$$\mathcal{F}_{N=1} = \text{Li}_2(zt^{-\frac{1}{2}}) - \text{Li}_2(zt^{\frac{1}{2}}) + \text{Li}_2(\hat{Q}t^{\frac{1}{2}}) - \text{Li}_2(\hat{Q}t^{-\frac{1}{2}}) - \text{Li}_2(1) - \frac{\xi}{2}\log t . \quad (5.2.32)$$

Now we make the saddle point analysis of the integral expression (5.2.11), at $N = 1$ and in the limit $\beta \to 0$. (5.2.11) in this setting becomes

$$Z_{N=1} \sim \int \frac{ds}{2\pi i s}\exp\left[-\frac{\xi}{2\beta}\log s + \frac{1}{2\beta}\left(\text{Li}_2(zt^{\frac{1}{2}}) - \text{Li}_2(zt^{-\frac{1}{2}}) + \text{Li}_2(t^{-1}) + \text{Li}_2(t^{\frac{1}{2}}s) - \text{Li}_2(t^{-\frac{1}{2}}s)\right)\right]$$

(5.2.33)

where the contour is over the unit circle $|s| = 1$. In the Cardy limit, we can ignore the quantization condition of ζ and keep general complex ξ. Taking ξ to

be purely imaginary, and t, z to be phases, we try to find the saddle point for s at $|\beta| \ll 1$. One needs to extremize

$$\xi \log s + \text{Li}_2(st^{-\frac{1}{2}}) - \text{Li}_2(st^{\frac{1}{2}}) \ . \tag{5.2.34}$$

The saddle point should satisfy

$$0 = \xi + \text{Li}_1(st^{-\frac{1}{2}}) - \text{Li}_1(st^{\frac{1}{2}}) = \xi - \log \frac{1 - st^{-\frac{1}{2}}}{1 - st^{\frac{1}{2}}} \ . \tag{5.2.35}$$

The solution is given by

$$s_0 = \frac{e^{\xi} - 1}{e^{\xi}t^{\frac{1}{2}} - t^{-\frac{1}{2}}} = \frac{\sinh \frac{\xi}{2}}{\sinh \frac{\xi + T}{2}} \tag{5.2.36}$$

with $t \equiv e^T$. s_0 is real for purely imaginary ξ, T. Plugging in this value to the integrand of (5.2.33), $s_0 = t^{-\frac{1}{2}} \frac{1 - t^{\frac{1}{2}}\hat{Q}}{1 - t^{-\frac{1}{2}}\hat{Q}}$, one obtains precisely the same $\mathcal{F}$ as (5.2.32). The last statement can be shown analytically by using the identity

$$\text{Li}_2(xy) - \text{Li}_2(x) - \text{Li}_2(y) + \text{Li}_2(1) = \text{Li}_2\left(\frac{1 - x}{1 - xy}\right) - \text{Li}_2\left(y\frac{1 - x}{1 - xy}\right) + \log(x) \log\left(\frac{1 - x}{1 - xy}\right) \ . \tag{5.2.37}$$

5.2.2 Factorization on $S^2 \times S^1$

So far, we examined the vortex partition function Z_{vortex} that is captured as a part of the $\mathbb{R}^2 \times S^1$ index, or equivalently the $D_2 \times S^1$ index with a certain boundary condition at the edge. In the literature, it was discussed that the vortex partition function can be a building block of many other supersymmetric partition functions on compact 3d manifolds such as $S^2 \times S^1$ and S_b^3 [175–182]. We shall develop a similar factorization formula along the line of [183]. More precisely, once we consider an S^1 fibration on S^2 where the angular momentum fugacity is turned on, the fields are effectively localized at the poles of S^2 and probe local $\mathbb{R}^2$ geometry. Thus, the supersymmetric partition functions on those

manifolds are written in terms of the vortex partition function as the following universal form:

$$Z = \sum_{\text{Higgs vacua}} Z_{\text{pert}} Z_{\text{vortex}} \overline{Z}_{\text{vortex}}. \qquad (5.2.38)$$

Only differences are the perturbative contribution Z_{pert} and how to glue two pieces of the vortex partition functions, i.e., how to define $\overline{Z}_{\text{vortex}}$, which has the same functional form as Z_{vortex} up to redefinitions of variables depending on the background geometry. For our example, the index on $S^2 \times S^1$ will take the form of

$$Z_{S^2 \times S^1}(\hat{Q}, t, z, q) = \sum_{\mathcal{Y} \in \text{Higgs}} Z_{\text{pert}}^{\mathcal{Y}}(t, z, q) Z_{\text{vortex}}^{\mathcal{Y}}(\hat{Q}, t, z, q) Z_{\text{vortex}}^{\mathcal{Y}}(\hat{Q}^{-1}, t^{-1}, z^{-1}, q^{-1}),$$

$$(5.2.39)$$

where the points $\mathcal{Y}$ in the Higgs branch will be specified below.

Our theory of interest includes one fundamental and one adjoint hypermultiplets. Since a 3d $\mathcal{N} = 4$ vector multiplet contains an $\mathcal{N} = 2$ chiral multiplet as well, we have in total three $\mathcal{N} = 2$ chirals in the adjoint representation. In the previous section, we showed that the chiral from the $\mathcal{N} = 4$ vector does not yield any contributing pole. Thus, the factorization of our partition function mimics that of a theory with two adjoints. The factorization of a 3d $\mathcal{N} = 2$ theory with two adjoints is recently discussed in [183]. It was shown that the D-term equations of the $\mathcal{N} = 2$ theory restrict its Higgs vacua such that they are represented by 2-dimensional box diagrams; e.g., see figure 5.1. Furthermore, if the theory has a superpotential, there will be extra conditions from the F-term equations. In our case, we have the following F-term condition:

$$q\tilde{q} + [\phi, \tilde{\phi}] = 0, \qquad (5.2.40)$$

which is a part of the $\mathcal{N} = 4$ D-term conditions. As we have shown in the previous section, the vacuum solutions have vanishing $\tilde{q}$ and accordingly vanishing
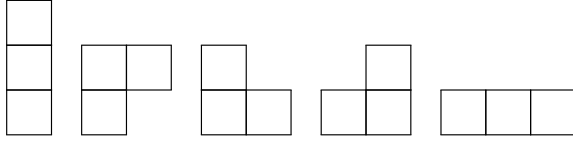
Figure 5.1: The Higgs vacua of the (massive) $\mathcal{N} = 2$ $U(3)$ theory with one fundamental and two adjoint chirals are represented by 2-dimensional box diagrams due to the D-term conditions. If there is a superpotential, they are further restricted.

$[\phi, \tilde{\phi}]$. The condition $[\phi, \tilde{\phi}] = 0$ demands that only the first, third and fifth diagrams in figure 5.1 are allowed; in general, only the Young diagram types are allowed.

To establish the factorization formula with the structures outlined in the previous paragraph, we start from the known expression for the index on $S^2 \times S^1$ [70, 164], which is [163, 165, 184]:

$$Z_{S^2 \times S^1}(\hat{Q}, z, t, q) = \tag{5.2.41}$$

$$\sum_{\{m\}=-\infty}^{\infty} \frac{1}{\mathrm{Weyl}(\{m\})} \oint \left(\prod_{a=1}^{N} \frac{ds_a}{2\pi i s_a} \hat{Q}^{m_a} t^{-|m_a|/2} q^{|m_a|/2} \right) \times$$

$$\left(\prod_{1 \le a \ne b \le N} \left(1 - s_a s_b^{-1} q^{|m_a - m_b|} \right) \right) \left(\prod_{a=1}^{N} \frac{(s_a^{-1} t^{-\frac{1}{2}} q^{\frac{3}{2}+|m_a|}; q^2)}{(s_a t^{\frac{1}{2}} q^{\frac{1}{2}+|m_a|}; q^2)} \frac{(s_a t^{-\frac{1}{2}} q^{\frac{3}{2}+|m_a|}; q^2)}{(s_a^{-1} t^{\frac{1}{2}} q^{\frac{1}{2}+|m_a|}; q^2)} \right) \times$$

$$\left(\prod_{a,b=1}^{N} \frac{(s_a^{-1} s_b t q^{1+|-m_a+m_b|}; q^2)(s_a^{-1} s_b z^{-1} t^{-\frac{1}{2}} q^{\frac{3}{2}+|-m_a+m_b|}; q^2)(s_a^{-1} s_b z t^{-\frac{1}{2}} q^{\frac{3}{2}+|-m_a+m_b|}; q^2)}{(s_a s_b^{-1} t^{-1} q^{1+|m_a-m_b|}; q^2)(s_a s_b^{-1} z t^{\frac{1}{2}} q^{\frac{1}{2}+|m_a-m_b|}; q^2)(s_a s_b^{-1} z^{-1} t^{\frac{1}{2}} q^{\frac{1}{2}+|m_a-m_b|}; q^2)} \right).$$

Here the integration contour for each s_a is taken to be the unit circle. $\mathrm{Weyl}(\{m\})$ is the order of the Weyl group remaining unbroken for given magnetic flux $\{m\} \in \mathbb{Z}^N/S_N$. In the following computation, however, it will be more convenient to distinguish the permutations in $\{m\}$ and to take the symmetry factor

$N!$ instead of Weyl($\{m\}$). In other words, we replace the flux summation by

$$\sum_{\{m\}=-\infty}^{\infty} \frac{1}{\text{Weyl}(\{m\})} \qquad \rightarrow \qquad \frac{1}{N!} \sum_{\{m\}\in\mathbb{Z}^N} . \qquad (5.2.42)$$

From here, we also use a shorthand expression $(a;q) \equiv (a;q)_\infty$ in the rest of this chapter.

We are aiming to evaluate this integral using the residue theorem. Assuming $|q| < 1$ and $|t| = |z| = 1$, we take the poles outside the unit circle, which are given by the intersections of the following hyperplanes:

$$\begin{aligned}
s_a &= t^{-\frac{1}{2}} q^{-\frac{1}{2}} q^{-|m_a|-2k_a}, \\
s_a &= s_b z^{-1} t^{-\frac{1}{2}} q^{-\frac{1}{2}} q^{-|m_a-m_b|-2k_a}, \\
s_a &= s_b z t^{-\frac{1}{2}} q^{-\frac{1}{2}} q^{-|m_a-m_b|-2k_a}, \\
s_a &= s_b t q^{-1} q^{-|m_a-m_b|-2k_a}
\end{aligned} \qquad (5.2.43)$$

where $k_a \geq 0$. However, poles sitting at the hyperplanes of the fourth type have vanishing residues. In the set-up of the previous paragraph, this implies that there are no poles from the adjoint chiral in the $\mathcal{N} = 4$ vector multiplet. The relevant poles are only determined by hyperplanes of the other types. Thus, as we noted already, the residue evaluation of our theory resembles that of the two adjoint theory. While a pole is typically determined by N hyperplanes, for a general two adjoint theory, it may happen that a set of hyperplanes degenerate such that more than N hyperplanes meet at the point. In such cases, one encounters a double or higher order pole when the N-dimensional integral is evaluated iteratively. Nevertheless, a particular choice of the superpotential sometimes yield extra zeros by imposing conditions on the fugacities so that the higher order poles become simple. Indeed, our $\mathcal{N} = 4$ SYM example turns out to be such a case.

At first let us forget about the issue of higher order poles and just focus on how we organize N linearly independent hyperplanes. Once we pick up N hyperplanes intersecting at a pole, they can be represented by a binary tree graph of N nodes where each node is accompanied by a label of three parameters (a, z_a, k_a). While the meanings of the tree and the labels (a, z_a, k_a) are rather clear from (5.2.43), let us explain them briefly. The first parameter a, which is an integer in the range $1 \leq a \leq N$ without repetition, can be used to label the nodes. Namely, we will refer to the node with (a, z_a, k_a) as the ath node. Then one can represent a tree graph using a map $p : \{1, \ldots, N\} \to \{0, \ldots, N\}$. p is defined such that $p(a) = b$ if the bth node is the parent node of the ath node. If the ath node is the root node, which doesn't have a parent node, $p(a) = 0$. The other two parameters are chosen such that

$$
z_a = \begin{cases} 1, & p(a) = 0, \\ z, z^{-1}, & p(a) \neq 0, \end{cases} \qquad k_a \geq 0. \tag{5.2.44}
$$

Note that z_a distinguishes whether the ath node is the left child or the right child of the parent node, which are two available choices in a binary tree. Once a tree p and (a, k_a, z_a) for each node are given, they specify the hyperplanes as follows:

$$
s_a = \begin{cases} t^{-\frac{1}{2}} q^{-\frac{1}{2}} q^{-|m_a| - 2k_a}, & p(a) = 0, \\ s_{p(a)} z_a^{-1} t^{-\frac{1}{2}} q^{-\frac{1}{2}} q^{-|m_a - m_{p(a)}| - 2k_a}, & p(a) \neq 0. \end{cases} \tag{5.2.45}
$$

Consequently, each s_a at the pole is given by

$$
s_a = \left(\prod_{n=0}^{l_a - 1} z_{p^n(a)}^{-1} \right) (tq)^{-\frac{l_a}{2}} q^{-\sum_{n=0}^{l_a - 1} |m_{p^n(a)} - m_{p^{n+1}(a)}| - 2 \sum_{n=0}^{l_a - 1} k_{p^n(a)}} \tag{5.2.46}
$$

where l_a is the integer satisfying $p^{l_a}(a) = 0$. For example, the root note has $l_a = 1$. We also define $m_0 = 0$.

Now let us evaluate the residue at the pole (5.2.46). First we consider $N < 4$, in which case, the pole (5.2.46) is always simple. We have to sum the residues for all possible p and (a, z_a, k_a). Combined with the flux summation, they give rise to the expression for the index factorized into the perturbative part and the vortex parts sketched earlier. In particular, the perturbative part can be extracted out by evaluating the residue for $m_a = k_a = 0$, which is given by

$$
Z_{\text{pert}}^p(z, t, q) = \left(\prod_{1 \leq a \neq b \leq N} \left(1 - v_a^{-1} v_b \right) \right) \left(\prod_{a=1}^{N} \frac{(v_a q^2; q^2)}{(v_a^{-1}; q^2)'} \frac{(v_a^{-1} u^{-2} q^2; q^2)}{(v_a u^2; q^2)} \right)
$$
$$
\times \left(\prod_{a,b=1}^{N} \frac{(v_a v_b^{-1} u^2; q^2)(v_a v_b^{-1} v^{-1} q^2; q^2)(v_a v_b^{-1} u^{-2} v q^2; q^2)}{(v_a^{-1} v_b u^{-2} q^2; q^2)(v_a^{-1} v_b v; q^2)'(v_a^{-1} v_b u^2 v^{-1}; q^2)'} \right)
$$

$$(5.2.47)$$

where

$$
v_a = \left(\prod_{n=0}^{l_a - 1} z_{p^n(a)} \right) (tq)^{\frac{l_a - 1}{2}},
$$
$$
u = t^{\frac{1}{2}} q^{\frac{1}{2}}, \qquad v = z t^{\frac{1}{2}} q^{\frac{1}{2}}.
$$

$$(5.2.48)$$

Note that v_a reduces to $v^{l_a - 1}$ if $z_b = z$ for all b. $(a; q^2)'$ is defined around (5.2.16). Namely, it is defined as an ordinary q-Pochhammer symbol up to the vanishing factors discarded. Note that there are N such vanishing factors, which arise due to the pole we have taken.

The expression (5.2.47) is specified by a binary tree p. Note that a binary tree of $N < 4$ nodes can be represented by a 2-dimensional box diagram; e.g., see figure 5.1 for $N = 3$. The left child node is placed on top of the parent node and the right child node is placed at the right side of the parent node. Among the box diagrams in figure 5.1, the second and the fourth diagrams have vanishing residues due to the factor $\prod_{a,b=1}^{N} (v_a v_b^{-1} u^2; q^2)$ in (5.2.47). This factor gives an extra zero whenever we have diagonally adjacent boxes along
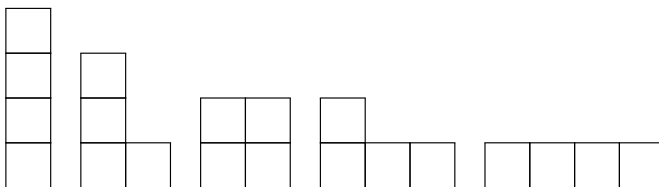
Figure 5.2: For our $\mathcal{N} = 4$ SYM example, the contributing poles are labeled by Young diagrams. For $N = 4$ there are five diagrams, among which the third diagram corresponds to a degenerate singularity where five hyperplanes intersect rather than four.

the top-right direction. Thus, for $N = 3$, only the first, third and fifth diagrams contribute.

Such box diagrams can label the residues for higher N as well. One may worry that the correspondence between the binary trees and the 2-dimensional box diagrams is not one-to-one for $N \geq 4$. Indeed, there are two such cases. First, there exist tree graphs that do not have box diagram counterparts. That happens only if two nodes of the binary tree are overlapped when they are represented in the 2-dimensional box diagram. However, such a tree with over-lapping nodes has the vanishing residue due to the first factor $\prod_{a \neq b} \left(1 - v_a^{-1} v_b\right)$ of (5.2.47). Thus, one can always find the corresponding box diagram unless the tree graph has the vanishing residue.

Second, there can be multiple tree graphs that are mapped to the same box diagram. This is related to the possibility of higher order poles, which will demand us to modify the formula (5.2.47). In that case, more than N vanishing factors appear in the denominator of (5.2.47) if we forget about the $'$ symbol for a moment. Such a case, for instance, happens for the third diagram in figure 5.2. One can associate two different tree graphs to this box diagram because the top-right box can be either the right child of the top-left node or the left child node of the bottom-right node. This is exactly due to the fact

that the five hyperplanes intersect at this pole rather than four. Although the singularity is unique, there are two ways of picking up four linearly independent hyperplanes defining this singularity. Therefore, (5.2.47) is wrong if p does not uniquely label the poles. Instead, we should seek for a formula in which the box diagrams rather than p label the residues.

Now recall that if there are diagonally adjacent boxes along the top-right direction, they yield an extra zero. For the third diagram in figure 5.2, this extra zero cancels out the extra pole from the degenerate hyperplanes such that the singularity becomes a simple pole. Thus, a simple modification of (5.2.47) will give the right residue formula if we discard the extra vanishing factors in the numerator and the denominator simultaneously. In our $\mathcal{N} = 4$ SYM example, for arbitrary box diagrams, an extra vanishing factor in the denominator is always accompanied by an extra zero in the numerator. Furthermore, a pole corresponding to a non-Young diagram has the vanishing residue as we have demonstrated for $N = 3$. Thus, the contributing poles are all simple and labeled by Young diagrams.

Collecting all, we write down a modification of (5.2.47) in terms of the Young diagrams. For a Young diagram $\mathcal{Y}$, the perturbative part is written as follows:

$$
Z_{\text{pert}}^{\mathcal{Y}}(z, t, q) = \left(\prod_{\mathsf{a} \neq \mathsf{b} \in \mathcal{Y}} \left(1 - v_{\mathsf{a}}^{-1} v_{\mathsf{b}} \right) \right) \left(\prod_{\mathsf{a} \in \mathcal{Y}} \frac{(v_{\mathsf{a}} q^2; q^2)}{(v_{\mathsf{a}}^{-1}; q^2)'} \frac{(v_{\mathsf{a}}^{-1} u^{-2} q^2; q^2)}{(v_{\mathsf{a}} u^2; q^2)} \right)
$$
$$
\times \left(\prod_{\mathsf{a}, \mathsf{b} \in \mathcal{Y}} \frac{(v_{\mathsf{a}} v_{\mathsf{b}}^{-1} u^2; q^2)'(v_{\mathsf{a}} v_{\mathsf{b}}^{-1} v^{-1} q^2; q^2)(v_{\mathsf{a}} v_{\mathsf{b}}^{-1} u^{-2} v q^2; q^2)}{(v_{\mathsf{a}}^{-1} v_{\mathsf{b}} u^{-2} q^2; q^2)(v_{\mathsf{a}}^{-1} v_{\mathsf{b}} v; q^2)'(v_{\mathsf{a}}^{-1} v_{\mathsf{b}} u^2 v^{-1}; q^2)'} \right).
$$
$$
(5.2.49)
$$

v_{a} is now given by

$$
v_{\mathsf{a}} = z^{\mathsf{i}(\mathsf{a}) - \mathsf{j}(\mathsf{a})} (tq)^{\frac{1}{2}(\mathsf{i}(\mathsf{a}) + \mathsf{j}(\mathsf{a}) - 2)} \tag{5.2.50}
$$

where $(\mathsf{i}(\mathsf{a}), \mathsf{j}(\mathsf{a}))$ is the position of box a in the Young diagram $\mathcal{Y}$. Again $'$ denotes that the vanishing factors are discarded. Note that the label $a = 1, \cdots, N$ of each node that we began with is now irrelevant. It will turn out that this is also true for the vortex parts, so we have $N!$ identical contributions, which are canceled by the symmetry factor $1/N!$.

Now we move on to the vortex parts. After evaluating the integral by taking the non-vanishing residues, we are left with the summation over Young diagrams as well as the two summations over m_a and k_a. The latter sums over m_a, k_a can be reorganized into the sums over the vorticity and the anti-vorticity, which are completely factorized for given Young diagram $\mathcal{Y}$. The detailed computation of the vortex parts is similar to what is done in [183]. It turns out that the result is simply given by making the following replacements in Z_{vortex} in (5.2.22), which we obtained from the $D_2 \times S^1$ index in the previous section:

$$\prod_{a=1}^{N} \to \prod_{\mathsf{a} \in \mathcal{Y}} \ , \quad v^{a-1} \to v_{\mathsf{a}} = z^{\mathsf{i}(\mathsf{a}) - \mathsf{j}(\mathsf{a})}(tq)^{\frac{1}{2}(\mathsf{i}(\mathsf{a}) + \mathsf{j}(\mathsf{a}) - 2)} \ , \quad k_a \to k_{\mathsf{a}} \ , \quad Q \to \hat{Q} t^{\frac{1}{2}} q^{-\frac{1}{2}} \ .$$
$$(5.2.51)$$

k_{a} is a non-negative integer assigned to each $\mathsf{a} \in \mathcal{Y}$ such that those integers are non-decreasing in each row and column of $\mathcal{Y}$. This resembles the standard Young tableau, in which the associated integers are strictly increasing rather than non-decreasing. Taking into account those modifications, we have the following expression of $Z_{\text{vortex}}^{\mathcal{Y}}$ for the Young diagram $\mathcal{Y}$:

$$\begin{aligned}
Z_{\text{vortex}}^{\mathcal{Y}}(\hat{Q}, z, t, q) &= \sum_{k_{\mathsf{a}}} (\hat{Q} t^{\frac{1}{2}} q^{-\frac{1}{2}})^{\sum_{\mathsf{a} \in \mathcal{Y}} k_{\mathsf{a}}} \left(\prod_{\mathsf{a} \in \mathcal{Y}} \frac{(v_{\mathsf{a}}^{-1}; q^2)_{-k_{\mathsf{a}}}}{(u^{-2} v_{\mathsf{a}}^{-1} q^2; q^2)_{-k_{\mathsf{a}}}} \right) \quad (5.2.52) \\
&\times \left(\prod_{\mathsf{a} \neq \mathsf{b} \in \mathcal{Y}} \frac{(v v_{\mathsf{a}}^{-1} v_{\mathsf{b}}; q^2)_{-k_{\mathsf{a}} + k_{\mathsf{b}}} (u^{-2} v_{\mathsf{a}}^{-1} v_{\mathsf{b}} q^2; q^2)_{-k_{\mathsf{a}} + k_{\mathsf{b}}}}{(v_{\mathsf{a}}^{-1} v_{\mathsf{b}}; q^2)_{-k_{\mathsf{a}} + k_{\mathsf{b}}} (u^{-2} v v_{\mathsf{a}}^{-1} v_{\mathsf{b}} q^2; q^2)_{-k_{\mathsf{a}} + k_{\mathsf{b}}}} \right) \ .
\end{aligned}$$

If we take $\mathcal{Y} = (1^N)$, (5.2.52) reduces to Z_{vort} in the previous section.

In the end, combining the perturbative part and the vortex parts, (5.2.41)

is written in the following factorized form

$$Z_{S^2 \times S^1}(\hat{Q}, z, t, q) = \sum_{|\mathcal{Y}|=N} Z_{\text{pert}}^{\mathcal{Y}}(z, t, q) \, Z_{\text{vortex}}^{\mathcal{Y}}(\hat{Q}, z, t, q) \, Z_{\text{vortex}}^{\mathcal{Y}}(\hat{Q}^{-1}, z^{-1}, t^{-1}, q^{-1}) \, .$$

$$(5.2.53)$$

The expression (5.2.53) is also checked numerically up to $N = 3$ as a series expansion in q up to q^3, and also at $N = 4$ up to q^2.

5.3   Cardy limit of the index on $S^2 \times S^1$: set-up

In this section, we set up a direct framework of making the Cardy limit approximation of the index on $S^2 \times \mathbb{R}$. The result will be connected to the vortex partition function that we studied in the previous section. Although we focus on the $\mathcal{N} = 4$ Yang-Mills theory for M2-branes introduced in the previous section, the framework applies to other 3d QFTs. We shall provide similar analysis for the ABJM theory in section 4.3.

The index of our $\mathcal{N} = 4$ gauge theories on $S^2 \times S^1$ is given by $(e^{-\hat{\xi}} \equiv \hat{Q})$ [163]

$$\begin{aligned}
Z \;=\; & \sum_{\{m\}=-\infty}^{\infty} \frac{1}{\text{Weyl}(\{m\})} \oint \frac{d\alpha_a}{2\pi} e^{-\hat{\xi} \sum_{a=1}^{N} m_a} \prod_{a=1}^{N} (qt^{-1})^{\frac{|m_a|}{2}} \frac{(e^{-i\alpha_a} q^{|m_a|} t^{-\frac{1}{2}} q^{\frac{3}{2}}; q^2)(e^{i\alpha_a} q^{|m_a|} t^{-\frac{1}{2}} q^{\frac{3}{2}}; q^2)}{(e^{i\alpha_a} q^{|m_a|} t^{\frac{1}{2}} q^{\frac{1}{2}}; q^2)(e^{-i\alpha_a} q^{|m_a|} t^{\frac{1}{2}} q^{\frac{1}{2}}; q^2)} \\[2mm]
& \times \prod_{a \neq b} q^{-\frac{|m_{ab}|}{2}} (1 - e^{i\alpha_{ab}} q^{|m_{ab}|}) \prod_{a,b=1}^{N} t^{\frac{|m_{ab}|}{2}} \frac{(e^{i\alpha_{ab}} t q^{1+|m_{ab}|}; q^2)}{(e^{i\alpha_{ab}} t^{-1} q^{1+|m_{ab}|}; q^2)} \quad (5.3.1) \\[2mm]
& \times \prod_{a,b=1}^{N} (qt^{-1})^{\frac{|m_{ab}|}{2}} \frac{(e^{i\alpha_{ab}} q^{|m_{ab}|} z^{-1} t^{-\frac{1}{2}} q^{\frac{3}{2}}; q^2)(e^{i\alpha_{ab}} q^{|m_{ab}|} z t^{-\frac{1}{2}} q^{\frac{3}{2}}; q^2)}{(e^{i\alpha_{ab}} q^{|m_{ab}|} z t^{\frac{1}{2}} q^{\frac{1}{2}}; q^2)(e^{i\alpha_{ab}} q^{|m_{ab}|} z^{-1} t^{\frac{1}{2}} q^{\frac{1}{2}}; q^2)}
\end{aligned}$$

Here, the factor $\prod_{a \neq b}(1 - e^{i\alpha_{ab}} q^{|m_{ab}|})$ coming from the Haar measure and the $\mathcal{N} = 2$ vector multiplet may be written as

$$\prod_{a \neq b}(1 - e^{i\alpha_{ab}} q^{|m_{ab}|}) = \prod_{a \neq b} \frac{(e^{i\alpha_{ab}} q^{|m_{ab}|}; q^2)}{(e^{i\alpha_{ab}} q^{2+|m_{ab}|}; q^2)} \, , \qquad (5.3.2)$$

which was relevant in section 2 when we discussed the factorization of this index into vortex partition functions.

We would first like to rewrite the index in the following way. Each chiral multiplet contributes the following factor to the contour integrand:

$$\left(e^{-i\rho(\alpha)}q^{1-R}y^{-1}\right)^{\frac{|\rho(m)|}{2}}\frac{(e^{-i\rho(\alpha)}q^{2-R+|\rho(m)|}y^{-1};q^2)}{(e^{i\rho(\alpha)}q^{R+|\rho(m)|}y;q^2)} \ . \qquad (5.3.3)$$

For the chiral multiplets in our $\mathcal{N}=4$ theory, $R=\frac{1}{2}$ and y is given by a suitable combination of t and z. For the adjoint chiral multiplet in the $\mathcal{N}=4$ vector multiplet, this formula applies with $R=1$ and $y=t^{-1}$. Even for the $\mathcal{N}=2$ vector multiplet, inverse of this expression applies at $R=0$ and $y=1$ if one uses the decomposition (5.3.2). One can show that [185]

$$\left(e^{-i\rho(\alpha)}q^{1-R}y^{-1}\right)^{\frac{|\rho(m)|}{2}}\frac{(e^{-i\rho(\alpha)}q^{2-R+|\rho(m)|}y^{-1};q^2)}{(e^{i\rho(\alpha)}q^{R+|\rho(m)|}y;q^2)} = \left(e^{-i\rho(\alpha)}q^{1-R}y^{-1}\right)^{-\frac{\rho(m)}{2}}\frac{(e^{-i\rho(\alpha)}q^{2-R-\rho(m)}y^{-1};q^2)}{(e^{i\rho(\alpha)}q^{R-\rho(m)}y;q^2)} \ .$$
$$(5.3.4)$$

This identity states that one can replace all $|\rho(m)|$'s by $-\rho(m)$. (Of course one can have a similar identity replacing $|\rho(m)| \to +\rho(m)$.) One also finds

$$\left(e^{i\rho(\alpha)}q^{1-R}\tilde{y}^{-1}\right)^{\frac{|\rho(m)|}{2}}\frac{(e^{i\rho(\alpha)}q^{2-R+|\rho(m)|}\tilde{y}^{-1};q^2)}{(e^{-i\rho(\alpha)}q^{R+|\rho(m)|}\tilde{y};q^2)} = \left(e^{i\rho(\alpha)}q^{1-R}\tilde{y}^{-1}\right)^{-\frac{\rho(m)}{2}}\frac{(e^{i\rho(\alpha)}q^{2-R-\rho(m)}\tilde{y}^{-1};q^2)}{(e^{-i\rho(\alpha)}q^{R-\rho(m)}\tilde{y};q^2)} \ .$$
$$(5.3.5)$$

In our $\mathcal{N}=4$ theory, one obtains a product of the two left hand sides of (5.3.4) and (5.3.5) for each hypermultiplet. The above identities state that this factor can be replaced by

$$\left(q^{1-R}y^{-\frac{1}{2}}\tilde{y}^{-\frac{1}{2}}\right)^{-\rho(m)}\frac{(e^{\rho(\bar{u})}q^{2-R}y^{-1};q^2)(e^{\rho(u)}q^{2-R}\tilde{y}^{-1};q^2)}{(e^{\rho(u)}q^{R}y;q^2)(e^{\rho(\bar{u})}q^{R}\tilde{y};q^2)} \qquad (5.3.6)$$

where $q=e^{-\beta}$ and $u \equiv \beta m + i\alpha$. We shall apply this formula for all weights ρ in a representation $\mathbf{R}$, so that there is a product $\prod_{\rho \in \mathbf{R}}$ which comes with holomorphic $\rho(u)$, while $\prod_{-\rho \in \overline{\mathbf{R}}}$ comes with anti-holomorphic $\rho(\bar{u})$. In other words, one obtains the following factorization of the integrand into 'holomophic' and 'anti-holomorphic' parts:

$$\prod_{a=1}^{N}(t/q)^{\frac{u_a}{4\beta}}\frac{(e^{u_a}t^{-\frac{1}{2}}q^{\frac{3}{2}};q^2)}{(e^{u_a}t^{\frac{1}{2}}q^{\frac{1}{2}};q^2)}\prod_{a,b=1}^{N}\frac{(e^{u_{ab}}zt^{-\frac{1}{2}}q^{\frac{3}{2}};q^2)}{(e^{u_{ab}}zt^{\frac{1}{2}}q^{\frac{1}{2}};q^2)} \cdot \prod_{a=1}^{N}(t/q)^{\frac{\bar{u}_a}{4\beta}}\frac{(e^{\bar{u}_a}t^{-\frac{1}{2}}q^{\frac{3}{2}};q^2)}{(e^{\bar{u}_a}t^{\frac{1}{2}}q^{\frac{1}{2}};q^2)}\prod_{a,b=1}^{N}\frac{(e^{\bar{u}_{ab}}z^{-1}t^{-\frac{1}{2}}q^{\frac{3}{2}};q^2)}{(e^{\bar{u}_{ab}}z^{-1}t^{\frac{1}{2}}q^{\frac{1}{2}};q^2)} \ .$$
$$(5.3.7)$$

Here, we inserted $R = \frac{1}{2}$ for all hypermultiplet fields, $y = \tilde{y} = t^{\frac{1}{2}}$ for fundamental hyper, and $y = t^{\frac{1}{2}}z$, $\tilde{y} = t^{\frac{1}{2}}z^{-1}$ for adjoint hyper. The 'holomorphic' part depending on u_a is part of the integrand appearing in the $D_2 \times S^1$ index (5.2.11) after setting $e^{u_a} = s_a$, except the factor $(t/q)^{\frac{u_a}{4\beta}}$ that will be accounted for shortly. The 'anti-holomorphic part' will also have a similar interpretation on $D_2 \times S^1$. As for the integrand coming from the $\mathcal{N} = 4$ vector multiplet,

$$\prod_{a \neq b} (e^{-i\alpha_{ab}}q)^{-\frac{|m_{ab}|}{2}} (1 - e^{i\alpha_{ab}}q^{|m_{ab}|}) \prod_{a,b=1}^{N} (e^{-i\alpha_{ab}}t)^{\frac{|m_{ab}|}{2}} \frac{(e^{-i\alpha_{ab}}tq^{1+|m_{ab}|}; q^2)}{(e^{i\alpha_{ab}}t^{-1}q^{1+|m_{ab}|}; q^2)} \quad (5.3.8)$$

$$= \prod_{a \neq b} (e^{-i\alpha_{ab}}q)^{-\frac{|m_{ab}|}{2}} \frac{(e^{i\alpha_{ab}}q^{|m_{ab}|}; q^2)}{(e^{-i\alpha_{ab}}q^{2+|m_{ab}|}; q^2)} \prod_{a,b=1}^{N} (e^{-i\alpha_{ab}}t)^{\frac{|m_{ab}|}{2}} \frac{(e^{-i\alpha_{ab}}tq^{1+|m_{ab}|}; q^2)}{(e^{i\alpha_{ab}}t^{-1}q^{1+|m_{ab}|}; q^2)} \,,$$

the first factor comes from the $\mathcal{N} = 2$ vector multiplet, and the second factor from the $\mathcal{N} = 2$ adjoint chiral multiplet within the $\mathcal{N} = 4$ vector multiplet. Applying (5.3.4), one obtains

$$\prod_{a \neq b} (e^{-i\alpha_{ab}}q)^{\frac{m_{ab}}{2}} \frac{(e^{u_{ab}}; q^2)}{(e^{\bar{u}_{ab}}q^2; q^2)} \prod_{a,b=1}^{N} (e^{-i\alpha_{ab}}t)^{-\frac{m_{ab}}{2}} \frac{(e^{\bar{u}_{ab}}tq; q^2)}{(e^{u_{ab}}t^{-1}q; q^2)} = \frac{\prod_{a \neq b}(e^{u_{ab}}; q^2)}{\prod_{a,b}(e^{u_{ab}}t^{-1}q; q^2)} \cdot \frac{\prod_{a,b}(e^{\bar{u}_{ab}}tq; q^2)}{\prod_{a \neq b}(e^{\bar{u}_{ab}}q^2; q^2)} \,.$$
$$(5.3.9)$$

The holomorphic part is again part of the integrand appearing in the $D_2 \times S^1$ index (5.2.11).

Finally, the fugacity factor $e^{-\hat{\xi}\sum_a m_a}$ for the topological $U(1)_T$ can be written as

$$e^{-\hat{\xi}\sum_a m_a} = e^{-\frac{\hat{\xi}}{2\beta}\sum_a u_a} e^{-\frac{\hat{\xi}}{2\beta}\sum_a \bar{u}_a} \,, \qquad (5.3.10)$$

which again factorizes to holomorphic and anti-holomorphic part. Combined with the factor $(t/q)^{\sum_a \frac{u_a}{4\beta}}$ from hypermultiplets, one obtains

$$e^{-\frac{\xi}{2\beta}\sum_a u_a} e^{-\frac{\xi}{2\beta}\sum_a \bar{u}_a} \qquad (5.3.11)$$

where

$$e^{-\xi} \equiv e^{-\hat{\xi}}(t/q)^{\frac{1}{2}} \qquad (5.3.12)$$

is the FI parameter that appeared in the $D_2 \times S^1$ index. (Recall that $2\pi r \zeta = \frac{\xi}{2\beta}$.) So one obtains a 'formal factorization' of the integrand of the index on $S^2 \times S^1$. This is not a true factorization yet, because $u_a, \bar{u}_a$ have to be partly integrated (imaginary part) while partly summed over discretely (real part).

Before proceeding, with the formula for the index with all absolute values of $\rho(m)$ removed as above, we identify the periods of the chemical potentials and present a natural basis. This will be useful later for understanding the precise structures of the saddle point free energy. From the integrand including the flux-dependent zero point energy factor, one identifies the following periodicities:

$$\hat{\xi} \quad \sim \quad \hat{\xi} + 2\pi i \tag{5.3.13}$$

$$(T, \beta) \quad \sim \quad (T \pm 2\pi i, \beta + 2\pi i)$$

$$f \quad \sim \quad f + 2\pi i$$

$$(\hat{\xi}, f, \beta; \alpha_a) \quad \sim \quad (\hat{\xi} \pm \pi i, f \pm \pi i, \beta + 2\pi i; \alpha_a + \pi) \tag{5.3.14}$$

$$(T, \hat{\xi}, f; \alpha_a) \quad \sim \quad (T + 2\pi i, \hat{\xi} \pm \pi i, f \pm \pi i; \alpha_a + \pi)$$

where $t = e^T$, $z = e^f$. The $\pm$ signs appearing on the right hand sides are independent. Note that the shift $\alpha_a \to \alpha_a + \pi$ of the integral variables is sometimes required to see that the integrand is invariant. Now let us define the variables,

$$\Delta_1 \equiv -\hat{\xi} + \frac{T}{2} + \frac{\beta}{2} , \quad \Delta_2 \equiv \hat{\xi} + \frac{T}{2} + \frac{\beta}{2} , \quad \Delta_3 \equiv f - \frac{T}{2} + \frac{\beta}{2} , \quad \Delta_4 \equiv -f - \frac{T}{2} + \frac{\beta}{2} .$$
$$\tag{5.3.15}$$

Note that these four variables can be regarded as four independent chemical potentials of the index. They are related to β as $\Delta_1 + \Delta_2 + \Delta_3 + \Delta_4 - 2\beta = 0$, so that the sum over them is approximately zero in the Cardy limit $\beta \to 0$. In terms of these variables, the 12 periodicities identified above can be rephrased as

$$(\Delta_I, \Delta_J) \sim (\Delta_I + 2\pi i, \Delta_J \pm 2\pi i) \tag{5.3.16}$$

shifts for 6 possible pairs Δ_I, Δ_J among $\Delta_{1,2,3,4}$. These are the basic periodicities expected for the $SO(8)$ chemical potentials, coupling to vector, spinors or their product representations. In terms of Δ_I's, the index can be written as

$$Z_{S^2 \times S^1}(\Delta_I) = \text{Tr} \left[(-1)^F e^{-\sum_{I=1}^4 \Delta_I (Q_I + J)} \right] \qquad (5.3.17)$$

where Q_I's are the $U(1)^4 \subset SO(8)$ Cartans, and J is the angular momentum on S^2. Δ_I should satisfy

$$\text{Re}(\Delta_I) > 0 \ , \quad \sum_{I=1}^4 \Delta_I = 2\beta \ , \qquad (5.3.18)$$

as they are conjugate the charges $Q_I + J$ which are non-negative in the BPS sector and furthermore can grow to $+\infty$.

Let us now take the $\beta \to 0$ Cardy limit of the index, keeping small complex β with $\text{Re}(\beta) > 0$. The idea [186] is to now regard $u_a = \beta m_a + i \alpha_a$ as a continuum complex variable, and replace the sum over m_a by integration. The N dimensional integral over α_a and sum over m_a are replaced by a $2N$ dimensional integral over u_a, $\bar{u}_a$. One obtains

$$Z \sim \int \prod_{a=1}^N du_a e^{-\frac{\xi}{2\beta} \sum_{a=1}^N u_a} \prod_{a=1}^N \frac{(e^{u_a} t^{-\frac{1}{2}} q^{\frac{3}{2}}; q^2)}{(e^{u_a} t^{\frac{1}{2}} q^{\frac{1}{2}}; q^2)} \prod_{a,b=1}^N \frac{(e^{u_{ab}} z t^{-\frac{1}{2}} q^{\frac{3}{2}}; q^2)}{(e^{u_{ab}} z t^{\frac{1}{2}} q^{\frac{1}{2}}; q^2)} \frac{\prod_{a \neq b}(e^{u_{ab}}; q^2)}{\prod_{a,b}(e^{u_{ab}} t^{-1} q; q^2)} (5.3.19)$$

$$\times \int \prod_{a=1}^N d\bar{u}_a e^{-\frac{\xi}{2\beta} \sum_{a=1}^N \bar{u}_a} \prod_{a=1}^N \frac{(e^{\bar{u}_a} t^{-\frac{1}{2}} q^{\frac{3}{2}}; q^2)}{(e^{\bar{u}_a} t^{\frac{1}{2}} q^{\frac{1}{2}}; q^2)} \prod_{a,b=1}^N \frac{(e^{\bar{u}_{ab}} z^{-1} t^{-\frac{1}{2}} q^{\frac{3}{2}}; q^2)}{(e^{\bar{u}_{ab}} z^{-1} t^{\frac{1}{2}} q^{\frac{1}{2}}; q^2)} \frac{\prod_{a,b}(e^{\bar{u}_{ab}} t q; q^2)}{\prod_{a \neq b}(e^{\bar{u}_{ab}} q^2; q^2)} \ .$$

Here, we have formally separated the integrands into u dependent parts and $\bar{u}$ dependent parts. Note that, with complex β (which will play crucial roles later in this chapter), u_a and $\bar{u}_a$ are not complex conjugate to each other. As we took $\beta \to 0$ limit to make the continuum approximation for the summation of m_a, the q-Pochhammer symbols appearing in the integrand should also be approximated to dilogarithm functions as follows:

$$(x q^a; q^2) \xrightarrow{\beta \to 0} \exp\left[-\frac{\text{Li}_2(x)}{2\beta} \right] \ . \qquad (5.3.20)$$

We shall seek for the saddle points of u_a, $\bar{u}_a$ which will approximate the integral in the $\beta \to 0$ limit. While seeking for the saddle points, one can separately consider the saddle points for u_a, $\bar{u}_a$ independently, since the integrand factorizes. During this course, whenever any of the x variables appearing in Li_2 functions are larger than 1, i.e. $|x| > 1$, analytic continuations are made for those $\mathrm{Li}_2(x)$ functions. Whenever $|x|$ is greater than 1, one would have to worry about the branch cut issues of $\mathrm{Li}_2(x)$ after making the analytic continuations. This issue will be treated later when we discuss concrete problems. (However, 'branch cuts' here should always be understood as singularities of the Cardy free energy rather than signaling multi-valued functions.)

Here, note that the first line of (5.3.19) is the $\beta \to 0$ limit of the vortex partition function on $D_2 \times S^1$, considered in section 2, corresponding to the vertical Young diagram (1^N). The holomorphic integrand is given by the exponential of

$$\frac{1}{2\beta}\left[-\xi \sum_a u_a + \sum_a \left(\mathrm{Li}_2(e^{u_a}t^{\frac{1}{2}}) - \mathrm{Li}_2(e^{u_a}t^{-\frac{1}{2}}) \right) \right. \tag{5.3.21}$$

$$\left. + \sum_{a,b} \left(\mathrm{Li}_2(e^{u_{ab}}zt^{\frac{1}{2}}) - \mathrm{Li}_2(e^{u_{ab}}zt^{-\frac{1}{2}}) + \mathrm{Li}_2(e^{u_{ab}}t^{-1}) \right) - \sum_{a \neq b} \mathrm{Li}_2(e^{u_{ab}}) \right] .$$

On the other hand, the $\beta \to 0$ limit of the integrand on the second line of (5.3.19) can be obtained from (5.3.21) by flipping $(\beta, \xi) \to (-\beta, -\xi)$ and $(t, z) \to (t^{-1}, z^{-1})$. This is the same as the Cardy limit of the anti-vortex partition function of section 2. Therefore, at least in the Cardy limit, the two factors in (5.3.19) can be interpreted as the vortex-anti-vortex factorization which refers to a particular point in the Higgs branch (corresponding to the vertical Young diagram). In particular, we have shown that the particular vortex partition function chosen in section 2.1 will provide the Cardy saddle point of the index on $S^2 \times S^1$, which is not clear at all in the factorization formula of section 2.2.

Note that, after the factorization, the periodicities (5.3.16) of the four chem-

ical potentials Δ_I are not manifest in each integrand. Therefore, when we study the Cardy (and large N) limits in the next section, we shall first make a suitable period shifts of Δ_I's to bring them into a canonical chamber, and then factorize using the setup of this section.

5.4   Cardy limit: results

In this section, we study the Cardy limit of our index on $S^2 \times S^1$. We shall discuss in sections 4.1 and 4.3 the large N and Cardy limits for our $\mathcal{N} = 4$ Yang-Mills theory and the ABJM theory, respectively. In section 4.2, we study the finite N Cardy limit. The Cardy limit is defined as $\beta \to 0$ with other chemical potentials (e.g. Δ_I's) imaginary and finite [75].

5.4.1   Large N Cardy free energy and black holes

In this subsection, we study the large N free energy of the index on $S^2 \times S^1$ in the Cardy limit. In section 3, we have seen its connection to the partition function $Z_{D_2 \times S^1}$ on $D_2 \times S^1 \sim \mathbb{R}^2 \times S^1$ at a particular point on the Higgs branch.

The holomorphic factorization of section 3 obscures the periodicities of chemical potentials if one pays attention to the holomorphic factor only. So before performing the factorization of section 3, we should first specify the ranges of the imaginary parts of ξ, T, f. (Recall that $t = e^T$, $z = e^f$, $2\pi r \zeta = \frac{\xi}{2\beta}$.) Note that these three variables are in the natural convention of the vortex partition function of section 2. Especially, ξ is related to the fugacity of the topological charge (on $S^2 \times S^1$) by $\hat{Q} \equiv e^{-\hat{\xi}} = q^{1/2} t^{-1/2} Q = e^{-\xi - T/2 - \beta/2}$. Without losing

generality, we take

$$2\pi p_1 < \mathrm{Im}(\xi) < 2\pi(p_1+1) \ , \quad 2\pi p_2 < \mathrm{Im}(T) < 2\pi(p_2+1) \tag{5.4.1}$$

$$2\pi p_3 < \mathrm{Im}\left(f - \frac{T}{2}\right) < 2\pi(p_3+1) \ , \quad 2\pi p_4 < \mathrm{Im}\left(-f - \frac{T}{2}\right) < 2\pi(p_4+1)$$

for certain integers $p_1, \cdots, p_4$. (It will be convenient later to set ranges as above.) Although we gave ranges to the imaginary parts of chemical potentials, they are (approximately) pure imaginary in the Cardy limit. This is because, as we take $\beta \to 0$ with $\mathrm{Re}(\beta) > 0$, (5.3.18) demands $\mathrm{Re}(\Delta_I) \to 0^+$ for all I's. Adding the last three inequalities of (5.4.1), one obtains

$$2\pi(p_1+p_2+p_3) < 0 < 2\pi(p_2+p_3+p_4+3) \ \to \ p_2+p_3+p_4 = -1, -2 \ . \tag{5.4.2}$$

We also recall the periodicities of these variables that we explained in section 3. Since we are now taking the Cardy limit $\beta \to 0$, we collect the periodic shifts which leave small β invariant:

$$(\xi, T, f) \sim (\xi + 2\pi i, T, f) \sim (\xi, T, f + 2\pi i) \sim (\xi, T + 2\pi i, f \pm \pi i) \ . \tag{5.4.3}$$

In terms of the variables $\xi, T, f - \frac{T}{2}, -f - \frac{T}{2}$, the four shifts above are rewritten as

$$\left(\xi, T, f - \frac{T}{2}, -f - \frac{T}{2}\right) \sim \left(\xi + 2\pi i, T, f - \frac{T}{2}, -f - \frac{T}{2}\right) \sim \left(\xi, T + 2\pi i, f - \frac{T}{2} - 2\pi i, -f - \frac{T}{2}\right)$$

$$\sim \left(\xi, T + 2\pi i, f - \frac{T}{2}, -f - \frac{T}{2} - 2\pi i\right) \sim \left(\xi, T, f - \frac{T}{2} + 2\pi i, -f - \frac{T}{2} - 2\pi i\right) \ . \tag{5.4.4}$$

Using these four period shifts, one can set p_1, p_2, p_3, p_4 to be one of the two cases:

$$\text{region I} \ : \ p_1 = -1 \ , \ p_2 = -1 \ , \ p_3 = 0 \ , \ p_4 = 0$$

$$\text{region II} \ : \ p_1 = 0 \ , \ p_2 = 0 \ , \ p_3 = -1 \ , \ p_3 = -1 \ . \tag{5.4.5}$$

Notice that, each of the last three shifts in (5.4.4) picks a pair in p_2, p_3, p_4, and shifts this pair by $(+1, -1)$. So the case I is for $p_2 + p_3 + p_4 = -1$ in (5.4.2), while the case II is for $p_2 + p_3 + p_4 = -2$. ξ has its own shift symmetry in (5.4.4), which we have suitably set as (5.4.5) for later convenience. Collecting all, it suffices to consider the two cases of (5.4.5) only.

Here, recall that the index on $S^2 \times S^1$ is related to that on $D_2 \times S^1$ as follows:

$$\lim_{\beta \to 0} Z_{S^2 \times S^1}(\beta, \hat{\xi}, f, T) \sim \lim_{\beta \to 0} Z_{D_2 \times S^1}(\beta, \xi, f, T) Z_{D_2 \times S^1}(-\beta, -\xi, -f, -T) \ . \tag{5.4.6}$$

From (5.4.6), we (formally) find the following expression

$$Z_{S^2 \times S^1}(\beta, \hat{\xi}, f, T) \sim Z_{S^2 \times S^1}(-\beta, -\hat{\xi}, -f, -T) \ , \tag{5.4.7}$$

for the free energy in the Cardy limit. Thus, from the Cardy index in the region I of (5.4.5), one can easily generate that in the region II, since the two regions

$$\text{I}: -2\pi < \text{Im}(\xi) < 0, \ -2\pi < \text{Im}(T) < 0, \ 0 < \text{Im}\left(f - \frac{T}{2}\right) < 2\pi, \ 0 < \text{Im}\left(-f - \frac{T}{2}\right) < 2\pi$$

$$\text{II}: 0 < \text{Im}(\xi) < 2\pi, \ 0 < \text{Im}(T) < 2\pi, \ -2\pi < \text{Im}\left(f - \frac{T}{2}\right) < 0, \ -2\pi < \text{Im}\left(-f - \frac{T}{2}\right) < 0 \tag{5.4.8}$$

are related to each other by the sign flips of (β, ξ, f, T). So from now on, we focus on the calculations in region I. Then, from (5.4.6), in order to obtain the Cardy index on $S^2 \times S^1$ in region I, one should compute two Cardy indices on $D_2 \times S^1$. However, we need not compute them independently. To see this, first note that the Cardy limit of the latter index takes the form of $\log Z_{D_2 \times S^1} \sim -\frac{\mathcal{F}(\xi, f, T)}{2\beta}$. Now consider the complex conjugation of this free energy. By definition of this index, which traces over the Hilbert space with integer coefficients and real charges, the complex conjugated free energy can be obtained by simply complex

conjugating the chemical potentials. So one obtains

$$\overline{\log Z_{D_2 \times S^1}(\beta, \xi, f, T)} \sim -\frac{\mathcal{F}(\bar{\xi}, \bar{f}, \bar{T})}{2\bar{\beta}} \sim \log Z_{D_2 \times S^1}(\bar{\beta}, -\xi, -f, -T) \ . \quad (5.4.9)$$

At the last step, we used the fact that ξ, f, T are all imaginary in our Cardy limit. Therefore, the nontrivial part $\mathcal{F}(-\xi, -f, -T)$ of $Z_{D_2 \times S^1}(-\beta, -\xi, -f, -T)$ in (5.4.6) can be obtained once we compute $\mathcal{F}(\xi, f, T)$ in region I.

We compute the large N and Cardy limit of $\log Z_{D_2 \times S^1}(\beta, \xi, f, T)$ in region I. The Cardy limit $\beta \to 0^+$ of $Z_{D_2 \times S^1}$ can be evaluated by the saddle point method as

$$Z_{D_2 \times S^1} \sim \exp\left(-\frac{1}{2\beta}\mathcal{W}^*\right) \ , \quad (5.4.10)$$

with $\mathcal{W}$ given by

$$\mathcal{W} = N\left(\mathrm{Li}_2(zt^{-1/2}q^{1/2}) - \mathrm{Li}_2(zt^{1/2}q^{-1/2}) - \mathrm{Li}_2(t^{-1})\right) + \sum_{a=1}^{N}\left(\xi \log s_a + \mathrm{Li}_2(s_a t^{-1/2}q^{1/2}) - \mathrm{Li}_2(s_a t^{1/2}q^{-1/2})\right)$$

$$+ \sum_{1 \le a \ne b \le N}\left(\mathrm{Li}_2(s_a s_b^{-1}q^{-1}) - \mathrm{Li}_2(s_a s_b^{-1}t^{-1}) + \mathrm{Li}_2(s_a s_b^{-1}zt^{-1/2}q^{1/2}) - \mathrm{Li}_2(s_a s_b^{-1}zt^{1/2}q^{-1/2})\right) \ .$$

$$(5.4.11)$$

Here, we used the asymptotic formula of the q-Pochhammer symbol in appendix A. $\mathcal{W}^*$ denotes the saddle point value of $\mathcal{W}$. Saddle point equations are given by (no summation for a):

$$s_a \partial_{s_a}\mathcal{W} = \xi + \mathrm{Li}_1(s_a t^{-1/2}q^{1/2}) - \mathrm{Li}_1(s_a t^{1/2}q^{-1/2}) + \sum_{b \ne a}\Big[\mathrm{Li}_1(s_a s_b^{-1}q^{-1}) - \mathrm{Li}_1(s_b s_a^{-1}q^{-1})$$

$$- \mathrm{Li}_1(s_a s_b^{-1}t^{-1}) + \mathrm{Li}_1(s_b s_a^{-1}t^{-1}) + \mathrm{Li}_1(s_a s_b^{-1}zt^{-1/2}q^{1/2})$$

$$- \mathrm{Li}_1(s_b s_a^{-1}zt^{-1/2}q^{1/2}) - \mathrm{Li}_1(s_a s_b^{-1}zt^{1/2}q^{-1/2}) + \mathrm{Li}_1(s_b s_a^{-1}zt^{1/2}q^{-1/2})\Big] = 0.$$

$$(5.4.12)$$

Note that $s_a = 0$ is a fake solution since the original equations $\partial_{s_a}\mathcal{W} = 0$ have $1/s_a$ factors. By redefining parameters and exponentiating both sides, one can see that the above saddle point equations (5.4.12) take the form of the Bethe

ansatz equations [171].[3] Finally, combining (5.4.6), (5.4.9), (5.4.10), one obtains

$$\log Z_{S^2 \times S^1}(\beta, \hat{\xi}, f, T) \sim -\frac{\mathcal{W}^*(\xi, f, T) - \overline{\mathcal{W}^*(\xi, f, T)}|_{(\bar{\xi}, \bar{f}, \bar{T}) = (-\xi, -f, -T)}}{2\beta}$$

$$= -\frac{2i \operatorname{Im}\left[\mathcal{W}^*(\xi, f, T)\right]|_{(\bar{\xi}, \bar{f}, \bar{T}) = (-\xi, -f, -T)}}{2\beta} ,$$
$$(5.4.13)$$

where ξ, f, T are taken to be pure imaginary while taking complex conjugations.

We now analytically find the relevant solution of (5.4.12). We will basically follow the procedures used in [66]. Based on the discussions made so far, we consider the region I of (5.4.5),

$$-2\pi < \operatorname{Im}(\xi) < 0, \ -2\pi < \operatorname{Im}(T) < 0, \ 0 < \operatorname{Im}\left(f - \frac{T}{2}\right) < 2\pi, \ 0 < \operatorname{Im}\left(-f - \frac{T}{2}\right) < 2\pi ,$$
$$(5.4.14)$$

where ξ, T, f are imaginary. Our ansatz for the eigenvalue distribution is given by

$$s_a = s_0 e^{N^\alpha x_{(a)} + iy(x_{(a)})} \quad (x_1 \le x_{(a)} \le x_2) , \qquad (5.4.15)$$

where $s_0 > 0$ is a positive real constant. Here $x_{(a)}$ and $y(x)$ are real, which we take to be at $\mathcal{O}(N^0)$. We introduced a factor N^α with $0 < \alpha < 1$. The constant α will be determined later. Also, we assumed that the eigenvalues are distributed in $[x_1, x_2]$ for some $x_1 < x_2$. Then, we introduce the continuum variable $x_{(a)} \to x$ assuming that we ordered the eigenvalues to make x to be an increasing function of a. This particular ordering cancels out the Weyl factor $N!$. In addition, we introduce the density function of the eigenvalues as $\rho(x) = \frac{1}{N}\frac{da}{dx}$. Here, we further assume a connected distribution of eigenvalues where ρ is always positive in (x_1, x_2).

---

[3]In (5.4.11) and (5.4.12), we have no essential need to keep $q \to 1^-$ in our Cardy limit. In fact we shall insert $q = 1$ in these formulae shortly, except that we temporarily need q^{-1} factors for the terms $\operatorname{Li}_2(s_a s_b^{-1} q^{-1})$ and $\operatorname{Li}_1(s_a s_b^{-1} q^{-1})$, as natural regulators to keep the saddle point slightly away from the branch cuts.

In this setting, we first take the continuum limit of $\mathcal{W}$. We will only consider the leading contribution at small β, plugging in $q = 1$ in (5.4.11) and (5.4.12). $\mathcal{W}$ can be divided into two parts, $\mathcal{W} = \mathcal{W}_{ext} + \mathcal{W}_{int}$. $\mathcal{W}_{ext}$ denotes the contribution from the external potential:

$$\mathcal{W}_{ext} = N \int_{x_1}^{x_2} dx \rho(x) \Big(\xi \log s(x) + \mathrm{Li}_2(s(x)t^{-1/2}) - \mathrm{Li}_2(s(x)t^{1/2}) \Big) .$$

$$(5.4.16)$$

$\mathcal{W}_{int}$ comes from the interactions of eigenvalue pairs:

$$
\begin{aligned}
\mathcal{W}_{int} = N^2 &\int_{x_1}^{x_2} dx \rho(x) \int_x^{x_2} dx' \rho(x') \Big(\mathrm{Li}_2(s(x)s(x')^{-1}) + \mathrm{Li}_2(s(x')s(x)^{-1}) \\
&- \mathrm{Li}_2(s(x)s(x')^{-1}t^{-1}) - \mathrm{Li}_2(s(x')s(x)^{-1}t^{-1}) + \mathrm{Li}_2(s(x)s(x')^{-1}zt^{-1/2}) \\
&+ \mathrm{Li}_2(s(x')s(x)^{-1}zt^{-1/2}) - \mathrm{Li}_2(s(x)s(x')^{-1}zt^{1/2}) - \mathrm{Li}_2(s(x')s(x)^{-1}zt^{1/2}) \Big) .
\end{aligned}
$$

$$(5.4.17)$$

The main strategy to extract the leading order contribution at in large N is to use the following integral formula [160]:

$$
\begin{aligned}
\int_0^{x>0} dx \rho(x) \mathrm{Li}_s(e^{-N^\alpha x + iy(x)}) &= \int_0^x dx \rho(x) \sum_{n=1}^\infty \frac{e^{n(-N^\alpha x + iy(x))}}{n^s} \\
&= \sum_{n=0}^\infty \frac{1}{n^s} \left[-\rho(x) e^{iny(x)} \frac{e^{-nN^\alpha x}}{nN^\alpha} \Big|_0^x + \int_0^x dx (\rho(x) e^{iny(x)})' \frac{e^{-nN^\alpha x}}{nN^\alpha} \right] \\
&= N^{-\alpha} \rho(0) \mathrm{Li}_{s+1}(e^{iy(0)}) + O(N^{-2\alpha}) ,
\end{aligned}
$$

$$(5.4.18)$$

where we used the power series definition of the polylogarithm function on the first line. One can see that the integral on the second line is suppressed by a factor of $1/N^\alpha$ compared to the boundary term, by performing integration by parts repeatedly. Note that we assumed $d\rho/dx$, $|dy/dx| < N^\alpha$.

Applying

$$\mathrm{Li}_n(a) + (-1)^n \mathrm{Li}_n(a^{-1}) = -\frac{(2\pi i)^n}{n!} B_n\left(\frac{\log a}{2\pi i} - p\right) \quad (2\pi p < \mathrm{Im}(\log a) < 2\pi(p+1),\ a \notin (0,1))$$

$$B_1(x) = x - \frac{1}{2}\ ,\quad B_2(x) = x^2 - x + \frac{1}{6}\ ,\quad B_3(x) = x^3 - \frac{3}{2}x^2 + \frac{1}{2}x\ ,\quad \cdots\ , \tag{5.4.19}$$

$\mathcal{W}_{ext}$ is approximated at large N as

$$\mathcal{W}_{ext} = N^{1+\alpha}\left[\xi \int_{x_1}^{x_2} dx \rho(x) x\right.$$

$$\left. + \left(T - 2\pi i \left(\left\lfloor \frac{2y(x) + \mathrm{Im}(T)}{4\pi} \right\rfloor - \left\lfloor \frac{2y(x) - \mathrm{Im}(T)}{4\pi} \right\rfloor\right)\right) \int_{\max(0,x_1)}^{\max(x_2,0)} dx \rho(x) x \right] + O(N^1)$$

$$\equiv N^{1+\alpha}\left[\xi \int_{x_1}^{x_2} dx \rho(x) x + \left(T - 2\pi i p_2'\right) \int_{\max(0,x_1)}^{\max(x_2,0)} dx \rho(x) x \right] + O(N^1)\ .$$

$$\tag{5.4.20}$$

Here, $\lfloor a \rfloor$ means the unique integer n satisfying $n \leq a < n + 1$. The last step is the definition of the integer p_2', whose values will be specified in a moment. One can see that the specific form of $y(x)$ does not affect to the leading order. Only the range of $y(x)$ contributes because it appears in the $\lfloor \ldots \rfloor$ symbols. (Its specific form may affect the sub-leading order in $1/N$, which is not of our interest here.) As part of our extremization problem, one should extremize $\mathcal{W}$ with respect to $y(x)$. However, it seems hard to make a fully general extremization of the functional containing a discrete function $\lfloor \ldots \rfloor$. To further manipulate, we assume that $y(x)$ does not pass across the branch cuts which cause the discrete jumps. One can regard it as part of our ansatz. There are two branch cuts from two $\lfloor \ldots \rfloor$'s. Hence, we should demand $y(x)$ to be within a specific region bounded by the two branch cuts. There are two possible regions, with the following values of p_2':

$$\text{(i)} \quad \frac{\mathrm{Im}(T)}{2} < y(x) < -\frac{\mathrm{Im}(T)}{2} \quad (\mathrm{mod}\ 2\pi)\ :\ p_2' = -1\ ,$$

$$\text{(ii)} \quad -\frac{\mathrm{Im}(T)}{2} < y(x) < 2\pi + \frac{\mathrm{Im}(T)}{2} \quad (\mathrm{mod}\ 2\pi)\ :\ p_2' = 0\ . \tag{5.4.21}$$

Later, we will determine which case yields nontrivial large N solutions.

We then consider the large N approximation of $\mathcal{W}_{int}$. Again to simplify the manipulations after using (5.4.19), (5.4.18), we assume that $y(x') - y(x)$ at $x' > x$ does not pass across the branch cuts. In particular, during this manipulation, one apparently encounters terms at order $O(N^{2+\alpha})$ whose coefficient is nonzero unless

$$\left\lfloor \frac{y(x') - y(x) + \mathrm{Im}(\beta)}{2\pi} \right\rfloor = -1 \quad (x' > x) . \tag{5.4.22}$$

(Here, we restored the subleading $\mathcal{O}(\beta)$ correction by not strictly plugging in $q = 1$ in (5.4.11), which is a convenient and natural regularization.) As we just started from a QFT with N^2 degrees of freedom, There will not be physical saddle points whose free energies scale like $N^{2+\alpha}$. So we impose the condition above on $y(x)$. There are other conditions for $y(x)$ so that no branch cuts are crossed at all. Collecting them all, one obtains the following conditions for $x' > x$:

$$-2\pi < y(x') - y(x) + \mathrm{Im}(\beta) < 0 \tag{5.4.23}$$
$$0 < y(x') - y(x) - \mathrm{Im}(T) < 2\pi$$
$$0 < y(x') - y(x) + \mathrm{Im}(f - T/2) < 2\pi$$
$$-2\pi < y(x') - y(x) + \mathrm{Im}(f + T/2) < 0 .$$

Here we quote a result that it we shall eventually pay attention to small β satisfying $\mathrm{Im}(\beta) < 0$. This is because, once we compute the free energy and go back to the microcanonical ensemble by the Legendre transformation, the dominant saddle point of our interest will always satisfy $\mathrm{Im}(\beta) < 0$. This is basically the result of [74], which we shall briefly review later in this subsection. With this assumed in foresight, the right inequality of the first line of (5.4.23) says that $y(x)$ is a non-increasing function, i.e. $y(x') - y(x) \leq 0$ at $x' > x$.

Here, the equality in $\leq$ is allowed because of the regularization with $\mathrm{Im}(\beta) < 0$. With this non-increasing property assumed, all the right inequalities of the second, third, fourth lines of (5.4.23) are automatically satisfied. Also, the left inequality on the first line of (5.4.23) is a consequence of the left inequality on the fourth line. Finally, the left inequalities of the second, third, fourth lines take the form of $y(x') - y(x) > A$ with negative real numbers A. With $y(x)$ being a non-increasing function in the interval (x_1, x_2), such a condition is equivalent to $y(x_2) - y(x_1) > A$, since $y(x_2) - y(x_1)$ is the minimum of $y(x') - y(x)$. So collecting all, (5.4.23) can be rephrased as

$$y(x') - y(x) \leq 0 \quad (\text{for } x' > x) \ , \quad y(x_2) - y(x_1) - \mathrm{Im}(T) > 0 \ , \qquad (5.4.24)$$
$$y(x_2) - y(x_1) + \mathrm{Im}(f - T/2) > 0 \ , \quad y(x_2) - y(x_1) + \mathrm{Im}(f + T/2) > -2\pi \ .$$

A particularly important possibility for $y(x)$ would be

$$y(x) = \text{constant} \ . \qquad (5.4.25)$$

Indeed, in the next subsection, we will numerically see that the Cardy saddle point solutions satisfy $y(x) = 0$ at arbitrary finite N. With the conditions (5.4.24), one obtains the following result for $\mathcal{W}_{\mathrm{int}}$ after some calculations:

$$\mathcal{W}_{int} = -\frac{N^2}{2}(T+2\pi i)\left(-f-\frac{T}{2}\right) - \frac{N^{2-\alpha}}{2}(T+2\pi i)\left(f-\frac{T}{2}\right)\left(-f-\frac{T}{2}\right)\int_{x_1}^{x_2}dx\rho(x)^2 + O(N^{2-2\alpha}) \ .$$
$$(5.4.26)$$

Here, we used $\int_{x_1}^{x_2}\rho(x)dx = 1$. $\mathcal{W}_{\mathrm{int}}$ in (5.4.26) shows short-ranged interactions only between nearby eigenvalues. One can see again that the specific form of $y(x)$ does not matter at the leading order. Since we are only interested in the leading free energy in N, we will not care about $y(x)$ below.

As a side remark before proceeding, we comment on the first term of (5.4.26) proportional to N^2, which does not depend on the eigenvalue distribution $\rho(x)$.

The terms in $\mathcal{W}_{\mathrm{ext}}$, $\mathcal{W}_{\mathrm{int}}$ which depend on $\rho(x)$ will be soon extremized below at $\alpha = \frac{1}{2}$, with the expected $N^{\frac{3}{2}}$ scaling for M2-branes. However, the first term of (5.4.26) proportional to N^2 might apparently look contradictory to the expected M2-brane behaviors. Here, we note that there is a very natural interpretation of such a term in the context of of the partition function on $D_2 \times S^1$. Namely, if one considers a 3d QFT on $D_2 \times \mathbb{R}$ or $D_2 \times S^1$, boundary chiral anomalies may be induced on $S^1 \times \mathbb{R}$ or T^2. We chose the boundary conditions so that the $U(N)$ gauge anomaly is canceled. But there are boundary 't Hooft anomalies for the global symmetries which are probed by the chemical potentials T, f. Since these boundary anomalies are proportional to N^2, the spectrum on $D_2 \times \mathbb{R}$ should contain such light degrees of freedom at the boundary. So even if the bulk physics would only see $N^{\frac{3}{2}}$ degrees of freedom, $\log Z_{D_2 \times S^1}$ will see certain terms at N^2 order. This is our interpretation of the first term of (5.4.26). If one combines two vortex partition functions to make an index on $S^2 \times S^1$ without any boundary using (5.4.13), the two terms proportional to N^2 indeed cancel,

$$ -\frac{N^2}{2}(T + 2\pi i)\left(-f - \frac{T}{2}\right) - (\text{complex conjugate}) = 0 \ . \qquad (5.4.27) $$

This is consistent with our interpretation. Also, note that we have no terms scaling like N^2 in (5.4.26) which depend on the dynamical gauge holonomy x (and accordingly not $\rho(x)$). This is because our QFT in section 2 has no boundary gauge anomaly. On the other hand, as commented briefly in footnote 2, p.7, we found it quite tricky (if not impossible) to provide simple boundary conditions for the ABJM theory without gauge anomaly. This will make the large N calculus very difficult. In section 4.3, we will introduce a rather ugly factorization for the ABJM index which breaks the $U(N) \times U(N)$ gauge symmetry, to circumvent this problem.

Collecting (5.4.20) and (5.4.26), one obtains

$$
\mathcal{W} \sim N^{1+\alpha} \left[\xi \int_{x_1}^{x_2} dx \rho(x) x + \left(T - 2\pi i p_2'\right) \int_{\max(0,x_1)}^{\max(x_2,0)} dx \rho(x) x \right]
$$
$$
- \frac{N^{2-\alpha}}{2} \left(T + 2\pi i\right) \left(f - \frac{T}{2}\right) \left(-f - \frac{T}{2}\right) \int_{x_1}^{x_2} dx \rho(x)^2 + \mathcal{W}_0 \tag{5.4.28}
$$

with $\mathcal{W}_0 \equiv -\frac{N^2}{2} \left(T + 2\pi i\right) \left(-f - \frac{T}{2}\right)$, where p_2' is either -1 or 0, as shown in (5.4.21). $\mathcal{W}_0$ can be ignored during our extremization problem. We extremize $\mathcal{W}$ with $\rho(x)$ in the set $\mathcal{C} = \left\{\rho \mid \int_{x_1}^{x_2} \rho(x) dx = 1; \ \rho(x) \geq 0 \text{ pointwise}\right\}$. As $N \to \infty$, in order to get nontrivial solutions, $\mathcal{W}_{ext}$ and $\mathcal{W}_{int} - \mathcal{W}_0$ should be at the same order in N. So we will now set $\alpha = \frac{1}{2}$. Introducing the Lagrange multiplier λ, we extremize the following functional, where $\hat{\mathcal{W}} \equiv \mathcal{W} - \mathcal{W}_0$:

$$
\begin{aligned}
\frac{\hat{\mathcal{W}}}{N^{\frac{3}{2}}} &= \xi \int_{\min(x_1,0)}^{\min(0,x_2)} dx \rho(x) x + \left(\xi + T - 2\pi i p_2'\right) \int_{\max(0,x_1)}^{\max(x_2,0)} dx \rho(x) x \\
&\quad - \frac{1}{2} \left(T + 2\pi i\right) \left(f - \frac{T}{2}\right) \left(-f - \frac{T}{2}\right) \int_{x_1}^{x_2} dx \rho(x)^2 + \lambda \left(\int_{x_1}^{x_2} dx \rho(x) - 1\right) .
\end{aligned} \tag{5.4.29}
$$

When $x_1 \leq x_2 \leq 0$ or $0 \leq x_1 \leq x_2$, one can see that there are no solutions for x_1, x_2 extremizing $\hat{\mathcal{W}}$. Thus, a nontrivial saddle point only exists when $x_1 \leq 0 \leq x_2$. In the last case, the extremal $\rho(x)$ is given by

$$
\rho(x) = \begin{cases} \frac{4\lambda + 4\xi x}{(T+2\pi i)(2f-T)(-2f-T)} , & x_1 \leq x \leq 0 \\ \frac{4\lambda + 4(\xi + T - 2\pi i p_2')x}{(T+2\pi i)(2f-T)(-2f-T)} , & 0 \leq x \leq x_2 \end{cases} . \tag{5.4.30}
$$

From the normalization condition $\int_{x_1}^{x_2} \rho(x) dx = 1$, the Lagrange multiplier λ is given by

$$
\lambda = \frac{(T + 2\pi i)(2f - T)(-2f - T) - 2(\xi + T - 2\pi i p_2')x_2^2 + 2\xi x_1^2}{4(x_2 - x_1)} . \tag{5.4.31}
$$

With pure imaginary ξ, f, T, $\rho(x)$ is automatically a real function. Inserting the above $\rho(x)$ and λ back to $\hat{\mathcal{W}}$, one obtains

$$
\hat{\mathcal{W}} = N^{\frac{3}{2}} \frac{-12\gamma^2 + 12\gamma(T'x_2^2 - \xi x_1^2) + \xi^2 x_1^4 + T'^2 x_2^4 - 4x_1 x_2(\xi^2 x_1^2 + T'^2 x_2^2) + 6\xi T' x_1^2 x_2^2}{24\gamma(x_2 - x_1)} ,
$$
$$
\tag{5.4.32}
$$

where $T' \equiv \xi + T - 2\pi i p_2'$, $\gamma \equiv (T + 2\pi i)\left(f - \frac{T}{2}\right)\left(-f - \frac{T}{2}\right)$. Then, differentiating the above $\hat{\mathcal{W}}$ with x_1, x_2, the extremal x_1, x_2 satisfies

$$
\begin{aligned}
x_1 x_2 &= \frac{(T + 2\pi i)(2f - T)(-2f - T)}{2(T - 2\pi i p_2')} < 0 \qquad\qquad (5.4.33) \\
x_1^2 &= \frac{(T + 2\pi i)(2f - T)(-2f - T)(\xi + T - 2\pi i p_2')}{2\xi(T - 2\pi i p_2')} > 0, \\
x_2^2 &= \frac{(T + 2\pi i)(2f - T)(-2f - T)\xi}{2(\xi + T - 2\pi i p_2')(T - 2\pi i p_2')} > 0 .
\end{aligned}
$$

The first condition is compatible with the product of last two, and we have been careful so far not to make any square roots. Here, negativity of $x_1 x_2$ demands $p_2' = -1$, so that one should choose the case (i) of (5.4.21). Also, the positivity of x_1^2, x_2^2 demands $-2\pi < \text{Im}(\xi + T) < 0$. (Its range was originally $-4\pi < \text{Im}(\xi + T) < 0$.) Otherwise, we do not find any large N Cardy saddle point for s_a's in the region I of (5.4.5). In this set up, non-negativity of $\rho(x)$ is guaranteed in the whole region (x_1, x_2). In particular, one finds $\rho(x_1) = \rho(x_2) = 0$ at this saddle point.

Inserting the above saddle point solution, the extremal value of $\mathcal{W}$ is given by

$$
\mathcal{W}^* \sim -N^{\frac{3}{2}} \frac{1}{3} \frac{(T + 2\pi i)(2f - T)(-2f - T)}{x_2 - x_1} + \mathcal{W}_0 . \qquad\qquad (5.4.34)
$$

We took no square-roots so far to avoid branch ambiguities. We now explain this final step. One should simply remember that, while taking the square roots of the expressions for x_1^2, x_2^2 in (5.4.33), one takes the negative root for x_1 and positive root for x_2. The final result can be phrased in a simple manner by recalling the allowed ranges of chemical potentials,

$$
0 < \text{Im}(-\xi),\ \text{Im}(\xi + T + 2\pi i),\ \text{Im}\left(f - \frac{T}{2}\right),\ \text{Im}\left(-f - \frac{T}{2}\right) < 2\pi . \qquad (5.4.35)
$$

Especially, all expressions appearing in Im above are i times positive numbers.

After plugging in the values of x_1, x_2 in (5.4.34), one obtains

$$\mathcal{W}^* \sim i\,\frac{2\sqrt{2}N^{\frac{3}{2}}}{3}\sqrt{(-\xi)(\xi+T+2\pi i)\left(f-\frac{T}{2}\right)\left(-f-\frac{T}{2}\right)}-\frac{N^2}{2}(T+2\pi i)\left(-f-\frac{T}{2}\right)\,.$$
(5.4.36)

Here, the expression appearing in the square-root is the product of the four numbers appearing in (5.4.35), where each of them is i times a positive real number in the Cardy limit. So the product of them is real and positive. Our convention for the formulae involving square-roots, starting from (5.4.36), is to take square roots of positive numbers only, and to take the positive root. This applies to all our formulae below for the free energies in the Cardy limit. Sometimes our formulae are used in the non-Cardy regime, e.g. in [74] to discuss dual AdS_4 black holes. In this case, one takes the unique root which reduces to the positive root in the Cardy limit.[4] Consequentially, the free energy $\log Z_{D_2\times S^1} \sim -\frac{\mathcal{W}^*}{2\beta}$ is given by

$$\begin{aligned}\log Z_{D_2\times S^1} &\sim -i\,\frac{\sqrt{2}N^{\frac{3}{2}}}{3\beta}\sqrt{(-\xi)(\xi+T+2\pi i)\left(f-\frac{T}{2}\right)\left(-f-\frac{T}{2}\right)}+\frac{N^2}{4\beta}(T+2\pi i)\left(-f-\frac{T}{2}\right)\\ &\equiv -i\,\frac{\sqrt{2}N^{\frac{3}{2}}}{3\beta}\sqrt{\left(-\hat{\xi}+\frac{T}{2}\right)\left(\hat{\xi}+\frac{T}{2}+2\pi i\right)\left(f-\frac{T}{2}\right)\left(-f-\frac{T}{2}\right)}+\log Z_0\,,\end{aligned}$$
(5.4.37)

where $\hat{\xi}=\xi+\frac{T}{2}+\frac{\beta}{2}$, $Z_0\equiv e^{-\frac{\mathcal{W}_0}{2\beta}}$.

Based on the studies made on $Z_{D_2\times S^1}$, we now compute the large N and Cardy limit of the index on $S^2\times S^1$, using (5.4.13). Recall that in this formula, we consider the imaginary part of $\mathcal{W}^*$ in (5.4.36) at pure imaginary ξ, f, T. Using (5.4.35), the first term in (5.4.36) is pure imaginary, while the second term is purely real. So multiplying two $Z_{D^2\times S^1}$'s in (5.4.13), $O(N^{\frac{3}{2}})$ term is doubled, while $O(N^2)$ term is canceled. In fact at this stage, we can present

---

[4]Equivalently but more concretely, the rule for taking the square root $\sqrt{z}$ of a complex number z in the free energy of [74] is to take z in the principal branch $-\pi < \text{Arg}(z) < \pi$.

both results in the two regions I and II as defined in (5.4.5). The large N Cardy free energies of $Z_{S^2 \times S^1}$ in the two cases are given by

$$\log Z_{S^2 \times S^1}(\beta, \hat{\xi}, f, T) \sim \mp 2i \frac{\sqrt{2} N^{\frac{3}{2}}}{3\beta} \sqrt{\left(-\hat{\xi} + \frac{T}{2}\right)\left(\hat{\xi} + \frac{T}{2} \pm 2\pi i\right)\left(f - \frac{T}{2}\right)\left(-f - \frac{T}{2}\right)} ,$$
(5.4.38)

where the upper/lower signs are for the region I/II, respectively. The existence of two regions will play a rather important physical role below. We summarize again that in the two regions, the chemical potentials satisfy

$$\text{region I} \quad : \quad 0 < \text{Im}\left(-\hat{\xi} + \frac{T}{2}\right), \text{Im}\left(\hat{\xi} + \frac{T}{2} + 2\pi i\right), \text{Im}\left(f - \frac{T}{2}\right), \text{Im}\left(-f - \frac{T}{2}\right) < 2\pi ,$$

$$\text{region II} \quad : \quad -2\pi < \text{Im}\left(-\xi_{ren} + \frac{T}{2}\right), \text{Im}\left(\hat{\xi} + \frac{T}{2} - 2\pi i\right), \text{Im}\left(f - \frac{T}{2}\right), \text{Im}\left(-f - \frac{T}{2}\right) < 0 .$$

To see the symmetry most transparently, we use the proper $SO(8)$ basis given by (5.3.15),

$$\Delta_1 \equiv -\hat{\xi} + \frac{T}{2} + \frac{\beta}{2} , \quad \Delta_2 \equiv \hat{\xi} + \frac{T}{2} + \frac{\beta}{2} \pm 2\pi i , \quad \Delta_3 \equiv f - \frac{T}{2} + \frac{\beta}{2} , \quad \Delta_4 \equiv -f - \frac{T}{2} + \frac{\beta}{2} ,$$
(5.4.39)

in the case I and II, respectively. This is an expression valid at finite β. Compared to (5.3.15), we have only made a $\pm 2\pi i$ shift for Δ_2 in the case I/II respectively.[5] These chemical potentials satisfy $0 < \pm \text{Im}(\Delta_I) < 2\pi$ in the Cardy limit, and further satisfy

$$\sum_{I=1}^{4} \Delta_I - 2\beta = \pm 2\pi i ,$$
(5.4.40)

where upper/lower signs are again for the case I/II, respectively. In the two cases, the free energy is given by

$$\log Z_{S^2 \times S^1} \sim \mp i \frac{4\sqrt{2} N^{\frac{3}{2}}}{3} \frac{\sqrt{\Delta_1 \Delta_2 \Delta_3 \Delta_4}}{2\beta} .$$
(5.4.41)

---

[5]Note that the index $\text{Tr}\left[(-1)^F e^{-\Delta_2 Q_2} \cdots \right]$ can be rewritten as $\text{Tr}\left[e^{-(\Delta_2 \pm 2\pi i)Q_2} \cdots \right]$ by absorbing $(-1)^F$ by $\pm 2\pi i$ shift of Δ_2. So the shifted variables are chemical potentials in the latter convention for the index.

This finishes the derivation of our large N Cardy free energy on $S^2 \times S^1$. The free energy in other chambers of $\mathrm{Im}\Delta_I$ can be obtained by the period shifts of Δ_I's.

One can make a similar Cardy approximation with the ABJM model for N M2-branes. We reported some difficulties in section 2 to study the vortex partition function for the ABJM theory on $D_2 \times S^1$, due to the diverse possibilities of anomaly-free boundary conditions. This will be closely related the asymptotic factorization in the Cardy limit in the set-up of section 3. Namely, we will have to factorize the integrand in a way that the 'holomorphic' and 'anti-holomorphic' factors separately do not respect the $U(N) \times U(N)$ Weyl symmetry. We will not cover this part in this chapter and simply write down the result:

$$\log Z_{S^2 \times S^1} \sim \mp \frac{2\sqrt{2}k^{\frac{1}{2}}N^{\frac{3}{2}}}{3\beta} i \sqrt{\Delta_1 \Delta_2 \Delta_3 \Delta_4} \ , \qquad (5.4.42)$$

where k is the Chern-Simons level of the ABJM theory. The derivation of the above formula can be found in section 4.3 in [79].

(5.4.41) describes the deconfined phase of our gauge theory as it scales like $N^{3/2}$ at large N. Together with (5.4.40), (5.4.41) precisely matches the entropy function of electrically charged rotating supersymmetric black holes in $\mathrm{AdS}_4 \times S^7$ [74], which we discussed in chapter 2. Namely, [74] performed the Legendre transformation, which is extremizing

$$S(Q_I, J; \Delta_I, \beta) = \log Z_{S^2 \times S^1} + \sum_{I=1}^{4} Q_I \Delta_I + 2\beta J \qquad (5.4.43)$$

with Δ_I, β, subject to (5.4.40). Then it was shown that the resulting microcanonical entropy agrees with the Bekenstein-Hawking entropy of the BPS black holes in $AdS_4 \times S^7$ [82], upon inserting a charge relation satisfied by known analytic black hole solutions. Therefore, we have statistically accounted for the

microstates of the supersymmetric AdS$_4$ black holes by deriving this free energy.

One important fact which is perhaps not emphasized in [74] is the following. As one extremizes (5.4.43), the dominant saddle point has complex Δ_I, β as well as complex value S_* for the extremized 'entropy.' Its interpretation is given as follows (See also [78]). The exponential of the saddle point 'entropy' S_* given by

$$e^{S_*(Q_I, J)} = e^{i\mathrm{Im}S_*(Q_I, J)} e^{\mathrm{Re}S_*(Q_I, J)} \qquad (5.4.44)$$

should somehow represent the large charge and large N degeneracies of BPS states. Here we present an interpretation of the charge-dependent phase factor $e^{i\mathrm{Im}S_*}$, as mimicking rapid oscillations between ± 1 as the macroscopic angular momentum charges Q_I, J are shifted by their minimal quantized units. If the macroscopic bosonic and fermionic states are not completely cancelled at a given charge order, the resulting integer after the partial cancelation can be either positive or negative, depending on the precise values of charges. Semi-classical Legendre transformation is not capable of deciding these signs, which should depend on the precise quantized values of macroscopic charges. Our interpretation is that, the macroscopic Legendre transformation can at least imitate the rapid ± 1 oscillation by having an imaginary part of the saddle point entropy S_* [78]. However, to make this story more precise, one should recall that the unitarity of the QFT demands the existence of complex conjugate pairs of saddle points if they are not real. Indeed, the two cases I/II of (5.4.41) guarantee that such a pair exists for the physical saddle point. Then, adding the contributions from the pair, one obtains

$$\sim e^{\mathrm{Re}S_*} \cos\left(\mathrm{Im}S_* + \cdots\right) \ , \qquad (5.4.45)$$

where now one obtains a real entropy $\mathrm{Re}S_*$ and the cos factor is interpreted as imitating the rapid oscillation between ± 1.

Let us illustrate that the physical value of complex β that is relevant for the Legendre transformation satisfies $\text{Im}(\beta) < 0$, which was assumed during the computations. The general studies are made in [74], so we illustrate this fact in the case when all $U(1)^4 \subset SO(8)$ charges are equal: $Q_1 = Q_2 = Q_3 = Q_4 \equiv Q$. We therefore set $\Delta_I \approx \frac{\pi i}{2}$ for all $I = 1, \cdots, 4$ in case I. Then (5.4.41) becomes

$$\log Z_{S^2 \times S^1} \sim -i \frac{\sqrt{2}\pi^2 N^{\frac{3}{2}}}{6} \beta^{-1} \equiv -i\frac{c}{\beta} \ . \tag{5.4.46}$$

c is a positive number. For any positive number c, the Legendre transformation will yield $\text{Im}\beta < 0$. This can be seen by considering the extremization of (5.4.43), which is now

$$S(Q, J; \beta) \approx -i\frac{c}{\beta} + 4Q\Delta + 2\beta J \approx -i\frac{c}{\beta} + 2J\beta + 2\pi i Q \ . \tag{5.4.47}$$

After extremization, one obtains

$$S_* = 2\sqrt{-2icJ} + 2\pi i Q \ , \quad \beta_* = \sqrt{\frac{-ic}{2J}} \ . \tag{5.4.48}$$

The square roots are taken so that $\text{Re}S_* > 0$ and $\text{Re}\beta_* > 0$. In particular, one obtains

$$\beta_* = \sqrt{\frac{c}{2J}} \, e^{-\frac{\pi i}{4}} \tag{5.4.49}$$

which indeed satisfies $\text{Im}\beta_* < 0$. So $\text{Im}\beta < 0$ is the region of the chemical potential which is relevant for our microstate counting, justifying this assumption made earlier in this section. The set-up $\text{Im}\beta < 0$ will also be assumed in the rest of this section even at finite N, which will be justified whenever the effective value of c in the free energy is positive.

Before concluding this subsection, let us comment on the physics of (de)confinement and the expectation value of the Wilson-Polyakov loops. These discussions will shed more lights on the dynamics of this system.

The reduction of the apparent N^2 degrees of freedom down to $N^{\frac{3}{2}}$ was triggered by the condensation of magnetic monopole operators at the saddle point. Let us discuss the relation in more detail. The condensation is measured by the eigenvalues $u_a = \beta m_a + i\alpha_a$ deviating from the unit circle, $|s_a| = |e^{u_a}| \neq 1$. The large N condensation is macroscopic, $\max |\beta m_a| \sim N^{\frac{1}{2}}$. More precisely, one finds

$$M_{ab} \equiv |\beta m_{ab} + i\alpha_{ab}| \approx |\mathrm{Re}(\beta m_{ab})| = \sqrt{N}|x(a) - x(b)| \ , \quad a(x) \equiv N \int_{x_1}^{x} \rho(x')dx' \ ,$$

$$(5.4.50)$$

with x and $\rho(x)$ being $\mathcal{O}(N^0)$. The approximation $\approx$ is possible because u_a are close to the real axis in our saddle point ansatz. $x(a)$ and $x(b)$ are given by the inverse function of $a(x)$. Therefore, M_{ab} becomes much larger than 1 when $|x(a) - x(b)| \gg N^{-\frac{1}{2}}$. From the fact that x and $\rho(x)$ do not scale with large N, one concludes that $M_{ab} \gg 1$ if $|a - b| \gg \sqrt{N}$.

M_{ab} is the effective mass of the off-diagonal mode at a'th row and b'th column of the adjoint fields in our QFT, provided by the magnetic monopole operator. This mass becomes much larger than 1 if the mode is 'deeply off-diagonal' $|a - b| \gg \sqrt{N}$. Therefore, the light modes which can contribute to the free energy in this monopole background should satisfy $|a - b| \lesssim \sqrt{N}$. These 'near-diagonal' modes are a small fraction of the N^2 matrix elements. Since the width of the near-diagonal region is $\sqrt{N}$, the number of the near-diagonal modes scales like $N \cdot N^{\frac{1}{2}} = N^{\frac{3}{2}}$, accounting for the desired scaling. Technically, the two-body interaction potential $\mathcal{W}_{\mathrm{int}}$ for the adjoint fields is approximated to a short-ranged interaction (5.4.26) after making the large N approximation. This is because only the near-diagonal modes remain light in the monopole background. Therefore, we realize that the $N^{\frac{3}{2}}$ scaling of the free energy is due to a partial confinement triggered by the magnetic monopole condensation. This

partial confinement happens even in the high temperature limit of the CFT.

It is also interesting to consider the saddle point value of the Polyakov loop in the fundamental representation, given by

$$\mathcal{P} \equiv \frac{1}{N} \sum_{a=1}^{N} e^{u_a} \sim e^{\sqrt{N} x_2} \tag{5.4.51}$$

with $x_2 > 0$ at $\mathcal{O}(N^0)$. $-\log \mathcal{P}$ measures the free energy of an external quark running along the temporal circle, in the grand canonical ensemble [57]. The fact that $-\log \mathcal{P} \sim -\sqrt{N} x_2$ is negative implies that the presence of such a quark loop is thermodynamically preferred by the system. Here, note that our $\mathcal{N} = 4$ Yang-Mills theory has dynamical fundamental fields. So at the saddle point with a large expectation value for the Polyakov loop, the loop amplitude for the dynamical fundamental fields will be amplified. In fact, this amplification did happen in our calculus. Namely, while approximating $\mathcal{W}_{\text{ext}}$ to (5.4.20), we encountered some $\text{Li}_2(s_a \cdots)$ with $|s_a| \gg 1$. These terms are the reason why $\mathcal{W}_{\text{ext}}$ is amplified as $N \to N^{1+\alpha}$ in (5.4.20).

To summarize, the loop amplification factor N^{α} for the fundamental fields in $\mathcal{W}_{\text{ext}}$ is balanced with the partial confinement factor $N^{-\alpha}$ for the adjoint fields in $\mathcal{W}_{\text{int}}$, to yield the $N^{\frac{3}{2}}$ scaling at $\alpha = \frac{1}{2}$. Both phenomena are triggered by the monopole condensation.

5.4.2 Finite N Cardy free energy

In this subsection, we study $\log Z_{S^2 \times S^1}$ in the finite N Cardy regime. We have already discussed in section 2 the Cardy limit at $N = 1$, on single M2-brane. Here we focus on the non-Abelian cases with $N \geq 2$. The main goal of this subsection is to explore a finite N version of the $N^{\frac{3}{2}}$ degrees of freedom. Namely,

we have obtained

$$\log Z_{(0)} \sim -i \frac{2\sqrt{2}N^{\frac{3}{2}}}{3\beta} \sqrt{\Delta_1 \Delta_2 \Delta_3 \Delta_4} \qquad (5.4.52)$$

as our large N free energy (in what we called region I). We are interested in the ratio $\frac{\log Z}{\log Z_{(0)}}$ of our finite N free energy $\log Z$ and the fiducial one $\log Z_{(0)}$, to see whether the partial confinement due to monopole condensation is stronger or weaker at finite N. At $N = 2$, we shall present an analytic solution for the Cardy semi-classical approximation. At higher N's, we shall rely on numerical methods to find the Cardy saddle points. Apparently, this might look similar to the numerical studies made on the 'saddle points' of the S^3 partition functions or the topological index at finite N [66, 160]. However, in the previous studies in the literautre, there are no small parameters to admit semi-classical saddle point approximations at finite N. On the other hand, we do have small $|\beta|$, which makes our finite N results physical. We will always find $\frac{\log Z}{\log Z_{(0)}} > 1$.

For simplicity, we first consider the case with $\Delta_1 = \Delta_2 = \Delta_3 = \Delta_4 = \frac{\pi i}{2}$ (after shifting Δ_2 by $2\pi i$ as (5.4.39)), which corresponds to the case with equal $U(1)^4 \subset SO(8)$ R-charges, $Q_1 = Q_2 = Q_3 = Q_4$. In terms of the variables of the Yang-Mills theory, this amounts to setting $\xi = -\frac{\pi i}{2}, f = 0, T = -\pi i$. Then, the saddle point equations (5.4.12) become

$$0 = -\frac{\pi i}{2} + \mathrm{Li}_1(is_a q^{\frac{1}{2}}) - \mathrm{Li}_1(-is_a q^{-\frac{1}{2}}) + \sum_{b(\neq a)} \Big[\mathrm{Li}_1(s_a s_b^{-1} q^{-1}) - \mathrm{Li}_1(s_b s_a^{-1} q^{-1}) - \mathrm{Li}_1(-s_a s_b^{-1})$$

$$+ \mathrm{Li}_1(-s_b s_a^{-1}) + \mathrm{Li}_1(is_a s_b^{-1} q^{\frac{1}{2}}) - \mathrm{Li}_1(is_b s_a^{-1} q^{\frac{1}{2}}) - \mathrm{Li}_1(-is_a s_b^{-1} q^{-\frac{1}{2}}) + \mathrm{Li}_1(-is_b s_a^{-1} q^{-\frac{1}{2}}) \Big] \quad (5.4.53)$$

Here, we again temporarily included $q(\approx 1^-)$ to regularize some variables sitting on top of the branch cuts, similar to the previous subsection. Exponentiating

162

both sides, one obtains

$$\frac{1+iq^{-1/2}s_a}{1-iq^{1/2}s_a} \prod_{\substack{b=1 \\ b \neq a}}^{N} \frac{1-q^{-1}s_b s_a^{-1}}{1-q^{-1}s_a s_b^{-1}} \frac{1+s_a s_b^{-1}}{1+s_b s_a^{-1}} \frac{1-iq^{1/2}s_b s_a^{-1}}{1-iq^{1/2}s_a s_b^{-1}} \frac{1+iq^{-1/2}s_a s_b^{-1}}{1+iq^{-1/2}s_b s_a^{-1}} = i \ ,$$

(5.4.54)

which are rational equations of s_a's. Some solutions of (5.4.54) do not satisfy the original equations (5.4.53). We are interested in the solution of (5.4.53).[6] So after solving (5.4.54), one should check whether the solutions satisfy (5.4.53) or not. Then, one should take $\beta \to 0$ (or $q \to 1$) limit on the solutions to remove the branch cut regulator.

Before proceeding, let us comment on a 'trivial solution' of (5.4.53), (5.4.54), which is

$$s_1 = s_2 = \cdots = s_N \equiv s_0 \ , \quad \frac{1+iq^{-\frac{1}{2}}s_0}{1-iq^{\frac{1}{2}}s_0} = i \ . \qquad (5.4.55)$$

s_0 is the Cardy saddle point solution to the Abelian M2-brane index, (5.2.36), which in (5.4.55) is given by $s_0 \to 1$. At $N = 1$, we have shown in section 2 that this is the one and only saddle point which yields the correct free energy for single M2-brane. At higher $N \geq 2$, there are good reasons to trust that they are forbidden saddle points, which we sketch now.

We first recall that a similar phenomenon was observed for the 3d vector-Chern-Simons models [166,167], in which one found an incompressible nature of the eigenvalue distribution for s_a in the high temperature limit. To understand this, one should first note that partition functions of 4d gauge theories on $S^3 \times S^1$ are also given in terms of the holonomy integrals, over α_a (or s_a). At high temperature, the general expectation is that these eigenvalues asymptotically

---

[6]We think that extra solutions to (5.4.54) may also be valid saddle points, which apparently look illegal in the current setting because we have replaced discrete magnetic flux sums into continuum integrals. More carefully doing the flux sum along the line of [167], we expect to reveal the relevance of these extra solutions. However, it happens that a natural finite N version of the saddle points encountered in section 4.1 solves (5.4.53).

approach the same value, $s_1 = \cdots = s_N$, so that the underlying gauge symmetry is asymptotically unbroken. This is the 'maximally deconfining' saddle point, at which quarks and gluons are maximally liberated to a deconfined plasma. However, in 3d gauge theories, partition functions are given by both integrals over α_a and sums over the GNO charges m_a. In particular, [167] discussed the thermal partition functions of 3d vector-Chern-Simons theories on $S^2 \times S^1$ at high temperature. They showed that the discrete sums over m_a yield the following factor in the integrand for α_a:

$$\prod_{a=1}^{N} \delta\left(k\alpha_a\right) \; , \tag{5.4.56}$$

where k is the Chern-Simons level for the $U(N)$ gauge symmetry, and $\delta(x)$ is the periodic delta function satisfying $\delta(x) = \delta(x + 2\pi)$. It has k sharply peaked solutions for N variables, $\alpha_a = \frac{2\pi n_a}{k}$, where $n_a = 0, 1, \cdots, k-1$. Therefore, if N is larger than k, more than one eigenvalues should assume exactly the same value. Then [167] argues that the Haar measure $\prod_{a<b}\left(2\sin\frac{\alpha_a - \alpha_b}{2}\right)^2$ provides exact 0, forbidding such a saddle point. To summarize, the GNO charge sums and the Haar measure of 3d gauge theories may impose extra exclusion principles on α_a, forbidding them to assume same values.

Since our naive saddle point (5.4.55) also has coinciding eigenvalues, one can suspect that similar exclusions may happen. Indeed, by following the procedure of [167] in our index, we find such exclusions at $N \geq 2$. To explain this, one should go one order beyond our Cardy approximation, which only keeps the leading β^{-1} order in the exponent. One starts from (5.3.1), with absolute values of the fluxes removed. Here, rather than making a continuum approximation of the flux sum, one keeps the discrete sums (which is a resolution needed to see the exclusion principle of coincident eigenvalues). Then in the Cardy limit, one

approximates

$$(xe^{-\beta y}; e^{-2\beta}) \approx \exp\left[-\frac{\mathrm{Li}_2(x)}{2\beta} + \frac{1-y}{2}\log(1-x) + \cdots\right] , \qquad (5.4.57)$$

keeping the subleading $\mathcal{O}(\beta^0)$ term. In (5.3.1), x will contain $e^{i\alpha_a}$. x will also contain the macroscopic condensation of m_a at the saddle point. y contains the fluctuation l_a of the monopole flux $m_a = m_a^* + l_a$ around the saddle point value m_a^*. Following [167], we would like to sum over the discrete l_a, rather than making a continuum approximation. Summing over l_a's, one obtains

$$\prod_{a=1}^{N} 2\pi\delta\left(-\frac{i}{2}\log\frac{(1-e^{\beta m_a^* + i\alpha_a}t^{-\frac{1}{2}})(1-e^{\beta m_a^* - i\alpha_a}t^{-\frac{1}{2}})}{(1-e^{\beta m_a^* + i\alpha_a}t^{\frac{1}{2}})(1-e^{\beta m_a^* - i\alpha_a}t^{\frac{1}{2}})} + i\hat{\xi} - \frac{iT}{2}\right) \quad (5.4.58)$$

in the integrand of α_a integrals. Here we used $2\pi\delta(x) = \sum_{l=-\infty}^{\infty} e^{ilx}$ for the periodic delta function $\delta(x) = \delta(x + 2\pi)$. The argument of (5.4.58) is real. The delta function is peaked when α_a solves

$$e^{-\hat{\xi} + \frac{T}{2}}\left[\frac{(1-e^{\beta m_a^* + i\alpha_a}t^{-\frac{1}{2}})(1-e^{\beta m_a^* - i\alpha_a}t^{-\frac{1}{2}})}{(1-e^{\beta m_a^* + i\alpha_a}t^{\frac{1}{2}})(1-e^{\beta m_a^* - i\alpha_a}t^{\frac{1}{2}})}\right]^{\frac{1}{2}} = 1 . \qquad (5.4.59)$$

We are interested in the fate of the saddle point (5.4.55), or more generally (5.2.36). In particular, plugging in the saddle point value of βm_a^*, there is a unique solution $\alpha_a = 0 \pmod{2\pi}$ for (5.4.59). Therefore, following the arguments of [167], only one eigenvalue can sit at this unique peak: otherwise, the Haar measure will provide 0. This leads to the conclusion that the naive saddle point (5.4.55) will be relevant only at $N = 1$.[7]

With these understood, let us first consider the case with $N = 2$. Among 4 solutions of (5.4.54), there are two solutions satisfying (5.4.53). One is given

---

[7]However, as commented in [167], this argument relies on the fact that the delta functions like (5.4.56), (5.4.58) do not spread as one includes further subleading corrections in β. To the best of our knowledge, this issue is not completely clarified so far. We hope to completely resolve this issue within the indices in the near future.

by (5.4.55), which is dismissed as explained. Another solution is given by

$$s_1 = \frac{1}{2}\left(1 - 3^{1/4}\sqrt{2} + \sqrt{3}\right) \approx 0.435421\,, \ \ s_2(= s_1^{-1}) = \frac{1}{2}\left(1 + 3^{1/4}\sqrt{2} + \sqrt{3}\right) \approx 2.29663\,,$$

(5.4.60)

in $\beta \to 0$ limit with $\text{Im}(\beta) < 0$, up to permutation. It is important to keep the regulator β, with the correct sign for $\text{Im}(\beta) < 0$ as explained in section 4.1, to get this solution. This is because of the presence of $\text{Li}_1(s_a s_b^{-1}) = -\log(1 - s_a s_b^{-1})$ and $\text{Li}_1(s_b s_a^{-1})$ in the saddle point equations at $q = 1$, since the solution (5.4.60) sits precisely at a branch cut. This solution satisfies (5.4.53) only when $\text{Im}(\beta) < 0$, which is our physical region for complex β. Finally, the Cardy free energy of $\log Z_{S^2 \times S^1}$ at this saddle point is given from (5.4.13) by

$$\log Z_{S^2 \times S^1}\Big|_{N=2} \sim \frac{i}{2\beta}\left[-8G - 2\,\text{Im}\left\{2\text{Li}_2(ix) + 2\text{Li}_2\left(\frac{i}{x}\right) + 2\text{Li}_2(ix^2) + 2\text{Li}_2\left(\frac{i}{x^2}\right) + \text{Li}_2\left(\frac{1}{x}\right)\right\}\right]$$
$$\approx -\frac{17.4771i}{2\beta}\,,$$

(5.4.61)

where $x \equiv s_1 = s_2^{-1} = \frac{1}{2}\left(1 - 3^{1/4}\sqrt{2} + \sqrt{3}\right) \approx 0.435421$, and

$$G \equiv \sum_{n=0}^{\infty} \frac{(-1)^n}{(2n+1)^2} = \frac{\text{Li}_2(i) - \text{Li}_2(-i)}{2i} \approx 0.915966 \tag{5.4.62}$$

is Catalan's constant.

When $N \geq 3$, we cannot solve (5.4.54) analytically since they are sextic equations even at $N = 3$. Thus, we numerically solve the saddle point equations at $\beta = 0$. At $\beta = 0$, (5.4.54) is simplified as

$$\frac{1 + is_a}{1 - is_a}\prod_{\substack{b=1\\b\neq a}}^{N}\left(\frac{1 + is_a s_b^{-1}}{1 - is_a s_b^{-1}}\right)^2 = i\,, \tag{5.4.63}$$

which is so-called the Bethe ansatz equations. We first find numerical solutions of (5.4.63) at $N = 3$. Having set $\beta = 0$, there could possibly be some solutions at finite β that we miss. We assume that the physical solution remains to

166

solve (5.4.63) and proceed. (This is obviously true at large N, as we confirm numerically below.) Note also that, since we solve the exponentiated equation (5.4.63), nonzero β as a branch-cut regulator is unnecessary. In this set-up, we found 13 numerical solutions of (5.4.63). Among them, there is only one solution (except (5.4.55)) satisfying (5.4.53), given by

$$s_1 \approx 0.230396, \ s_2 \approx 1, \ s_3 \approx 4.34035 \ , \tag{5.4.64}$$

up to permutations of s_a's. As before, this solution exactly lies on the branch cut of the vector multiplet part when $\beta = 0$. The correct sign of $\mathrm{Im}(\beta)$, which makes the above solution satisfy (5.4.53), is $\mathrm{Im}(\beta) < 0$. The Cardy free energy from (5.4.13) is given by

$$\log Z_{S^2 \times S^1} \Big|_{N=3} \approx \frac{-29.8009i}{2\beta} \ , \tag{5.4.65}$$

assuming $\mathrm{Im}(\beta) < 0$.

For $N \geq 4$, we will directly solve (5.4.53) numerically, rather than (5.4.54). Since we have been obtaining solutions with real positive $s_a s_b^{-1}$ till $N \leq 3$, we should carefully treat the branch cuts on the real axis of the $s_a s_b^{-1}$ planes in the $\beta \to 0$ limit. The functions in (5.4.53) to be careful about are $\mathrm{Li}_1(q^{-1} s_a s_b^{-1}) - \mathrm{Li}_1(q^{-1} s_b s_a^{-1})$, as we take $q \to 1^-$ with $\mathrm{Re}(\beta) > 0$, $\mathrm{Im}(\beta) < 0$. In the numerics, we plugged in very small $\mathrm{Im}(\beta) < 0$ to get the solutions, resolving the branch cut ambiguity. (On the other hand, we find no solutions after plugging in very small $\mathrm{Im}(\beta) > 0$.)

Now we show the numerical results. We used Newton's method to find the roots of (5.4.53).[8] For $N \leq 100$, we found that all eigenvalues s_a are positive real in our solutions. These eigenvalues can be sorted in ascending order:

---

[8]The Newton method may in principle miss some solutions, as it depends on the choice of initial values. However, even after trying many initial values, we found no more solutions than those presented below.
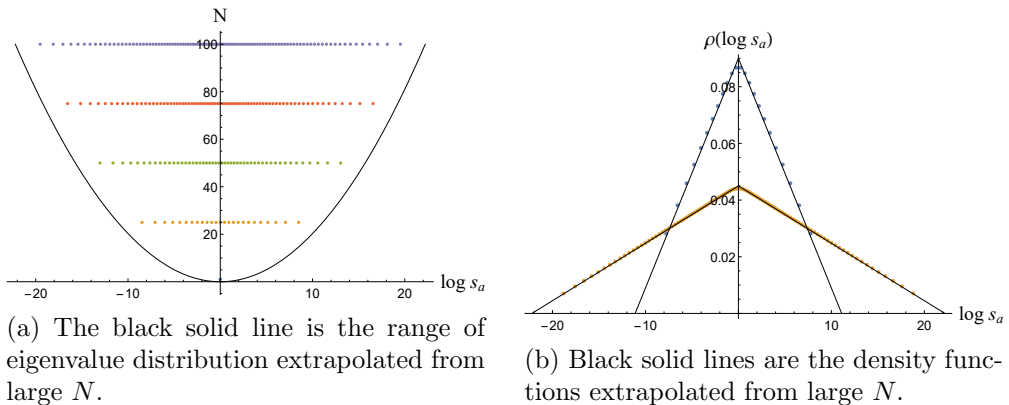
(a) The black solid line is the range of eigenvalue distribution extrapolated from large N.

(b) Black solid lines are the density functions extrapolated from large N.

Figure 5.3: (a) Eigenvalue distributions at $N = 25, 50, 75, 100$, (b) Densities of eigenvalues at $N = 25$ (blue) and $N = 100$ (yellow)

$y_a = 0, \quad 0 < s_1 < s_2 < \ldots < s_N$. We also mention that our finite N numerical solutions also satisfy all the assumptions (5.4.21), (5.4.24) made in section 4.1 for large N analysis, coming from the eigenvalue distributions not crossing branch cuts. The N eigenvalues spread out from s_0 ($\to 1$ in the Cardy limit) with the width roughly proportional to $N^{1/2}$. The detailed eigenvalue distributions at various N are given by Fig. 5.3. The density of the eigenvalues is defined as $\rho(x) = \frac{1}{N}\frac{da}{dx}$.

$\log Z_{S^2 \times S^1}$ at various N are given by Fig. 5.4. One finds that the large N analytic approximation of section 4.1 is well-fitted with the numerical result at large enough N. The difference between the numerical result and the fiducial one in Fig. 5.4(a) increases as N grows, which seems to scale like $O(N^{\frac{1}{2}})$. In addition, we find that the finite N Cardy free energy ($F = -\mathrm{Re}\,(\log Z)$) is always smaller than the fiducial one. Although we do not display the relevant plot here, we found that the numerical result for $\mathrm{Re}(\mathcal{W}^*)$ is also well-fitted to the analytically computed $\mathcal{W}_0$ at large enough N.

Our numerical solutions for s_a are very simple, staying at the positive real
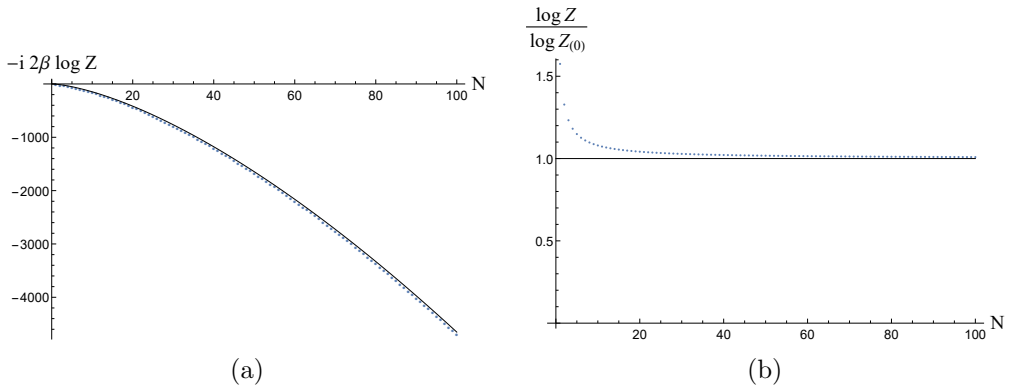
Figure 5.4: (a) Imaginary parts of $2\beta \log Z$ (dots) and $2\beta \log Z_{(0)}$ (solid line). (b) Ratio of the finite N free energy $\log Z$ and the fiducial free energy $\log Z_{(0)}$ (dots). Solid line is drawn just as a reference line.

axis. One may wonder that such simple distributions are due to the simplified setting $\Delta_1 = \Delta_2 = \Delta_3 = \Delta_4$. However, we found that the eigenvalues are positive real even at unequal Δ_I's. As the qualitative behaviors are very similar, we shall not plot the results for unequal Δ_I's here.

As long as we are aware of, our results are first quantitatively explored finite N versions of $N^{\frac{3}{2}}$ on M2-branes. Especially, it will be interesting to see if there are any further implications of the analytic coefficient of (5.4.61), which should be replacing $N^{\frac{3}{2}}$ at $N = 2$.

5.5 Conclusion and remarks

In this chapter, we explored the Cardy limit of the index for the M2-brane SCFTs on $S^2 \times \mathbb{R}$. Our studies are made by analyzing the vortex partition functions, and also suitably approximating the GNO charge sum for the magnetic monopole operators. At large N, we have quantitatively shown that the deconfined free energy scales like $N^{\frac{3}{2}}$. This free energy statistically accounts for the Bekenstein-Hawking entropies of large BPS black holes in $AdS_4 \times S^7$. We dis-

covered the important roles played by the condensation of magnetic monopole operators, which provides a mechanism for partial confinement of N^2 degrees of freedom. We have also found finite N versions of $N^{\frac{3}{2}}$ degrees of freedom by studying the Cardy limit of the index.

We believe that these discoveries will shed very concrete lights on the strongly interacting dynamics of 3d (S)CFTs, including the M2-brane CFTs.

One important issue that has been treated rather briefly in this chapter is the exclusion behavior of eigenvalues in our index. This phenomenon has been first explored in the 3d vector-Chern-Simons theories, either using semi-classical arguments [166] or based on path integral approach [167]. We employed the strategy of [167] and studied the index of our M2-brane QFT. The key result is that the GNO charge sum forbids eigenvalues to assume same values, not even asymptotically in the high temperature limit. In the vector-Chern-Simons model, this phenomenon played important roles to make certain dualities to hold. In our M2-brane QFT, similar exclusion principle forbids the naive saddle point whose free energy is proportional to N^2. Both in the study of [167] and this chapter, there are further issues to clarify concerning the small spreading of the delta functions of α_a's, as explained in the conclusion of [167].

As a technical remark, we mainly used the $\mathcal{N} = 4$ Yang-Mills-matter theory engineered on the D2-D6-brane system, rather than the ABJM theory. When we first started our project, this was because we were aiming to use the vortex partition function in the Higgs branch and the factorization of $Z_{S^2 \times S^1}$. In Chern-Simons-matter theories, studies of vortex partition functions are more difficult. Apparently, this seems to be due to the difficulty in finding natural anomaly-free boundary condition on $D_2 \times S^1$. More physically, with Chern-Simons terms, there may be so-called non-topological vortices in the symmetric

phase, apart from the topological vortices in the Higgs phase. This is because once we have electrically charged configurations in the symmetric phase, magnetic flux is induced due to the Gauss' law of Chern-Simons-matter theory. It is natural that these non-topological vortices may play roles in the factorization formulae of the ABJM theory, if there is one at all. However, our alternative asymptotic factorization of section 3 (in the Cardy limit) can be applied to the ABJM theory, as we explained in section 4.3 of [79].

Chapter 6

Universal 3d Cardy block and various AdS$_4$ black holes

In this chapter, we discuss the Cardy limit of 3d supersymmetric partition functions which allow the factorization into the hemisphere indices: the generalized superconformal index, the refined topologically twisted index and the squashed sphere partition function. In the Cardy limit, the hemisphere index can be evaluated by the saddle point approximation where there exists a dominant saddle point contribution, which we call the *Cardy block*. The Cardy block turns out to be a simple but powerful object as it is a building block of other partition functions in the Cardy limit. The factorization to the Cardy block allows us to find universal relations among the partition functions, which we formulate as index theorems. Furthermore, if we consider a holographic 3d SCFT and its large N limit, those partition functions relate to various entropic quantities of the dual gravity theory in AdS$_4$. As a result, our result provides the microscopic derivation of the universal relations among those entropic quantities of

the gravity theory. We also discuss explicit examples, which confirm our general index theorems.

6.1   Introduction and summary

Last few years, the localization has played an important role in understanding supersymmetric theories on compact manifolds. Thanks to this technique, one can compute various exact BPS observables such as partition functions and Wilson loops, which turn out very useful to test the non-perturbative phenomena in strongly coupled systems.

One of those observables is the holomorphic block, which can be defined as a partition function on $D^2 \times S^1$ in 3d [176] and as that on $D^2 \times S^2$ in 4d [187]. The holomorphic block is of particular interest because it is a basic building block of various other supersymmetric partition functions. A partition function defined on a circle fibered, either trivially or nontrivially, over a sphere is written in terms of holomorphic blocks as follows:

$$\mathcal{Z}_{\mathcal{M}} = \sum_{\alpha} ||\mathcal{B}^{\alpha}||_{\mathcal{M}}^2 \qquad (6.1.1)$$

where the fusion rule $|| \cdots ||^2$ depends on the manifold $\mathcal{M}$. α specifies the boundary condition defining the holomorphic block, and one can obtain a new supersymmetric partition function $\mathcal{Z}_{\mathcal{M}}$ by summing the square of the holomorphic block over those boundary conditions. The holomorphic block also relates to the open topological string amplitude and the vortex partition function on Ω-deformed $\mathbb{R}^2 \times S^1$ [175–178]. The holomorphic block appears in various contexts such as the AGT-like correspondence [188] and supersymmetric dualities. See, e.g., [189, 190] and [174, 176, 177, 182, 183, 191].

While the holomorphic block turns out to be a useful quantity in various contexts, its matrix integral expression needs some care as one should specify the integration contour depending on the boundary condition α. See [176] for explicit examples. On the other hand, if one is interested in the Cardy limit, which is usually called the semi-classical limit, of the blocks and especially the dominant contribution, one may perform a saddle point approximation of the integral and pay particular attention only to the leading saddle point. In this way, one can circumvent the explicit determination of the integration contour and can extract the dominant contribution in the Cardy limit. In this chapter, we give a particular name for such dominant contribution, *Cardy block*, as it plays an important role in our discussion.

Such Cardy block has been somehow overlooked due to its simplicity. However, recently it was found that the 3d Cardy block is indeed extremely useful, especially for the microstate counting of AdS_4 black holes. As we discussed in chapter 5, the large N computation of the 3d superconformal index is challenging due to the existence of supersymmetric monopole operators. The localization saddles of the 3d superconformal index include infinite monopole configurations, whose individual contribution has to be summed to obtain the exact superconformal index. This problem can be rephrased in a slightly different way using the holomorphic block. According to (6.1.1), the superconformal index is also written in terms of the holomorphic blocks where the *Cardy block* gives the dominant contribution. Furthermore, the Cardy block itself can be independently computed using the localization, which provides another way to compute the superconformal index in the Cardy limit. In that case, the infinite monopole summation is already encoded in the Cardy block. Indeed, it was shown in [79], which was discussed in chapter 5, that the large N limit of the Cardy block, more precisely its square, successfully reproduces the known

entropy function of the rotating BPS black hole in $\text{AdS}_4 \times S^7$ [74], considered in chapter 2, using the ABJM theory and the mirror dual of the maximal SYM theory [44, 162]. The Legendre transformation of such entropy function yields the Bekenstein-Hawking entropy of the dual black hole with the large angular momentum.

In this chapter, we extend this analysis to more general theories and partition functions. We will consider the Cardy limit of the hemisphere index and various other partition functions allowing the factorization into the holomorphic blocks: the generalized superconformal index, the refined topologically twisted index[1] and the squashed sphere partition function. Especially in the Cardy limit, the free energies of those partition functions, defined by $F_{\mathcal{M}} = -\log Z_{\mathcal{M}}$, are written in terms of the Cardy block $\mathcal{C}$ in a much simpler manner than (6.1.1):

$$
\begin{aligned}
F_{D^2}(t; \beta) &\approx -\log \mathcal{C}(t; \beta)\,, \\
F_{S^2}(\mathfrak{t}, n; \beta) &\approx N \log \beta - \log \mathcal{C}(t; \beta) - \log \overline{\mathcal{C}}(\bar{t}; -\beta)\,, \\
F_{S^2}^{\text{twisted}}(\mathfrak{t}, n; \beta) &\approx N \log \beta - \log \mathcal{C}(t; \beta) - \log \mathcal{C}(\bar{t}^{-1}; -\beta)\,, \\
F_{S_b^3}(\Delta; \beta) &\approx \frac{N}{2} \log \beta - \log \mathcal{C}(e^{\Delta}; \beta)\,,
\end{aligned}
\tag{6.1.2}
$$

which only refer to the dominant saddle. We may call those formulae *Cardy factorizations*. We should mention that the Cardy factorization of the topologically twisted index happens only in special circumstances such as the large N limit. See section 6.2 for more detailed discussions including the notation. Also note that our analysis will be applied on generic 3d $\mathcal{N} = 2$ supersymmetric

---

[1]While the topologically twisted index can be defined on a generic Riemann surface Σ_g of arbitrary genus g, the refined version is only available for S^2, which has $U(1)$ isometry [181, 192, 193]. In this chapter, we focus on the refined topologically twisted index on S^2 because such refinement is essential for the factorization and the Cardy limit, which play crucial roles in our discussion.

theories having UV Lagrangian description.

Surprisingly, the Cardy factorization allows us to find various universal relations among those partition functions in the Cardy limit, some of which, in particular, are phrased as index theorems in section 6.3. For example, we formulate an index theorem relating the generalized superconformal index and the squashed sphere partition function:

$$F_{S^2}(e^{\Delta}, n; \beta) = F_{S^3_b}(\Delta + \beta n; \beta) + \overline{F}_{S^3_b}(-\Delta + \beta n; -\beta) + \mathcal{O}(\beta) \qquad (6.1.3)$$

where Δ denotes flavor chemical potentials while n denotes flavor magnetic flux collectively. For the superconformal index, β is the chemical potential for the angular momentum on S^2, with a shift by the R-charge due to the supersymmetry condition, while, for the squashed sphere partition function, it is related to the squashing parameter b of the sphere by $\beta = \pi i b^2$. In our Cardy limit, β is taken to zero: $\beta \to 0^+$.

In addition to the Cardy limit, the large N limit of 3d superconformal field theories is of particular interest because a large class of 3d SCFTs are known to have holographic dual gravity theories in AdS$_4$ in the large N limit. Accordingly, if we further assume large N, we find another index theorem relating the superconformal index and the topologically twisted index to the round sphere partition function:

$$F_{S^2}(\Delta, n; \beta) = \frac{(\pi i + \beta)^2}{4\pi i \beta} F_{S^3}\left(-\frac{\Delta + \beta n}{\pi i + \beta}\right) + \frac{(\pi i + \beta)^2}{4\pi i \beta} \overline{F}_{S^3}\left(-\frac{\Delta - \beta n}{\pi i + \beta}\right),$$

$$F_{S^2}^{\text{twisted}}(\Delta, n; \beta) = \frac{(\pi i + \beta)^2}{4\pi i \beta} F_{S^3}\left(-\frac{\Delta + \beta n}{\pi i + \beta}\right) - \frac{(\pi i - \beta)^2}{4\pi i \beta} F_{S^3}\left(-\frac{\Delta - \beta n}{\pi i - \beta}\right),$$

$$(6.1.4)$$

which relies on the large N relation between the squashed and round sphere

partition functions found in [194]:

$$F_{S_b^3}\left(-\pi i b Q \delta; \pi i b^2\right) = \frac{Q^2}{4} F_{S^3}\left(\delta\right) \qquad (6.1.5)$$

where $Q = b + 1/b$ and δ parametrizes trial R-charges. While our derivation of (6.1.4) is valid up to $\mathcal{O}(\beta)$, there is strong evidence that it is indeed exact even for finite β in the large N limit, at least for the known large N saddle point capturing the dual black hole microstates. Especially, those indices in the large N limit statistically account for the microstates of rotating dyonic BPS black holes in AdS$_4$. While the superconformal index should have the vanishing magnetic flux for the R-symmetry, the topologically twisted index has the non-zero R-symmetry flux, which leads to a particular asymptotically locally AdS$_4$ spacetime, dubbed mAdS$_4$ [195], on the dual gravity side. We expect that those indices give entropy functions of dual black holes for arbitrary β, which is confirmed for some examples in section 6.4 and 6.5. In addition, the squashed sphere partition function relates to the supersymmetric Rényi entropy [196], which accounts for the Bekenstein-Hawking entropy of a charged topological black hole in AdS$_4$ [197, 198]. Also note that the right hand side is written in terms of the round sphere partition function, which, with the superconformal R-charge, is identified with the entanglement entropy for a spherical entangling surface [199, 200]. By the AdS/CFT dictionary, it corresponds to the Euclidean on-shell action in AdS$_4$ [36]. In that regard, our index theorem shows that various entropic quantities in dual AdS are not independent and indeed mutually related. While we provide a field theoretic derivation of such relations, interestingly, similar relations are discussed in the gravity context recently [201], using the gravitational blocks, which are supposed to be dual to our Cardy blocks in the large N limit.

Moreover, if we turn off all the magnetic flux for the flavor symmetry for

the generalized superconformal index, it reduces to the ordinary superconformal index, which satisfies

$$F_{S^2}(\Delta, n = 0; \beta) = \frac{(\pi i + \beta)^2}{2\pi i \beta} \text{Re} \left[F_{S^3} \left(-\frac{\Delta}{\pi i + \beta} \right) \right] \qquad (6.1.6)$$

where $\text{Re}[\dots]$ should be understood with the conjugation defined by (6.2.36). If we further turn off the flavor chemical potentials while restore the superconformal R-charge, the right hand side is simply written as

$$F_{S^2}(\beta) = \frac{\Delta_R^2}{2\pi i \beta} \text{Re} \left[F_{S^3} \left(\delta_* \right) \right] \qquad (6.1.7)$$

where $\Delta_R = \pi i + \beta$ is the chemical potential for the superconformal R-symmetry and $F_{S^3}(\delta_*)$ is the round sphere free energy at the superconformal R-charge, which is determined by the F-maximization [202]. This is reminiscent of the Cardy formula for 2d CFTs [12] or 4d $\mathcal{N} = 1$ SCFTs [138] in the large N limit, where the real part of the round sphere free energy, $\text{Re}[F_{S^3}(\delta_*)]$, plays the role of central charges in 2d and in 4d. Recently the same formula has been obtained both on the gravity side and on the field theory side for a particular class of theories called class $\mathcal{R}$, which is obtained from M5-branes wrapped on hyperbolic 3-manifolds, using the 3d-3d correspondence [203, 204]. Our result validates this formula for generic 3d $\mathcal{N} = 2$ SCFTs with UV Lagrangian.

Lastly, one can also find interesting relations from the leading term of the right hand side of (6.1.4). If we expand the right hand side with respect to β and take the leading term, we find

$$F_{S^2}(\mathfrak{t}e^{-\beta\delta}, n; \beta) \approx -\frac{\pi}{2\beta} \text{Re} \left[F_{S^3} \left(-\frac{\Delta}{\pi i} \right) \right],$$

$$F_{S^2}^{\text{twisted}}(\mathfrak{t}, n; \beta) \approx \frac{\pi i}{2} \sum_i \left(n_i - \frac{\Delta_i}{\pi i} \right) \frac{\partial}{\partial \Delta_i} F_{S^3} \left(-\frac{\Delta}{\pi i} \right) + F_{S^3} \left(-\frac{\Delta}{\pi i} \right). \qquad (6.1.8)$$

Especially, the strict Cardy limit of the topologically twisted index is essentially the unrefined limit of the index, which accounts for the static dyonic BPS black

holes in AdS$_4$. Indeed, the second relation is a rederivation of the index theorem for the unrefined topologically twisted indices, and therefore the entropy functions of static black holes, discovered by Hosseini and Zaffaroni [205]. For such unrefined indices with $\beta = 0$, the index theorem was later generalized for those on generic Riemann surfaces with arbitrary genera [206, 207].

Note that the interpretation of our results as black hole entropy functions should be understood only when they give rise to positive macroscopic entropy, which is not guaranteed for an arbitrary choice of the background, such as the existence of the topological twist or the magnetic fluxes for flavor symmetries. For instance, recently [204] have made use of the 3d-3d correspondence to show that the refined topologically twisted index is exponentially suppressed in the large N limit, and also exactly vanishes for some finite N, for a particular class of theories with the universal twist, the twist along the exact superconformal R-symmetry. Such universal twist corresponds to the so-called universal black holes [206], and the vanishing of the index is consistent with the fact that there is no universal black hole solution with near-horizon geometry AdS$_2 \times S^2$.

This shows that macroscopic entropy and dual black hole solutions are not always guaranteed for an arbitrary choice of background. Nonetheless, as long as we have macroscopic entropy from the index, we expect this entropy captures the microstates of some black hole, regardless of whether or not such a black hole solution has been found already. This suggests that our index computation can be a probe for a new black hole solution. Indeed, recently the Macdonald index of 4d $\mathcal{N} = 4$ SYM theory has been used to predict a new black hole in AdS$_5$ [75]. It will be also interesting if such predictions can be made for black holes in AdS$_4$ using our results for 3d field theories.

The rest of this chapter is organized as follows. In section 6.2 we first review the localization results of 3d $\mathcal{N} = 2$ supersymmetric partition functions and examine their Cardy limits, especially focusing on their factorization properties. In section 6.3, we derive universal relations among the partition functions by combining the results of section 6.2. In particular, we formulate two index theorems: one relating the generalized superconformal index and the squashed sphere partition function in the Cardy limit and the other relating the generalized superconformal index, the refined topologically twisted index and the round sphere partition function in the large N limit. In section 6.4, we address the $\mathcal{N} = 4$ $U(N)$ SYM with one fundamental and one adjoint matters as an explicit example. We demonstrate how to obtain four different partition functions in the large N limit using the factorization. Lastly, in section 6.5, we provide more examples of 3d $\mathcal{N} \geq 2$ SCFTs. We discuss the large N Cardy limit of the generalized superconformal indices for those examples. We also examine the finite N Cardy formulae for some examples, which provide nontrivial tests for known supersymmetric dualities.

6.2 3d Cardy block and factorization

In this section, we first review the localization results of 3d $\mathcal{N} = 2$ supersymmetric partition functions and examine their Cardy limits, especially focusing on their factorization properties. Since the partition functions are 1-loop exact in the context of the supersymmetric localization, the results are given by finite dimensional matrix integrals whose integrands consist of the classical action contributions as well as the 1-loop determinants. Also the factorization of 3d partition functions have been extensively discussed in the literature; e.g.,

see [175–180, 182, 183, 187, 191]. Here we revisit them in our notation, which is chosen to be convenient for our Cardy limit analysis. In particular, we start with the hemisphere index on $D^2 \times S^1$ defined in [171], which is closely related to the holomorphic block discussed in [176]. This is a building block of the other supersymmetric partition functions we will discuss. We then move on to those partition functions on a circle fibered over a sphere, which are known to be factorized, and examine their Cardy limits.

6.2.1 Hemisphere index

The first example we discuss is the hemisphere index on $D^2 \times S^1$ [171], which is defined by

$$I_{D^2} = \mathrm{tr}_{\mathcal{H}(D^2;\alpha)} \left[(-1)^F e^{-\beta_1(\mathsf{D}-\mathsf{R}-\mathsf{J}_3)} e^{-\beta_2(\mathsf{D}+\mathsf{J}_3)} e^{-F_l M_l} \right] \qquad (6.2.1)$$

where D is the translation generator along S^1; R is the $\mathcal{N}=2$ $U(1)$ R-charge; J_3 is the angular momentum; and F_l's are the Cartan charges of the flavor symmetry. The trace is taken over the Hilbert space on D^2 with the boundary condition α. As usual, this index counts the BPS states saturating $\mathsf{D}-\mathsf{R}-\mathsf{J}_3 \geq 0$ and is thus independent of β_1 unless there is a flat direction appearing while β_1 changes. While the hemisphere index itself does not have a factorized structure mentioned in the introduction, it plays a role of a building block of the other partition functions we will consider.

F, a fermion number, is typically chosen to be $F = 2\mathsf{J}_3$. On the other hand, to define an index, one can also use other choices of F; one useful alternative, especially for the factorization, is $F = \mathsf{R}$. Recall that, for 3d $\mathcal{N}=2$ supersymmetric theories, the IR superconformal R-charge is determined by the F-maximization [202]. However, to define an index, one can use a trial, or UV,

value of the R-charge, from which the IR superconformal value can be achieved as a mixture of the UV R-charge and various $U(1)$ flavor charges. For convenience, we take the integer quantized UV R-charge and use it to define the index. For the integer quantized R-charge, $(-1)^F$ is merely a sign while it would be a nontrivial phase otherwise. In fact, the integer R-charge will be eventually required for the comparison with the topologically twisted index, which demands the integer R-charge due to twisting. This choice of F will make the comparison between the hemisphere index and other partition functions, especially the squashed sphere partition function, more clear as noted in [176].

From the definition of the index, one can see that those two choices are related by the shift of β_1, β_2:

$$
\begin{aligned}
\beta_1 &\to \beta_1 - \pi i, \\
\beta_2 &\to \beta_2 + \pi i,
\end{aligned}
\tag{6.2.2}
$$

which yields extra sign $(-1)^{\mathsf{R}+2\mathsf{J}_3}$. Note that if R is even integer quantized, the two choices are identical. Using this shift, one can easily obtain the formula for $F = \mathsf{R}$ from the localization result for $F = 2\mathsf{J}_3$ in [171]. Setting $\beta_2 = \beta + \pi i$, the hemisphere index with $F = \mathsf{R}$ is given by

$$
I_{D^2} = \frac{1}{|W_G|} \oint \left(\prod_{a=1}^{\mathrm{rk}(G)} \frac{dz_a}{2\pi i z_a} \right) \mathcal{Z}_{\text{classical}} \, \mathcal{Z}_{\text{vector}} \, \mathcal{Z}_{\text{chiral}}^{N/D} \, \mathcal{Z}_{\text{vector}}^{2d} \, \mathcal{Z}_{\text{chiral/Fermi}}^{2d}
\tag{6.2.3}
$$

where $W(G)$ is the Weyl group of the gauge group G. The nontrivial classical action contribution $\mathcal{Z}_{\text{classical}}$ consists of various Chern-Simons terms:

$$
e^{\frac{k}{4\beta} \mathrm{tr} u^2}
\tag{6.2.4}
$$

182

for a canonical Chern-Simons term with level k and

$$e^{\frac{1}{2\beta}\operatorname{tr}(u_A u_B)} \tag{6.2.5}$$

for a mixed Chern-Simons term between $U(1)_A \times U(1)_B$, each of which is either gauge or global $U(1)$. Each u is defined by $u = \log z$ where z is the holonomy for the corresponding (either gauge or global) symmetry.

The 1-loop determinants of the 3d bulk fields are as follows:

$$\mathcal{Z}_{\text{vector}} = \prod_{\alpha \in \Delta} e^{-\frac{1}{8\beta}(\alpha(u) \pm \pi i)^2} \left(z^{\alpha}; x^2 \right), \tag{6.2.6}$$

$$\mathcal{Z}_{\text{chiral}}^{N} = \prod_{\rho \otimes \sigma \in \mathfrak{R}^N} e^{\frac{\beta}{8}\left((r_\sigma - 1)^2 - \frac{1}{3}\right) - \frac{r_\sigma - 1}{4}(\rho(u) + \sigma(v) - \pi i(r_\sigma \mp 1)) + \frac{1}{8\beta}(\rho(u) + \sigma(v) - \pi i(r_\sigma \mp 1))^2}$$

$$\times \left(z^{\rho} t^{\sigma} x^{r_\sigma} e^{-\pi i r_\sigma}; x^2 \right)^{-1}, \tag{6.2.7}$$

$$\mathcal{Z}_{\text{chiral}}^{D} = \prod_{\rho \otimes \sigma \in \mathfrak{R}^D} e^{-\frac{\beta}{8}\left((r_\sigma - 1)^2 - \frac{1}{3}\right) + \frac{r_\sigma - 1}{4}(\rho(u) + \sigma(v) - \pi i(r_\sigma \mp 1)) - \frac{1}{8\beta}(\rho(u) + \sigma(v) - \pi i(r_\sigma \mp 1))^2}$$

$$\times \left(z^{-\rho} t^{-\sigma} x^{2 - r_\sigma} e^{\pi i r_\sigma}; x^2 \right) \tag{6.2.8}$$

with

$$z^{\rho} = e^{\rho(u)}, \qquad t^{\sigma} = e^{\sigma(v)}, \qquad x = e^{-\beta} \tag{6.2.9}$$

where Δ is the set of non-zero roots of the gauge group; $\mathfrak{R}^{N/D}$ are the representations of the chiral multiplets with the Neumann/Dirichlet boundary conditions respectively, with gauge weight ρ and global weight σ, which includes $U(1)_R$ charge r_σ. Here we use the shorthand expression $(a; x^2)$ for q-Pochhammer symbol $(a; x^2)_\infty$:

$$(a; x^2)_\infty = \prod_{k=0}^{\infty} \left(1 - a x^{2k} \right). \tag{6.2.10}$$

Due to our choice $F = \mathsf{R}$, there are extra $e^{-\pi i r_\sigma}$ in contrast to the result of [171].

Note that the exponential factor in each determinant spoils the invariance of the determinant under the large gauge transformation. Such exponential factors are remnant of the gauge non-invariant regularization, which should disappear if one regularizes the determinant in a gauge invariant way with the appropriate definitions of the UV Chern-Simons levels understood. However, we here stick to the above definition of the determinants for easy comparisons with the earlier literature. Indeed, the exponential factors should be completely canceled out once the boundary matter contributions are taken into account. Thus, the entire integrand is again invariant under the large gauge transformation. Nevertheless, since each determinant is not invariant under the large gauge transformation, we have to fix the ambiguity; namely, we take the above definition for the arguments in chambers $-2\pi < \pm\text{Im}(\alpha(u))$, $\pm\text{Im}(\rho(u) + \sigma(v) - \pi i r_\sigma) < 0$. If we don't specify the chamber explicitly, we take the upper plus sign of $\pm$.

The exponential factor in each determinant makes an effective shift of Chern-Simons levels. The effective Chern-Simons terms, dictated by such exponential factors as well as the classical action contribution, yield anomalies at the boundary, which should be canceled by extra boundary degrees of freedom, at least up to a u-independent constant. The 1-loop determinants of the boundary matters are

$$\mathcal{Z}_{\text{vector}}^{2d} = \prod_{\alpha \in \Delta^{2d}} e^{-\frac{1}{4\beta}(\alpha(u) \pm \pi i)^2} \theta\left(z^\alpha; x^2\right), \tag{6.2.11}$$

$$\mathcal{Z}_{\text{chiral}}^{2d} = \prod_{\rho \otimes \sigma \in \mathfrak{R}_{\text{chiral}}^{2d}} e^{\frac{\beta}{4}\left((r_\sigma-1)^2 - \frac{1}{3}\right) - \frac{r_\sigma-1}{2}(\rho(u)+\sigma(v)-\pi i(r_\sigma \mp 1)) + \frac{1}{4\beta}(\rho(u)+\sigma(v)-\pi i(r_\sigma \mp 1))^2}$$

$$\times \theta\left(z^\rho t^\sigma x^{r_\sigma} e^{-\pi i r_\sigma}; x^2\right)^{-1}, \tag{6.2.12}$$

$$\mathcal{Z}_{\text{Fermi}}^{2d} = \prod_{\rho \otimes \sigma \in \mathfrak{R}_{\text{Fermi}}^{2d}} e^{-\frac{\beta}{4}\left((r_\sigma-1)^2 - \frac{1}{3}\right) + \frac{r_\sigma-1}{2}(\rho(u)+\sigma(v)-\pi i(r_\sigma \mp 1)) - \frac{1}{4\beta}(\rho(u)+\sigma(v)-\pi i(r_\sigma \mp 1))^2}$$

$$\times \theta\left(z^\rho t^\sigma x^{r_\sigma} e^{-\pi i r_\sigma}; x^2\right) \tag{6.2.13}$$

where $\theta\left(a; x^2\right)$ is defined by

$$\theta\left(a; x^2\right) = \left(a; x^2\right)_\infty \left(a^{-1}x^2; x^2\right)_\infty .$$ (6.2.14)

The 3d determinants and 2d determinants satisfy

$$\frac{\mathcal{Z}^N_{\text{chiral}}}{\mathcal{Z}^D_{\text{chiral}}} = Z^{2d}_{\text{chiral}} = \frac{1}{Z^{2d}_{\text{Fermi}}}$$ (6.2.15)

once we assign the same representation and the R-charge. Note that those 2d degrees of freedom are engineered so that the net exponential factor of the integrand is completely canceled.

In the Cardy limit, i.e., $\beta \to 0^+$ while the other variables kept finite, the 3d determinants are given by

$$\lim_{\beta \to 0} \log \mathcal{Z}_{\text{vector}}(z; \beta) = -\frac{1}{2\beta} \sum_\alpha \left[\frac{1}{4}(\alpha(u) \pm \pi i)^2 + \text{Li}_2(z^\alpha x^{-1}) \right],$$

$$\lim_{\beta \to 0} \log \mathcal{Z}^N_{\text{chiral}}(z, t; \beta)$$
$$= \frac{1}{2\beta} \sum_{\rho \otimes \sigma} \left[\frac{1}{4}(\rho(u) + \sigma(v) - \pi i(r_\sigma \mp 1) - \beta(r_\sigma - 1))^2 + \text{Li}_2(z^\rho t^\sigma x^{r_\sigma - 1} e^{-\pi i r_\sigma}) \right],$$

$$\lim_{\beta \to 0} \log \mathcal{Z}^D_{\text{chiral}}(z, t; \beta)$$
$$= -\frac{1}{2\beta} \sum_{\rho \otimes \sigma} \left[\frac{1}{4}(\rho(u) + \sigma(v) - \pi i(r_\sigma \mp 1) - \beta(r_\sigma - 1))^2 + \text{Li}_2(z^{-\rho} t^{-\sigma} x^{1 - r_\sigma} e^{\pi i r_\sigma}) \right]$$

(6.2.16)

up to $\mathcal{O}(\beta)$. On the other hand, the 2d determinants become

$$\lim_{\beta \to 0} \log \mathcal{Z}^{2d}_{\text{vector}}(z; \beta) = \frac{\pi^2}{6\beta}$$

$$\lim_{\beta \to 0} \log \mathcal{Z}^{2d}_{\text{chiral}}(z, t; \beta) = -\frac{\pi^2}{12\beta}$$ (6.2.17)

$$\lim_{\beta \to 0} \log \mathcal{Z}^{2d}_{\text{Fermi}}(z, t; \beta) = \frac{\pi^2}{12\beta}.$$

for each pair of $(\alpha, -\alpha)$ and for each $\rho \otimes \sigma$. While those do not vanish in the Cardy limit, we will see that their role is rather minimal when we construct other 3d partition functions upon the hemisphere index. Since $\mathcal{Z}^N_{\mathrm{chiral}}$ and $\mathcal{Z}^D_{\mathrm{chiral}}$ are related by $\mathcal{Z}^{2d}_{\mathrm{chiral/Fermi}}$, also their distinction will not be very significant in such situations. Thus, we mostly call them $\mathcal{Z}_{\mathrm{chiral}}$ unless their distinction is necessary.

Note that, in each determinant, β always appears in a combination with v: $\sigma(v) - \pi i r_\sigma - \beta(r_\sigma - 1)$ except β^{-1} in front. From now on, for convenience, let us distinguish β in a combination with v and β in front by denoting the former by $\hat{\beta}$. And we also introduce $\mathsf{t} = (t, -\hat{x}e^{-\pi i})$, on which σ act as follows:

$$\mathsf{t}^\sigma = t^\sigma \hat{x}^{r_\sigma - 1} e^{-\pi i r_\sigma} \tag{6.2.18}$$

where $\hat{x} = e^{-\hat{\beta}}$. In this way, the explicit β-dependence of the above determinants is only β^{-1} in front. At the end, we should restore $\hat{\beta}$ to β. Also note that although we have set r_σ to be the UV integer value, one can obtain the index with the non-integer R-charge, such as the IR superconformal one, by shifting the flavor chemical potentials v by $v \to v - (\beta + \pi i)\delta$. Then the deformed value of the R-charge is $r_\sigma + \sigma(\delta)$.

In the small β limit, one can evaluate the integral (6.2.3) using the saddle point approximation as follows:

$$I_{D^2} = \left(\frac{\beta}{\pi}\right)^{\frac{N}{2}} \sum_* \exp\left(-\frac{1}{2\beta}\mathcal{W}^*\right) \left(\det(-\partial_z^2 \mathcal{W})^*\right)^{-\frac{1}{2}} \left(\prod_{a=1}^N \frac{1}{z_a^*} + \mathcal{O}(\beta)\right), \tag{6.2.19}$$

where N is the gauge group rank. Our effective potential is defined by

$$-\frac{1}{2\beta}\mathcal{W} = \sum \lim_{\beta \to 0} \log \mathcal{Z}, \tag{6.2.20}$$

where the summation is taken over the collection of the above determinants. The β-dependence of $\mathcal{W}$ is hidden in t as $\hat{\beta}$, which will be taken back to be β at the end. * denotes the value at each saddle point, which is a solution to the equation

$$\partial_z \mathcal{W} = 0. \tag{6.2.21}$$

As long as there is a saddle satisfying $\text{Re}(\mathcal{W}^*/\beta) < 0$, the index exponentially grows in the Cardy limit. In such cases, there is a dominant saddle such that

$$I_{D^2}(t; \beta) \approx \mathcal{C}(t; \beta) \tag{6.2.22}$$

where $\mathcal{C}$ is the contribution at the dominant saddle, which we call the *Cardy block*. Thus, the free energy, $F_{D^2} = -\log I_{D^2}$, is written as

$$F_{D^2}(t; \beta) = -\log \mathcal{C}(t; \beta) + \mathcal{O}\left(e^{-\beta^{-1}}\right) = \frac{1}{\beta} G^{(0)}(\mathsf{t}) - \frac{N}{2} \log \beta + G^{(1)}(\mathsf{t}) + \mathcal{O}(\beta) \tag{6.2.23}$$

where $G^{(0)} = \frac{1}{2}\mathcal{W}^*$ is the dominant saddle value of the effective potential while the other saddle point contributions are suppressed exponentially. $G^{(1)}$ is the collection of the remaining contributions at the dominant saddle, e,g,. that of the Hessian. One should remember that t includes $\hat{\beta} = \beta$ in such way that $\mathsf{t}^\sigma = t^\sigma \hat{x}^{r_\sigma - 1} e^{-\pi i r_\sigma}$.

6.2.2   Generalized superconformal index

Our next example is the generalized superconformal index [70, 164, 208], which is defined by

$$I_{S^2} = \text{tr}_{\mathcal{H}_{BPS}(S^2; n)} \left[(-1)^F e^{-\beta(\mathsf{R} + 2\mathsf{J}_3)} e^{-F_l M_l} \right] \tag{6.2.24}$$

where the BPS condition $D - R - J_3 = 0$ is understood. n denotes the external magnetic flux for the flavor symmetry collectively. Again, while a typical choice of F is $F = 2J_3$, our choice here is $F = R$. Those two are related by shift of β: $\beta \to \beta - \pi i$. Also R will be taken to be integer quantized. The superconformal R can be restored by shifting M_l.

One can evaluate such superconformal index using the supersymmetric localization. The localization result for $F = J_3$ was obtained in [165, 184]. Similarly, the superconformal index with $F = R$ is written as

$$I_{S^2} = \frac{1}{|W_G|} \sum_{m \in \Gamma_G^\vee} \oint \left(\prod_{a=1}^{\mathrm{rk}(G)} \frac{d\mathfrak{z}_a}{2\pi i \mathfrak{z}_a} \right) Z_{\mathrm{classical}} \, Z_{\mathrm{vector}} \, Z_{\mathrm{chiral}} \, . \qquad (6.2.25)$$

m runs over the GNO charges including the Weyl equivalent ones. Thus, the symmetry factor is just the order of the Weyl group of the gauge group G. The 1-loop determinants of the vector multiplet and the chiral multiplet are

$$Z_{\mathrm{vector}} = \prod_{\alpha \in \Delta} \left(x e^{-\pi i} \right)^{-\frac{|\alpha(m)|}{2}} \left(1 - \mathfrak{z}^\alpha x^{|\alpha(m)|} \right) , \qquad (6.2.26)$$

$$Z_{\mathrm{chiral}} = \prod_{\rho \otimes \sigma \in \mathfrak{R}} \left(\mathfrak{z}^\rho \mathfrak{t}^\sigma x^{r_\sigma - 1} e^{-\pi i (r_\sigma - 1)} \right)^{-\frac{|\rho(m) + \sigma(n)|}{2}} \frac{\left(\mathfrak{z}^{-\rho} \mathfrak{t}^{-\sigma} x^{2 - r_\sigma + |\rho(m) + \sigma(n)|} e^{\pi i r_\sigma} ; x^2 \right)}{\left(\mathfrak{z}^\rho \mathfrak{t}^\sigma x^{r_\sigma + |\rho(m) + \sigma(n)|} e^{-\pi i r_\sigma} ; x^2 \right)}$$

$$(6.2.27)$$

with

$$\mathfrak{z}^\rho = e^{i\rho(a)} , \qquad \mathfrak{t}^\sigma = e^{i\sigma(b)} , \qquad x = e^{-\beta} . \qquad (6.2.28)$$

Δ is the set of non-zero roots. $\mathfrak{R}$ is the representation of the chiral multiplets under the gauge and global symmetry groups, including the R-symmetry, with weights ρ and σ respectively. Note that there are extra $e^{-\pi i r_\sigma}$ compared to the usual localization result due to the choice $F = R$. The nontrivial contribution of the classical action again comes from various Chern-Simons terms. A canonical

Chern-Simons term with level k gives rise to

$$e^{ik\,\mathrm{tr}(am)} \tag{6.2.29}$$

while a mixed Chern-Simons term between $U(1)_A \times U(1)_B$ gives

$$\mathfrak{z}_A^{m_B} \mathfrak{z}_B^{m_A} \tag{6.2.30}$$

where $U(1)_{A,B}$ are either gauge or global $U(1)$. Each pair of $\mathfrak{z} = e^{ia}$ and m denote the holonomy and the magnetic flux for the corresponding symmetry, either gauge or global.

One can massage the 1-loop determinants to be written in terms of *formal* holomorphic and anti-holomorphic variables. Using the identity [185]

$$\left(-zx^{-1}\right)^{\frac{|m|+m}{2}} \frac{\left(z^{-1}x^{2-m}; x^2\right)_{\frac{|m|+m}{2}}}{\left(zx^{-m}; x^2\right)_{\frac{|m|+m}{2}}} = 1, \tag{6.2.31}$$

we have

$$Z_{\text{vector}} = \prod_{\alpha} e^{-\frac{1}{8\beta}\left(\alpha(u)^2 - \alpha(\bar{u})^2\right)} \frac{\left(z^{\alpha}; x^2\right)}{\left(\bar{z}^{\alpha}x^2; x^2\right)}, \tag{6.2.32}$$

$$Z_{\text{chiral}} = \prod_{\rho \otimes \sigma} e^{-\frac{r_{\sigma}-1}{4}(\rho(u)+\sigma(v)+\rho(\bar{u})+\sigma(\bar{v})) + \frac{1}{8\beta}\left((\rho(u)+\sigma(v)-\pi i(r_{\sigma}-1))^2 - (\rho(\bar{u})+\sigma(\bar{v})+\pi i(r_{\sigma}-1))^2\right)}$$

$$\times \frac{\left(\bar{z}^{\rho}\bar{t}^{\sigma}x^{2-r_{\sigma}}e^{\pi i r_{\sigma}}; x^2\right)}{\left(z^{\rho}t^{\sigma}x^{r_{\sigma}}e^{-\pi i r_{\sigma}}; x^2\right)} \tag{6.2.33}$$

where we have defined that

$$z^{\rho} = e^{\rho(u)} = \mathfrak{z}^{\rho}x^{-\rho(m)}, \qquad t^{\sigma} = e^{\sigma(v)} = \mathfrak{t}^{\sigma}x^{-\sigma(m)},$$
$$\bar{z}^{\rho} = e^{\rho(\bar{u})} = \mathfrak{z}^{-\rho}x^{-\rho(m)}, \qquad \bar{t}^{\sigma} = e^{\sigma(\bar{v})} = \mathfrak{t}^{-\sigma}x^{-\sigma(m)}; \tag{6.2.34}$$

i.e.,

$$u = \log z = ia + \beta m, \qquad v = \log t = ib + \beta n,$$
$$\bar{u} = \log \bar{z} = -ia + \beta m, \qquad \bar{v} = \log \bar{t} = -ib + \beta n. \tag{6.2.35}$$

When a, b and β are real, the barred variables are the complex conjugates of the unbarred variables. On the other hand, if we relax such reality conditions, the barred variables should be understood as the formal conjugates defined by the following map:

$$
\begin{aligned}
a &\to -a\,, \\
m &\to -m\,, \\
\beta &\to -\beta
\end{aligned}
\tag{6.2.36}
$$

and similarly for b and n. This formal conjugate will be understood throughout this chapter.

Note that each 1-loop determinant is completely factorized into a holomorphic piece and an anti-holomorphic piece:

$$
\begin{aligned}
Z_{\text{vector}} &= \mathscr{Z}_{\text{vector}}(z;\beta) \times \overline{\mathscr{Z}}_{\text{vector}}(\bar{z};-\beta)\,, \\
Z_{\text{chiral}} &= \mathscr{Z}_{\text{chiral}}(z,t;\beta) \times \overline{\mathscr{Z}}_{\text{chiral}}(\bar{z},\bar{t};-\beta)
\end{aligned}
\tag{6.2.37}
$$

where $\mathscr{Z}_{\text{vector}}$ and $\mathscr{Z}_{\text{chiral}}$ are defined by

$$
\mathscr{Z}_{\text{vector}}(z;\beta) = \prod_{\alpha} e^{-\frac{1}{8\beta}(\alpha(u)+\pi i)^2}\left(z^{\alpha};x^2\right)\,,
$$

$$
\mathscr{Z}_{\text{chiral}}(z,t;\beta) = \prod_{\rho\otimes\sigma} e^{\frac{\beta}{8}\left((r_\sigma-1)^2-\frac{1}{3}\right)-\frac{r_\sigma-1}{4}(\rho(u)+\sigma(v)-\pi i(r_\sigma-1))+\frac{1}{8\beta}(\rho(u)+\sigma(v)-\pi i(r_\sigma-1))^2}
$$

$$
\times \left(z^\rho t^\sigma x^{r_\sigma} e^{-\pi i r_\sigma};x^2\right)^{-1}\,.
$$

Here $\overline{\mathscr{Z}}$ is defined such that any imaginary coefficient flips its sign. Also the following definition of $(a;x^2)$ for $|x|\neq 1$ is understood:

$$
\left(a;x^2\right) =
\begin{cases}
\left(a;x^2\right)_\infty\,, & |x| < 1\,, \\
\left(ax^{-2};x^{-2}\right)_\infty^{-1}\,, & |x| > 1\,.
\end{cases}
\tag{6.2.38}
$$

While we have introduced the exponential factor $e^{\frac{\beta}{8}\left((r_\sigma-1)^2-\frac{1}{3}\right)+\frac{\pi i}{4}(r_\sigma-1)^2}$ in $\mathscr{Z}_{\text{chiral}}(z,t;\beta)$ to be matched with the hemisphere determinant, it is irrelevant

because it is canceled by the same factor of $\overline{\mathcal{Z}}_{\text{chiral}}(\bar{z}, \bar{t}; -\beta)$. Their Cardy limits are given by

$$\lim_{\beta \to 0} \log \mathcal{Z}_{\text{vector}}(z; \beta) = -\frac{1}{2\beta} \sum_{\alpha} \left[\frac{1}{4}(\alpha(u) + \pi i)^2 + \text{Li}_2(z^{\alpha} x^{-1}) \right],$$

$$\lim_{\beta \to 0} \log \mathcal{Z}_{\text{chiral}}(z, t; \beta) = \frac{1}{2\beta} \sum_{\rho \otimes \sigma} \left[\frac{1}{4}(\rho(u) + \sigma(v) - (\beta + \pi i)(r_{\sigma} - 1))^2 + \text{Li}_2(z^{\rho} t^{\sigma} x^{r_{\sigma} - 1} e^{-\pi i r_{\sigma}}) \right]$$

$$(6.2.39)$$

up to $\mathcal{O}(\beta)$.

We should comment that there is another way of factorizing the 1-loop determinant of the chiral multiplet:

$$Z_{\text{chiral}} = \mathcal{Z}_{\text{chiral}}(z, t; \beta) \times \overline{\mathcal{Z}}_{\text{chiral}}(\bar{z}, \bar{t}; -\beta), \tag{6.2.40}$$

$$\mathcal{Z}_{\text{chiral}}(z, t; \beta) = \prod_{\rho \otimes \sigma} e^{-\frac{\beta}{8}\left((r_{\sigma}-1)^2 - \frac{1}{3}\right) + \frac{r_{\sigma}-1}{4}(\rho(u)+\sigma(v)-\pi i r_{\sigma})} e^{-\frac{1}{8\beta}(\rho(u)+\sigma(v)-\pi i r_{\sigma})^2}$$

$$\times \left(z^{-\rho} t^{-\sigma} x^{2-r_{\sigma}} e^{\pi i r_{\sigma}} \right), \tag{6.2.41}$$

which can be obtained by replacing m by $-m$ in the identity (6.2.31). The Cardy limit is given by

$$\lim_{\beta \to 0} \log \mathcal{Z}_{\text{chiral}}(z, t; \beta)$$

$$= -\frac{1}{2\beta} \sum_{\rho \otimes \sigma} \left[\frac{1}{4}(\rho(u) + \sigma(v) - (\beta + \pi i)(r_{\sigma} - 1))^2 + \text{Li}_2(z^{-\rho} t^{-\sigma} x^{1-r_{\sigma}} e^{\pi i r_{\sigma}}) \right].$$

$$(6.2.42)$$

One should note that the holomorphic part of the first factorization (6.2.38) is identified with the determinant on $D^2 \times S^1$ with the Neumann boundary condition (6.2.7) while the holomorphic part of the second factorization (6.2.41) is identified with the determinant on $D^2 \times S^1$ with the Dirichlet boundary condition (6.2.8). As we have seen in the previous subsection, they differ by the determinant of a boundary chiral multiplet, or equivalently a boundary

Fermi multiplet. Recall that the 2d determinants in the Cardy limit are given by (6.2.17):

$$\lim_{\beta \to 0} \log \mathcal{Z}_{\text{chiral}}^{2d} = - \lim_{\beta \to 0} \log \mathcal{Z}_{\text{Fermi}}^{2d} = -\frac{\pi^2}{12\beta}. \qquad (6.2.43)$$

They simply vanish when we glue two copies of them following the fusion rule (6.2.37). Thus, we need not to worry about the boundary matters when we factorize the superconformal index into two copies of the hemisphere indices in the Cardy limit; and also the distinction between the two boundary conditions, i.e., how we factorize the determinants, is not significant.

Lastly, let us examine the Chern-Simons terms. In terms of the holomorphic variables, they are written as follows:

$$e^{ik\,\text{tr}(am)} = e^{\frac{k}{2\beta}\,\text{tr}\left(\frac{1}{2}u^2 - \frac{1}{2}\bar{u}^2\right)}, \qquad (6.2.44)$$

$$z_A^{m_B} z_B^{m_A} = e^{\frac{1}{2\beta}\,\text{tr}(u_A u_B - \bar{u}_A \bar{u}_B)} \qquad (6.2.45)$$

where the definition of u is given in (6.2.35). Thus, the classical action contribution is also factorized in the same way:

$$Z_{\text{classical}} = \mathcal{Z}_{\text{classical}}(z, t; \beta) \times \overline{\mathcal{Z}}_{\text{classical}}(\bar{z}, \bar{t}; -\beta) \qquad (6.2.46)$$

where $\mathcal{Z}_{\text{classical}}(z, t; \beta)$ consists of two types of contributions:

$$e^{\frac{k}{2\beta}\,\text{tr}\left(\frac{1}{2}u^2\right)} \qquad (6.2.47)$$

for a level k Chern-Simons term and

$$e^{\frac{1}{2\beta}\,\text{tr}(u_A u_B)} \qquad (6.2.48)$$

for a mixed Chern-Simons term between $U(1)_A \times U(1)_B$, which are exactly what appears in the hemisphere index.

Combining those Cardy limits of the 1-loop determinants and the classical action contributions, the entire superconformal index is completely factorized into the holomorphic integral and the anti-holomorphic integral. In particular, the superconformal index has the holonomy integration as well as the magnetic flux sum where the latter is replaced by another integration in the Cardy limit [79, 186]. Combined with the original holonomy integration, it gives rise to

$$
\sum_{m=-\infty}^{\infty} \oint_{|\mathfrak{z}|=1} \frac{d\mathfrak{z}}{2\pi i \mathfrak{z}} = \sum_{r \in e^{\beta \mathbb{Z}}} \int_{0}^{2\pi} \frac{d\theta}{2\pi} \quad \rightarrow \quad \int_{\mathbb{C}} \frac{dz d\bar{z}}{4\pi \beta |z|^2} \tag{6.2.49}
$$

up to $\mathcal{O}(\beta)$. If we consider a $U(N)$ theory for simplicity, the Cardy limit of the superconformal index is given by

$$
\lim_{\beta \to 0} I_{S^2} = \frac{1}{N!} \int_{\mathbb{C}^N} \left(\prod_{a=1}^{N} \frac{dz_a d\bar{z}_a}{4\pi \beta |z_a|^2} \right) e^{-\frac{1}{2\beta} \left(\mathcal{W}(z,\mathsf{t}) - \overline{\mathcal{W}(z,\mathsf{t})} \right)} \tag{6.2.50}
$$

where

$$
-\frac{1}{2\beta} \mathcal{W}(z,\mathsf{t}) = \lim_{\beta \to 0} \left[\log \mathcal{Z}_{\text{classical}}(z,t;\beta) + \log \mathcal{Z}_{\text{vector}}(z;\beta) + \log \mathcal{Z}_{\text{chiral}}(z,t;\beta) \right] \tag{6.2.51}
$$

with each component described above. As seen in the previous subsection, there is no explicit β-dependence in $\mathcal{W}$ as long as we use $\mathsf{t} = (t, -\hat{x}e^{-\pi i})$, on which the global weight σ acts such that $\mathsf{t}^\sigma = t^\sigma \hat{x}^{r_\sigma - 1} e^{-\pi i r_\sigma}$. According to the rule (6.2.36), $\bar{\mathsf{t}}$ is defined by

$$
\bar{\mathsf{t}} = (\bar{t}, -\hat{x}^{-1} e^{\pi i}). \tag{6.2.52}
$$

In the Cardy limit, the superconformal index can be also evaluated by the saddle point approximation. One should note that the holomorphic part of (6.2.50) is nothing but the hemisphere index in the Cardy limit:

$$
\frac{1}{N!} \int \left(\prod_{a=1}^{N} \frac{dz_a}{2\pi i z_a} \right) e^{-\frac{1}{2\beta} \mathcal{W}(z,\mathsf{t})} \tag{6.2.53}
$$

while the anti-holomorphic part is given by its conjugate defined by (6.2.36). Naively the holomorphic variable and anti-holomorphic variable may solve the saddle point equations independently as they are formal conjugate variables rather than complex conjugate. However, regarding $\hat{\beta}$ as an independent variable, if $\hat{\beta}$ is pure imaginary, such conjugate variables are truly complex conjugate because they are related by $\hat{\beta} \leftrightarrow -\hat{\beta}$. In that case, the two saddle point equations are essentially the same; and there is no reason to solve the equations independently because it is basically the saddle point approximation of a real function on the real axis. If $\hat{\beta}$ is slightly away from the imaginary axis, however, $\hat{\beta} \to -\hat{\beta}$ is not compatible with the complex conjugate anymore, in which case, the two saddle point equations should be solved independently. Nevertheless, if we assume a smooth transition when $\hat{\beta}$ moves away from the imaginary axis, the saddle point should be determined such that z and $\bar{z}$ at a saddle should become complex conjugate to each other as $\hat{\beta}$ approaches the imaginary axis; i.e., there is a natural one-to-one map between the holomorphic saddles and the anti-holomorphic saddles, and only the pairs of saddles related by this map contributes to the index. Thus, the saddle points are determined by the same equation for the hemisphere index, and each saddle point contribution is that for the hemisphere index times its conjugate.

While we have assumed a smooth transition when $\hat{\beta}$ moves aways from the imaginary axis, it would be worth studying the behavior of those saddles more rigorously. Nevertheless, in spite of such a subtlety in dealing with the two complex saddle point equations, it is not very significant at the end as long as the index exponentially grows in the Cardy limit. Recall that the free energy for the hemisphere index is determined by the contribution of the dominant saddle because the contributions of the other saddles are exponentially suppressed. As the same thing happens for the superconformal index, we find a simple relation

between their free energies:

$$F_{S^2}(\mathfrak{t}, n; \beta) = N \log \beta + F_{D^2}(t; \beta) + \overline{F}_{D^2}(\bar{t}; -\beta) - \log\left[N! \, \pi^N\right] + \mathcal{O}(\beta) \,,$$
(6.2.54)

or in terms of the Cardy block in (6.2.23),

$$F_{S^2}(\mathfrak{t}, n; \beta) = N \log \beta - \log \mathcal{C}(t; \beta) - \log \overline{\mathcal{C}}(\bar{t}; -\beta) - \log\left[N! \, \pi^N\right] + \mathcal{O}(\beta) \,,$$
(6.2.55)

with

$$t = \mathfrak{t} \, e^{\beta n} \,, \qquad \bar{t} = \mathfrak{t}^{-1} \, e^{\beta n} \,,$$
(6.2.56)

where only the dominant saddle plays the role. While the formula is written for a $U(N)$ theory for simplicity, the generalization is straightforward.

6.2.3 Refined topologically twisted index

One can also define an index for a topologically twisted theory on a circle fibered over a Riemann surface of genus g [181, 192, 193, 209, 210]. If $g = 0$, i.e., if the Riemann surface is a sphere, one can refine the index by turning on the angular momentum fugacity. In that case, the index is defined by

$$I_{S^2}^{\text{twisted}} = \text{tr}_{\mathcal{H}_{BPS}(S^2; n, n_R = -1)} \left[(-1)^F e^{-2\beta \mathsf{J}_3} e^{-F_l M_l} \right]$$
(6.2.57)

where the trace is taken over the Hilbert space on S^2 in the presence of the R-symmetry flux $n_R = -1$. Again n denotes the external magnetic flux for the flavor symmetry. Using the supersymmetric localization, we have

$$I_{S^2}^{\text{twisted}} = \frac{1}{|W_G|} \sum_{m \in \Gamma_G^\vee} \oint \left(\prod_{a=1}^{\text{rk}(G)} \frac{d\mathfrak{z}_a}{2\pi i \mathfrak{z}_a} \right) Z_{\text{classical}}^{\text{twisted}} \, Z_{\text{vector}}^{\text{twisted}} \, Z_{\text{chiral}}^{\text{twisted}} \,.$$
(6.2.58)

where the integration contour is determined by the rule of the Jeffrey-Kirwan residue [181]. The 1-loop determinants of the vector multiplet and the chiral multiplet are given by

$$Z_{\text{vector}}^{\text{twisted}} = \prod_{\alpha \in \Delta} \left(x e^{-\pi i} \right)^{-\frac{|\alpha(m)|}{2}} \left(1 - \mathfrak{z}^{\alpha} x^{|\alpha(m)|} \right), \tag{6.2.59}$$

$$Z_{\text{chiral}}^{\text{twisted}} = \prod_{\rho \otimes \sigma \in \mathfrak{R}} \frac{\left(\mathfrak{z}^{\rho} \mathfrak{t}^{\sigma} e^{-\pi i (r_\sigma - 1)} \right)^{\frac{\rho(m) + \sigma(n) - r_\sigma + 1}{2}}}{\left(\mathfrak{z}^{\rho} \mathfrak{t}^{\sigma} x^{r_\sigma - \rho(m) - \sigma(n)} e^{-\pi i r_\sigma}; x^2 \right)_{\rho(m) + \sigma(n) - r_\sigma + 1}}. \tag{6.2.60}$$

The twist by the (non-superconformal) R-symmetry demands that the R-charge of a matter should be an integer. Again please note extra $e^{-\pi i r_\sigma}$ due to our choice $F = \mathsf{R}$. The classical action contributions are given by

$$e^{i k \, \text{tr}(am)} \tag{6.2.61}$$

for a canonical Chern-Simons term with level k and

$$z_A^{m_B} z_B^{m_A} \tag{6.2.62}$$

for a mixed Chern-Simons term between $U(1)_A \times U(1)_B$, each of which is either gauge or global $U(1)$. Again each pair of $\mathfrak{z} = e^{ia}$ and m denote the holonomy and the magnetic flux for the corresponding symmetry.

One can manipulate the determinants in a similar way to the superconformal index:

$$Z_{\text{vector}}^{\text{twisted}} = \prod_{\alpha} e^{-\frac{1}{8\beta} \left(\alpha(u)^2 - \alpha(\bar{u})^2 \right)} \frac{\left(z^{\alpha}; x^2 \right)}{\left(\bar{z}^{-\alpha} x^2; x^2 \right)}, \tag{6.2.63}$$

$$Z_{\text{chiral}}^{\text{twisted}} = \prod_{\rho \otimes \sigma} e^{-\frac{r_\sigma - 1}{4} \left(\rho(u) + \sigma(v) - \rho(\bar{u}) - \sigma(\bar{v}) - 2\pi i (r_\sigma - 1) \right) + \frac{1}{8\beta} \left((\rho(u) + \sigma(v) - \pi i (r_\sigma - 1))^2 - (\rho(\bar{u}) + \sigma(\bar{v}) + \pi i (r_\sigma - 1))^2 \right)}$$
$$\times \frac{\left(\bar{z}^{-\rho} \bar{t}^{-\sigma} x^{2 - r_\sigma} e^{-\pi i r_\sigma}; x^2 \right)}{\left(z^{\rho} t^{\sigma} x^{r_\sigma} e^{-\pi i r_\sigma}; x^2 \right)}, \tag{6.2.64}$$

$$z^\rho = e^{\rho(u)} = \mathfrak{z}^\rho x^{-\rho(m)}, \qquad t^\sigma = e^{\sigma(v)} = \mathfrak{t}^\sigma x^{-\sigma(m)},$$

$$\bar{z}^\rho = e^{\rho(\bar{u})} = \mathfrak{z}^{-\rho} x^{-\rho(m)}, \qquad \bar{t}^\sigma = e^{\sigma(\bar{v})} = \mathfrak{t}^{-\sigma} x^{-\sigma(m)},$$

(6.2.65)

which lead to the following factorization

$$Z_{\text{vector}}^{\text{twisted}} = \mathcal{Z}_{\text{vector}}(z; \beta) \times \mathcal{Z}_{\text{vector}}(\bar{z}^{-1}; -\beta),$$

(6.2.66)

$$Z_{\text{chiral}}^{\text{twisted}} = \mathcal{Z}_{\text{chiral}}(z, t; \beta) \times \mathcal{Z}_{\text{chiral}}(\bar{z}^{-1}, \bar{t}^{-1}; -\beta)$$

(6.2.67)

where $\mathcal{Z}_{\text{vector}}$ and $\mathcal{Z}_{\text{chiral}}$ are defined exactly in the same way as the hemisphere determinants:

$$\mathcal{Z}_{\text{vector}}(z; \beta) = \prod_\alpha e^{-\frac{1}{8\beta}(\alpha(u)+\pi i)^2} \left(z^\alpha; x^2\right),$$

(6.2.68)

$$\mathcal{Z}_{\text{chiral}}(z, t; \beta) = \prod_{\rho \otimes \sigma} e^{\frac{\beta}{8}\left((r_\sigma-1)^2-\frac{1}{3}\right) - \frac{r_\sigma-1}{4}(\rho(u)+\sigma(v)-\pi i(r_\sigma-1)) + \frac{1}{8\beta}(\rho(u)+\sigma(v)-\pi i(r_\sigma-1))^2}$$

$$\times \left(z^\rho t^\sigma x^{r_\sigma} e^{-\pi i r_\sigma}; x^2\right)^{-1}.$$

(6.2.69)

The Cardy limits of those are given in (6.2.16). In the Cardy limit, the boundary matters are irrelevant for the factorization of the topologically twisted index, due to the same reason as the superconformal index.

Next, the classical action contribution is factorized into

$$Z_{\text{classical}}^{\text{twisted}} = \mathcal{Z}_{\text{classical}}(z, t; \beta) \times \mathcal{Z}_{\text{classical}}(\bar{z}^{-1}, \bar{t}^{-1}; -\beta)$$

(6.2.70)

where $\mathcal{Z}_{\text{classical}}(z, t; \beta)$ consists of two types of contributions:

$$e^{\frac{k}{2\beta} \text{tr}\left(\frac{1}{2}u^2\right)}$$

(6.2.71)

for a level k Chern-Simons term and

$$e^{\frac{1}{2\beta} \text{tr}(u_A u_B)}$$

(6.2.72)

for a mixed Chern-Simons term between $U(1)_A \times U(1)_B$.

Like the superconformal index, the entire topologically twisted index is completely factorized into the holomorphic integral and the anti-holomorphic integral given that the magnetic flux sum is replaced by an integration in the Cardy limit:

$$\lim_{\beta \to 0} I_{S^2}^{\text{twisted}} = \frac{1}{N!} \int_{\mathbb{C}^N} \left(\prod_{a=1}^{N} \frac{dz_a d\bar{z}_a}{4\pi\beta|z_a|^2} \right) e^{-\frac{1}{2\beta}\left(\mathcal{W}(z,\mathsf{t}) - \mathcal{W}(\bar{z}^{-1},\tilde{\mathsf{t}}^{-1}) \right)} \qquad (6.2.73)$$

where

$$-\frac{1}{2\beta}\mathcal{W}(z,\mathsf{t}) = \lim_{\beta \to 0} \left[\log \mathcal{Z}_{\text{classical}}(z,t;\beta) + \log \mathcal{Z}_{\text{vector}}(z;\beta) + \log \mathcal{Z}_{\text{chiral}}(z,t;\beta) \right].$$

$$(6.2.74)$$

$\mathsf{t} = (t, -\hat{x}e^{-\pi i})$ is defined such that $\mathsf{t}^\sigma = t^\sigma \hat{x}^{r_\sigma - 1} e^{-\pi i r_\sigma}$ as before, and $\tilde{\mathsf{t}} = (\bar{t}, -\hat{x}e^{\pi i})$. While this form of the topologically twisted index and that of the superconformal index are very much alike, there is a crucial difference that the topologically twisted index does not grow in the small β limit because β^{-1} terms should be canceled out at the end. This is anticipated because the strict Cardy limit is basically the unrefined limit of the topologically twisted index, which is $\mathcal{O}(1)$. Thus, if one does the saddle point approximation, every saddle democratically contributes to the index, which ends up with the BAE formula for the unrefined index [181]. Nevertheless, if there happens to be only one saddle or if there is a dominant saddle due to other large parameters such as large N, one can write down the free energy in a simple manner as before:

$$F_{S^2}^{\text{twisted}}(\mathsf{t}, n; \beta) = N \log \beta + F_{D^2}(t;\beta) + F_{D^2}(\bar{t}^{-1}; -\beta) - \log\left[N! \pi^N \right] + \mathcal{O}(\beta),$$

$$= N \log \beta - \log \mathcal{C}(t;\beta) - \log \mathcal{C}(\bar{t}^{-1}; -\beta) - \log\left[N! \pi^N \right] + \mathcal{O}(\beta)$$

$$(6.2.75)$$

where $t = \mathfrak{t}\,e^{\beta n}$, $\bar{t} = \mathfrak{t}^{-1}\,e^{\beta n}$, and $\mathcal{C}$ is the Cardy block in (6.2.23). Furthermore, although the strict Cardy limit is the unrefined limit of the topologically twisted index, (6.2.74) will suggest a conjecture for finite β in the large N limit. We will discuss it with explicit examples in section 6.4 and 6.5.

6.2.4 Squashed sphere partition function

Lastly, we consider the supersymmetric partition function on the squashed sphere S_b^3. Again using the supersymmetric localization, it is given by [211–213]

$$Z_{S_b^3} = \frac{1}{|W_G|} \int d^{\mathrm{rk}(G)}\hat{u}\, Z_{\mathrm{classical}}^{S_b^3}\, Z_{\mathrm{vector}}^{S_b^3}\, Z_{\mathrm{chiral}}^{S_b^3}. \tag{6.2.76}$$

The 1-loop determinants of the vector multiplet and the chiral multiplet are

$$Z_{\mathrm{vector}}^{S_b^3} = \prod_{\alpha \in \Delta} s_b\left(i\frac{Q}{2} - \alpha(\hat{u})\right)^{-1}, \tag{6.2.77}$$

$$Z_{\mathrm{chiral}}^{S_b^3} = \prod_{\rho \otimes \sigma \in \mathfrak{R}} s_b\left(i\frac{Q}{2}(1 - r_\sigma) - \rho(\hat{u}) - \sigma(\hat{v})\right) \tag{6.2.78}$$

with $Q = b + \frac{1}{b}$. $s_b(\hat{u})$ is the double-sine function defined by

$$s_b\left(i\frac{Q}{2} - \hat{u}\right) = e^{-\frac{\pi i}{2}\left(\left(i\frac{Q}{2} - \hat{u}\right)^2 + \frac{Q^2}{12} - \frac{1}{6}\right)} \frac{(e^{-2\pi b^{-1}\hat{u} + 2\pi i b^{-2}}; e^{2\pi i b^{-2}})}{(e^{-2\pi b\hat{u}}; e^{-2\pi i b^2})} \tag{6.2.79}$$

for $\mathrm{Im}(b^2) \neq 0$, which leads to the following factorization of the determinants:

$$Z_{\mathrm{vector}}^{S_b^3} = \mathcal{Z}_{\mathrm{vector}}^{S_b^3}\left(e^{-2\pi b\hat{u}}; \pi i b Q\right) \times \mathcal{Z}_{\mathrm{vector}}^{S_b^3}\left(e^{-2\pi b^{-1}\hat{u}}; \pi i b^{-1} Q\right),$$

$$Z_{\mathrm{chiral}}^{S_b^3} = \mathcal{Z}_{\mathrm{chiral}}^{S_b^3}\left(e^{-2\pi b\hat{u}}, e^{-2\pi b\hat{v}}; \pi i b Q\right) \times \mathcal{Z}_{\mathrm{chiral}}^{S_b^3}\left(e^{-2\pi b^{-1}\hat{u}}, e^{-2\pi b^{-1}\hat{v}}; \pi i b^{-1} Q\right)$$

$$\tag{6.2.80}$$

where

$$\mathcal{Z}^{S_b^3}_{\text{vector}}(z;\beta) = \prod_\alpha e^{-\frac{\beta}{12}-\frac{\pi i}{24}-\frac{1}{8\beta}\alpha(u)^2}\left(z^\alpha;x^2\right), \tag{6.2.81}$$

$$\mathcal{Z}^{S_b^3}_{\text{chiral}}(z,t;\beta) = \prod_{\rho\otimes\sigma} e^{\frac{\beta}{8}\left((r_\sigma-1)^2-\frac{1}{3}\right)-\frac{r_\sigma-1}{4}(\rho(u)+\sigma(v))+\frac{\pi i}{24}+\frac{1}{8\beta}(\rho(u)+\sigma(v))^2}\frac{1}{(z^\rho t^\sigma x^{r_\sigma};x^2)} \tag{6.2.82}$$

$$u = \log z, \qquad v = \log t, \qquad \beta = -\log x. \tag{6.2.83}$$

For the sphere partition function the limit of our interest is the highly squashed limit of the sphere. More precisely, we take the limit $b^2 \to i0^+$ with fixed $u = -2\pi b \hat{u}$ and $v = -2\pi b \hat{v}$. We will compare this limit with the Cardy limits of the other partition functions we have discussed. An interesting thing is that in this limit, unlike the other partition functions, the holomorphic part and the anti-holomorphic part do not contribute democratically. Indeed, even though the squashed sphere partition function has the factorized structure as in (6.2.80), what corresponds to the hemisphere index in the Cardy limit is the entire squashed partition function rather than its holomorphic part. To see this,

let us first take the highly squashed limit of each component in (6.2.80):

$$\lim_{b \to 0} \log \mathcal{Z}_{\text{vector}}^{S_b^3} \left(e^{-2\pi b \hat{u}}; \pi i b Q \right) = -\frac{1}{2\pi i b^2} \sum_\alpha \text{Li}_2 \left(z^\alpha e^{\pi i b^2} \right) - \frac{1}{8\pi i} \sum_\alpha (\alpha(u) + \pi i)^2,$$

$$(6.2.84)$$

$$\lim_{b \to 0} \log \mathcal{Z}_{\text{vector}}^{S_b^3} \left(e^{-2\pi b^{-1} \hat{u}}; \pi i b^{-1} Q \right)$$

$$= -\frac{1}{2\pi i b^2} \sum_\alpha \left[\frac{\pi^2}{12} + \frac{1}{4}(\alpha(u) + \pi i)^2 \right] + \frac{1}{8\pi i} \sum_\alpha \left[\alpha(u)^2 + \pi^2 \right], \qquad (6.2.85)$$

$$\lim_{b \to 0} \log \mathcal{Z}_{\text{chiral}}^{S_b^3} \left(e^{-2\pi b \hat{u}}, e^{-2\pi b \hat{v}}; \pi i b Q \right)$$

$$= \frac{1}{2\pi i b^2} \sum_{\rho \otimes \sigma} \text{Li}_2 \left(z^\rho t^\sigma e^{-\pi i r_\sigma - \pi i b^2 (r_\sigma - 1)} \right) + \frac{1}{8\pi i} \sum_{\rho \otimes \sigma} \left[\rho(u) + \sigma(v) - \pi i (r_\sigma - 1) \right]^2,$$

$$(6.2.86)$$

$$\lim_{b \to 0} \log \mathcal{Z}_{\text{chiral}}^{S_b^3} \left(e^{-2\pi b^{-1} \hat{u}}, e^{-2\pi b^{-1} \hat{v}}; \pi i b^{-1} Q \right)$$

$$= \frac{1}{2\pi i b^2} \sum_{\rho \otimes \sigma} \left[\frac{\pi^2}{12} + \frac{1}{4} \left(\rho(u) + \sigma(v) - \pi i (r_\sigma - 1) \right)^2 \right] - \frac{1}{8\pi i} \sum_{\rho \otimes \sigma} \left[(\rho(u) + \sigma(v))^2 + \pi^2 (r_\sigma - 1)^2 \right],$$

$$(6.2.87)$$

provided that the argument sits in a chamber: $-2\pi < \text{Im}(\rho(u) + \sigma(v) - \pi i r_\sigma) < 0$. As mentioned above, the holomorphic part and the anti-holomorphic part do not contribute democratically. Indeed, the holomorphic and anti-holomorphic parts combined give rise to

$$\lim_{b \to 0} \log Z_{\text{vector}}^{S_b^3} = -\frac{1}{2\pi i b^2} \sum_\alpha \left[\frac{\pi^2}{12} + \frac{1}{4}(\alpha(u) + \pi i)^2 + \text{Li}_2 \left(z^\alpha e^{\pi i b^2} \right) \right] - \frac{\pi i}{4} |\Delta|,$$

$$(6.2.88)$$

$$\lim_{b \to 0} \log Z_{\text{chiral}}^{S_b^3}$$

$$= \frac{1}{2\pi i b^2} \sum_{\rho \otimes \sigma} \left[\frac{\pi^2}{12} + \frac{1}{4} \left(\rho(u) + \sigma(v) - \pi i (1 + b^2)(r_\sigma - 1) \right)^2 + \text{Li}_2 \left(z^\rho t^\sigma e^{-\pi i r_\sigma - \pi i b^2 (r_\sigma - 1)} \right) \right]$$

$$(6.2.89)$$

up to $\mathcal{O}(b^2)$, which are the same as the hemisphere determinants up to constant terms. Indeed, such constant terms are just a phase or remnants of the 2d boundary matter contributions, which however do not affect the factorization of the superconformal index and of the topologically twisted index. Thus, one can ignore such constant terms.

Next, the classical action contribution $Z_{\text{classical}}^{S_b^3}$ includes two types of contributions:

$$e^{-\pi i k \, \text{tr}(\hat{u}^2)} \tag{6.2.90}$$

for a canonical Chern-Simons term with level k and

$$e^{-2\pi i \, \hat{u}_A \hat{u}_B} \tag{6.2.91}$$

for a mixed Chern-Simons term between $U(1)_A \times U(1)_B$, which can be factorized in the same way as the determinants. Moreover, in the highly squashed limit, they become

$$e^{\frac{k}{2\pi i b^2} \, \text{tr}\left(\frac{1}{2} u^2\right)}, \tag{6.2.92}$$

$$e^{\frac{1}{2\pi i b^2} u_A u_B} \tag{6.2.93}$$

since we are keeping $u = -2\pi b \hat{u}$ and $v = -2\pi b \hat{v}$ finite.

Therefore, the sphere partition function in the highly squashed limit is given in the following form:

$$\lim_{b \to 0} Z_{S_b^3} = \frac{1}{(ib)^N} \frac{1}{N!} \int \left(\prod_{a=1}^N \frac{dz_a}{2\pi i z_a} \right) e^{-\frac{1}{2\pi i b^2} \mathcal{W}(z,\text{t})} \tag{6.2.94}$$

where

$$-\frac{1}{2\pi i b^2} \mathcal{W}(z,\text{t}) = \lim_{b \to 0} \left[\log \mathcal{Z}_{\text{classical}}(z, t; \pi i b^2) + \log \mathcal{Z}_{\text{vector}}(z; \pi i b^2) + \log \mathcal{Z}_{\text{chiral}}(z, t; \pi i b^2) \right] \tag{6.2.95}$$

As before, we have used the variable $\mathsf{t} = (t, -e^{-\pi i - \pi i b^2})$, which is defined such that $\mathsf{t}^\sigma = t^\sigma e^{-\pi i r_\sigma - \pi i b^2 (r_\sigma - 1)}$. In terms of the hemisphere index, the highly squashed sphere partition function is given by

$$
\begin{aligned}
F_{S_b^3}(\Delta; \beta) &= \frac{N}{2} \log \beta + F_{D^2}(e^\Delta; \beta) - \frac{N}{2} \log[-\pi i] + \mathcal{O}(\beta) \,, \\
&= \frac{N}{2} \log \beta - \log \mathcal{C}(e^\Delta; \beta) - \frac{N}{2} \log[-\pi i] + \mathcal{O}(\beta) \,.
\end{aligned}
\tag{6.2.96}
$$

with $\Delta = -2\pi b \hat{v}$, $\beta = \pi i b^2$ and the Cardy block $\mathcal{C}$ in (6.2.23).

6.3 Universal formula

In this section, we discuss the universal relations in the Cardy limit among the partition functions we have discussed in the previous section. So far we have seen that those quantities can be solely written in terms of the Cardy block. We examine this relation more carefully and propose general index theorems for those quantities in the Cardy limit. In particular, such index theorems will prove very useful when we consider the large N limit of those quantities, which relates to the entropic quantities of the dual gravity.

In the previous section, we have already found how the hemisphere index, or the Cardy block, relates to the other three partition functions. See (6.2.55), (6.2.75) and (6.2.96). Since the topologically twisted index needs more care, let us first focus on the generalized superconformal index and the squashed sphere partition function:

$$
\begin{aligned}
F_{S^2}(\mathsf{t}, n; \beta) &= N \log \beta - \log \mathcal{C}(t; \beta) - \log \overline{\mathcal{C}}(\bar{t}; -\beta) + \mathcal{O}(\beta) \,, \\
F_{S_b^3}(\Delta; \beta) &= \frac{N}{2} \log \beta - \log \mathcal{C}(e^\Delta; \beta) + \mathcal{O}(\beta)
\end{aligned}
\tag{6.3.1}
$$

up to irrelevant numerical constants. $t = \mathfrak{t}\,e^{\beta n}$ and $\bar{t} = \mathfrak{t}^{-1}\,e^{\beta n}$ are understood for the superconformal index while $\Delta = -2\pi b\hat{v}$ and $\beta = \pi i b^2$ are understood for the squashed sphere partition function. Combining those, we find our first index theorem:

$$F_{S^2}(e^\Delta, n; \beta) = F_{S_b^3}(\Delta + \beta n; \beta) + \overline{F}_{S_b^3}(-\Delta + \beta n; -\beta) + \mathcal{O}(\beta) \,. \qquad (6.3.2)$$

One may recall that we have taken integer r_σ. This is necessary condition for the topologically twisted index while it is not for the other partition functions. Even for the other partition functions, however, the R-charges are not completely arbitrary and are restricted by the superpotential of the theory. Indeed, such restricted R-charges can be parametrized by the flavor chemical potentials. Namely, one can obtain any allowed R-charges, which are generically non-integer values, by shifting the flavor chemical potentials by $\Delta_i \to \Delta_i - (\beta + \pi i)\delta_i$. Then, the R-charge is deformed from r_σ to $r_\sigma + \sigma(\delta)$. From now on, this deformed R-charge is understood except the topologically twisted index.

One can also expand the right hand side with respect to β. Recall that $-\log \mathcal{C}(t; \beta) \approx F_{D^2}(t; \beta)$ has the form

$$-\log \mathcal{C}(t; \beta) = \frac{1}{\beta}G^{(0)}(\mathfrak{t}) - \frac{N}{2}\log\beta + G^{(1)}(\mathfrak{t}) + \mathcal{O}(\beta) \qquad (6.3.3)$$

where $\mathfrak{t} = (t, -\hat{x}e^{-\pi i})$ is defined such that

$$\mathfrak{t}^\sigma = t^\sigma \hat{x}^{r_\sigma - 1} e^{-\pi i r_\sigma} \,. \qquad (6.3.4)$$

t has a different definition for each partition function, but most generally it is defined by

$$t = \mathfrak{t}e^{\beta(n-\delta)-\pi i\delta} \,, \qquad \bar{t} = \mathfrak{t}^{-1}e^{\beta(n+\delta)+\pi i\delta} \qquad (6.3.5)$$

where the R-charge deformation is taken into account. For later convenience, we include $e^{-\pi i \delta}$ in the definition of t from now on. The small β expansion of $-\log \mathcal{C}(t; \beta)$ is thus given by

$$-\log \mathcal{C}(t; \beta) = \left[\frac{1}{\beta} G^{(0)}(\mathsf{t}) - \frac{N}{2} \log \beta + \frac{d\mathsf{t}}{d\beta} \cdot \frac{\partial}{\partial \mathsf{t}} G^{(0)}(\mathsf{t}) + G^{(1)}(\mathsf{t}) \right]_{\hat{\beta} \to 0} + \mathcal{O}(\beta).$$
(6.3.6)

Here, the third term can be expanded as

$$\frac{d\mathsf{t}}{d\beta} \cdot \frac{\partial}{\partial \mathsf{t}} G^{(0)}(\mathsf{t}) = \sum_i (n_i - \delta_i) t_i \frac{\partial}{\partial t_i} G^{(0)}(\mathsf{t}) - \hat{x} \frac{\partial}{\partial \hat{x}} G^{(0)}(\mathsf{t})$$
(6.3.7)

where we have used $\frac{d\hat{\beta}}{d\beta} = 1$. Using this expansion, we have the following expressions for $-\log \mathcal{C}$ and $-\log \overline{\mathcal{C}}$:

$$-\log \mathcal{C}(t; \beta) =$$
$$\frac{1}{\beta} G^{(0)}(\mathsf{t}) - \frac{N}{2} \log \beta + \sum_i (n_i - \delta_i) t_i \frac{\partial}{\partial t_i} G^{(0)}(\mathsf{t}) - \frac{\partial}{\partial \hat{x}} G^{(0)}(\mathsf{t}) \bigg|_{\hat{\beta} \to 0} + G^{(1)}(\mathsf{t}) + \mathcal{O}(\beta),$$
(6.3.8)

$$-\log \overline{\mathcal{C}}(\bar{t}; -\beta) =$$
$$-\frac{1}{\beta} \overline{G}^{(0)}(\mathsf{t}^{-1}) - \frac{N}{2} \log(-\beta) - \sum_i (n_i + \delta_i) \mathsf{t}_i^{-1} \frac{\partial}{\partial \mathsf{t}_i^{-1}} \overline{G}^{(0)}(\mathsf{t}^{-1}) - \frac{\partial}{\partial \hat{x}^{-1}} \overline{G}^{(0)}(\bar{\mathsf{t}}) \bigg|_{\hat{\beta} \to 0} + \overline{G}^{(1)}(\mathsf{t}^{-1})$$
$$+ \mathcal{O}(\beta)$$
(6.3.9)

where $\bar{\mathsf{t}} = (\bar{t}, -\hat{x}^{-1} e^{\pi i})$. In addition, we have used a shorthand expression

$$G^{(0,1)}(\mathsf{t}) \equiv G^{(0,1)}(\mathsf{t}) \bigg|_{\beta \to 0} = G^{(0,1)}(\mathsf{t}, -e^{-\pi i})$$
(6.3.10)

where σ acts on $-e^{\pi i}$ as $e^{-\pi i r_\sigma}$. n is nontrivial for the superconformal index while it is set to be zero for the hemisphere index and the squashed sphere

205

partition function. Combining all those expansions, in the end, we find that

$$F_{S^2}(\mathsf{t}e^{-\beta\delta}, n; \beta) = \frac{2}{\beta}i\,\mathrm{Im}\left[G^{(0)}(\mathsf{t})\right] + 2\sum_i n_i i\,\mathrm{Im}\left[\mathsf{t}_i\frac{\partial}{\partial\mathsf{t}_i}G^{(0)}(\mathsf{t})\right]$$

$$- 2\sum_i \delta_i\,\mathrm{Re}\left[\mathsf{t}_i\frac{\partial}{\partial\mathsf{t}_i}G^{(0)}(\mathsf{t})\right] - 2\,\mathrm{Re}\left[\frac{\partial}{\partial\hat{x}}G^{(0)}(\mathsf{t})\right]\Big|_{\hat{\beta}\to0} + 2\mathrm{Re}\left[G^{(1)}(\mathsf{t})\right] + \mathcal{O}(\beta)$$

$$(6.3.11)$$

$$F_{S^3_b}\left(\Delta - (\beta + \pi i)\delta; \beta\right) = \frac{1}{\beta}G^{(0)}(\mathsf{t}) - \sum_i \delta_i \mathsf{t}_i\frac{\partial}{\partial\mathsf{t}_i}G^{(0)}(\mathsf{t}) - \frac{\partial}{\partial\hat{x}}G^{(0)}(\mathsf{t})\Big|_{\hat{\beta}\to0} + G^{(1)}(\mathsf{t}) + \mathcal{O}(\beta)$$

$$(6.3.12)$$

up to numerical constants one can ignore. For the squashed sphere partition function, $\mathsf{t} = e^{\Delta - \pi i\delta} = e^{-2\pi b\hat{v} - \pi i\delta}$, $\hat{x} = e^{-\hat{\beta}} = e^{-\pi i b^2}$ is understood. Here the real part and the imaginary part should be understood with the conjugate (6.2.36).

On the other hand, for the topologically twisted index, we have seen that the Cardy limit is not completely determined by a dominant saddle. Nevertheless, it is worth mentioning the case that there is only one saddle or there is a dominant saddle due to other large parameters. In such situations, the topologically twisted index is written in terms of the Cardy block as

$$F_{S^2}^{\mathrm{twisted}}(\mathsf{t}, n; \beta) = N\log\beta - \log\mathcal{C}(t; \beta) - \log\mathcal{C}(\bar{t}^{-1}; -\beta) + \mathcal{O}(\beta). \qquad (6.3.13)$$

The expansion of the second term is given by (6.3.8) with $\delta = 0$ while the third term is expanded as follows:

$$-\log\mathcal{C}(\bar{t}^{-1}; -\beta) =$$

$$-\frac{1}{\beta}G^{(0)}(\mathsf{t}) - \frac{N}{2}\log(-\beta) + \sum_i n_i \mathsf{t}_i\frac{\partial}{\partial\mathsf{t}_i}G^{(0)}(\mathsf{t}) - \frac{\partial}{\partial\hat{x}^{-1}}G^{(0)}(\tilde{\mathsf{t}}^{-1})\Big|_{\hat{\beta}\to0} + G^{(1)}(\mathsf{t}) + \mathcal{O}(\beta)$$

$$(6.3.14)$$

where $\tilde{\mathsf{t}} = (\bar{t}, -\hat{x}e^{\pi i})$. Combining the two contributions, therefore, we find

$$F_{S^2}^{\text{twisted}}(\mathsf{t}, n; \beta) = 2\sum_i n_i \mathsf{t}_i \frac{\partial}{\partial \mathsf{t}_i} G^{(0)}(\mathsf{t}) - 2\left.\frac{\partial}{\partial \hat{x}} G^{(0)}(\mathsf{t})\right|_{\hat{\beta}\to 0} + 2G^{(1)}(\mathsf{t}) + \mathcal{O}(\beta),$$

(6.3.15)

which is only valid if there is only one saddle or if there is a dominant saddle due to other large parameters such as large N, which we discuss shortly. Also note that

$$F_{S^2}^{\text{twisted}}(e^{\Delta}, n; \beta) = F_{S_b^3}(\Delta + \beta n; \beta) + F_{S_b^3}(\Delta - \beta n; -\beta) + \mathcal{O}(\beta) \qquad (6.3.16)$$

in such cases.

Large N limit

So far we have seen that the Cardy limits discussed in the previous section are determined by two functions $G^{(0,1)}(\mathsf{t})$. See (6.3.8), (6.3.11), (6.3.12) and (6.3.15). On the other hand, we will see that, in the large N limit, only $G^{(0)}$ plays the crucial role.

Before jumping into the large N limit, let us recall that a large class of 3d supersymmetric gauge theories are known to have their gravity dual on AdS$_4$. In the large N limit, for example, the superconformal and topologically twisted indices are supposed to count the microstates of the corresponding dual black holes. This has been confirmed for a wide class of theories for the topologically twisted index [160, 161, 205, 206, 214–216] and is also recently tested for the superconformal index using the ABJM theory and its mirror dual theory [79]. Also the squashed sphere partition function relates to the supersymmetric Rényi entropy [196], which accounts for the Bekenstein-Hawking entropy of a charged topological black hole in AdS$_4$ [197, 198]. Furthermore, although we have not

discussed it so far, the round sphere partition function, which is a basic quantity counting the degrees of freedom in odd dimensions, relates to the Euclidean on-shell action in AdS_4 [36] as well as the holographic entanglement entropy of Ryu-Takayanagi [199, 200, 217].

As such, many observables of a field theory directly capture the entropic quantities of its gravity dual. More surprisingly, in the large N limit, some of those different looking quantities are proven to be related to each other. For example, there is an index theorem between the topologically twisted index and the round sphere partition function [205]:

$$
F_{S^2}^{\text{twisted}}(\mathfrak{t}, n; \beta) = \frac{\pi i}{2} \sum_i \left(n_i - \frac{\Delta_i}{\pi i} \right) \frac{\partial}{\partial \Delta_i} F_{S^3} \left(-\frac{\Delta}{\pi i} \right) + F_{S^3} \left(-\frac{\Delta}{\pi i} \right) ,
$$

(6.3.17)

which is written in our notation. This index theorem relates two different entropic quantities of the dual gravity theory: the black hole entropy and the holographic entanglement entropy for a spherical entangling surface. Here we extend this index theorem to include the superconformal index, which is supposed to capture the entropy of the rotating black hole, and also rederive the above index theorem in our factorization context.

First, we note an interesting relation between the squashed sphere partition function and the round sphere partition function in the large N limit [194]:

$$
F_{S_b^3} \left(-\pi i b Q \delta; \pi i b^2 \right) = \frac{Q^2}{4} F_{S^3} \left(\delta \right) ,
$$

(6.3.18)

or equivalently

$$
F_{S_b^3} \left(\Delta; \beta \right) = \frac{(\pi i + \beta)^2}{4 \pi i \beta} F_{S^3} \left(-\frac{\Delta}{\pi i + \beta} \right) .
$$

(6.3.19)

The explicit field theoretic derivation of this relation is discussed in [194], where the relation is derived for non-chiral Chern-Simons quiver gauge theories dual to M-theory on $\mathrm{AdS}_4 \times SE_7$. On the other hand, we will see that this relation holds more generally, in particular for theories dual to massive IIA string theory as well. Note that flavor chemical potentials are turned off while the deformations of the R-charges are parametrized by δ. Putting this back into the index theorem (6.3.2), and (6.3.16), we find our second index theorem in the large N limit:

$$F_{S^2}(\Delta, n; \beta) = \frac{(\pi i + \beta)^2}{4\pi i \beta} F_{S^3}\left(-\frac{\Delta + \beta n}{\pi i + \beta}\right) + \frac{(\pi i + \beta)^2}{4\pi i \beta}\overline{F}_{S^3}\left(-\frac{\Delta - \beta n}{\pi i + \beta}\right) + \mathcal{O}(\beta),$$

$$F_{S^2}^{\text{twisted}}(\Delta, n; \beta) = \frac{(\pi i + \beta)^2}{4\pi i \beta} F_{S^3}\left(-\frac{\Delta + \beta n}{\pi i + \beta}\right) - \frac{(\pi i - \beta)^2}{4\pi i \beta} F_{S^3}\left(-\frac{\Delta - \beta n}{\pi i - \beta}\right) + \mathcal{O}(\beta),$$
$$(6.3.20)$$

which relates two types of black hole entropies with the holographic entanglement entropy for a spherical entangling surface. Note that, for parity invariant theories, F_{S^3} is a real function. Furthermore although we have derived (6.3.20) in the Cardy limit, many examples suggest that they are exact for arbitrary β in the large N limit, at least for the known large N saddle point capturing the black hole microstates. In particular, recall that the Cardy block is given by

$$-\log \mathcal{C}(t; \beta) = \frac{1}{\beta} G^{(0)}(\mathsf{t}) - \frac{N}{2} \log \beta + G^{(1)}(\mathsf{t}) + \mathcal{O}(\beta). \qquad (6.3.21)$$

In the next section, we will show that $G^{(1)}$ is subdominant in N compared to $G^{(0)}$ at the large N saddle point for the M2-brane example. In the same manner, we expect that the $\mathcal{O}(\beta)$ corrections are also all subdominant at the large N saddle, which implies that our formula (6.3.20) is indeed exact for arbitrary β. We will come back to this point in section 6.4 and 6.5. Also note that recently similar relations are found in terms of gravitational blocks on the dual gravity side [201], which are also inspired by the holomorphic blocks. It

will be interesting to obtain those relations using the equivariant localization in supergravity [218, 219].

In particular, one can consider the ordinary superconformal index by turning off all the magnetic flux for the flavor symmetry, $n = 0$. In that case, we have

$$F_{S^2}(\Delta, n = 0; \beta) = \frac{(\pi i + \beta)^2}{2\pi i \beta} \mathrm{Re} \left[F_{S^3} \left(-\frac{\Delta}{\pi i + \beta} \right) \right] \qquad (6.3.22)$$

where $\mathrm{Re}[\dots]$ should be understood with the conjugation defined by (6.2.36). Indeed, one can further unrefine the index by turning off the flavor chemical potentials as well. Restoring the superconformal R-charge by setting $\Delta = -(\pi i + \beta)\delta_* \equiv -\Delta_R \delta_*$, we obtain a simple formula

$$F_{S^2}(\beta) = \frac{\Delta_R^2}{2\pi i \beta} \mathrm{Re} \left[F_{S^3}(\delta_*) \right] \qquad (6.3.23)$$

where $\Delta_R = \pi i + \beta$ is the chemical potential for the superconformal R-symmetry and δ_* is the shift of R-charges restoring the superconformal values, which are determined by the F-maximization. This relates the unrefined superconformal index and the round sphere partition function at the superconformal point in a very simple manner, where the latter accounts for the degrees of freedom of 3d SCFTs [202]. This is reminiscent of the Cardy formula for 2d CFTs [12][2] or 4d $\mathcal{N} = 1$ SCFTs [138] in the large N limit, where the real part of the round sphere free energy, $\mathrm{Re}\left[F_{S^3}(\delta_*) \right]$, plays the role of central charges in 2d and in 4d. Recently the same relation has been observed for 3d SCFTs arising from M5-branes wrapped on hyperbolic three-manifolds [203, 204], which show N^3 degrees of freedom in the large N limit. Our result shows that this relation holds much more generally. Also we would like to mention that similar universal relations among quantities in different dimensions are discussed in [207, 222].

---

[2]Recently, it is shown that the 2d Cardy formula can be derived in a rigorous way using Tauberian theorems [220, 221].

Again one can expand the right hand side with respect to β. First, comparing (6.3.18) with our formula (6.3.12), we obtain the following expression for the round sphere:

$$F_{S^3}(\delta) = \frac{4}{\pi i} G^{(0)}(e^{-\pi i \delta}) = \frac{2}{\pi i} \sum_i \delta_i \frac{\partial}{\partial \delta_i} G^{(0)}(e^{-\pi i \delta}) - 2 \frac{\partial}{\partial \hat{x}} G^{(0)}(\mathfrak{t}) \bigg|_{\mathfrak{t} \to e^{-\pi i \delta}, \hat{\beta} \to 0} + 2 G^{(1)}(e^{-\pi i \delta}),$$

(6.3.24)

which implies that

$$\frac{2}{\pi i} G^{(0)}(\mathfrak{t}) = \frac{1}{\pi i} \sum_i (\Delta_i - \pi i \delta_i) \mathfrak{t}_i \frac{\partial}{\partial \mathfrak{t}_i} G^{(0)}(\mathfrak{t}) - \frac{\partial}{\partial \hat{x}} G^{(0)}(\mathfrak{t}) \bigg|_{\hat{\beta} \to 0} + G^{(1)}(\mathfrak{t}) \quad (6.3.25)$$

where $\mathfrak{t} = e^{\Delta - \pi i \delta}$. Putting this back into the general formula above, we obtain

$$F_{D^2}(\mathfrak{t}e^{-\beta \delta}; \beta) = \frac{1}{\beta} G^{(0)}(\mathfrak{t}) - \frac{N}{2} \log \beta - \frac{1}{\pi i} \sum_i \Delta_i \mathfrak{t}_i \frac{\partial}{\partial \mathfrak{t}_i} G^{(0)}(\mathfrak{t}) + \frac{2}{\pi i} G^{(0)}(\mathfrak{t}) + \mathcal{O}(\beta),$$

(6.3.26)

$$F_{S^2}(\mathfrak{t}e^{-\beta \delta}, n; \beta) =$$
$$\frac{2}{\beta} i \operatorname{Im}\left[G^{(0)}(\mathfrak{t})\right] + 2 \sum_i n_i i \operatorname{Im}\left[\mathfrak{t}_i \frac{\partial}{\partial \mathfrak{t}_i} G^{(0)}(\mathfrak{t})\right] - 2 \sum_i \operatorname{Re}\left[\frac{\Delta_i}{\pi i} \mathfrak{t}_i \frac{\partial}{\partial \mathfrak{t}_i} G^{(0)}(\mathfrak{t})\right] + \frac{4}{\pi} \operatorname{Im}\left[G^{(0)}(\mathfrak{t})\right]$$
$$+ \mathcal{O}(\beta),$$

(6.3.27)

$$F_{S^2}^{\text{twisted}}(\mathfrak{t}, n; \beta) = 2 \sum_i \left(n_i - \frac{\Delta_i}{\pi i}\right) \mathfrak{t}_i \frac{\partial}{\partial \mathfrak{t}_i} G^{(0)}(\mathfrak{t}) + \frac{4}{\pi i} G^{(0)}(\mathfrak{t}) + \mathcal{O}(\beta) \quad (6.3.28)$$

for the three indices and

$$F_{S_b^3}\left(-2\pi b\hat{v} - \pi i b Q \delta; \pi i b^2\right) = \frac{1}{\pi i b^2} G^{(0)}(e^{-2\pi b\hat{v} - \pi i \delta}) - \frac{1}{\pi i} \sum_i \hat{v}_i \frac{\partial}{\partial \hat{v}_i} G^{(0)}(e^{-2\pi b\hat{v} - \pi i \delta})$$
$$+ \frac{2}{\pi i} G^{(0)}(e^{-2\pi b\hat{v} - \pi i \delta}) + \mathcal{O}(\beta), \quad (6.3.29)$$

$$F_{S^3}(\delta) = \frac{4}{\pi i} G^{(0)}(e^{-\pi i \delta}) \quad (6.3.30)$$

for the sphere partition functions. $\mathfrak{t}$ is defined by $\mathfrak{t} = e^{\Delta - \pi i \delta}$; n_i vanishes for the hemisphere index; δ_i vanishes for the topologically twisted index; and finite $b\hat{v}$ is understood for the squashed sphere partition function.

Especially, if we only look at the leading term in each partition function,

$$F_{D^2}(\mathfrak{t}e^{-\beta\delta};\beta) = \frac{1}{\beta}G^{(0)}(\mathfrak{t})\,, \tag{6.3.31}$$

$$F_{S^2}(\mathfrak{t}e^{-\beta\delta},n;\beta) = \frac{2}{\beta}i\mathrm{Im}\left[G^{(0)}(\mathfrak{t})\right]\,, \tag{6.3.32}$$

$$F_{S^2}^{\mathrm{twisted}}(\mathfrak{t},n;\beta) = 2\sum_i\left(n_i - \frac{\Delta_i}{\pi i}\right)\mathfrak{t}_i\frac{\partial}{\partial\mathfrak{t}_i}G^{(0)}(\mathfrak{t}) + \frac{4}{\pi i}G^{(0)}(\mathfrak{t})\,, \tag{6.3.33}$$

$$F_{S^3_b}\left(-2\pi b\hat{v} - \pi ibQ\delta;\pi ib^2\right) = \frac{1}{\pi ib^2}G^{(0)}(e^{-2\pi b\hat{v}-\pi i\delta})\,, \tag{6.3.34}$$

$$F_{S^3}(\delta) = \frac{4}{\pi i}G^{(0)}(e^{-\pi i\delta})\,, \tag{6.3.35}$$

from which one can read off various relations among those partition functions in the strict Cardy limit. For example, one can write down the superconformal index and the topologically twisted index in terms of the round sphere partition function as follows:

$$F_{S^2}(\mathfrak{t}e^{-\beta\delta},n;\beta) \approx -\frac{\pi}{2\beta}\mathrm{Re}\left[F_{S^3}\left(-\frac{\Delta}{\pi i}\right)\right]\,,$$

$$\tag{6.3.36}$$

$$F_{S^2}^{\mathrm{twisted}}(\mathfrak{t},n;\beta) \approx \frac{\pi i}{2}\sum_i\left(n_i - \frac{\Delta_i}{\pi i}\right)\frac{\partial}{\partial\Delta_i}F_{S^3}\left(-\frac{\Delta}{\pi i}\right) + F_{S^3}\left(-\frac{\Delta}{\pi i}\right)$$

where the former provides a new universal formula for the large N superconformal indices of 3d $\mathcal{N} = 2$ supersymmetric non-chiral Chern-Simons quiver theories dual to M-theory on $\mathrm{AdS}_4 \times SE_7$ while the latter reproduces the known index theorem for the unrefined topologically twisted index [205].

Indeed, the relations in (6.3.36), and (6.3.20), hold more generally, in particular, for theories dual to massive IIA string theory. Recall that the second relation in [205] is derived not only for theories dual to M-theory but also for those dual to massive IIA string theory. Thus, by reversing the logic, combining the index theorem of [205] and our formula (6.3.16), which relates the topologically twisted index and the squashed sphere partition function, one can find

that the relation (6.3.19) should hold for massive IIA duals as well as M-theory duals. Therefore, the resulting relations in (6.3.20) and (6.3.36) also hold for massive IIA duals. We will encounter such a massive type IIA example in section 6.5. Furthermore, the Cardy limit formula (6.3.2) without the large N limit is even more general as it does not have any such restrictions.

6.4 Example: $\mathcal{N} = 4\, U(N)$ SYM with one fundamental and one adjoint hypermultiplets

In this section, we examine the $\mathcal{N} = 4\, U(N)$ SYM theory with one fundamental and one adjoint hypermultiplets as an explicit example. It lives on N D2-branes and 1 D6-brane, and flows in IR to $\mathcal{N} = 8$ SCFT on M2-branes. Its holographic dual is the 11d SUGRA, or M-theory, on $\text{AdS}_4 \times S^7$. The partition functions of this theory are already discussed in the literature. For example, the Cardy limits of the superconformal and hemisphere indices are discussed in [79], which we review in chapter 5, and the (unrefined) topologically twisted index in the large N limit is discussed in [214]. Here, we reexamine those partition functions in the perspective of the Cardy factorization, which sheds more light on their relations and the universal structure such as (6.3.20) or (6.3.36). For simplicity, we will only consider the large N limit. The finite N superconformal index in the Cardy limit can be found in [79], which we discussed in chapter 5.

6.4.1 Hemisphere index

We first examine the hemisphere index. Following [171], the hemisphere index of the theory is given by

$$
I_{D^2}(\hat{Q}, z, t^{\frac{1}{2}}; \beta) = \mathrm{tr}_{\mathcal{H}(D^2;\alpha)} \left[(-1)^{\mathsf{R}} x^{\mathsf{R}+2\mathsf{J}_3} t^{l-r} z^{2m} \hat{Q}^T \right]
$$

$$
= \frac{1}{N!} \left(\frac{\theta(zt; x^2)}{\theta(zx^2; x^2)} \right)^{\frac{N^2-N}{2}} \left(\frac{\theta(zt^{\frac{1}{2}}; x^2)\theta(t^{\frac{1}{2}}e^{-\pi i}x; x^2)}{\theta(ze^{-\pi i}x; x^2)} \right)^N
$$

$$
\times \oint \left(\prod_{a=1}^{N} \frac{ds_a}{2\pi i s_a} \right) \left(\prod_{a=1}^{N} \frac{\theta(s_a \hat{Q} t^{\frac{1}{2}}; x^2)}{\theta(s_a e^{-\pi i}x; x^2)\theta(\hat{Q} t^{\frac{1}{2}}; x^2)} \right) \left(\prod_{1 \le a \ne b \le N} (s_a s_b^{-1}; x^2) \right)
$$

$$
\times \left(\prod_{a=1}^{N} \frac{(s_a t^{-\frac{1}{2}} x^2; x^2)}{(s_a t^{\frac{1}{2}}; x^2)} \right) \left(\prod_{a,b=1}^{N} \frac{(s_a s_b^{-1} z t^{-\frac{1}{2}} x^2; x^2)}{(s_a s_b^{-1} t^{-1} x^2; x^2)(s_a s_b^{-1} z t^{\frac{1}{2}}; x^2)} \right) , \quad (6.4.1)
$$

where $x = e^{-\beta}$. s_a's denote the gauge holonomies on S^1, which were originally denoted by z_a's in section 6.2. Our theory has $\mathcal{N} = 4$ SUSY in UV, which is associated with $SO(4) \cong SU(2)_l \times SU(2)_r$ R-symmetry. Also, the adjoint hypermultiplet can be decomposed into two half-hypermultiplets being a doublet of $SU(2)_m$ flavor symmetry. Finally, there is a topological $U(1)_T$ symmetry coming from the conserved current of the $U(N)$ gauge symmetry $j^\mu = \mathrm{tr}(\star F)^\mu$. l, r, m denote the Cartan charges of $SU(2)_l \times SU(2)_r \times SU(2)_m$, and T is the $U(1)_T$ charge. From the $\mathcal{N} = 2$ viewpoint, $l+r$ corresponds to the $SO(2) \cong U(1)$ superconformal R-charge while $l - r$ is a flavor charge. As explained in section 6.2, we will take the integer quantized R-charge to define the index with $(-1)^{\mathsf{R}}$, $\mathsf{R} = 2r$ in this case, instead of the superconformal one. Those two merely differ by a shift of the chemical potentials. Then, the adjoint chiral multiplet in the $\mathcal{N} = 4$ vector multiplet has R-charge 2, while the other chiral multiplets have vanishing R-charges. This can be achieved by successive replacing $t \to tx^{-1}$ and $x \to e^{-\pi i}x$ for the index in [79], which made use of the superconformal R-charge and $F = 2\mathsf{J}_3$, where J_3 is the angular momentum on D^2. Further note

that $\hat{Q} = e^{-\hat{\xi}}, z = e^f, t^{\frac{1}{2}} = e^{\frac{T}{2}}$ are the fugacities conjugate to the integer quantized flavor charges. Lastly we have introduced 2d degrees of freedom to cancel the boundary mixed/flavor anomalies such that there is no UV mixed/flavor Chern-Simons term except the one between the diagonal gauge $U(1)$ and the topological $U(1)$. In particular, the θ functions in front of the integral are due to the flavor anomalies while the θ functions inside the integral are due to the mixed anomalies between the gauge and the flavor symmetries.

For this particular model, one may avoid 2d degrees of freedom by turning on appropriate mixed/flavor Chern-Simons terms, as done in [79]. On the other hand, here we keep 2d degrees of freedom and assume no extra mixed/flavor Chern-Simons terms. In particular, if $Q = e^{-\xi} \equiv \hat{Q}t^{\frac{1}{2}}e^{\pi i}x^{-1}$ has discrete value x^{2n} with an integer n, the θ functions inside the integral are simplified to

$$\prod_{a=1}^{N} \frac{\theta(s_a\hat{Q}t^{\frac{1}{2}};x^2)}{\theta(s_a e^{-\pi i}x;x^2)\theta(\hat{Q}t^{\frac{1}{2}};x^2)}\Bigg|_{\hat{Q}t^{\frac{1}{2}}e^{\pi i}x^{-1}=x^{2n}} = \frac{1}{(e^{-\pi i}x;x^2)^2} \prod_{a=1}^{N} s_a^{-\frac{\xi}{2\beta}} , \quad (6.4.2)$$

which can be regarded as the classical contribution of the Fayet-Iliopoulos action, whose coupling constant should have a quantized real value on D^2, up to a gauge holonomy independent factor. In this regard, the above θ functions incorporate a generalized FI parameter $\hat{\xi} = \log \hat{Q}$, which can take any complex value. This is because, in 3d, the Fayet-Iliopoulos action can be realized as a mixed Chern-Simons action between the gauge $U(1)$ and the topological $U(1)$. For computational convenience, we will temporarily use the parameter $\xi = \hat{\xi} - \frac{T}{2} - \pi i - \beta$ rather than $\hat{\xi}$. At the final answer, we will convert it back to $\hat{\xi}$.

In the Cardy limit $\beta \to 0$, all the other chemical potentials ξ, f, T may be taken as pure imaginary and finite [75]. We will restrict the parameter region

215

as

$$-2\pi < \text{Im}(\xi) < 0\,, \qquad -2\pi < \text{Im}(T) < 0\,,$$

$$0 < \text{Im}\left(f - \frac{T}{2}\right) < 2\pi\,, \qquad 0 < \text{Im}\left(-f - \frac{T}{2}\right) < 2\pi\,. \qquad (6.4.3)$$

After gluing two hemisphere indices to make the superconformal index, or the topologically twisted index, the resulting index at the other parameter regions can be easily generated by periodic shifts of the chemical potentials and complex conjugation of the index [79]. So, it suffices to consider the above case only to cover the whole parameter region. Then, recall that the Cardy limit $\beta \to 0$ of the hemisphere index (6.4.1) can be evaluated by the saddle point method as

$$I_{D^2} = \left(\frac{\beta}{\pi}\right)^{\frac{N}{2}} \exp\left(-\frac{1}{2\beta}\mathcal{W}^*\right) \left(\det(-\partial_s^2 \mathcal{W})^*\right)^{-\frac{1}{2}} \left(\prod_{a=1}^{N} \frac{1}{s_a^*} + \mathcal{O}(\beta)\right)\,, \quad (6.4.4)$$

with an effective twisted superpotential [79, 171]

$$\mathcal{W} =$$

$$\frac{N^2 - N}{2}(T - 2\pi i(p_1 - p_2) + 2\beta)\left(-f - \frac{T}{2} + \pi i(p_1 + p_2 + 1)\right)$$

$$+ \frac{N}{2}(T + 2\pi i + 2\beta)\left(-f - \frac{T}{2}\right)$$

$$+ N\left(-\frac{3}{2}\pi^2 + 2\pi^2((p_3 - p_4)(p_3 + p_4 + 2) - p_5(p_5 + 2)) - 2\pi i(p_3 - p_5)\xi - \frac{1}{2}\beta(2\pi i + \beta)\right)$$

$$+ N\left(-\text{Li}_2(t^{-1}x) + \text{Li}_2(zt^{-\frac{1}{2}}x) - \text{Li}_2(zt^{\frac{1}{2}}x^{-1})\right)$$

$$+ \sum_{a=1}^{N}\left(\left(\xi + 2\pi i(p_3 - p_4)\right)\log s_a + \text{Li}_2(s_a t^{-\frac{1}{2}}x) - \text{Li}_2(s_a t^{\frac{1}{2}}x^{-1})\right)$$

$$+ \sum_{1 \le a \ne b \le N}\left(\text{Li}_2(s_a s_b^{-1}x^{-1}) - \text{Li}_2(s_a s_b^{-1}t^{-1}x) + \text{Li}_2(s_a s_b^{-1}zt^{-\frac{1}{2}}x) - \text{Li}_2(s_a s_b^{-1}zt^{\frac{1}{2}}x^{-1})\right)$$

$$+ \mathcal{O}(\beta^2)\,,$$

$$(6.4.5)$$

where

$$2\pi p_1 < \mathrm{Im}\,(f+T) < 2\pi(p_1+1)\,,$$

$$2\pi p_2 < \mathrm{Im}\,(f) < 2\pi(p_2+1)\,,$$

$$2\pi p_3 < \mathrm{Im}\,(\log s_a - \xi - \pi i) < 2\pi(p_3+1)\,, \qquad (6.4.6)$$

$$2\pi p_4 < \mathrm{Im}\,(\log s_a - \pi i) < 2\pi(p_4+1)\,,$$

$$2\pi p_5 < \mathrm{Im}\,(-\xi - \pi i) < 2\pi(p_5+1)\,.$$

Here, we used the asymptotic formulae (A.0.2), (A.0.10). Also, we assumed that the eigenvalue distribution s_a does not pass across the branch cuts, and $\mathcal{O}(\beta)$ corrections do not change the branches of the arguments. Due to the conditions (6.4.3),

$$(p_1, p_2) = (-2,-1)\,, (-1,-1)\,, (-1,0)\,, (0,0)\,,$$

$$p_3 - p_4 = 0,\, 1\,, \qquad p_5 = -1,\, 0\,. \qquad (6.4.7)$$

Focusing on the gauge holonomy dependent parts of (6.4.5), $2\pi i(p_3 - p_4)$ effectively shifts the range of $\mathrm{Im}(\xi)$ to $(2\pi(p_3 - p_4 - 1), 2\pi(p_3 - p_4))$. However, according to [79], the known Cardy saddle point of the hemisphere index (6.4.1) only exists when $-2\pi < \mathrm{Im}(\xi) < 0$. Therefore, we will set $p_3 - p_4 = 0$. This restricts the possible range of the argument of s_a's. The known Cardy saddle point belongs to that range. When $p_3 - p_4 = 1$, there is no known saddle point. Also, as the hemisphere index (6.4.1) is invariant under $s_a \to e^{2\pi i} s_a$, due to the large gauge invariance of our QFT, we can freely tune the value of p_4. We shall

set $p_3 = p_4 = p_5 \equiv p$, which can be either -1 or 0. Then, $\mathcal{W}$ becomes

$$
\mathcal{W} =
$$

$$
\frac{N^2 - N}{2}(T - 2\pi i(p_1 - p_2) + 2\beta)\left(-f - \frac{T}{2} + \pi i(p_1 + p_2 + 1)\right)
$$

$$
+ \frac{N}{2}(T + 2\pi i + 2\beta)\left(-f - \frac{T}{2}\right)
$$

$$
+ N\left(-\frac{4p+3}{2}\pi^2 - \frac{1}{2}\beta(2\pi i + \beta) - \mathrm{Li}_2(t^{-1}x) + \mathrm{Li}_2(zt^{-\frac{1}{2}}x) - \mathrm{Li}_2(zt^{\frac{1}{2}}x^{-1})\right)
$$

$$
+ \sum_{a=1}^{N}\left(\xi \log s_a + \mathrm{Li}_2(s_a t^{-\frac{1}{2}}x) - \mathrm{Li}_2(s_a t^{\frac{1}{2}}x^{-1})\right)
$$

$$
+ \sum_{1 \le a \neq b \le N}\left(\mathrm{Li}_2(s_a s_b^{-1}x^{-1}) - \mathrm{Li}_2(s_a s_b^{-1}t^{-1}x) + \mathrm{Li}_2(s_a s_b^{-1}zt^{-\frac{1}{2}}x) - \mathrm{Li}_2(s_a s_b^{-1}zt^{\frac{1}{2}}x^{-1})\right)
$$

$$
+ \mathcal{O}(\beta^2)\,.
$$

$$(6.4.8)$$

The first and second lines become $\frac{N^2}{2}(T + 2\pi i + 2\beta)\left(-f - \frac{T}{2}\right)$ when $(p_1, p_2) = (-1, 0)$, which is proportional to N^2. This exactly cancels $\mathcal{W}_0$ in [79], which is the term proportional to N^2 of $\mathcal{W}^*$ in the large N limit. Namely, by introducing appropriate boundary degrees of freedom, we can get rid of the term proportional to N^2 in the large N Cardy free energy, which does not come from the degrees of freedom of N M2-branes. However, one may suspect what happens in the other branches as it will not exactly cancels $\mathcal{W}_0$ in those cases. First note that it does not depend on s_a's, so it does not affect the saddle point. Furthermore, as explained in [79], this term cancels out when we glue two hemisphere indices to make the superconformal index or the topologically twisted index. Therefore, this term does not affect the resulting indices at all so that we can effectively ignore it in the hemisphere index even in the other branches.

To analytically compute $\mathcal{W}^*$, let us consider the large N limit. It was basically studied in [79]. Carefully following section 4.1 of [79], it is not hard to

keep $\mathcal{O}(\beta)$ terms in $\mathcal{W}$. We obtain

$$-\frac{\mathcal{W}^*}{2\beta} = -i\frac{\sqrt{2}N^{\frac{3}{2}}}{3\beta}\sqrt{\left(-\hat{\xi} + \frac{T}{2} + \pi i + \beta\right)\left(\hat{\xi} + \frac{T}{2} + \pi i + \beta\right)\left(f - \frac{T}{2}\right)\left(-f - \frac{T}{2}\right)}$$

$$+ \frac{o(N^{\frac{3}{2}})}{\beta} + o(N^{\frac{3}{2}})\beta^0 + \mathcal{O}(\beta) , \tag{6.4.9}$$

where $\hat{\xi} = \xi + \frac{T}{2} + \pi i + \beta$.[3] This large N Cardy saddle point value exists only when we further restrict the parameters as

$$0 < \mathrm{Im}\left(\hat{\xi} + \frac{T}{2} + \pi i + \beta\right) < 2\pi , \quad \mathrm{Im}(\beta) < 0 . \tag{6.4.10}$$

Note that we shifted $T \to T + \beta$ and removed $\mathcal{W}_0$ in [79] as explained before.

According to (6.4.4), the following also contributes to the hemisphere index at $\mathcal{O}(\beta^0)$:

$$\left(\frac{\beta}{\pi}\right)^{\frac{N}{2}} \left(\det(-\partial_s^2 \mathcal{W})^*\right)^{-\frac{1}{2}} \prod_{a=1}^{N} \frac{1}{s_a^*} . \tag{6.4.11}$$

Also, from [79], one can find that the Cardy saddle point satisfies $\mathrm{Im}(s_a) = 0$, $\mathrm{Re}(s_a) > 0$ for our parameter region. Then, we may sort the eigenvalues in the ascending order as follows:

$$0 < s_1 < s_2 < \cdots < s_N . \tag{6.4.12}$$

Assuming $\mathrm{Im}(\beta) < 0$ as before, which is the relevant region for our microstate

---

[3]Indeed, the subleading correction in N turns out to be not $\mathcal{O}(N)$ but $\mathcal{O}(N^{\frac{1}{2}})$, according to the numerical analysis [79]. So, one may replace $o(N^{\frac{3}{2}}) \to \mathcal{O}(N^{\frac{1}{2}})$ in (6.4.9). Nevertheless, we shall keep using $o(N^{\frac{3}{2}})$ as we do not have its analytic proof yet.

counting, the Hessian of $\mathcal{W}$ at $\beta \to 0$ is given by

$$\frac{\partial^2 \mathcal{W}}{\partial s_a \partial s_b} = \frac{1}{s_a s_b} \left[1 + \sum_\mu s_\mu \left(\frac{1}{1 - e^{-\mu} s_a s_b^{-1}} + \frac{1}{1 - e^{-\mu} s_a^{-1} s_b} \right) \right] , \qquad (a \neq b) ,$$

$$\frac{\partial^2 \mathcal{W}}{\partial s_a^2} =$$
$$\frac{1}{s_a^2} \left[-(N-1) - (N - 2a + 1)\pi i - \xi + \mathrm{Li}_1(t^{1/2} s_a) - \mathrm{Li}_1(t^{-1/2} s_a) + \frac{1}{1 - t^{-1/2} s_a^{-1}} - \frac{1}{1 - t^{1/2} s_a^{-1}} \right.$$
$$\left. + \sum_{\substack{b=1 \\ b \neq a}}^N \left\{ \log(s_a s_b^{-1}) + \sum_\mu s_\mu \left(-\mathrm{Li}_1(e^\mu s_a s_b^{-1}) + \mathrm{Li}_1(e^\mu s_a^{-1} s_b) - \frac{1}{1 - e^{-\mu} s_a s_b^{-1}} - \frac{1}{1 - e^{-\mu} s_a^{-1} s_b} \right) \right\} \right] ,$$

$$(6.4.13)$$

where $\mu = -T, f - \frac{T}{2}, f + \frac{T}{2}$ and $s_{-T} = -1$, $s_{f - \frac{T}{2}} = +1$, $s_{f + \frac{T}{2}} = -1$. At the large N Cardy saddle point [79]

$$s_a^* = s_0 e^{N^{1/2} x_a} , \quad s_0 = \frac{\sinh(\xi/2)}{\sinh(\xi/2 + T/2)} , \qquad (6.4.14)$$

the above Hessian becomes

$$\frac{\partial^2 \mathcal{W}}{\partial s_a \partial s_b} = -\frac{1}{s_a^* s_b^*} \left[\left(\sum_\mu 2 s_\mu \sinh \mu \right) e^{-N^{1/2} |x_a - x_b|} + \mathcal{O}\left(\left(e^{-N^{1/2}} \right)^2 \right) \right] , \quad (a \neq b) ,$$

$$\frac{\partial^2 \mathcal{W}}{\partial s_a^2} = -\frac{1}{s_a^{*2}} \left[\xi + \theta(x_a)(T + 2\pi i) - \delta_{x_a, 0} \left(\xi + \frac{1}{1 - t^{-1/2} s_0^{-1}} - \frac{1}{1 - t^{1/2} s_0^{-1}} \right) + \mathcal{O}\left(e^{-N^{1/2}} \right) \right] ,$$

$$(6.4.15)$$

where $\theta(x > 0) = 1$, $\theta(x \leq 0) = 0$, and $\delta_{x_a, 0}$ is the Kronecker delta. Then, the Hessian determinant is given by

$$\det(-\partial_s^2 \mathcal{W})^* = \prod_{a=1}^N \frac{1}{s_a^{*2}} \, \Delta^N \left(1 + \mathcal{O}\left(e^{-N^{1/2}} \right) \beta^0 + \mathcal{O}(\beta) \right) , \qquad (6.4.16)$$

where $\Delta^N \equiv \prod_{a=1}^N \left[\xi + \theta(x_a)(T + 2\pi i) - \delta_{x_a, 0} \left(\xi + \frac{1}{1 - t^{-1/2} s_0^{-1}} - \frac{1}{1 - t^{1/2} s_0^{-1}} \right) \right]$, i.e. Δ is an $\mathcal{O}(1)$ constant. Finally, we obtain

$$\log \left[\left(\frac{\beta}{\pi} \right)^{\frac{N}{2}} \left(\det(-\mathcal{W}_{ss}'') \right)^{-\frac{1}{2}} \prod_{a=1}^N \frac{1}{s_a^*} \right] = \frac{N}{2} \log \left(\frac{\beta}{\pi \Delta} \right) + \mathcal{O}\left(e^{-N^{1/2}} \right) \beta^0 + \mathcal{O}(\beta) ,$$

$$(6.4.17)$$

which contributes as $\mathcal{O}(N)$ to the large N Cardy free energy. Therefore, together with (6.4.9), the large N Cardy free energy of the hemisphere index is given by

$$
\begin{aligned}
&\log I_{D^2}(e^{-\hat{\xi}}, e^f, e^{\frac{T}{2}}; \beta) \\
&= \log \mathcal{C}(e^{-\hat{\xi}}, e^f, e^{\frac{T}{2}}; \beta) \\
&= -i \frac{\sqrt{2} N^{\frac{3}{2}}}{3\beta} \sqrt{\left(-\hat{\xi} + \frac{T}{2} + \pi i + \beta\right)\left(\hat{\xi} + \frac{T}{2} + \pi i + \beta\right)\left(f - \frac{T}{2}\right)\left(-f - \frac{T}{2}\right)} \\
&\quad + \frac{N}{2} \log\left(\frac{\beta}{\pi\Delta}\right) + \frac{o(N^{\frac{3}{2}})}{\beta} + o(N^{\frac{3}{2}})\beta^0 + \mathcal{O}(\beta) \,,
\end{aligned}
$$

(6.4.18)

when

$$
0 < \mathrm{Im}\left(-\hat{\xi} + \frac{T}{2} + \pi i + \beta\right),\ \mathrm{Im}\left(\hat{\xi} + \frac{T}{2} + \pi i + \beta\right),\ \mathrm{Im}\left(f - \frac{T}{2}\right),\ \mathrm{Im}\left(-f - \frac{T}{2}\right) < 2\pi \,,
$$

(6.4.19)

with

$$
\mathrm{Im}(\beta) < 0 \,.
$$

(6.4.20)

Note that the $\log \beta$ term is correct even at finite N as explained in section 6.2. One can also restore the superconformal R-charge by shifting $T \to T - \pi i - \beta$.

6.4.2 Generalized superconformal index

In this subsection, we construct the large N Cardy limit of the generalized superconformal index from (6.4.18). This index should statistically account for the microstates of the electrically charged [82] or dyonic [97] rotating BPS black holes with vanishing magnetic charge for the R-symmetry and large angular momentum $J/N^{\frac{3}{2}} = \mathcal{O}(\beta^{-2})$ in $\mathrm{AdS}_4 \times S^7$ [79]. In order to preserve SUSY, the black holes should have both electric charges and angular momentum while it is free to turn off the magnetic charges for the (non-R) flavor symmetries [74, 82, 97].

Recall that, in the Cardy limit, the generalized superconformal index is given in terms of the Cardy block (6.2.55) as follows:

$$F_{S^2}(\mathfrak{t}, n; \beta) = N \log \beta - \log \mathcal{C}(e^{-\hat{\xi}+\beta n_\xi}, e^{f+\beta n_f}, e^{\frac{T}{2}+\beta n_T}; \beta)$$
$$- \log \overline{\mathcal{C}}(e^{\hat{\xi}+\beta n_\xi}, e^{-f+\beta n_f}, e^{-\frac{T}{2}+\beta n_T}; -\beta) - \log\left[N!\,\pi^N\right] + \mathcal{O}(\beta)$$
(6.4.21)

Applying (6.4.18) to the above factorization formula, we obtain

$$\log I_{S^2}(\Delta_I, n_I; \beta) = -i\frac{2\sqrt{2}N^{\frac{3}{2}}}{3}\frac{\sqrt{(\Delta_1 + n_1\beta)(\Delta_2 + n_2\beta)(\Delta_3 + n_3\beta)(\Delta_4 + n_4\beta)}}{2\beta}$$
$$- i\frac{2\sqrt{2}N^{\frac{3}{2}}}{3}\frac{\sqrt{(\Delta_1 - n_1\beta)(\Delta_2 - n_2\beta)(\Delta_3 - n_3\beta)(\Delta_4 - n_4\beta)}}{2\beta} + o(N^{\frac{3}{2}})$$
$$+ \mathcal{O}(\beta)\,,$$
(6.4.22)

where

$$\Delta_1 \equiv -\hat{\xi} + \frac{T}{2} + \pi i + \beta\,,\ \Delta_2 \equiv \hat{\xi} + \frac{T}{2} + \pi i + \beta\,,\ \Delta_3 \equiv f - \frac{T}{2}\,,\ \Delta_4 \equiv -f - \frac{T}{2}\,,$$

$$n_1 \equiv n_\xi + n_T\,,\ n_2 \equiv -n_\xi + n_T\,,\ n_3 \equiv n_f - n_T\,,\ n_4 \equiv -n_f - n_T\,,$$
(6.4.23)

which satisfy

$$\sum_{I=1}^{4}\Delta_I - 2\beta = 2\pi i\,,\quad \sum_{I=1}^{4}n_I = 0\,,\quad 0 < \text{Im}(\Delta_I) < 2\pi\,,\quad \text{Im}(\beta) < 0\,.\ (6.4.24)$$

Here, Δ_I's are the four Cartan chemical potentials for $SO(8)$ R-symmetry of the $\mathcal{N} = 8$ SCFT in IR, and n_I's denote the magnetic fluxes for the Cartan subgroup. Then, the first constraint of (6.4.24) can be considered as the index-like condition implied on a partition function defined without $(-1)^F$ [75, 79]. Also, the second constraint reveals that we do not turn on magnetic flux on S^2 for the R-symmetry; i.e., there is no topological twist.

The above large N Cardy free energy (6.4.22) statistically accounts for the

microstates of dyonic rotating BPS black holes in $\text{AdS}_4 \times S^7$ [97, 201]. In particular, turning off all the magnetic fluxes for the flavor symmetries, we get

$$\log I_{S^2}(\Delta_I; \beta) = -i \frac{4\sqrt{2} N^{\frac{3}{2}}}{3} \frac{\sqrt{\Delta_1 \Delta_2 \Delta_3 \Delta_4}}{2\beta} + o(N^{\frac{3}{2}}) + \mathcal{O}(\beta) \ . \qquad (6.4.25)$$

This large N Cardy free energy of the superconformal index accounts for the microstates of electrically charged rotating BPS black holes in $\text{AdS}_4 \times S^7$ [74]. Namely, performing the Legendre transformation of the above free energies with respect to Δ_I's and 2β under the constraints (6.4.24), one obtains the Bekenstein-Hawking entropy of the corresponding BPS black holes in $\text{AdS}_4 \times S^7$. Further note that although we derive these large N free energies in the Cardy limit $\beta \to 0$, they in fact perfectly capture the entropy of the BPS black holes even at finite β.

6.4.3 Refined topologically twisted index

In this subsection, we construct the large N Cardy limit of the refined topologically twisted index from (6.4.18). This index should statistically account for the microstates of the magnetically charged or dyonic, static [223–225] or rotating [226] BPS black holes with the non-vanishing magnetic flux for the gauged R-symmetry in $\text{mAdS}_4 \times S^7$ [160], which is a particular asymptotically locally AdS spacetime [195]. For these black holes, one can freely turn off the electric charges, angular momentum, and magnetic charges for the (non-R) flavor symmetries. The magnetic charge for the R-symmetry should be properly tuned to preserve SUSY by a topological twist.

Recall that, in the Cardy limit, the refined topologically twisted index is

given in terms of the Cardy block (6.2.75) as follows:

$$F_{S^2}^{\text{twisted}}(\mathfrak{t}, n; \beta) = N \log \beta - \log \mathcal{C}(e^{-\hat{\xi}+\beta n_\xi}, e^{f+\beta n_f}, e^{\frac{T}{2}+\beta n_T}; \beta)$$

$$- \log \mathcal{C}(e^{-\hat{\xi}-\beta n_\xi}, e^{f-\beta n_f}, e^{\frac{T}{2}-\beta n_T}; -\beta) - \log \left[N! \pi^N\right] + \mathcal{O}(\beta) \,.$$

$$(6.4.26)$$

Applying (6.4.18) to the above factorization formula, we obtain

$$\log I_{S^2}^{\text{twisted}}(\Delta_I, n_I; \beta) = -i \frac{2\sqrt{2}N^{\frac{3}{2}}}{3} \frac{\sqrt{(\Delta_1 + n_1\beta)(\Delta_2 + n_2\beta)(\Delta_3 + n_3\beta)(\Delta_4 + n_4\beta)}}{2\beta}$$

$$+ i \frac{2\sqrt{2}N^{\frac{3}{2}}}{3} \frac{\sqrt{(\Delta_1 - n_1\beta)(\Delta_2 - n_2\beta)(\Delta_3 - n_3\beta)(\Delta_4 - n_4\beta)}}{2\beta}$$

$$+ o(N^{\frac{3}{2}}) + \mathcal{O}(\beta) \,,$$

$$(6.4.27)$$

where

$$\Delta_1 \equiv -\hat{\xi} + \frac{T}{2} + \pi i \,, \ \Delta_2 \equiv \hat{\xi} + \frac{T}{2} + \pi i \,, \ \Delta_3 \equiv f - \frac{T}{2} \,, \ \Delta_4 \equiv -f - \frac{T}{2} \,,$$

$$n_1 \equiv 1 + n_\xi + n_T \,, \ n_2 \equiv 1 - n_\xi + n_T \,, \ n_3 \equiv n_f - n_T \,, \ n_4 \equiv -n_f - n_T \,,$$

$$(6.4.28)$$

which satisfy

$$\sum_{I=1}^{4} \Delta_I = 2\pi i \,, \quad \sum_{I=1}^{4} n_I = 2 \,, \quad 0 < \text{Im}(\Delta_I) < 2\pi \,, \quad \text{Im}(\beta) < 0 \,. \quad (6.4.29)$$

Here, Δ_I's are again the four Cartan chemical potentials for $SO(8)$ R-symmetry of the $\mathcal{N} = 8$ SCFT in IR, and n_I's denote the magnetic fluxes for each Cartan subgroup. The first constraint of (6.4.29) comes from the index-like condition for the partition function without $(-1)^F$ while the second constraint implies the topological twist by the magnetic flux for the R-symmetry on S^2.

The above large N Cardy free energy (6.4.27) statistically accounts for the microstates of magnetically charged or dyonic rotating BPS black holes in mAdS$_4 \times S^7$ [201, 226]. As before, this large N free energy gives the correct

entropy of the BPS black holes at arbitrary β. Also, expanding the free energy in β, one can find that it is regular at $\beta = 0$. Then, setting $\beta = 0$, we get

$$\log I_{S^2}^{\text{twisted}}(\Delta_I, n_I) = -i\frac{\sqrt{2}N^{\frac{3}{2}}}{3}\sqrt{\Delta_1\Delta_2\Delta_3\Delta_4}\sum_{I=1}^{4}\frac{n_I}{\Delta_I} + o(N^{\frac{3}{2}}) \,, \quad (6.4.30)$$

whose Legendre transformation in Δ_I's yields the entropy of the magnetically charge or dyonic static BPS black holes in $\text{mAdS}_4 \times S^7$ [160].

6.4.4 Squashed sphere partition function

In this subsection, we construct the large N Cardy limit of the squashed sphere partition function from (6.4.18). This partition function should be related to the round sphere partition function by (6.3.18) [194]. Then, the free energy of the round sphere partition function [66] is supposed to be identified with the regularized Euclidean on-shell action on $\text{AdS}_4 \times S^7$ [65, 227].

Recall that, in the Cardy limit, the squashed sphere partition function is given in terms of the Cardy block (6.2.96) as follows:

$$F_{S_b^3}(-\pi i bQ\delta; \pi i b^2) = \frac{N}{2}\log\left[-b^2\right] - \log\mathcal{C}(e^{-\pi i bQ\delta_\xi}, e^{-\pi i bQ\delta_f}, e^{-\pi i bQ\delta_T}; \pi i b^2) + \mathcal{O}(b^2)$$

$$(6.4.31)$$

where $Q = b + \frac{1}{b}$; δ_μ's are the R-charge deformations by $U(1)_\mu$ flavor charges; and we turned off all the mass parameters on S_b^3 for simplicity. Applying (6.4.18) to the above formula, we obtain

$$\log Z_{S_b^3}(\Delta_I; \pi i b^2) = -\frac{1}{4}\left(b + \frac{1}{b}\right)^2\frac{4\sqrt{2}\pi N^{\frac{3}{2}}}{3}\sqrt{\Delta_1\Delta_2\Delta_3\Delta_4} + o(N^{\frac{3}{2}}) + \mathcal{O}(b^2) \,,$$

$$(6.4.32)$$

where

$$\Delta_1 \equiv 1 - \delta_\xi - \delta_T \,, \ \Delta_2 \equiv 1 + \delta_\xi - \delta_T \,, \ \Delta_3 \equiv -\delta_f + \delta_T \,, \ \Delta_4 \equiv \delta_f + \delta_T \,, \ (6.4.33)$$

which satisfy

$$\sum_{I=1}^{4} \Delta_I = 2 \ . \tag{6.4.34}$$

Here, Δ_I's parametrize trial R-charges of the theory, which are constrained as above due to the condition that the superpotential should have R-charge 2. As before, this large N free energy (6.4.32) is indeed exact at arbitrary b.

Using the relation between the squashed and round sphere partition function (6.3.18), we get the following large N limit of the round sphere partition function with arbitrary R-charges:

$$\log Z_{S^3}(\Delta_I) = 4 \left(b + \frac{1}{b}\right)^{-2} \log Z_{S_b^3}(\Delta_I; \pi i b^2) = -\frac{4\sqrt{2}\pi N^{\frac{3}{2}}}{3}\sqrt{\Delta_1 \Delta_2 \Delta_3 \Delta_4} + o(N^{\frac{3}{2}}) \ , \tag{6.4.35}$$

which exactly agrees with the known field theory result [228] and the confirmation on the gravity side [229]. In particular, setting $\delta_T = \frac{1}{2}$ and $\delta_\xi = \delta_f = 0$, one can restore the superconformal R-charge. In that case, we find $\Delta_1 = \Delta_2 = \Delta_3 = \Delta_4 = \frac{1}{2}$, which indeed maximize $F = -\log Z_{S^3}(\Delta_I)$ [202]. Then, the large N limit of the round sphere partition function at the superconformal R-charge is given by

$$\log Z_{S^3} = -\frac{\sqrt{2}\pi N^{\frac{3}{2}}}{3} + o(N^{\frac{3}{2}}) \ , \tag{6.4.36}$$

which precisely matches the regularized Euclidean on-shell action on $AdS_4 \times S^7$ [66]. In addition, one can easily check that our second index theorem (6.3.20) indeed holds for the results obtained in this section.

6.5   Other examples

In this section, we study the Cardy limit of the superconformal index of various $\mathcal{N} \geq 2$ SCFTs applying (6.3.1) or (6.3.20). For the definiteness, we shall only

consider the SCFTs which can be obtained from M-theory or string theory.

Before moving on to explicit examples, we first make a comment on the Hessian determinant of the hemisphere index in the large N limit. While computing the Hessian determinant in section 6.4, the crucial point was that the eigenvalues spread as $s_a \sim e^{N^{1/2} x_a}$. This eigenvalue spreading is a common feature of 3d SCFTs while the precise factor N^α depends on a specific model. For SCFTs with M-theory dual, $\alpha = \frac{1}{2}$; for SCFTs with massive IIA dual, $\alpha = \frac{1}{3}$. As one can see in section 6.4, the precise factor is not important in the computation. Thus, we expect that the log of the Hessian determinant is $\mathcal{O}(N)$ in general. Namely, for generic $\mathcal{N} = 2$ SCFTs, we expect that

$$G^{(1)} = \mathcal{O}(N) + \mathcal{O}(\beta) . \tag{6.5.1}$$

It is well known that $G^{(0)} = \mathcal{O}(N^{\frac{3}{2}})$ for the M-theory dual while $G^{(0)} = \mathcal{O}(N^{\frac{5}{3}})$ for massive IIA dual. Therefore, we expect that $G^{(1)}$ is negligible in the large N limit.

There are lots of examples whose round sphere partition functions [65, 66, 228, 230] or topologically twisted indices on $S^2 \times S^1$ [214–216, 231] are known in the large N limit. Using (6.3.20), one can easily read off the large N Cardy limit of the superconformal index from the round sphere partition function. Also, in the literature, the topologically twisted index was computed via its index theorem (6.3.17), which was expressed in terms of the Bethe potential $\overline{\mathcal{V}}$. In our notation, the Bethe potential is translated as

$$\overline{\mathcal{V}}(\Delta) = \frac{2}{i} G^{(0)}(e^{-i\Delta}) . \tag{6.5.2}$$

Since $G^{(1)}$ can be ignored in the large N limit, reading off $\overline{\mathcal{V}}$ from the topologically twisted index suffices to compute the superconformal index in the large N Cardy limit by (6.3.1). We will illustrate such examples whose large N Cardy

limit of the superconformal indices can be obtained either from the round sphere partition functions or the topologically twisted indices.

Furthermore, we will also provide finite N Cardy results of the superconformal indices for a few examples, with rank less than 3 for simplicity, which are severed as nontrivial tests of known dualities of those examples.

6.5.1 M2-Branes probing a CY 4-fold singularity

In this subsection, we consider quiver gauge theories, which describe the low energy dynamics of M2-branes probing a conical Calabi-Yau 4-fold singularity. For this class of theories, the sum of the CS levels for each gauge group vanishes, i.e. $\sum_g k_g = 0$. Also, those theories are parity invariant so that the round sphere free energy F_{S^3} is real. Then, from (6.3.20), the generalized superconformal index can be expressed as

$$F_{S^2}(\Delta, n; \beta) = \frac{F_{S^2}(\Delta + n\beta, 0; \beta) + F_{S^2}(\Delta - n\beta, 0; \beta)}{2} \ . \qquad (6.5.3)$$

Keeping the above formula in mind, we shall turn off all the magnetic fluxes for the flavor symmetries. The generalization can be easily done by the above formula. There are two relevant regimes for these theories: M-theory regime, and type IIA string theory regime.

M-theory regime

One can take the large N limit with fixed CS levels $k \sim \mathcal{O}(1)$. Then, the field theory is supposed to be dual to the M-theory or 11d SUGRA on $\mathrm{AdS}_4 \times \mathrm{SE}_7$ where SE_7 is the Sasaki-Einstein 7-manifold serving as the base of a conical CY 4-fold. The characteristic large N behavior of the free energy in this M-theory

regime is

$$F \sim k^{\frac{1}{2}} N^{\frac{3}{2}} \ . \tag{6.5.4}$$

First, the round sphere free energy at the superconformal R-charge is given by [66]

$$F_{S^3} = N^{\frac{3}{2}} \sqrt{\frac{2\pi^6}{27\mathrm{Vol}(\mathrm{SE}_7)}} \ . \tag{6.5.5}$$

Applying (6.3.23), the (unrefined) superconformal index in the large N Cardy limit, for the generic $\mathcal{N} \geq 2$ SCFTs describing the low energy dynamics of M2-branes, is given by

$$F_{S^2} = \frac{\Delta_R^2}{2\pi i \beta} N^{\frac{3}{2}} \sqrt{\frac{2\pi^6}{27\mathrm{Vol}(\mathrm{SE}_7)}} \ , \tag{6.5.6}$$

which precisely matches the result from the dual supergravity analysis on universal spinning black holes in AdS$_4$ [203], even in the non-Cardy regime.

Example 1: ABJM theory

The most common example in this class is the ABJM$_k$ theory, which describes the low energy dynamics of N M2-branes probing $\mathbb{C}_4/\mathbb{Z}_k$ singularity [44]. Its holographic dual is given by 11d SUGRA on AdS$_4 \times S^7/\mathbb{Z}_k$. The round sphere free energy with generic R-charge assignment is given by [228]

$$F_{S^3} = \frac{4\sqrt{2}\pi k^{\frac{1}{2}} N^{\frac{3}{2}}}{3} \sqrt{\Delta_1 \Delta_2 \Delta_3 \Delta_4} \ . \tag{6.5.7}$$

The large N Cardy free energy of the superconformal index is given by [79]

$$F_{S^2} = i\frac{4\sqrt{2}k^{\frac{1}{2}} N^{\frac{3}{2}}}{3} \frac{\sqrt{\Delta_1 \Delta_2 \Delta_3 \Delta_4}}{2\beta} \ . \tag{6.5.8}$$

Indeed, they satisfy our large N Cardy formula (6.3.20):

$$F_{S^2}(\Delta; \beta) = \frac{(\pi i + \beta)^2}{2\pi i \beta} F_{S^3}\left(-\frac{\Delta}{\pi i + \beta}\right) \ . \tag{6.5.9}$$

Note that the above large N Cardy free energy of the superconformal index, in fact, precisely captures the entropy of dual BPS black holes in $\mathrm{AdS}_4 \times S^7/\mathbb{Z}_k$ [74, 82, 97], even in the non-Cardy regime.

$SL(2, \mathbb{Z})$ **duality** When $k = 1$, the ABJM theory is supposed to be dual to $\mathcal{N} = 4$ $U(N)$ SYM with one fundamental and one adjoint hypermultiplets in section 6.4 by the $SL(2, \mathbb{Z})$ duality [44]. Indeed, in the large N Cardy limit, two free energies (6.4.25), (6.5.8) coincide. One can also test this duality in the finite N Cardy limit using (6.3.1). When $N = 1$, the Cardy free energy of the ABJM_1 theory is given by

$$F_{S^2} \sim \frac{8iG}{2\beta} \approx \frac{7.33i}{2\beta} \ , \tag{6.5.10}$$

at $\Delta_1 = \Delta_2 = \Delta_3 = \Delta_4 = \frac{\pi i}{2}$. G is Catalan's constant, which is defined by

$$G = \frac{\mathrm{Li}_2(i) - \mathrm{Li}_2(-i)}{2i} \approx 0.915966 \,. \tag{6.5.11}$$

It turns out that (6.5.10) is identical to the Cardy free energy of the dual theory when $N = 1$ [79]. One would test this duality at $N > 1$ by numerical analysis.

Now we discuss a few more examples belonging to this class. The topologically twisted indices of those examples are examined in [214]. We examine their superconformal indices in the Cardy limit, mainly with large N but also with finite N for a few theories with rank less than 3.

Example 2: $\mathcal{N} = 4$ $U(N)$ SYM with N_f fundamental and one adjoint hypermultiplets

This theory is a natural generalization of the theory we have considered in section 6.4. This theory describes N M2-branes probing $\mathbb{C}^2 \times \mathbb{C}^2/\mathbb{Z}_{N_f}$ singularity.

Referring to the topologically twisted index in [214], we obtain the following large N Cardy free energy of the superconformal index from (6.3.1):

$$F_{S^2} = i \frac{4\sqrt{2} N_f^{\frac{1}{2}} N^{\frac{3}{2}}}{3} \frac{\sqrt{\Delta_1 \Delta_2 \Delta_3 \Delta_4}}{2\beta} \ . \qquad (6.5.12)$$

Also, at $N_f = 2$, we give the Cardy free energy at finite N. When $N = 1$,

$$\begin{aligned} F_{S^2} &\sim \frac{i}{2\beta} \left[4G + 8\mathrm{Im} \left\{ \mathrm{Li}_2((-1+\sqrt{2})i) \right\} - \pi \log(-1+\sqrt{2}) \right] \\ &\approx \frac{9.68691i}{2\beta} \ , \end{aligned} \qquad (6.5.13)$$

and when $N = 2$,

$$F_{S^2} \approx \frac{22.6365i}{2\beta} \ , \qquad (6.5.14)$$

at $\Delta_1 = \Delta_2 = \Delta_3 = \Delta_4 = \frac{\pi i}{2}$. Note that the above free energies comes from the dominant one among several saddle points.

Example 3: $\mathcal{N} = 4$ $U(N)^g$ necklace quiver SYM with N_f fundamental hypermultiplets for the g-th gauge group

This theory contains $g > 1$ bifundamental hypermultiplets, each of which connects adjacent gauge nodes, as well as N_f fundamental hypermultiplets attached to the last gauge node. The theory lives on N M2-branes probing $\mathbb{C}^2/\mathbb{Z}_g \times \mathbb{C}^2/\mathbb{Z}_{N_f}$ singularity. The large N Cardy free energy of the superconformal index is given by

$$F_{S^2} = i \frac{4\sqrt{2}(gN_f)^{\frac{1}{2}} N^{\frac{3}{2}}}{3} \frac{\sqrt{\Delta_1 \Delta_2 \Delta_3 \Delta_4}}{2\beta} \ . \qquad (6.5.15)$$

Mirror symmetry This theory at $g = 2, N_f = 1$ is dual to the former theory at $N_f = 2$ by the mirror symmetry [232]. Indeed, the Cardy free energies of two theories, (6.5.12) and (6.5.15), agree at large N limit. Also, when $g =$

$2, N_f = 1$ and $N = 1$,

$$
\begin{aligned}
F_{S^2} &\sim \frac{i}{2\beta} \left[4G + 4\text{Im} \left\{ \text{Li}_2(e^{\frac{\pi i}{4}}) + \text{Li}_2(e^{\frac{3\pi i}{4}}) \right\} \right] \\
&\approx \frac{9.68691i}{2\beta} \ ,
\end{aligned}
\tag{6.5.16}
$$

at $\Delta_1 = \Delta_2 = \Delta_3 = \Delta_4 = \frac{\pi i}{2}$. Hence, two Cardy free energies, (6.5.13) and (6.5.16), also agree at $N = 1$.

Example 4: $\mathcal{N} = 3$ $U(N)^g$ necklace quiver CS matter theory with CS levels $(+k, -k, 0, 0, \ldots, 0)$

This theory lives on N M2-branes probing $(\mathbb{C}^2 \times \mathbb{C}^2/\mathbb{Z}_{g-1})/\mathbb{Z}_k$ singularity. The large N Cardy free energy is given by

$$
F_{S^2} = i \frac{4\sqrt{2}[(g-1)k]^{\frac{1}{2}} N^{\frac{3}{2}}}{3} \frac{\sqrt{\Delta_1 \Delta_2 \Delta_3 \Delta_4}}{2\beta} \ .
\tag{6.5.17}
$$

This theory with g gauge nodes at $k = 1$ is dual to the third example with $g - 1$ gauge nodes at $N_f = 1$ by the $SL(2, \mathbb{Z})$ duality [233]. Indeed, the large N Cardy free energies of two theories, (6.5.15) and (6.5.17), are identical.

Example 5: $\mathcal{N} = 3$ $U(N)^{2g}$ necklace quiver CS matter theory with alternating CS levels $\pm k$

This theory describes the low energy dynamics of N M2-branes probing $(\mathbb{C}^2/\mathbb{Z}_g \times \mathbb{C}^2/\mathbb{Z}_g)/\mathbb{Z}_k$ singularity. The large N Cardy free energy is

$$
F_{S^2} = i \frac{4\sqrt{2} g k^{\frac{1}{2}} N^{\frac{3}{2}}}{3} \frac{\sqrt{\Delta_1 \Delta_2 \Delta_3 \Delta_4}}{2\beta} \ .
\tag{6.5.18}
$$

Type IIA string theory regime

One can take the large N limit with large but fixed 't Hooft couplings $\lambda = \frac{N}{k} \gg 1 \sim \mathcal{O}(N^0)$. Then, the field theory in this 't Hooft limit is dual to type

IIA string theory. The characteristic large N, λ behavior of the free energy in this type IIA string theory regime is

$$F \sim \frac{N^2}{\sqrt{\lambda}} \ . \tag{6.5.19}$$

Our example is the ABJM$_k$ theory. In the above 't Hooft limit, the ABJM$_k$ theory is dual to type IIA SUGRA on AdS$_4 \times \mathbb{CP}^3$ [44]. This can be understood as the 10d reduction of the M-theory on AdS$_4 \times S^7/\mathbb{Z}_k$ where S^7 is a $U(1)$ bundle over $\mathbb{CP}^3$. Using (6.3.1), the Cardy free energy of the superconformal index in the large N, λ limit can be read off from the topologically twisted index in [231] as follows:

$$F_{S^2} = i\frac{4\sqrt{2}N^2}{3\sqrt{\lambda}}\frac{\sqrt{\Delta_1\Delta_2\Delta_3\Delta_4}}{2\beta} \ . \tag{6.5.20}$$

The above large N Cardy free energy perfectly captures the entropy of dual BPS black holes in AdS$_4 \times \mathbb{CP}^3$ [74, 231].

6.5.2 D2-Branes probing a CY 3-fold singularity in massive IIA string theory

In this subsection, we consider Chern-Simons matter gauge theories describing the low energy dynamics of D2-branes probing a conical CY 3-fold singularity in the presence of a non-vanishing quantized Romans mass, i.e. in massive IIA string theory [230, 234]. For this class of theories, sum of the CS levels for each gauge group does not vanish, i.e. $\sum_g k_g \neq 0$. Hence, those theories are not parity invariant so that the round sphere free energy F_{S^3} is complex.

We shall consider the large N limit with fixed CS levels $k \sim \mathcal{O}(1)$. The holographic dual is given by massive IIA SUGRA on AdS$_4 \times M_6$ where $M_6 = \mathcal{S}Y_5$ is the suspension of a Sasaki-Einstein 5-manifold Y_5, which serves as the

base of a conical CY 3-fold. The characteristic large N behavior of the free energy of this class is given by [234]

$$F \sim n^{\frac{1}{3}} N^{\frac{5}{3}} , \qquad (6.5.21)$$

where $n = \sum_g k_g$, sum of the CS levels for each gauge node. The round sphere free energy at the superconformal R-charge is given by [230]

$$\mathrm{Re}[F_{S^3}] = \frac{2^{1/3}3^{1/6}\pi^3}{5\mathrm{Vol}(Y_5)^{2/3}} n^{\frac{1}{3}} N^{\frac{5}{3}} = \frac{2^{5/3}3^{1/6}\pi}{5}(nN)^{\frac{1}{3}}(a_{4d})^{\frac{2}{3}} , \qquad (6.5.22)$$

where a_{4d} is the a-anomaly coefficient of the parent 4d SCFT, which lives on D3-branes probing the same CY 3-fold singularity. Applying (6.3.23), the (unrefined) superconformal index in the large N Cardy limit, for the generic $\mathcal{N} \geq 2$ SCFTs describing the low energy dynamics of D2-branes in massive IIA string theory, is given by

$$F_{S^2} = \frac{\Delta_R^2}{2\pi i \beta} \frac{2^{1/3}3^{1/6}\pi^3}{5\mathrm{Vol}(Y_5)^{2/3}} n^{\frac{1}{3}} N^{\frac{5}{3}} = \frac{\Delta_R^2}{2\pi i \beta} \frac{2^{5/3}3^{1/6}\pi}{5}(nN)^{\frac{1}{3}}(a_{4d})^{\frac{2}{3}} , \qquad (6.5.23)$$

as expected from the dual gravity side in the non-Cardy regime [203].

For a generic $\mathcal{N} = 2$ $U(N)^g$ quiver theory with equal CS level k and bifundamental and adjoint matters, the large N Cardy free energy of the generalized superconformal index can be read off from the round sphere partition function [230] using (6.3.20) as follows:

$$F_{S^2} =$$

$$\frac{2^{1/3}3^{3/2}}{80i\beta}\left(1 - \frac{i}{\sqrt{3}}\right)\left[\sum_{I \in \mathrm{matters}}(\Delta_I + n_I\beta)(\Delta_I + n_I\beta + \pi i + \beta)(\Delta_I + n_I\beta + 2\pi i + 2\beta)\right]^{\frac{2}{3}} n^{\frac{1}{3}} N^{\frac{5}{3}}$$

$$+ \frac{2^{1/3}3^{3/2}}{80i\beta}\left(1 + \frac{i}{\sqrt{3}}\right)\left[\sum_{I \in \mathrm{matters}}(\Delta_I - n_I\beta)(\Delta_I - n_I\beta + \pi i + \beta)(\Delta_I - n_I\beta + 2\pi i + 2\beta)\right]^{\frac{2}{3}} n^{\frac{1}{3}} N^{\frac{5}{3}} .$$

$$(6.5.24)$$

One particular example is an $\mathcal{N} = 2$ CS deformation of the maximal SYM. This SCFT is dual to massive IIA SUGRA on $\mathrm{AdS}_4 \times S^6$. The large N Cardy free energy of the generalized superconformal index can be read off from the topologically twisted index [215, 216] using (6.3.1) as

$$F_{S^2} = \frac{2^{1/3} 3^{13/6}}{80 i \beta} k^{\frac{1}{3}} N^{\frac{5}{3}} \left[\left(1 - \frac{i}{\sqrt{3}} \right) [(\Delta_1 + n_1 \beta)(\Delta_2 + n_2 \beta)(\Delta_3 + n_3 \beta)]^{\frac{2}{3}} \right.$$
$$\left. + \left(1 + \frac{i}{\sqrt{3}} \right) [(\Delta_1 - n_1 \beta)(\Delta_2 - n_2 \beta)(\Delta_3 - n_3 \beta)]^{\frac{2}{3}} \right],$$
$$(6.5.25)$$

which is consistent with the above general formula. This large N Cardy free energy is supposed to account for the microstates of the dyonic rotating BPS black holes with vanishing magnetic charge for the R-symmetry in the massive IIA SUGRA background $\mathrm{AdS}_4 \times S^6$.

6.6 Concluding remarks

In this chapter, we have examined the Cardy limit of 3d supersymmetric partition functions using their factorization into the Cardy block, which is defined as the dominant saddle point contribution to the hemisphere index in the Cardy limit. The Cardy block plays the role of a building block of other 3d partition functions such as the generalized superconformal index, the refined topologically twisted index and the squashed sphere partition function. The factorization to the Cardy block allows us to find universal relations among those partition functions in the Cardy limit.

Furthermore, our analysis can be applied to holographic SCFTs in 3d, which are dual to AdS_4 gravity in the large N limit. In the large N limit, such universal relations extend to include the round sphere partition function, which is known to count the degrees of freedom of a SCFT in odd dimensions and is

also dual to the holographic entanglement entropy in dual AdS$_4$ for a spherical entangling surface. In addition, the two supersymmetric indices we have examined correspond to the entropy functions of BPS black holes in AdS$_4$; the generalized superconformal index, in the presence of the magnetic flux for the flavor symmetry, captures the microstates of rotating dyonic BPS black holes in AdS$_4$ while the refined topologically twisted index captures the microstates of rotating dyonic BPS black holes in mAdS$_4$, an asymptotically locally AdS$_4$ spacetime. Therefore, our analysis provides a field theoretic derivation of universal relations among the black hole entropies and the holographic entanglement entropy in AdS$_4$. We have also provided explicit examples, which confirm the universal relations we have found.

We would like to remark a few interesting points and future directions.

- **Black hole microstate counting in the non-Cardy regime**

  In section 6.4, we have seen that our Cardy formulae for the M2-brane theory, which are derived in the $\beta \to 0$ limit, exactly account for the microstates of various BPS black holes in AdS$_4 \times S^7$ even at finite β. Those BPS black holes are supposed to be realized as the local large N saddle points on the dual field theory side. Indeed, there are a lot of examples showing that the Cardy formula is exact at finite β: from the pioneering work of Strominger and Vafa counting the microstates of the D1-D5-P black holes [11] to recent works counting the microstates of the electrically charged rotating BPS black holes in AdS$_5$ [75, 138], AdS$_7$ [75,159], AdS$_6$ [78], AdS$_4$ [79]. Remarkably, the resulting Cardy free energy of the index at large N perfectly captures the Bekenstein-Hawking entropy of the dual BPS black holes even in the non-Cardy regime.

Accordingly, we expect that our Cardy formulae such as (6.3.20) are exact in the non-Cardy regime as long as we consider the large N saddle point corresponding to the dual BPS black holes in AdS$_4$. For example, let us consider the superconformal index without magnetic flux for the flavor symmetry. The form of the entropy function of generic rotating electric BPS black holes in AdS$_4$ can be found in [97], which is the same as our Cardy free energy once we identify Im $\left[G^{(0)}\right]$ with the supergravity prepotential $\mathcal{F}$ up to some multiplicative constant factors. We expect that $G^{(1)}$ and all $\mathcal{O}(\beta)$ corrections are subdominant in N at the large N saddle point capturing the dual black hole microstates. Also the unrefined superconformal index leads to the Cardy formula (6.3.23), which is proven exact by the supergravity analysis for the universal spinning black holes in AdS$_4$ [203]. It is worth studying such exactness of our Cardy formulae further, both on the field theory side and on the gravity side.

- **Cardy limit for finite N**

  In section 6.5, we have examined the superconformal indices in the Cardy limit of some examples for finite N. In [79], which we discussed in chapter 5, the finite N Cardy limit of the superconformal index was examined for $\mathcal{N} = 4$ SYM with one fundamental and one adjoint matters both analytically and numerically. In particular, for $N = 2$, we obtained the exact coefficient of the free energy:

$$
\begin{aligned}
\log I_{S^2} \\
&\sim \frac{i}{2\beta}\left[-8G - 2\,\mathrm{Im}\left\{2\mathrm{Li}_2(ix) + 2\mathrm{Li}_2\left(\frac{i}{x}\right) + 2\mathrm{Li}_2(ix^2) + 2\mathrm{Li}_2\left(\frac{i}{x^2}\right) + \mathrm{Li}_2\left(\frac{1}{x}\right)\right\}\right] \\
&\approx \frac{-17.4771i}{2\beta} \tag{6.6.1}
\end{aligned}
$$

with

$$G = \frac{\text{Li}_2(i) - \text{Li}_2(-i)}{2i} \approx 0.915966\,,$$
$$x = \frac{1}{2}(1 - 3^{\frac{1}{4}}\sqrt{2} + \sqrt{3}) \approx 0.435421\,, \tag{6.6.2}$$

which is the finite N version of the $N^{\frac{3}{2}}$ scaling of the M2-brane degrees of freedom. Our analysis provides similar results for more examples, and it would be interesting to find the physical interpretation of those numbers. Also our Cardy free energy is a simple but nontrivial observable of a theory. For example, its matching can be regarded as a nontrivial test of a duality for 3d SCFTs. We have illustrated such examples in section 6.5, where the Cardy free energy shows perfect matches under 3d mirror symmetry or $SL(2, \mathbb{Z})$ duality. While our analysis is restricted for theories of rank less than 3, it would be worth studying higher rank theories.

- **Twisted compactification of 5d, 6d SCFTs**

While our analysis relies on the localization computation of supersymmetric partition functions, and thus on the Lagrangian description of a theory, recently similar results are obtained for class $\mathcal{R}$ theories, which are generically non-Lagrangian theories, realized as twisted compactification of 6d (2,0) A_{N-1} theory on hyperbolic 3-manifolds [185,235,236]. The superconformal indices of those theories can be computed as topological invariants of $SL(N, \mathbb{C})$ Chern-Simons theories by the 3d-3d correspondence and are shown to capture N^3 degrees of freedom of N M5-branes [203, 204]. Remarkably, they satisfy the same relation (6.3.23):

$$F_{S^2}(\Delta = -\Delta_R \delta_*, n = 0; \beta) = \frac{\Delta_R^2}{2\pi i \beta}\text{Re}\left[F_{S^3}(\delta_*)\right], \tag{6.6.3}$$

which we derive for 3d SCFTs with Lagrangian descriptions. Also the same relation is expected by the supergravity analysis [203] for 3d the-

ories obtained as the twisted compactification of 5d SCFTs [237]. From those results, we may expect that our Cardy analysis for Lagrangian theories would hold for a broader class of 3d SCFTs, which will be interesting to clarify.

Chapter 7

Background field analysis for large AdS$_{5,7}$ black holes

In this chapter, we use a background field method on S^3 and S^5 to analyze the asymptotic free energy of the indices on $S^3 \times S^1$ and $S^5 \times S^1$ in the Cardy limit. This method can be useful for non-Lagrangian QFTs. In 4d case, we revisit the $\mathcal{N} = 4$ SYM discussed in chapter 3. In 6d case, we analyze the $\mathcal{N} = (2,0)$ SCFT. We will show that the Chern-Simons terms of the background fields yield the asymptotic free energy. The relevant Chern-Simons terms are determined by the 't Hooft anomalies. The resulting Cardy free energies exactly agree with the entropy functions of the BPS black holes in AdS$_5 \times S^5$ and AdS$_7 \times S^4$ respectively, thus statistically accounting for their microstates.

7.1 Large supersymmetric AdS$_5$ black holes

In this chapter, we consider an alternative approach to compute the asymptotic free energy of the index in the Cardy limit. As an exercise, in this section, we

revisit the index of 4d $\mathcal{N} = 4$ SYM on $S^3 \times S^1$, discussed in chapter 3. The chemical potentials β, ω_i are reflected in the background metric of $S^3 \times S^1$ as

$$ds^2 = r^2 \left[d\theta^2 + \sum_{i=1}^{2} n_i^2 \left(d\phi_i - \frac{i\omega_i}{\beta} d\tau \right)^2 \right] + d\tau^2 \ , \qquad (7.1.1)$$

where $(n_1, n_2) = (\cos\theta, \sin\theta)$, $0 \leq \theta \leq \frac{\pi}{2}$. The Euclidean time τ has period $\tau \sim \tau + \beta$, and we restored the radius r of S^3. Δ_I are encoded in the background $U(1)^3 \subset SO(6)$ gauge fields

$$A^I = -\frac{i\Delta_I}{\beta} d\tau \ . \qquad (7.1.2)$$

The partition function is given by a path integral over the $\mathcal{N} = 4$ Yang-Mills fields at coupling constant g_{YM}, coupled to these background fields in a canonical manner. Again having in mind imposing

$$\sum_{I=1}^{3} \Delta_I - \sum_{i=1}^{2} \omega_i = 2\pi i \qquad (7.1.3)$$

to get the index, we take $\beta \to 0^+$. Very naively, one might think that a Kaluza-Klein reduction to S^3 would be possible, integrating out heavy KK fields, because the circle size β is small. If one can integrate out the heavy fields, they will contribute to an effective action of the background fields, arranged in the derivative expansion which is a series in small β. This will turn out to be a much subtler issue, because β^{-1} appears in other background fields. Indeed, naively doing the KK reduction, one would see shortly that the 3d metric, dilaton and $U(1)^3$ fields all see inverse powers of β. Still, when $\omega_{1,2} \ll 1$, we will show that the KK fields can be integrated out, whose effect will be arranged in a derivative expansion. The expansion will be a series in small $\beta, \omega_{1,2}$, whose leading terms will be given by Chern-Simons terms. The effect of 3d zero modes is also expected to be subleading in our model. The analysis is similar to [73], except that our setting is subtler with new aspects.

Having these in mind, we arrange the 4d background fields as 3d background fields. To this end, we rewrite (7.1.1) in terms of 3d metric, gravi-photon a, and the dilaton Φ as

$$ds_4^2 = r^2 \left[d\theta^2 + \sum_i n_i^2 d\phi_i^2 + \frac{r^2(\sum_i \omega_i n_i^2 d\phi_i)^2}{\beta^2(1 - r^2 \sum_i \frac{n_i^2 \omega_i^2}{\beta^2})} \right] + e^{-2\Phi} (d\tau + a)^2 \equiv ds_3^2 + e^{-2\Phi}(d\tau + a)^2$$

$$e^{-2\Phi} = 1 - r^2 \sum_i \frac{n_i^2 \omega_i^2}{\beta^2} \quad , \quad a = -i \frac{r^2 \sum_i \omega_i n_i^2 d\phi_i}{\beta(1 - r^2 \sum_i \frac{n_i^2 \omega_i^2}{\beta^2})} \quad . \tag{7.1.4}$$

The 4d $U(1)^3$ background fields A^I are arranged to 3d gauge field $\mathcal{A}^I$ and the scalar A_4^I as $A^I = A_4^I(d\tau + a) + \mathcal{A}^I$, where

$$A_4^I = -\frac{i\Delta^I}{\beta} \equiv \frac{\alpha^I}{\beta} \quad , \quad \mathcal{A}^I = -A_4^I a \ . \tag{7.1.5}$$

We take β to be the smallest variable, eventually intending to take the limit $\beta \to 0^+$. $\omega_i \ll 1$ are also small, but still satisfying $\frac{\beta}{r\omega_i} \ll 1$. One might worry that some background fields may behave badly due to the factor $1 - r^2 \sum_i \frac{n_i^2 \omega_i^2}{\beta^2}$ in denominators. We temporarily circumvent this issue by taking ω_i to be complex and generic, evading the poles. Physically, this has to do with the fact that non-BPS derivatives' effect is present before imposing (7.1.3).

We first consider the limiting behaviors of the 3d background fields for $\frac{\beta}{r} \ll |\omega_i| \ll 1$:

$$ds_3^2 \sim r^2 \left[ds^2(S_{\text{round}}^3) - \frac{(\sum_i \omega_i n_i^2 d\phi_i)^2}{\sum_i n_i^2 \omega_i^2} + \cdots \right]$$

$$\beta^2 e^{-2\Phi} \sim -r^2 \sum_i n_i^2 \omega_i^2 + \cdots \quad , \quad \frac{a}{\beta} \sim \frac{i(\sum_i \omega_i n_i^2 d\phi_i)}{2 \sum_i n_i^2 \omega_i^2} + \cdots \ . \tag{7.1.6}$$

The omitted terms $\cdots$ are suppressed by positive powers of $\frac{\beta}{r\omega_i} \ll 1$. Note that in the 3d metric, one has a canonical round sphere metric, accompanied by the second term which is an $\mathcal{O}(1)$ negative length element along one direction. For instance, if $\omega_1 = \omega_2 \equiv \omega$, this direction is the Hopf fiber of S^3. Along

this direction, leading $\mathcal{O}(1)$ length elements cancel and its [length]^2 becomes smaller, at a positive power in $\frac{\beta}{\omega}$. This is one reason why a naive KK reduction becomes subtle in our case. The dilaton field $\beta^2 e^{-2\Phi}$ for the [circumference]^2 of temporal circle is suppressed to be small $|\omega_i| \ll 1$, which is an intuitive reason why we should also keep ω_i small to trust the derivative expansion. The 3d background fields are highly singular (e.g. ω, β dependence), presumably having short wavelength components on S^3, so that one might wonder if the whole spirit of using derivative expansion is relevant or not. In general, using these fields will be highly problematic in the general effective field theory. For instance, if one wishes to make variation of this effective action in background fields to generate correlation functions, this probably might be tricky. However, our strategy here is very practical, having in mind using this EFT just for our particular background. In other words, we use it just as a way of expressing the series expansion of a particular observable $\log Z$ in $\beta, \omega_1, \omega_2$. So no matter how singular the fields may look, we just care about whether the actual values of terms after spatial integrals are sequentially suppressed as an infinite series. We will show (more precisely, strongly illustrate) that this is indeed true.

In this background, we consider the path integral of 4d $\mathcal{N} = 4$ Yang-Mills theory. We formally decompose the 4d dynamical fields into 3d 'zero modes' and 'KK fields,' depending on the momentum mode on S^1. We schematically call the zero modes Φ_L and KK modes Φ_H, where L/H stand for 'light/heavy.' Φ_H couples to the background field a, while Φ_L does not. The path integral is done by integrating over Φ_H at fixed Φ_L, and then integrating over Φ_L.

We discuss the structure of the path integral over Φ_H, at fixed Φ_L. In our scaling limit of small S^1 radius, the path integral over Φ_H gives an effective action that depends only on the 3d background fields, but not on Φ_L which are

243

held fixed for the moment. To see this, consider the schematic structure of the 3d action for Φ_H. It takes the form of

$$\mathcal{L} \sim \Phi_H(\partial^2 + M_{\mathrm{KK}}^2)\Phi_H + g_{3\mathrm{d}}^2 V(\Phi_L, \Phi_H) \qquad (7.1.7)$$

where V denotes a potential quartic in Φ_H, Φ_L, with order 1 coefficients. Here we consider the case in which Φ_H, Φ_L are bosonic, for simplicity. Both M_{KK} and $g_{3\mathrm{d}}^2$ have dimension of mass, proportional to the inverse-radius of the temporal circle $\sim \frac{1}{r\omega}$ (where $\omega \sim \omega_{1,2}$.) The solution to Φ_H at given Φ_L is schematically given by $\Phi_H \sim \frac{g_{3\mathrm{d}}^2}{\partial^2 + M_{\mathrm{KK}}^2}\partial_{\Phi_H} V$. The propagator factor scales like $\frac{g_{3\mathrm{d}}^2}{\partial^2 + M_{\mathrm{KK}}^2} \lesssim r\omega$, which suppresses the Φ_H tadpole and fluctuations depending on Φ_L.[1] Φ_H's path integral is effectively Gaussian, depending on background fields only. So after integrating out Φ_H, Z consists of two factors: one given by the 3d background fields, and another given by the path integral of 'zero modes' Φ_L canonically coupled to 3d background fields, obtained by classical dimensional reduction of 4d $\mathcal{N} = 4$ Yang-Mills theory. In the latter sector, the dilaton appears as the 3d coupling constant (which may depend on spatial coordinate if $\omega_1 \neq \omega_2$), while the gravi-photon $\beta^{-1}a$ does not couple to the classical 3d Yang-Mills.

We first consider the factor coming from the path integral over Φ_L. It consists of the fields of 3d maximal super-Yang-Mills, whose action is deformed to be less supersymmetric by various parameters. Here, we simply discuss how its contribution to $\log Z$ will depend on various parameters. The 3d effective coupling is given by $g_{3\mathrm{d}}^2 \sim \frac{1}{r\omega}$. The 3d metric consists of 2d base whose length scale is r, and a fiber whose length scale is $\frac{\beta}{\omega} \ll r$. As we shall see below from background effective actions (which is also obvious from BPS kinematics), the

---

[1] We expect a caveat when Φ_L has zero modes held at large value without a potential cost, making $\partial_{\Phi_H} V$ large. There are two types of such modes, again depending on the IR divergent behaviors of Z_{S^3} for Φ_L [114]. In our 4d $U(N)$ theory, or 6d $(2,0)$ theory for N M5-branes, we assume the absence of such dangerous modes. See the next two paragraphs for more discussions.

leading free energy will be of order $\sim \frac{\beta^0}{\omega^2}$ at $\frac{\beta}{r} \ll \omega \ll 1$. We can argue that the path integral of Φ_L will yield much smaller terms than this. Suppose otherwise, and the Φ_L's path integral contributes a term at this order. Then, the divergent ω^{-2} part would come either from positive power in the 3d gauge coupling $g_{3d}^2 \sim \frac{g_{YM}^2}{r\omega}$, or positive power in the Hopf fiber radius $\sim (\beta\omega^{-1})^\#$. But acquiring this factor from the Hopf fiber radius is accompanied by a positive power in β, which is subleading. So $\beta^0\omega^{-2}$ dependence would come from the divergent 3d coupling, $g_{3d}^2 \sim \omega^{-1}$.

However, it is also hard to imagine (probably inconsistent) that a 3d QFT partition function diverges as the coupling grows, as the 3d QFT seems to be perfectly well defined. The only way in which we can imagine a divergent dependence on large g_{3d} is when the observable suffers from infrared divergence, since $g_{3d} \to \infty$ is a sort of IR limit in 3d. More concretely, the partition function of 3d maximal SYM on S^3 is well known to have an IR divergence [162]. As studied in [73,114], this is due to the N gauge holonomies of $U(N)$ on S^1 being non-compact in the small circle limit. At small but finite circle radius, $\sim r\omega$, the holonomies have period given by $\sim \frac{1}{r\omega}$, thus providing an IR cutoff. This would yield a factor of $\sim \omega^{-N}$ to Z, contributing at a subleading order $\sim N \log \omega$ to the free energy. Thus, we expect the divergent leading part $\propto \beta^0\omega^{-2}$ of the net free energy to be unaffected by the 3d dynamical fields.

So it suffices to consider the effect of integrating out the 'KK fields' Φ_H, yielding an effective action of $g_{\mu\nu}$, a_μ, Φ, $\mathcal{A}_\mu^I$, A_4^I. There are infinitely many terms in this effective action, arranged in a derivative expansion, whose coefficients are mostly unknown. At generic points of the background fields, before imposing the BPS index constraint (7.1.3), all fermions of the 4d theory will go to Φ_H, due to the anti-periodic boundary conditions. At (7.1.3), some fermion modes may be

massless. Across this surface, as we shall see, these transiently massless fermions at (7.1.3) will simply change some Chern-Simons coefficients, without further effects on the effective action. Below, we will show that: (1) the derivative expansion is arranged in a series of $\beta, \omega_1, \omega_2$; (2) the leading terms are at order $\frac{\beta^0}{\omega_1 \omega_2}$, completely coming from the Chern-Simons terms; (3) the Chern-Simons coefficients can be determined either from the free 4d QFT, or by an anomaly consideration. We shall discuss these issues in the order of $(3) \to (2) \to (1)$.

We first discuss possible Chern-Simons terms of $\mathcal{A}^I$, a. (One might also think of the gravitational Chern-Simons term $\sim \omega \wedge R$. We think its coefficient is zero, but anyway it will be subleading in our scaling limit, as illustrated below.) There can be standard gauge-invariant Chern-Simons terms of the forms [73, 238]

$$\beta^{-2} \int a \wedge da \ , \ \ \beta^{-1} \int \mathcal{A}^I \wedge da \ , \ \ \int \mathcal{A}^I \wedge d\mathcal{A}^J \ , \qquad (7.1.8)$$

whose coefficients are dimensionless and quantized. There can also be gauge non-invariant Chern-Simons terms which are needed for anomaly matching [73, 238]. Since their coefficients are all quantized, either from gauge invariance or anomaly matching, one can determine them by integrating out KK fermions of the 4d QFT at weak coupling.

We follow [73] to compute these coefficients for $U(1)^3 \subset SO(6)$ times the gravi-photon $U(1)$. There are four Weyl fermions $\Psi_\alpha^{Q_1, Q_2, Q_3}$, where $\alpha = \pm \frac{1}{2}$, and with $(Q_1, Q_2, Q_3) = (-, +, +), (+, -, +), (+, +, -), (-, -, -)$. $\pm$'s for Q_I's denote $\pm \frac{1}{2}$. The fermions with anti-periodic boundary conditions are labeled by the Kaluza-Klein level $n \in \mathbb{Z} + \frac{1}{2}$. The contributions to the Chern-Simons terms from the n'th KK modes are given by [73][2]

$$S_{\text{CS}}^{(n)} = \frac{iN^2}{8\pi} \sum_{(Q_1, Q_2, Q_3)} \text{sgn}\left(n - \frac{\beta}{2\pi} A_4^I Q_I\right) \int_{S^3} \left(Q_I Q_J \mathcal{A}^I \wedge d\mathcal{A}^J + 2Q_I \frac{2\pi n}{\beta} \mathcal{A}^I \wedge da + \frac{(2\pi n)^2}{\beta^2} a \wedge da\right) .$$
$$(7.1.9)$$

---

[2]The overall sign is chosen to be consistent with our chirality/parity convention.

There are infinitely many contributions from the tower of KK modes, which should be regularized. Following [73], we sum over all $n \in \mathbb{Z} + \frac{1}{2}$ using the zeta function regularization.[3] To start with, when $-\frac{1}{2} < \mu \equiv \frac{\beta}{2\pi} Q_I A_4^I < \frac{1}{2}$ for a fermion mode with given Q_I, one obtains [73]

$$\sum_n \mathrm{sgn}(n-\mu) \sim 2\mu \ , \quad \sum_n \mathrm{sgn}(n-\mu)n \sim \mu^2 + \frac{1}{12} \ , \quad \sum_n \mathrm{sgn}(n-\mu)n^2 \sim \frac{2}{3}\mu^3 \ . \tag{7.1.10}$$

If A_4^I's are chosen so that $\frac{\beta}{2\pi} Q_I A_4^I$ is in the range $(-\frac{1}{2}, \frac{1}{2})$ for all possible Q_I's, one obtains

$$S_{\mathrm{CS}} = \frac{iN^2}{4\pi} \sum_{(Q_1,Q_2,Q_3)} \int \left[\frac{\beta}{2\pi} Q_I Q_J Q_K A_4^I \mathcal{A}^J \wedge d\mathcal{A}^K + \frac{2\pi}{\beta} Q_I \left(Q_J Q_K \frac{\beta^2}{(2\pi)^2} A_4^J A_4^K + \frac{1}{12} \right) \mathcal{A}^I \wedge da \right.$$
$$\left. + \frac{\beta}{3 \cdot 2\pi} Q_I Q_J Q_K A_4^I A_4^J A_4^K a \wedge da \right] \ . \tag{7.1.11}$$

Here, note that

$$\sum_{(Q_1,Q_2,Q_3)} Q_I Q_J Q_K = -\frac{1}{2} C_{IJK} \ , \qquad \sum_{(Q_1,Q_2,Q_3)} Q_I = 0 \ , \tag{7.1.12}$$

where C_{IJK} is symmetric in I, J, K, $C_{123} = 1$, and $C_{IJK} = 0$ if any two of I, J, K are same. (These are the anomaly coefficients of $U(1)^3$.) Using these facts, one obtains

$$S_{\mathrm{CS}} = -\frac{iN^2}{8\pi} \cdot \frac{\beta}{2\pi} \int_{S^3} C_{IJK} \left(A_4^I \mathcal{A}^J \wedge d\mathcal{A}^K + A_4^I A_4^J \mathcal{A}^K \wedge da + \frac{1}{3} A_4^I A_4^J A_4^K a \wedge da \right) \ . \tag{7.1.13}$$

---

[3]There are various proposals for regularizing $Z[S^3 \times S^1]$ [73, 239–241], concerning the supersymmetric Casimir energy [150, 242, 243]. Employing the regularization of [73], we obtain a free energy unspoiled by the formal Casimir energy factor of [242]. Although we have no clear reasoning for this, note that Casimir energy is very sensitive to regularization, while the integral spectrum part should be more robust. Especially, our setup respects all the periodicities of holonomies, which is a property of the spectral part of $\log Z$ but not of the Casimir energy [242]. So our regularization appears to disallow a room for vacuum energy factor like [242].

Note that the gauge invariant Chern-Simons terms (7.1.8) are all zero in this chamber, with $-\frac{1}{2} \leq \frac{\beta}{4\pi}(\pm A_4^1 \pm A_4^2 \pm A_4^3) \leq \frac{1}{2}$ for all four possible sign choices satisfying $\pm \cdot \pm \cdot \pm = -1$.

In general chambers of A_4^I, one takes

$$-\frac{1}{2} + p_Q \leq \frac{\beta}{2\pi} Q_I A_4^I \leq \frac{1}{2} + p_Q \ , \tag{7.1.14}$$

where Q runs over 4 possible cases, with integral p_Q's. In this chamber, the regularized sums are now given by

$$\sum_n \mathrm{sgn}(n-\mu) = \sum_{n'} \mathrm{sgn}(n'-\mu') \sim 2(\mu - p) \tag{7.1.15}$$

$$\sum_n \mathrm{sgn}(n-\mu)n = \sum_{n'} \mathrm{sgn}(n'-\mu')(n'+p) \sim (\mu - p)^2 + \frac{1}{12} + 2p(\mu - p)$$

$$\sum_n \mathrm{sgn}(n-\mu)n^2 = \sum_{n'} \mathrm{sgn}(n'-\mu')((n')^2 + 2pn' + p^2) \sim \frac{2}{3}(\mu - p)^3 + 2p(\mu - p)^2 + \frac{p}{6} + 2p^2(\mu - p) \ ,$$

where $n' = n - p$, $\mu' = \mu - p$. In this chamber, one obtains

$$S_{\mathrm{CS}} = \frac{iN^2}{4\pi} \cdot \frac{\beta}{2\pi} \sum_{(Q_1,Q_2,Q_3)} \int \left[\left(Q_I A_4^I - \frac{2\pi p_Q}{\beta} \right) Q_J Q_K \mathcal{A}^J \wedge d\mathcal{A}^K \right. \tag{7.1.1}$$

$$+ Q_I \left(\left(Q \cdot A_4 - \frac{2\pi p_Q}{\beta} \right)^2 + \frac{1}{12} \cdot \frac{(2\pi)^2}{\beta^2} + 2p_Q \cdot \frac{2\pi}{\beta} \left(Q \cdot A_4 - \frac{2\pi p_Q}{\beta} \right) \right) \mathcal{A}^I \wedge da$$

$$+ \left(\frac{1}{3} \left(Q \cdot A_4 - \frac{2\pi p_Q}{\beta} \right)^3 + \frac{2\pi p_Q}{\beta} \left(Q \cdot A_4 - \frac{2\pi p_Q}{\beta} \right)^2 + \frac{(2\pi p_Q)^2}{\beta^2} \left(Q \cdot A_4 - \frac{2\pi p_Q}{\beta} \right) + \frac{p_Q}{12} \cdot \frac{(2\pi)^3}{\beta^3} \right) a \wedge da \right]$$

We shall mostly work with the result (7.1.13) in the canonical chamber.

One can also determine (7.1.13) by just knowing 't Hooft anomalies and discrete symmetries. Firstly, the gauge non-invariant terms (7.1.13) are completely fixed in [73, 238], by demanding that its gauge variation yields the expected 't Hooft anomaly of the 4d $U(1)^3 \subset SO(6)_R$ symmetry. (More precisely, (7.1.13) matches the covariant anomalies.) To complete the argument, we discuss why gauge invariant CS terms (7.1.8) should vanish. Firstly, $a \wedge da$ is forbidden by

the 3d parity after S^1 reduction, which is a symmetry of the mother 4d theory if an object is blind to $SO(6)_R$, such as $a \wedge da$. Similarly, $\mathcal{A}^I \wedge d\mathcal{A}^I$ with a given I is forbidden since the mother 4d $\mathcal{N} = 4$ theory is invariant under parity with sign flip of odd number of $\mathcal{A}^I$ fields. The latter flip is charge conjugation, flipping $\mathbf{4} \leftrightarrow \overline{\mathbf{4}}$. The remaining gauge invariant CS terms are forbidden simply from the Weyl symmetry of $SO(6)$. We consider the Weyl reflections which reflects two of the three $\mathcal{A}^I$'s, leaving one invariant. This reflection also acts on A_4^I. But they cannot affect the gauge invariant CS terms, so in the canonical chamber which is left invariant under these reflections, the gauge invariant CS terms should respect this symmetry. For $\mathcal{A}^I \wedge da$ with any given I, a reflection which flips I and another $J(\neq I)$ flips sign of this term, forbidding its generation. Similarly, for $\mathcal{A}^I \wedge d\mathcal{A}^J$ at given pair $I \neq J$, reflection of I and $K(\neq I, J)$ forbids its generation. This completes a symmetry-based argument for (7.1.13). Such an approach may be useful for some non-Lagrangian theories, if there are enough discrete symmetries. In section 4, we shall make similar studies with 6d $(2, 0)$ theory, although it appears that such intrinsic arguments are less predictive there.

We now evaluate these CS terms for our backgrond fields, in the canonical chamber. We first consider the background R-symmetry fields (7.1.5) with real $\alpha^I = -i\Delta^I$, and later continue to complex Δ^I. Also, we keep $\epsilon_i \equiv -i\omega_i$ real for a moment, and later continue to complex ω_i. (7.1.13) is given by

$$S_{\text{CS}} = -\frac{iN^2}{48\pi^2\beta^2} C_{IJK} \alpha^I \alpha^J \alpha^K \int_{S^3} a \wedge da . \qquad (7.1.17)$$

Inserting a in (7.1.4), one finds

$$\int a \wedge da \ = \ \frac{r^4}{\beta^2} \int \frac{\epsilon_i n_i^2 d\phi_i \wedge \epsilon_j d(n_j^2) \wedge d\phi_j}{\left(1 + \frac{r^2 n_i^2 \epsilon_i^2}{\beta^2}\right)^2} = \frac{(2\pi)^2 r^4 \epsilon_1 \epsilon_2}{\beta^2} \int \frac{y dx - x dy}{\left(1 + \frac{r^2(\epsilon_1^2 x + \epsilon_2^2 y)}{\beta^2}\right)^2} \quad (7.1.18)$$

$$= \ \frac{(2\pi)^2 r^4 \epsilon_1 \epsilon_2}{\beta^2} \int_0^1 \frac{dx}{\left(1 + \frac{r^2}{\beta^2}(\epsilon_2^2 + (\epsilon_1^2 - \epsilon_2^2)x)\right)^2} = \frac{(2\pi)^2 r^4 \epsilon_1 \epsilon_2}{\beta^2(1 + \frac{r^2 \epsilon_1^2}{\beta^2})(1 + \frac{r^2 \epsilon_2^2}{\beta^2})} \ ,$$

where $x \equiv n_1^2$, $y \equiv n_2^2 = 1 - x$. So one finds

$$S_{\mathrm{CS}} = -\frac{i N^2 r^4 \epsilon_1 \epsilon_2}{12 \beta^4 (1 + \frac{r^2 \epsilon_1^2}{\beta^2})(1 + \frac{r^2 \epsilon_2^2}{\beta^2})} C_{IJK} \alpha^I \alpha^J \alpha^K \qquad (7.1.19)$$

in the canonical chamber. Inserting $\alpha^I = -i\Delta^I$, $\epsilon_i = -i\omega_i$ and taking $\beta \to 0^+$, one obtains

$$S_{\mathrm{CS}} \to -\frac{N^2 C_{IJK} \Delta^I \Delta^I \Delta^K}{12 \omega_1 \omega_2} = -\frac{N^2 \Delta_1 \Delta_2 \Delta_3}{2 \omega_1 \omega_2} \qquad (7.1.20)$$

in the canonical chamber. If S_{CS} is the dominant term in the effective action (which we will show shortly), this yields the asymptotic free energy by the relation $Z \sim e^{-S_{\mathrm{CS}}}$. So $\log Z \sim -S_{\mathrm{CS}}$ completely agrees with the free QFT analysis in chapter 3, and the entropy function of the supersymmetric AdS_5 black holes, thus accounting for their microstates. The extension of this result to different chambers also agrees with the result from free QFT.

Now to complete the analysis of the free energy, we show that all the other terms in the effective action are subleading in our scaling limit, suppressed by small $\beta, \omega_{1,2}$. The background fields are the 3d metric $g_{\mu\nu}$, dilaton Φ, graviphoton a_μ, gauge boson $\mathcal{A}_\mu^I$, and scalar A_4^I. Greek indices run over the coordinates $\{\phi_1, \phi_2, \theta\}$, and small Latin indices used below will run over the locally flat coordinates $\{1, 2, 3\}$. There are rich possibilities in constructing the effective action. However, many possible terms are eliminated by taking into account the actual background value (7.1.4) and (7.1.5). First, the Riemann curvature $\mathcal{R}_{\mu\nu\rho\sigma}$ has non-zero components only at $\{\mu, \nu\} = \{\rho, \sigma\}$ or $\{\mu, \nu\} \cap \{\rho, \sigma\} = \{\theta\}$. Second,

the background value (7.1.4) and (7.1.5) depends only on the θ coordinate, so that the field strengths $\mathcal{F}^0_{\mu\nu} \equiv \frac{1}{2\beta}(\partial_\mu a_\nu - \partial_\nu a_\mu)$ and $\mathcal{F}^I_{\mu\nu} \equiv \frac{1}{2}(\partial_\mu \mathcal{A}^I_\nu - \partial_\nu \mathcal{A}^I_\mu)$ of the graviphoton a_μ and gauge field $\mathcal{A}^I_\mu$ have non-zero components only at $\{\mu, \nu\} \supset \{\theta\}$. For the same reason, the derivative of any scalar function of the background fields $\partial_\mu f(\omega_\rho{}^{ab}, \Phi, a_\rho, \mathcal{A}^I_\rho, A^I_4)$ can have non-zero components only at $\{\mu\} = \{\theta\}$. Third, the graviphoton a_μ and gauge field $\mathcal{A}^I_\mu$ have non-zero components only at $\{\mu\} \not\supset \{\theta\}$. We will further assume that $\omega_1 = \omega_2 \equiv \omega$ for simplification, so that the dilaton Φ becomes a constant.

Let us first examine the possible terms that involve the volume integral $\int d^3x \sqrt{g}$ of gauge-invariant Lagrangian densities, formed by contracting tensors without $\epsilon^{\mu\nu\rho}$. When we consider the scalar contraction between the curvature $\mathcal{R}_{\mu\nu\rho\sigma}$ and the field strength $\mathcal{F}^0_{\mu\nu}$ or $\mathcal{F}^I_{\mu\nu}$, only an *even* number of $\mathcal{F}^0_{\mu\nu}$ or $\mathcal{F}^I_{\mu\nu}$ can appear in the non-vanishing Lagrangian densities. It can be shown as follows: the scalar contraction of $\mathcal{R}_{\mu\nu\rho\sigma}$, $\mathcal{F}^0_{\mu\nu}$, $\mathcal{F}^I_{\mu\nu}$ can be encoded in the circular sequence of antisymmetric pairs of tensor indices $[\alpha\beta][\gamma\delta]\cdots[\zeta\alpha]$, where adjacent indices in adjoining pairs are contracted to each other. We distinguish the curvature tensor indices by using capital letters. Then the contraction to a Lorentz scalar can be generally written as

$$[\alpha_{1,1}\beta_{1,1}]\cdots[\alpha_{1,n_1}\beta_{1,n_1}][A_1 B_1][\alpha_{2,1}\beta_{2,1}]\cdots[\alpha_{2,n_2}\beta_{2,n_2}][A_2 B_2]\cdots[A_{2j}B_{2j}] \quad \text{with} \quad \sum_{i=1}^{2j} n_i \in 2\mathbb{Z}+1.$$

The set of the field strength indices $\{\alpha_{k,1}, \beta_{k,n_k}\}$ in $[\alpha_{k,1}\beta_{k,1}]\cdots[\alpha_{k,n_k}\beta_{k,n_k}]$ can only be either

$$\{a_{k,1}, b_{k,n_k}\} = \begin{cases} \{\phi_1, \theta\} \text{ or } \{\phi_2, \theta\} & \text{if } n_k \in 2\mathbb{Z}+1 \\ \{\theta\} \text{ or } \{\phi_1, \phi_2\} \text{ or } \{\phi_1\} \text{ or } \{\phi_2\} & \text{if } n_k \in 2\mathbb{Z}. \end{cases} \tag{7.1.21}$$

Collecting the sets of the curvature indices $\{A_k, B_k\}$ for $k = 1, \cdots, 2j$, there are always an odd number of $\{\phi_1, \theta\}$ or $\{\phi_2, \theta\}$ and an odd number of $\{\phi_1, \phi_2\}$. Any

complete pairings in this collection have at least one pair between $\{\phi_1, \phi_2\}$ and $\{\phi_{1,2}, \theta\}$, so each term in the contraction refers to $\mathcal{R}_{\phi_1 \phi_2 \phi_i \theta} = 0$. This exhausts many possible terms in the effective action. Here we evaluate and list all non-vanishing terms which involve up to 4 derivatives: (Below we assume I, J, K, L run over $0, 1, 2, 3$, and $\Delta^0 \equiv -i$.)

$$\frac{1}{(2\pi)^2} \int \beta^{-3} e^{3\Phi} \sqrt{g} = \frac{\beta r^3}{2(\beta^2 - r^2\omega^2)^2} = \frac{\beta}{2r\omega^4} + \mathcal{O}\left(\frac{\beta^3}{r^3\omega^6}\right)$$

(7.1.22)

$$\frac{1}{(2\pi)^2} \int \beta^{-1} e^{\Phi} \sqrt{g}\, \mathcal{R}^{ab}{}_{ab} = \frac{r(3\beta^3 - 4\beta r^2\omega^2)}{(\beta^2 - r^2\omega^2)^2} = -\frac{4\beta}{r\omega^2} + \mathcal{O}\left(\frac{\beta^3}{r^3\omega^4}\right)$$

$$\frac{1}{(2\pi)^2} \int \beta e^{-\Phi} \sqrt{g}\, \mathcal{F}^I_{ab} \mathcal{F}^J_{ab} = \frac{\beta \Delta^I \Delta^J r^3 \omega^2}{(\beta^2 - r^2\omega^2)^2} = \frac{\beta \Delta^I \Delta^J}{r\omega^2} + \mathcal{O}\left(\frac{\beta^3}{r^3\omega^4}\right)$$

$$\frac{1}{(2\pi)^2} \int \beta^3 e^{-3\Phi} \sqrt{g}\, (\nabla_c \mathcal{F}^I_{ab})(\nabla^c \mathcal{F}^{Jab}) = \frac{2\beta^3 r\omega^2 \Delta^I \Delta^J}{(\beta^2 - r^2\omega^2)^2} = \frac{2\beta^3 \Delta^I \Delta^J}{r^3\omega^2} + \mathcal{O}\left(\frac{\beta^5}{r^5\omega^4}\right)$$

$$\frac{1}{(2\pi)^2} \int \beta^3 e^{-3\Phi} \sqrt{g}\, (\nabla_c \mathcal{F}^I_{ab})(\nabla^a \mathcal{F}^{Jcb}) = \frac{\beta^3 r\omega^2 \Delta^I \Delta^J}{(\beta^2 - r^2\omega^2)^2} = \frac{\beta^3 \Delta^I \Delta^J}{r^3\omega^2} + \mathcal{O}\left(\frac{\beta^5}{r^5\omega^4}\right)$$

$$\frac{1}{(2\pi)^2} \int \beta e^{-\Phi} \sqrt{g}\, \mathcal{R}^{ab}{}_a{}^c \mathcal{R}_b{}^d{}_{cd} = \frac{2\beta(8r^4\omega^4 - 8\beta^2 r^2\omega^2 + 3\beta^4)}{r(\beta^2 - r^2\omega^2)^2} = \frac{16\beta}{r} + \mathcal{O}\left(\frac{\beta^3}{r^3\omega^2}\right)$$

$$\frac{1}{(2\pi)^2} \int \beta e^{-\Phi} \sqrt{g}\, \mathcal{R}_{abcd} \mathcal{R}^{abcd} = \frac{32\beta r^4\omega^4 - 16\beta^3 r^2\omega^2 + 6\beta^5}{r(\beta^2 - r^2\omega^2)^2} = \frac{32\beta}{r} + \mathcal{O}\left(\frac{\beta^3}{r^3\omega^2}\right)$$

$$\frac{1}{(2\pi)^2} \int \beta^3 e^{-3\Phi} \sqrt{g}\, \mathcal{F}^{Iab} \mathcal{F}^{Jc}_a \mathcal{R}_b{}^d{}_{cd} = \frac{2\beta \Delta^I \Delta^J r\omega^2(\beta^2 - 2r^2\omega^2)}{(\beta^2 - r^2\omega^2)^2} = -\frac{4\beta \Delta^I \Delta^J}{r} + \mathcal{O}\left(\frac{\beta^3}{r^3\omega^2}\right)$$

$$\frac{1}{(2\pi)^2} \int \beta^3 e^{-3\Phi} \sqrt{g}\, \mathcal{F}^I_{ab} \mathcal{F}^J_{cd} \mathcal{R}^{abcd} = \frac{2\beta \Delta^I \Delta^J r\omega^2(\beta^2 - 4r^2\omega^2)}{(\beta^2 - r^2\omega^2)^2} = -\frac{8\beta \Delta^I \Delta^J}{r} + \mathcal{O}\left(\frac{\beta^3}{r^3\omega^2}\right)$$

$$\frac{1}{(2\pi)^2} \int \beta^5 e^{-5\Phi} \sqrt{g}\, \mathcal{F}^{Iab} \mathcal{F}^{Jc}_a \mathcal{F}^{Kd}_b \mathcal{F}^L_{cd} = \frac{\beta \Delta^I \Delta^J \Delta^K \Delta^L r^3 \omega^4}{(\beta^2 - r^2\omega^2)^2} = \frac{\beta \Delta^I \Delta^J \Delta^K \Delta^L}{r} + \mathcal{O}\left(\frac{\beta^3}{r^3\omega^2}\right)$$

$$\frac{1}{(2\pi)^2} \int \beta^5 e^{-5\Phi} \sqrt{g}\, \mathcal{F}^{Iab} \mathcal{F}^J_{ab} \mathcal{F}^{Kcd} \mathcal{F}^L_{cd} = \frac{2\beta \Delta^I \Delta^J \Delta^K \Delta^L r^3 \omega^4}{(\beta^2 - r^2\omega^2)^2} = \frac{2\beta \Delta^I \Delta^J \Delta^K \Delta^L}{r} + \mathcal{O}\left(\frac{\beta^3}{r^3\omega^2}\right) .$$

These terms are all much smaller than (7.1.19) in the scaling limit $\beta/r \ll \omega \ll 1$. Extrapolating a pattern from the above terms, an action made of n_1 curvature tensors, n_2 graviphoton field strengths, n_3 background $U(1) \subset SO(6)$ field

strengths, and n_4 derivatives should behave as

$$\frac{\beta^{1+n_4}\Delta^{n_3}}{r^{1+n_4}\omega^{4-2n_1-n_2-n_3}} + \mathcal{O}\left(\frac{\beta^{3+n_4}}{r^{3+n_4}\omega^{6-2n_1-n_2-n_3}}\right) \tag{7.1.23}$$

which would be suppressed in the limit $\beta/r \ll \omega \ll 1$.

As a next step, we turn to the effective action that contains a totally antisymmetric tensor $\epsilon^{\mu\nu\rho}$. This consists of Chern-Simons terms and those terms associated with a gauge invariant Lagrangian density. We can further distinguish the gauge non-invariant Chern-Simons terms from the gauge invariant ones. The gauge non-invariant Chern-Simons terms are entirely dictated by the chiral anomaly, so that no other terms than (7.1.11) can arise [73,238]. And also, the gauge invariant Chern-Simons terms displayed in (7.1.8) are already shown to be absent in the canonical chamber. The gravitational Chern-Simons term $\mathrm{tr}\,(\omega \wedge \mathcal{R} + \frac{2}{3}\omega \wedge \omega \wedge \omega)$, even if present, makes only a sub-dominant contribution in the limit $\beta/r \ll \omega \ll 1$:

$$\frac{1}{3!}\frac{1}{(2\pi)^2}\int \epsilon^{\mu\nu\rho}\left(\omega_\mu{}^{ab}\mathcal{R}_{\nu\rho}{}^{ab} + \frac{2}{3}\omega_\mu{}^{ab}\omega_\nu{}^{bc}\omega_\rho{}^{ca}\right) = -\frac{4\beta^2}{r^2\omega^2} + \mathcal{O}\left(\frac{\beta^4}{r^4\omega^4}\right).$$
$$\tag{7.1.24}$$

Other gauge invariant Lagrangian densities containing $\epsilon^{\mu\nu\rho}$ are constrained by the symmetry-based argument, which was used to argue the gauge invariant CS terms (7.1.8) are absent. Each allowed term should have odd numbers of three different $U(1) \subset SO(6)$ field strengths $\mathcal{F}_{\mu\nu}^{1,2,3}$. So even a minimal term of this sort has 3 $U(1)^3 \subset SO(6)$ field strengths coupled to one another. Some non-vanishing sample terms are evaluated and displayed below:

$$\int \frac{\beta^6 e^{-6\Phi}}{3!\,(2\pi)^2}\,\epsilon^{\mu\nu\rho}\mathcal{F}_{\mu\nu}^1(\nabla_\alpha\mathcal{F}_{\rho\beta}^2)\mathcal{F}^{3\alpha\sigma}\mathcal{F}_\sigma^{0\beta} = -\frac{i\beta^2 r^2\omega^4\Delta_1\Delta_2\Delta_3}{3(\beta^2-r^2\omega^2)^2} = -\frac{i\beta^2\Delta_1\Delta_2\Delta_3}{3r^2} + \mathcal{O}\left(\frac{\beta^4}{r^4\omega^2}\right)$$

$$\int \frac{\beta^{10} e^{-10\Phi}}{3!\,(2\pi)^2}\,\epsilon^{\mu\nu\rho}\mathcal{F}_{\mu\alpha}^1\mathcal{F}_{\nu\beta}^1\mathcal{F}^{1\alpha\beta}(\nabla_\lambda\mathcal{F}_{\rho\sigma}^2)\mathcal{F}^{3\lambda\delta}\mathcal{F}_\delta^{0\sigma} = -\frac{i\beta^2 r^2\omega^6\Delta_1^3\Delta_2\Delta_3}{3(\beta^2-r^2\omega^2)^2} = -\frac{i\beta^2\omega^2\Delta_1\Delta_2\Delta_3}{3r^2} + \mathcal{O}\left(\frac{\beta^4}{r^4}\right)$$
$$\tag{7.1.25}$$

Notice that these leading corrections exhibit the same scaling behavior as (7.1.23). In any case, all these terms become sub-dominant in the limit $\beta/r \ll \omega \ll 1$. One can probably make a systematic proof of this statement, but we content ourselves here by illustrating the suppressions. This establishes our claimed result (7.1.20), rederived from an effective action approach.

7.2 Large supersymmetric AdS$_7$ black holes

In this section, we apply the method of the former section to the 6d $\mathcal{N} = (2,0)$ SCFT living on N M5-branes. We shall again rely on a background field method on S^5, reducing the system on small temporal S^1 in a Cardy-like limit. We show that gauge non-invariant Chern-Simons terms determined by 't Hooft anomalies derive the free energy suggested in [91] in the Cardy limit, which completely captures the large supersymmetric AdS$_7$ black holes. And then we explain that other higher derivative terms are suppressed in our BPS Cardy limit. Then, we are left with finite number of gauge invariant Chern-Simons terms of background fields. The absence or $\frac{1}{N}$ suppression of some of them are partly addressed in the literature [73, 150], as we shall explain below. For the complete arguments for ignoring them, refer to [159].

The SCFT is put on $S^5 \times \mathbb{R}$. The 6d partition function is given by

$$Z = \text{Tr}\left[e^{-\beta E} e^{-\Delta_1 Q_1 - \Delta_2 Q_2} e^{-\sum_{i=1}^3 \omega_i J_i} \right] , \qquad (7.2.1)$$

where Q_1, Q_2 are two charges for $U(1)^2 \subset SO(5)_5$, and $J_{1,2,3}$ are three $U(1)^3 \subset SO(6)$ angular momenta on S^5. The 6d theory has 16 Poincare supercharges $\mathcal{Q}_{J_1,J_2,J_3}^{Q_1,Q_2}$ where $(Q_1, Q_2) = (\pm\frac{1}{2}, \pm\frac{1}{2})$, and $J_i = \pm\frac{1}{2}$ with the product of three $\pm$ signs of J_i's being -1. We choose $\mathcal{Q} \equiv \mathcal{Q}_{---}^{++}$ and its conjugate $\mathcal{S}$, and constrain $\Delta_I, \omega_i, \beta$ to make Z an index. One should constrain

$$\Delta_1 + \Delta_2 - \omega_1 - \omega_2 - \omega_3 = 2\pi i \pmod{4\pi i} \qquad (7.2.2)$$

and take $\beta \to 0^+$. We will study $\log Z$ at $|\omega_i| \ll 1$, again keeping finite imaginary parts of Δ_I to admit saddle points in which boson/fermion cancelations are obstructed.

We consider the 6d QFT on $S^5 \times S^1$ coupled to the following background fields:

$$ds^2 \;=\; r^2 \sum_{i=1}^{3} \left[dn_i^2 + n_i^2 \left(d\phi_i - \frac{i\omega_i}{\beta} d\tau \right)^2 \right] + d\tau^2 \qquad (7.2.3)$$

where n_i label two of the coordinates of S^5, constrained as $n_1^2 + n_2^2 + n_3^2 = 1$. The other angles satisfy $\phi_i \sim \phi_i + 2\pi$. τ has period β. The $U(1)^2 \subset SO(5)_R$ gauge fields are given by

$$A^I = -\frac{i\Delta_I}{\beta} d\tau \; . \qquad (7.2.4)$$

In the absence of any 6d Lagrangian description, we find it awkward to concretely discuss the KK modes and follow all the discussions presented in section 2.2. However, the structure of zero modes are well known, given by 5d maximal SYM (deformed by various parameters) on S^5. If the S^1 radius for KK reduction is small, the 5d zero modes are weakly coupled. Also, we simply assume here that nontrivial holonomy issues of [114] are absent, at least for the A_{N-1} type theory which is of our main concern.[4] The contribution from 5d zero modes' perturbative partition function on S^5 can surely be ignored. This can be seen either by relying on arguments similar to the former section, or simply by a $\frac{1}{N}$ suppression since this part will be proportional to N^2.

So we study the structure of the effective action of our background fields, which encodes the effects of 6d KK modes along S^1. We organize the background

---

[4]It will be interesting if one can address whether there are nontrivial issues with outer automorphism twists [244], whose zero modes are 5d Yang-Mills theories with non-ADE gauge groups. [245] studied such partition functions on $\mathbb{R}^4 \times T^2$ from 5d instanton calculus, which may provide microscopic clues to this question.

fields to the following 5d fields after the KK reduction:

$$ds_6^2 = ds_5^2 + e^{-2\Phi}(d\tau + a)^2$$

$$ds_5^2 = r^2\left[d\theta_1^2 + \sin^2\theta_1 d\theta_2^2 + n_i^2 d\phi_i^2 + \frac{r^2(\omega_i n_i^2 d\phi_i)^2}{\beta^2(1 - r^2\frac{n_i^2\omega_i^2}{\beta^2})}\right] \tag{7.2.5}$$

where the dilaton field Φ and the gravi-photon field a are given by

$$e^{-2\Phi} = 1 - r^2\frac{n_i^2\omega_i^2}{\beta^2}, \quad a = -i\frac{r^2\omega_i n_i^2 d\phi_i}{\beta(1 - r^2\frac{n_i^2\omega_i^2}{\beta^2})} \tag{7.2.6}$$

The 6d background fields A^I are rewritten as 5d gauge fields $\mathcal{A}^I$ and scalars A_6^I as $A^I = A_6^I(d\tau + a) + \mathcal{A}^I$, where

$$A_6^I = -\frac{i\Delta_I}{\beta}, \quad \mathcal{A}^I = -A_6^I a \ . \tag{7.2.7}$$

In our scaling limit ($\beta \ll |\omega_i| \ll 1$), the leading terms will turn out to come from Chern-Simons terms, at order $\frac{\beta^0}{\omega_1\omega_2\omega_3}$. So it is crucial to know all their coefficients to get the free energy in our Cardy limit. The gauge non-invariant CS terms are again dictated by the 't Hooft anomalies of $SO(5)_R$, which will be presented below. The gauge invariant Chern-Simons terms of $\mathcal{A}^I$ and a take the forms of [73]

$$\beta^{-3}a \wedge da \wedge da, \quad \beta^{-2}\mathcal{A}^I \wedge da \wedge da, \quad \beta^{-1}\mathcal{A}^I \wedge d\mathcal{A}^J \wedge da, \quad \mathcal{A}^I \wedge d\mathcal{A}^J \wedge d\mathcal{A}^K \ . \tag{7.2.8}$$

Here, just like in the former section, we do not discuss Chern-Simons terms involving gravitational fields since they will be absent or subleading in our scaling limit. (See below in this section.) Now, unlike the 3d CS terms for 4d $\mathcal{N} = 4$ theory, we are not given enough discrete symmetries of 6d $(2,0)$ theory to forbid them all. In fact, some of them are believed to be nonzero.

Trying to see if one can use abstract symmetry-based arguments to forbid CS terms, one can only partly achieve the goal. Firstly, $\mathcal{A}^I \wedge d\mathcal{A}^J \wedge d\mathcal{A}^K$ at

$I, J, K = 1, 2$, $\mathcal{A}^I \wedge d\mathcal{A}^J \wedge da$ at $I \neq J$ and $\mathcal{A}^I \wedge da \wedge da$ can be forbidden from the Weyl symmetry of $SO(5)_R$, just like we excluded $\mathcal{A}^I \wedge da$ or $\mathcal{A}^I \wedge d\mathcal{A}^J$ at $I \neq J$ in the former section. In the former section, one used parity (suitably blind to $SO(6)_R$) to forbid other terms. However, in 6d $(2, 0)$ theory, the system is intrinsically chiral, so that we have no simple argument to forbid

$$\beta^{-3} a \wedge da \wedge da \quad , \quad \beta^{-1} \sum_{I=1}^{2} \mathcal{A}^I \wedge d\mathcal{A}^I \wedge da \ . \tag{7.2.9}$$

A proposal made in [73] had a consequence that the coefficient of $a \wedge da \wedge da$ is zero for the $(2, 0)$ theory. This is partly supported from a SUSY calculus of the index on $S^5 \times S^1$ at high temperature [150], by not exhibiting a free energy at order β^{-3} (although the calculus was carried out after turning off many chemical potentials). Also, the β^{-1} term of the free energy studied in [150] was at order N^1. This may be related to an argument that the second term of (7.2.9) is $\frac{1}{N}$ suppressed. Anyway, in the remaining part of this section, we shall assume the vanishing or suppression of (7.2.9). For the complete arguments proving this assumptions, refer to [159].

The gauge non-invariant Chern-Simons terms for $\mathcal{A}^I$, A_6^I can be determined from the 't Hooft anomaly of $SO(5)_R$. Note that the anomaly 8-form of 6d (2,0) A_{N-1} theory is

$$I_8 = \frac{N^3 - N}{24} p_2(N) + \frac{N}{48} \left[p_2(N) - p_2(T) + \frac{1}{4}(p_1(T) - p_1(N))^2 \right] \tag{7.2.10}$$

with

$$p_1(N) = -\frac{1}{2(2\pi)^2} \mathrm{tr} F^2, \quad p_2(N) = \frac{1}{(2\pi)^4} \left(-\frac{1}{4} \mathrm{tr} F^4 + \frac{1}{8} (\mathrm{tr} F^2)^2 \right) \ . \tag{7.2.11}$$

[158] discussed the gauge non-invariant Chern-Simons term for $A_6^1 + A_6^2 = 0$, $\mathcal{A}^1 + \mathcal{A}^2 = 0$, to study certain asymptotic aspects of the free energy of $(2, 0)$

theory on $\mathbb{R}^4 \times T^2$. Generalizing the calculus of [158] for $U(1)^2$, one obtains[5]

$$
S_{CS} = \frac{i(N^3 - \frac{N}{4})\beta}{192\pi^3} \int_{S^5} \Big[2\Big(A_6^1 \mathcal{A}^1 \wedge d\mathcal{A}^2 \wedge d\mathcal{A}^2 + A_6^2 \mathcal{A}^2 \wedge d\mathcal{A}^1 \wedge d\mathcal{A}^1 \Big)
$$

$$
+ \Big(4 A_6^1 A_6^2 \mathcal{A}^1 \wedge d\mathcal{A}^2 \wedge da + (A_6^1)^2 \mathcal{A}^2 \wedge d\mathcal{A}^2 \wedge da + (A_6^2)^2 \mathcal{A}^1 \wedge d\mathcal{A}^1 \wedge da \Big)
$$

$$
+ 2\Big((A_6^2)^2 A_6^1 \mathcal{A}^1 \wedge da \wedge da + (A_6^1)^2 A_6^2 \mathcal{A}^2 \wedge da \wedge da \Big) + (A_6^1)^2 (A_6^2)^2 a \wedge da \wedge da \Big]
$$

$$
+ \frac{iN\beta}{1536\pi^3} \sum_{I=1}^{2} \int_{S^5} \Big[4 A_6^I \mathcal{A}^I \wedge d\mathcal{A}^I \wedge d\mathcal{A}^I + 6(A_6^I)^2 \mathcal{A}^I \wedge d\mathcal{A}^I \wedge da
$$

$$
+ 4(A_6^I)^3 \mathcal{A}^I \wedge da \wedge da + (A_6^I)^4 a \wedge da \wedge da \Big] . \tag{7.2.12}
$$

Inserting (7.2.6), (7.2.7) to (7.2.12), one obtains

$$
S_{CS} = -\frac{iN^3}{192\pi^3} \frac{\Delta_1^2 \Delta_2^2}{\beta^3} \int_{S^5} a \wedge da \wedge da + \mathcal{O}(N^1) . \tag{7.2.13}
$$

Evaluating $\int a \wedge da \wedge da$ with (7.2.6), one obtains

$$
\int_{S^5} a \wedge da \wedge da = -\frac{(2\pi)^3 (-i)^3 r^6 \omega_1 \omega_2 \omega_3}{\beta^3} \frac{1}{\Big(1 - \frac{r^2\omega_1^2}{\beta^2}\Big)\Big(1 - \frac{r^2\omega_2^2}{\beta^2}\Big)\Big(1 - \frac{r^2\omega_3^2}{\beta^2}\Big)} . \tag{7.2.14}
$$

Taking the $\beta \to 0^+$ limit, one obtains

$$
S_{CS} = \frac{N^3}{24} \frac{\Delta_1^2 \Delta_2^2}{\omega_1 \omega_2 \omega_3} . \tag{7.2.15}
$$

Therefore, the asymptotic free energy one obtains from S_{CS} is

$$
\log Z \sim -S_{CS} = -\frac{N^3}{24} \frac{\Delta_1^2 \Delta_2^2}{\omega_1 \omega_2 \omega_3} , \tag{7.2.16}
$$

supposing that other higher derivative terms are suppressed. If S_{CS} is the dominant term in the effective action (which we will show shortly), the asymptotic free energy completely agrees with the entropy function of the supersymmetric

---

[5]We flipped the overall sign of S_{CS} compared with [158], due to opposite 6d chirality conventions. E.g., in [158], supercharges contain (anti-chiral)$_{\mathbb{R}^4} \times$ (right chiral)$_{T^2}$, which is in $(0,2)$ spinors in our convention here.

AdS$_7$ black holes discussed in chapter 2. Thus, we have statistically accounted for the microstates of the large supersymmetric AdS$_7$ black holes.

Now to complete the analysis of the asymptotic free energy, we examine other background terms in the S^5 effective action, assuming the absences or large N suppressions of particular low-order terms (7.2.8), as discussed above. All other terms arranged in an infinite tower of derivative expansion will turn out to be suppressed in the scaling limit $\beta/r \ll \omega \ll 1$, as we shall illustrate with sample terms below. We shall study the case without $\epsilon^{\mu\nu\rho\sigma\lambda}$ first and then the other case. The analysis on the S^5 background action will be parallel to that on the S^3 action done in the former section. So we shall keep our discussion more concise, inspecting a few sample terms rather than attempting an exhaustive list of corrections to certain order, as in (7.1.22). Below we assume $\omega_1 = \omega_2 = \omega_3 \equiv \omega$ for simplification, so that the dilaton Φ becomes a constant.

We first consider the background action built from the scalar contraction of tensors without $\epsilon^{\mu\nu\rho\sigma\lambda}$. Evaluating a few terms which involve 0, 2, and 4 derivatives, we find

$$\frac{1}{(2\pi)^3}\int \beta^{-5}e^{5\Phi}\sqrt{g} = \frac{\beta r^5}{8(\beta^2 - r^2\omega^2)^3} = -\frac{\beta}{8r\omega^6} + \mathcal{O}\left(\frac{\beta^3}{r^3\omega^8}\right) \quad (7.2.17)$$

$$\frac{1}{(2\pi)^3}\int \beta^{-3}e^{3\Phi}\sqrt{g}\,\mathcal{R}^{\mu\nu}{}_{\mu\nu} = \frac{5\beta^3 r^3 - 6\beta r^5\omega^2}{2(\beta^2 - r^2\omega^2)^3} = \frac{3\beta}{r\omega^4} + \mathcal{O}\left(\frac{\beta^3}{r^3\omega^6}\right)$$

$$\frac{1}{(2\pi)^3}\int \beta^{-1}e^{\Phi}\sqrt{g}\,\mathcal{F}^I_{ab}\mathcal{F}^{Jab} = \frac{\beta r^5\omega^2\Delta^I\Delta^J}{2(\beta^2 - r^2\omega^2)^3} = -\frac{\beta\Delta^I\Delta^J}{2r\omega^4} + \mathcal{O}\left(\frac{\beta^5}{r^5\omega^8}\right)$$

$$\frac{1}{(2\pi)^3}\int \beta e^{-\Phi}\sqrt{g}\,(\nabla_c\mathcal{F}^I_{ab})(\nabla^c\mathcal{F}^{Jab}) = \frac{\beta^3\Delta^I\Delta^J r^3\omega^2}{(\beta^2 - r^2\omega^2)^3} = -\frac{\beta^3\Delta^I\Delta^J}{r^3\omega^4} + \mathcal{O}\left(\frac{\beta^5}{r^5\omega^6}\right)$$

$$\frac{1}{(2\pi)^3}\int \beta^{-1}e^{\Phi}\sqrt{g}\,\mathcal{R}_{\mu\nu\rho\sigma}\mathcal{R}^{\mu\nu\rho\sigma} = \frac{24\beta r^5\omega^4 - 12\beta^3 r^3\omega^2 + 5\beta^5 r}{(\beta^2 - r^2\omega^2)^3} = -\frac{24\beta}{r\omega^2} + \mathcal{O}\left(\frac{\beta^3}{r^3\omega^4}\right)$$

$$\frac{1}{(2\pi)^3}\int \beta e^{-\Phi}\sqrt{g}\,\mathcal{F}^I_{ab}\mathcal{F}^J_{cd}\mathcal{R}^{abcd} = -\frac{\Delta^I\Delta^J(6\beta r^5\omega^4 - \beta^3 r^3\omega^2)}{(\beta^2 - r^2\omega^2)^3} = \frac{6\beta\Delta^I\Delta^J}{r\omega^2} + \mathcal{O}\left(\frac{\beta^3}{r^3\omega^4}\right)$$

$$\frac{1}{(2\pi)^3}\int \beta^5 e^{-5\Phi}\sqrt{g}\,\mathcal{F}^{Iab}\mathcal{F}^J_{ab}\mathcal{F}^{Kcd}\mathcal{F}^L_{cd} = \frac{2\beta r^5\omega^4 \cdot \Delta^I\Delta^J\Delta^K\Delta^L}{(\beta^2 - r^2\omega^2)^3} = -\frac{2\beta \cdot \Delta^I\Delta^J\Delta^K\Delta^L}{r\omega^2} + \mathcal{O}\left(\frac{\beta^3}{r^3\omega^4}\right).$$

where the indices I, J, K, L run over $0, 1, 2, 3$ and $\Delta^0 \equiv -i$. These terms are all much smaller than (7.2.15) in the scaling limit $\beta/r \ll \omega \ll 1$. Moreover, their leading behavior is consistent with the following speculation: An action made of n_1 curvature tensors, n_2 graviphoton field strengths, n_3 background $U(1)^2 \subset SO(5)_R$ field strengths, n_4 derivatives scales as

$$\frac{\beta^{1+n_4} \Delta^{n_3}}{r^{1+n_4} \omega^{6-2n_1-n_2-n_3}} + \mathcal{O}\left(\frac{\beta^{3+n_4}}{r^{3+n_4} \omega^{8-2n_1-n_2-n_3}}\right), \tag{7.2.18}$$

Notice that it differs from (7.1.23) due to the additional factor $r^2 \cdot (\beta e^{-\Phi})^{-2} \sim \omega^{-2}$. All these terms would be suppressed by taking the scaling limit $\beta/r \ll \omega \ll 1$.

Now we turn to the background action associated to a pseudo-scalar Lagrangian density which has $\epsilon^{\mu\nu\rho\sigma\lambda}$. It can be either a Chern-Simons action or the action coming from a gauge invariant Lagrangian density. Gauge non-invariant CS terms have been determined to be (7.2.12) from 6d 't Hooft anomaly. The analogue of the gravitational CS term (2.60) that involves the spin connection ω_μ^{ab} cannot exist in 5 dimensions, but only in $3, 7, 11$ dimensions [246]. The Weyl symmetry of $SO(5)_R$ restricts the other gauge invariant CS terms to be invariant under the simultaneous sign flip of $\mathcal{A}^{I=1}$ and $\mathcal{A}^{I=2}$. Displaying all possible CS terms,

$$\frac{\beta^{-3}}{5!(2\pi)^3} \int \epsilon^{\mu\nu\rho\sigma\lambda} a_\mu (da)_{\nu\rho} (da)_{\sigma\lambda} = \frac{ir^6\omega^3}{120 \left(\beta^2 - r^2\omega^2\right)^3} = -\frac{i}{120\omega^3} + \mathcal{O}\left(\frac{\beta^2}{r^2\omega^5}\right) \tag{7.2.19}$$

$$\frac{\beta^{-1}}{5!(2\pi)^3} \int \epsilon^{\mu\nu\rho\sigma\lambda} a_\mu \mathcal{R}_{\nu\rho}{}^{\alpha\beta} \mathcal{R}_{\sigma\lambda\alpha\beta} = -\frac{ir^6\omega^5}{5 \left(\beta^2 - r^2\omega^2\right)^3} = \frac{i}{5\omega} + \mathcal{O}\left(\frac{\beta^2}{r^2\omega^3}\right) \tag{7.2.20}$$

$$\frac{\beta^{-1}}{5!(2\pi)^3} \int \epsilon^{\mu\nu\rho\sigma\lambda} \mathcal{A}_\mu^I \mathcal{F}_{\nu\rho}^J (da)_{\sigma\lambda} = -\frac{i\Delta^I \Delta^J r^6 \omega^3}{120 \left(\beta^2 - r^2\omega^2\right)^3} = \frac{i\Delta^I \Delta^J}{120\omega^3} + \mathcal{O}\left(\frac{\beta^2}{r^2\omega^3}\right). \tag{7.2.21}$$

In fact, as asserted earlier, CS terms containing gravitational terms are suppressed, while other gauge invariant CS terms are not. As noted above, here we assume that their coefficients are either exactly zero or $\frac{1}{N}$ suppressed, but indeed that can be proved as in [159]. Then we move to study the action associated to the gauge invariant Lagrangian density containing $\epsilon^{\mu\nu\rho\sigma\lambda}$. We compute some non-vanishing terms of this kind, e.g.,

$$\frac{1}{5!(2\pi)^3} \int \beta^6 e^{-6\Phi} \, \epsilon^{\mu\nu\rho\sigma\lambda} \mathcal{F}^I_{\mu\nu} \mathcal{F}^I_{\rho\sigma} (\nabla_\alpha \mathcal{F}^J_{\lambda\beta}) \mathcal{F}^{J\alpha\delta} \mathcal{F}^{0\beta}_\delta = \frac{i\beta^2 r^4 \omega^5 (\Delta^I \Delta^J)^2}{30 \left(\beta^2 - r^2\omega^2\right)^3} = -\frac{i\beta^2 (\Delta^I \Delta^J)^2}{30 r^2 \omega} + \mathcal{O}\left(\frac{\beta^4}{r^4 \omega^3}\right)$$

$$\frac{1}{5!(2\pi)^3} \int \beta^{14} e^{-14\Phi} \, \epsilon^{\mu\nu\rho\sigma\lambda} \mathcal{F}^I_{\mu\alpha} \mathcal{F}^I_{\nu\beta} \mathcal{F}^{I\alpha\beta} \mathcal{F}^I_{\rho\kappa} \mathcal{F}^J_{\sigma\iota} \mathcal{F}^{J\kappa\iota} (\nabla_\psi \mathcal{F}^J_{\lambda\gamma}) \mathcal{F}^{J\psi\tau} \mathcal{F}^{0\gamma}_\tau = \frac{i\beta^2 r^4 \omega^9 (\Delta^I \Delta^J)^4}{30 \left(\beta^2 - r^2\omega^2\right)^3}$$

$$= -\frac{i\beta^2 \omega^3 (\Delta^I \Delta^J)^4}{30 r^2} + \mathcal{O}\left(\frac{\beta^4 \omega^1}{r^4}\right) \ .$$

We observe that their scaling behavior in the limit $\beta/r \ll \omega \ll 1$ follows (7.2.18). All these terms would be subleading corrections to the free energy. This establishes our claimed result (7.2.16) derived from an effective action approach.

As a final comment, it may be useful to employ the background field approach at small S^1, to explore large non-BPS AdS black holes. Of course in this case, we expect that additional dynamical information has to be put in, unlike BPS black holes. Maybe not too surprisingly, we find similar structures as the hydrodynamic approach to the large AdS black holes [247].

Chapter 8

AdS black holes and finite N indices

In this chapter, we study the index of 4d $\mathcal{N} = 4$ Yang-Mills theory with $U(N)$ gauge group, focussing on the physics of the dual BPS black holes in $AdS_5 \times S^5$. Certain aspects of these black holes can be studied from finite N indices with reasonably large N^2. We make numerical studies of the index for $N \leq 6$, by expanding it up to reasonably high orders in the fugacity. The entropy of the index agrees very well with the Bekenstein-Hawking entropy of the dual black holes, say at $N^2 = 25$ or 36. Our data clarifies and supports the recent ideas which allowed analytic studies of these black holes from the index, such as the complex saddle points of the Legendre transformation and the oscillating signs in the index. In particular, the complex saddle points naturally explain the $\frac{1}{N}$-subleading oscillating patterns of the index. We also illustrate the universality of our ideas by studying a model given by the inverse of the MacMahon function.

8.1 Introduction and summary

In this chapter, we want to present our numerical study of the 4d $\mathcal{N} = 4$ superconformal index, showing that some aspects of the BPS black holes in AdS$_5$ [83–86] can be investigated by numerically studying the index at finite N. Our numerical data will also nontrivially support certain recent ideas which enabled the analytic studies of these AdS black holes.

We define the Witten index of 4d $\mathcal{N} = 4$ superconformal field theory on $S^3 \times S^1$ as [69]

$$Z(\Delta_I, \omega_i) = \text{Tr}\left[(-1)^F e^{-\sum_{I=1}^{3} \Delta_I Q_I - \sum_{i=1}^{2} \omega_i J_i}\right] \tag{8.1.1}$$

with the constraint $\Delta_1 + \Delta_2 + \Delta_3 - \omega_1 - \omega_2 = 0$ on the chemical potentials. Q_I with $I = 1, 2, 3$ denote the $U(1)^3 \subset SO(6)$ R-charges of $\mathcal{N} = 4$ superalgebra, and J_i with $i = 1, 2$ denote the $U(1)^2 \subset SO(4)$ angular momenta on S^3. Only the BPS states with the energy $E = \sum_{I=1}^{3} Q_I + \sum_{i=1}^{2} J_i$ can contribute to the index. Since the supersymmetric index is invariant under the continuous deformation of the gauge coupling, one can evaluate the index from the weakly interacting QFT. It can be done in a few steps. First, we obtain the following single-letter index [69]

$$I_{\text{single}}(\Delta_I, \omega_i) = 1 - \frac{(1 - e^{-\Delta_1})(1 - e^{-\Delta_2})(1 - e^{-\Delta_3})}{(1 - e^{-\omega_1})(1 - e^{-\omega_2})} \tag{8.1.2}$$

by counting all single-letter operators in the $\mathcal{N} = 4$ vector multiplet that satisfy the above mentioned BPS energy condition. Next, we apply the Plethystic exponential to this index I_{single} multiplied by the adjoint character $\chi_{\mathfrak{g}}(\mathbf{z})$ of the gauge algebra $\mathfrak{g}$, [69]

$$\text{PE}[I_{\text{single}}(\Delta_I, \omega_i)\,\chi_{\mathfrak{g}}(z_a)] \equiv \exp\left[\sum_{n=1}^{\infty} \frac{I_{\text{single}}(n\Delta_I, n\omega_i)\,\chi_{\mathfrak{g}}(z_a^n)}{n}\right]. \tag{8.1.3}$$

Finally, we project to the set of gauge invariant states by integrating over z_a with the Haar measure of the gauge group. The index of the 4d $\mathcal{N} = 4$ theory with a gauge group corresponding to the Lie algebra $\mathfrak{g}$ reduces to a matrix model calculation giving the following integral [69]:

$$Z_\mathfrak{g} = \oint d\mu_\mathfrak{g}(\mathbf{z}) \, \mathrm{PE}\Big[I_{\mathrm{single}}(\Delta_I, \omega_i)\chi_\mathfrak{g}(\mathbf{z}) \Big] \; . \qquad (8.1.4)$$

Here $d\mu_\mathfrak{g}(\mathbf{z})$ is the Haar measure of $\mathfrak{g}$. Explicitly, it can be written as

$$\oint d\mu_\mathfrak{g}(\mathbf{z}) = \frac{1}{(2\pi i)^r} \frac{1}{|W|} \oint_{|z_1|=1} \cdots \oint_{|z_r|=1} \frac{dz_1 \ldots dz_r}{z_1 \ldots z_r} \prod_{\alpha \in \Delta} (1 - \mathbf{z}^\alpha) \; , \qquad (8.1.5)$$

where W is the Weyl group of $\mathfrak{g}$, r is the rank, z_a is the fugacity corresponding to its a-th Cartan generator and Δ is the set of its roots. It turns out that for numerical purposes it is more efficient to use a slightly modified definition of the Haar measure given by restricting the product in (8.1.5) to only the positive roots of $\mathfrak{g}$ [248]:

$$\oint d\mu_\mathfrak{g}(\mathbf{z}) = \frac{1}{(2\pi i)^r} \oint_{|z_1|=1} \cdots \oint_{|z_r|=1} \frac{dz_1 \ldots dz_r}{z_1 \ldots z_r} \prod_{\alpha \in \Delta^+} (1 - \mathbf{z}^\alpha) \; . \qquad (8.1.6)$$

This helps by removing the need to normalize the integral by the order of the Weyl group. From (8.1.4) and (8.1.2), $Z(\Delta_I, \omega_i)$ is invariant under $2\pi i$ shift of each of Δ_I, ω_i. So one can equivalently study the index at the surface $\sum_I \Delta_I - \sum_i \omega_i = 2\pi i \mathbb{Z}$. Below, we shall often choose the right hand side to be $2\pi i$.

For our purposes it suffices to consider a special unrefined case of the above integral by setting $e^{-\Delta_1} = e^{-\Delta_2} = e^{-\Delta_3} \equiv e^{-\Delta}$, $e^{-\omega_1} = e^{-\omega_2} \equiv e^{-\omega}$. If one Legendre transforms to the microcanonical ensemble at macroscopic charges, this amounts to taking equal charges and equal angular momenta, $Q_1 = Q_2 = Q_3 = Q$ and $J_1 = J_2 = J$. From $3\Delta - 2\omega = 2\pi i \mathbb{Z}$, one can set $x^2 = e^{-\Delta}$, $x^3 = $

$e^{-\omega}$ for certain x. The fugacity x is now conjugate to the charge $j \equiv 6(Q + J)$. The expression in (8.1.4) then becomes

$$Z_{\mathfrak{g}} = \oint d\mu_{\mathfrak{g}}(\mathbf{z}) \; \mathrm{PE}\Big[\Big(1 - \frac{(1 - x^2)^3}{(1 - x^3)^2} \Big) \chi_{\mathfrak{g}}(\mathbf{z}) \Big] \; . \qquad (8.1.7)$$

The resulting index can be expanded as

$$Z = \sum_{j=0}^{\infty} \Omega_j x^j \qquad (8.1.8)$$

where $j \equiv 6(Q + J)$ and Ω_j are integers which count the number of BPS states (with -1 factor for fermions). For $U(N)$ gauge group, we shall study this index at $N = 2, 3, 4, 5, 6$, by computing the coefficients of the fugacity expansion in x up to fairly high orders, till $\mathcal{O}(x^{100})$ for $N \leq 5$, and till $\mathcal{O}(x^{70})$ for $N = 6$. Naively, finite N indices will be irrelevant for studying emergent gravitational phenomena expected in the large N limit. In particular, one would like to study the large N limit of Ω_j when j is of order $N^2 \gg 1$. In this limit, black hole like degeneracy will grow like $\log |\Omega_i| \sim N^2$ when $j \sim N^2$. Our starting point is that, in practice, taking $N = 5$ or 6 has already large enough N^2, so that we can hope to see the black hole like exponential growth of Ω_j quite convincingly. In fact, plugging in $N^2 = 25$ or 36 to the geometric Bekenstein-Hawking entropy formula for the known AdS$_5$ black holes, we shall find very good agreements with the field theory calculus of $\log |\Omega_j|$. In non-Abelian gauge theories, how small $\frac{1}{N}$ should be at finite N to exhibit large N behaviors depends on the type of physics one is interested in. So not too surprisingly, our finite N approach does not clearly see certain types of black holes. For instance, we empirically find that the charge range for the so-called 'small black holes' is not clearly resolved in our finite N discretized analysis. (See section 2 for more explanations.) The detailed physics that can be learned is outlined below, and will be elaborated more in section 3.

Our finite (but reasonably large) N calculus reveals various interesting structures which shed more concrete lights on the recent analytic studies of these black holes. After computing the large N free energy $\log Z$ as a function of chemical potentials Δ_I, ω_i, one makes a Legendre transformation to the microcanonical ensemble to compute the entropy. Legendre transformation is a saddle point approximation of the inverse Laplace transformation

$$\Omega_j = \frac{1}{2\pi i} \oint \frac{dx}{x} x^{-j} Z(x) \tag{8.1.9}$$

at macroscopic charge j. (The formula can be generalized to refined Δ_I, ω_i, but we present the above unrefined formula for simplicity.) The fact is that the dominant saddle point values x_* of x (or Δ_I, ω_i) are complex, at real j (or Q_I, J_i). The naively computed saddle point value of the integral, $\Omega_j(x_*) \equiv e^{S(j)}$, at real positive j is therefore complex. Somewhat surprisingly, this simple fact apparently seems to have confused many people, leading to a number of ad hoc prescriptions and interpretations on how to extract the correct physics out of this result. We stick to the natural interpretation of [75, 76, 78] and find extremely nontrivial evidences supporting it from our numerical studies. We think this will confirm our interpretation to be the canonical picture, which goes as follows. From the unitarity of the underlying QFT, it is always guaranteed that one can find the complex conjugate saddle point $\bar{x}_*$ for any complex x_*. The conjugate saddle point value is given by $\Omega_j(\bar{x}_*) = e^{\overline{S(j)}}$. Adding the two equally dominant contributions, one obtains

$$\Omega_j \sim \Omega_j(x_*) + \Omega_j(\bar{x}_*) \sim \exp\left[\text{Re}(S(j)) + \cdots\right] \cos\left[\text{Im}(S(j)) + \cdots\right] , \quad (8.1.10)$$

where $\cdots$ denote possible subleading corrections at large N^2 and large j. (Note that $\text{Re}(S(j))$ and $\text{Im}(S(j))$ scale like N^2.) As will be manifest from our data in the next section, the integers Ω_j at macroscopic j grow exponentially fast to

account for the dual black holes, but come with possible minus signs at certain j's. Namely, Ω_j as a function of (quantized) j oscillates between positive and negative integers as j changes. However, the macroscopic Legendre transformation calculus is not sensitive to the precise quantized nature of j and Ω_j. Therefore, the best one can expect to see from this calculus is an exponentially growing envelope function, which is provided by $e^{\mathrm{Re}(S(j))}$, multiplied by a factor which oscillates between $+1$ and -1, which is provided by $\cos\left[\mathrm{Im}(S(j)) + \cdots\right]$ in the above expression.

Our numerical calculus will justify this interpretation. Firstly, the computed entropy $\log|\Omega_j|$ from the integers Ω_j indeed takes the form of

$$\mathrm{Re}(S(j)) + \log\left[\cos(\mathrm{Im}(S(j) + \cdots)\right] \;, \tag{8.1.11}$$

where $\mathrm{Re}[S(j)]$ and $\mathrm{Im}[S(j)]$ are those computed recently from the index using various analytic methods (in the large N and/or large charge limit). Furthermore, more importantly, investigating the overall signs in Ω_j from our numerical calculus, the sign oscillating pattern is also determined by the sign oscillation of $\cos\left(\mathrm{Im}(S(j)) + \cdots\right)$, upon fitting a constant $\mathcal{O}(1)$ phase shift in '$\cdots$' that has not yet been computed by any analytic methods. Therefore, a precise interpretation is given to $\mathrm{Im}(S(j))$, as containing the overall sign information of Ω_j.

While comparing our numerically computed $\log|\Omega_j|$ with (8.1.11), confirming the appearance of the second term is nontrivial. This is because, while the first term is proportional to N^2, the second term is typically subleading because the macroscopic quantity $\mathrm{Im}(S(j)) \sim N^2$ is inside the cosine function. To detect the second term, it is crucial to make a precision computation of the index which sees this '$\frac{1}{N}$ corrections.' Our finite N indices (say at $N = 5, 6$) provide a perfect setup to confirm such structures, as these values of N^2 are large enough

to provide a large N hierarchy to various contributions to the entropy, while not being too large so that the subleading corrections are visible. We think our numerical support to the formula (8.1.11) is compelling. See section 3 for the details.

The interpretations outlined above appear to be universal, which may appear in any index-like generating functions that have negative integer coefficients at various orders. We illustrate that this is actually the case, by studying in detail the inverse of the MacMahon function

$$f(x) \equiv \prod_{n=1}^{\infty}(1-x^n)^n = \sum_{j=0}^{\infty}\Omega_j x^j = 1-x-2x^2-x^3+0x^4+4x^5+4x^6+7x^7+3x^8-2x^9-9x^{10}-17x^{11}-\cdots.$$

(8.1.12)

At large j, one can analytically compute the macroscopic entropy given by $\log|\Omega_j| \sim \frac{3}{4}\left[2\zeta(3)j^2\right]^{\frac{1}{3}} + \cdots$, where '$\cdots$' denotes small $\frac{1}{j}$ corrections which can be concretely computed to any desired accuracy. On the other hand, Ω_j exhibits a characteristic oscillation between positive and negative integers. We shall illustrate that this is precisely realized in the Legendre transformation as the complex saddle points, where a formula like (8.1.11) will provide a perfect match. As we can explicitly compute the $\frac{1}{j}$ corrections to high orders, including the finite phase shifts in the second term of (8.1.11), our interpretation can be tested to very high accuracy in this model.

The remaining part of this chapter is organized as follows. Section 2 summarizes our numerical results for the integers Ω_j. We also explain some salient structures of the series Ω_j, and also provide a comparison with the Bekenstein-Hawking entropy of black holes. In section 3, we take a closer look at the structures of Ω_j and the $\frac{1}{N}$ correction, and provide various interpretations and discussions.

8.2 Numerical study of the $\mathcal{N} = 4$ index

We now specialize to the case of 4d $\mathcal{N} = 4$ theories with a $U(N)$ gauge group. We would like to probe the regime

$$Q_I, J_i \sim N^2 \gg 1 \ . \tag{8.2.1}$$

However, the last inequality will be reasonably met by trying to take N^2 and charges to be as large as possible within our computational capability. We expand the index in x (as introduced in section 1), perform the integral over N variables on computer, to obtain various coefficients of

$$Z_{U(N)} = \sum_{j=0}^{\infty} \Omega_j x^j \qquad \text{with} \qquad j \equiv 6(Q + J) \ . \tag{8.2.2}$$

This is a straightforward exercise, with the main impediment coming from the availability of sufficient computing power. The computational-complexity of the integral grows extremely quickly as the rank of the gauge group increases. We were able to explicitly evaluate the above integral for $2 \leq N \leq 5$ up to $\mathcal{O}(x^{100})$, as given in appendix A of [80]. For $U(6)$ we evaluated it up to $\mathcal{O}(x^{70})$. The

explicit expression of the $U(6)$ index is given by:

$$
\begin{aligned}
Z_{U(6)} = {}& 1 + 3x^2 - 2x^3 + 9x^4 - 6x^5 + 21x^6 - 18x^7 + 48x^8 - 42x^9 + 99x^{10} - 96x^{11} \\
& + 200x^{12} - 198x^{13} + 345x^{14} - 340x^{15} + 540x^{16} - 426x^{17} + 564x^{18} - 234x^{19} \\
& + 189x^{20} + 636x^{21} - 1026x^{22} + 2262x^{23} - 2583x^{24} + 3438x^{25} - 1851x^{26} \\
& - 794x^{27} + 8757x^{28} - 20460x^{29} + 40398x^{30} - 63054x^{31} + 88401x^{32} \\
& - 99388x^{33} + 80856x^{34} + 4680x^{35} - 184576x^{36} + 494910x^{37} - 920943x^{38} \\
& + 1392360x^{39} - 1690101x^{40} + 1451568x^{41} - 114147x^{42} - 2931498x^{43} + 8129358x^{44} \\
& - 15183836x^{45} + 22398435x^{46} - 25748382x^{47} + 18439724x^{48} + 8645112x^{49} \\
& - 64166661x^{50} + 150570130x^{51} - 254339973x^{52} + 334069536x^{53} - 310532838x^{54} \\
& + 68770386x^{55} + 514459605x^{56} - 1501534768x^{57} + 2775637323x^{58} - 3887229606x^{59} \\
& + 3923925613x^{60} - 1520426502x^{61} - 4814089191x^{62} + 15863550944x^{63} \\
& - 30282658596x^{64} + 42802285428x^{65} - 42817602705x^{66} + 14831924490x^{67} \\
& + 57170104014x^{68} - 179436305580x^{69} + 331894244529x^{70} + \mathcal{O}(x^{71}) \,. \qquad (8.2.3)
\end{aligned}
$$

It was pointed out in [76] that the alternation of $\pm$ signs of Ω_j demands special care when one attempts to extract it out at large j using Legendre transformation. These sign alternations are generic: they also happen at lower N's. See the results in appendix A of [80]. We shall later observe more organized patterns of the sign alternations, as will be explained in section 3. Here, we simply note that the absolute degeneracy $|\Omega_j|$ indeed grows very fast at large j. For instance, one finds $|\Omega_{70}| \sim 3.3 \times 10^{11}$ at $N = 6$, and $|\Omega_{100}| \sim 1.4 \times 10^{16}$ at $N = 5$. We will see shortly that Ω_j grows quantitatively like the black hole entropy even at $N = 5, 6$. See Fig. 8.1 for $\log |\Omega_j|$ and the signs of Ω_j at $N = 5, 6$.

We want to compare our indices at reasonably large N with the spectra in the gravitational dual. At low energies, the BPS spectrum can be computed
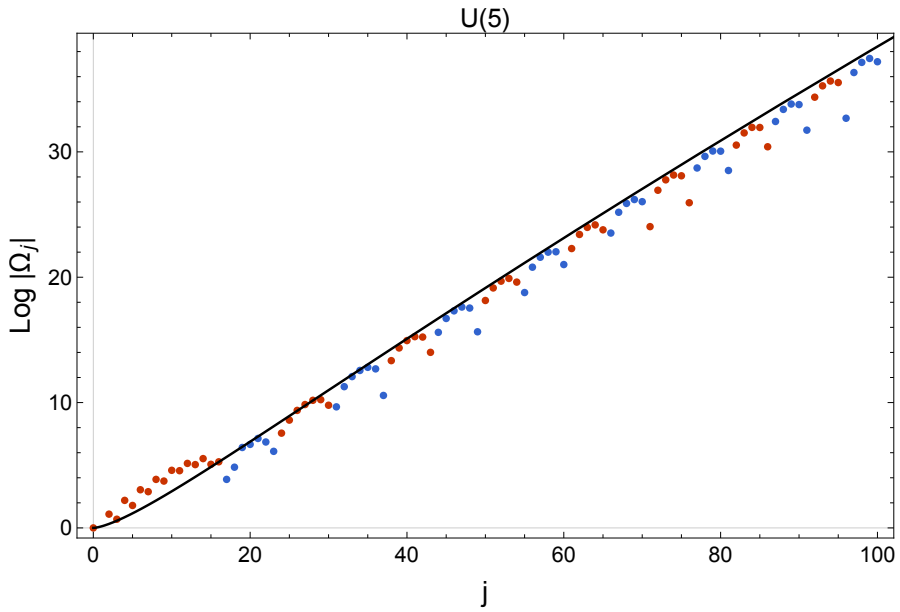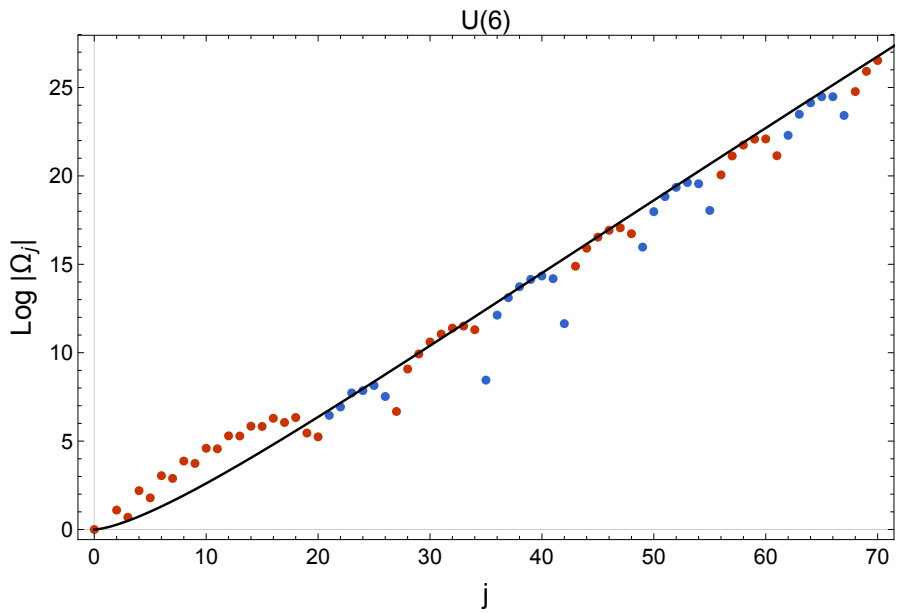
Figure 8.1: Plots of $\log |\Omega_j|$ for $U(5)$ and $U(6)$ indices. The colors of the points encode the sign of $(-1)^j \Omega_j$: red being positive and blue being negative. $\mathrm{Re}(S(j))$ computed from the black hole entropy function is the Bekenstein-Hawking entropy, given by the curve drawn with a solid black line.

from the gas of gravitons [69]. A BPS graviton particle corresponds to a particular single trace BPS operator in the QFT dual. It is a valid approach when the energy E satisfies $E \ll N$. In this limit, the BPS multi-graviton states correspond to multi-trace operators obtained by multiplying the above mentioned single trace operators, where one does not have to consider trace relations. As the energy grows, the finite N effects of these graviton states have been studied in some detail in the BPS sector. The trace relations will start to enter from an energy of order N, reducing the number of independent operators than the naive multi-particle spectrum beyond this threshold. To see how this picture is reflected in our Ω_j's, we first consider the index over BPS gravitons given by [69]

$$\sum_{j=0}^{\infty} \Omega_j^g x^j \equiv \prod_{n=1}^{\infty} \frac{(1-x^{3n})^2}{(1-x^{2n})^3} \ . \tag{8.2.4}$$

Comparing our Ω_j and Ω_j^g, one finds that $\Omega_j = \Omega_j^g$ holds for $j \leq 2N+1$. This can be seen exactly for all $N = 2, \cdots, 6$, and presumably holds exactly for other values of N. Slightly beyond this point, $j \gtrsim 2N+1$, $|\Omega_j|$ is smaller than $|\Omega_j^g|$ for a certain while. So $j = 2N + 1$ is naturally interpreted as the threshold where the trace relation starts to reduce the BPS states.

Now we consider the regime in which j is substantially larger than this threshold, so that the resulting $|\Omega_j|$ cannot be explained from $|\Omega_j^g|$ with the trace relation reduction. ($|\Omega_j|$ becomes bigger than $|\Omega_j^g|$ for sufficiently large j.) Eventually we enter a region with $j \sim N^2$, whose gravitational dual description will be the BPS black holes in AdS. To provide the comparison with the Bekenstein-Hawking entropy of these black holes, let us first explain the entropy function approach to understand its structures in a simple manner [90]. We present the results in the version which only keeps one fugacity x [75, 76]. The entropy function we shall discuss assumes the convention $3\Delta - 2\omega = 2\pi i$.

Then $x^2 = e^{-\Delta}$, $x^3 = e^{-\omega}$ can be solved as

$$x = e^{-\frac{\omega}{3} + \frac{2\pi i}{3}} = -e^{-\frac{\Delta}{2}} \ . \tag{8.2.5}$$

In this setup, consider the following entropy function of j and ω:

$$S(\omega, j) = \frac{N^2 \Delta^3}{2\omega^2} + \frac{\omega - 2\pi i}{3} j = \frac{N^2}{2\omega^2} \left(\frac{2\pi i + 2\omega}{3} \right)^3 + \frac{\omega - 2\pi i}{3} j \ . \tag{8.2.6}$$

The first term on the right hand side originates from $\log Z$ in the grand canonical ensemble, and the second term is the Legendre transformation factor, whose exponential becomes x^{-j} of (8.1.9). At fixed charge $j > 0$, one extremizes $S(\omega, j)$ with ω. This yields a cubic equation in ω, which yields three different solutions ω_*. Among these three, we take the one which yields maximal $\mathrm{Re}(S(j)) > 0$ where $S(j) \equiv S(\omega_*, j)$. At this solution, one finds

$$\omega_* = -\xi \sqrt{\frac{3\pi + 3\xi}{\pi - 3\xi}} + i\xi \tag{8.2.7}$$

$$j = -\frac{N^2}{9} \frac{(\pi - 2\xi)^2 (\pi + \xi)}{\xi^3}$$

$$\log Z = +\frac{N^2}{18} \frac{\pi^3 - 9\pi\xi^2 - 8\xi^3}{\xi^2} \sqrt{\frac{\pi + \xi}{3\pi - 9\xi}} - i \frac{N^2}{54} \frac{(\pi - 8\xi)(\pi + \xi)^2}{\xi^2} \ ,$$

where ξ is a real number satisfying $-\pi < \xi < 0$. It parametrizes the imaginary part of ω, and is a monotonically increasing function of j implicitly given by the second line. Inserting this value back to $S(\omega, j)$, one obtains $S(j)$ given by

$$\mathrm{Re}(S(j)) = \frac{N^2}{6} \frac{\pi(\pi^2 - 2\pi\xi - 3\xi^2)}{\xi^2} \sqrt{\frac{\pi + \xi}{3\pi - 9\xi}} \tag{8.2.8}$$

$$\mathrm{Im}(S(j)) = -\frac{N^2}{18} \frac{\pi(\pi - 5\xi)(\xi + \pi)}{\xi^2} - \frac{2\pi}{3} j$$

where the relation $j(\xi)$ is assumed. The fact is that $\mathrm{Re}(S(j))$ is precisely the Bekenstein-Hawking entropy of the BPS AdS black holes of [83, 84, 86] at $Q \equiv Q_1 = Q_2 = Q_3$ and $J \equiv J_1 = J_2$. More precisely, [83, 84, 86] found black

hole solutions carrying two charges Q, J, depending on only one independent parameter. The entropy is a function of this parameter, which is in one to one correspondence with $j \equiv 6(Q + J)$. Therefore, expressing the one-parameter Bekenstein-Hawking entropy in terms of j, one obtains the above $\mathrm{Re}(S(j))$. Here, N^2 in the gravity side is related to the inverse Newton constant G_5^{-1} of the 5d gravity as $N^2 = \frac{\pi \ell^3}{2 G_5}$, where ℓ is the radius of AdS_5.

The classical gravity description will be reliable at small enough Newton constant, i.e. $N^2 \gg 1$. To compare with our numerical results at $N = 5, 6$, we plug in $N^2 = 25$ or 36 to (8.2.8) expecting that N^2 is reasonably large. In Fig. 8.1, we have drawn these $\mathrm{Re}(S(j))$ by the black solid lines. At large enough charge j (especially for $U(5)$ where we could do numerical calculations for larger charges), this agrees very well with the numerically computed entropy $\log|\Omega_j|$ of the index. There appear intriguing oscillations of our numerical $\log|\Omega_j|$, which appear to be subleading in $\frac{1}{N}$ at large enough charges. We shall comment on these subleading fluctuations in the next section.

Similar plots are shown for lower N in appendix A of [80]. Of course, inserting the finite values of N^2 to (8.2.8) becomes less meaningful for those lower values. As one can see from these figures, the numerical $\log|\Omega_j|$ and $\mathrm{Re}(S(j))$ do not agree that well for $N = 2$ or $N = 3$. Here we note that, although $S(j)$ of (8.2.8) is introduced here as the entropy function for the black hole, valid at $N^2 \gg 1$, it has been shown [75] that (8.2.6) and (8.2.8) are true at any finite N^2 when ω becomes small (or equivalently, when $j \gg N^2$). This is called the 'Cardy limit' of higher dimensional SCFTs in the recent literature. In this case, (8.2.8) and (8.2.6) have been derived from the field theory side for any value of N. As one can see gaps between $\log|\Omega_j|$ and $\mathrm{Re}(S(j))$ for $N = 2, 3$ in Figs. 4 and 5 in appendix A of [80], it appears that the charge $j = 100$ has not yet

274

reached the Cardy regime.

We can also try to characterize which kinds of black holes are well described by our numerical data, and which kinds are not well visible. In AdS, one can classify black holes into 'small black holes' and 'large black holes' depending on various (closely related) criteria. The classification was originally made for AdS-Schwarzschild black holes. However, similar notion exists for our BPS black holes by the charge playing the role of energy, and the inverse chemical potential playing the role of temperature. The most intuitive way to distinguish the AdS black holes is whether the 'size' of the black hole is smaller than the AdS radius ℓ, or larger than it. To make it more precise, consider the temperature T of the black hole given by $\frac{1}{T} = \frac{dS(E)}{dE}$. For our BPS black holes, $\text{Re}(\omega)$, j, $\text{Re}(S(j))$ play the role of T^{-1}, E, $S(E)$ respectively. They satisfy the analogous relation

$$\frac{1}{3}\text{Re}(\omega) = \frac{d[\text{Re}S(j)]}{dj} \ . \tag{8.2.9}$$

Now consider taking the second derivative with energy (or j),

$$\frac{dT^{-1}(E)}{dE} = \frac{d^2 S(E)}{dE^2} \quad , \quad \frac{1}{3}\frac{d\text{Re}(\omega(j))}{dj} = \frac{d^2[\text{Re}S(j)]}{dj^2} \ , \tag{8.2.10}$$

where the first and second expressions apply for Schwarzschild black holes and our BPS black holes. The negativity of these expressions implies that the black holes are stable in the canonical and grand canonical ensemble, respectively, due to the heat capacity or susceptibility being positive. We call these black holes 'large black holes.' They are characterized by the entropy being a convex function of E or j. Our BPS black holes are in the large black hole branch for $j > j_0 \equiv \frac{(5+3\sqrt{3})N^2}{9}$ (or $-\frac{\pi}{\sqrt{3}} < \xi < 0$). On the other hand, for $j < j_0$ (or $-\pi < \xi < -\frac{\pi}{\sqrt{3}}$), the curve $S(j)$ is concave and one is in the small black hole branch. As one sees from the black curves in Fig. 8.1, the visibly concave region is at so small charges, that they are essentially overlapping with the region

275

$j \leq 2N+1$ in which the graviton description is good. Namely, we find that the small black hole branch squeezed by the graviton region from the left and j_0 from the right is not clearly visible from our finite N indices. At large enough N, the two charge scales $j \sim 2N+1$ and $j \sim j_0$ will be given enough hierarchy to allow a visible small black hole region. However, our finite N index does not seem to have large enough N to make this region clearly visible. Indeed, this can be clearly seen from our numerical plots in Fig. 8.1. In the small black hole region, $S(j)$ will increase very fast in j. However, our numerical $\log |\Omega_j|$ does not manifestly exhibit such an inflating region. It will be interesting to compute Ω_j's for larger N's to see this region.

So far, we explained how to compare our $\log |\Omega_j|$ with $\mathrm{Re}(S(j))$ of the dual black holes. There is other interesting information that one can get from our numerical data, concerning $\mathrm{Im}(S(j))$, the signs of Ω_j, and the subleading oscillations that one sees in the figures. These will be discussed in more detail in the next section.

8.3 Interpretations and discussions

In this section, we discuss more detailed information encoded in our numerical Ω_j, and relate it to the interpretations made on (8.2.6).

We first study the signs of Ω_j. The pattern of the signs visible in the series $Z(x) = \sum_j \Omega_j x^j$ apparently looks very complicated. However, one observes simplifications upon inserting $x \to -x$:

$$Z(-x) = \sum_j (-1)^j \Omega_j x^j \ . \tag{8.3.1}$$

The signs of $(-1)^j \Omega_j$ are shown in Fig. 8.1 and also in the figures of appendix A of [80] by the colors of the dots. After this substitution, one finds that the sign

276

change pattern is correlated to the subleading oscillation pattern of $\log |\Omega_j|$. Namely, the sign changes only at the local minima of the oscillation.

At this point, we revisit the interpretation of complex $S(j)$ at the saddle point of the Legendre transformation at macroscopic charges, that we outlined in section 1. The interpretation asserts that the sign of $\cos[\mathrm{Im}(S(j)) + \cdots]$ equals the sign of the integers Ω_j. Since we have observed very simple sign oscillation patterns of our data $(-1)^j \Omega_j$, let us try to understand this also from the entropy function (8.2.6). Since $(-1)^j = e^{\pi i j}$, one finds that

$$(-1)^j \Omega_j \sim \exp\left[\frac{N^2(\frac{2\pi i}{3} + \frac{2\omega_*}{3})^3}{2\omega_*^2} + \frac{\omega_* + \pi i}{3} j + \cdots\right] + c.c. \ , \qquad (8.3.2)$$

where $\cdots$ are possible subleading corrections in small $\frac{1}{N^2}$ and $\frac{1}{j}$ that have not been computed to date. From this, one obtains

$$(-1)^j \Omega_j \sim \exp\left[\mathrm{Re}(S(j)) + \cdots\right] \cos\left[\mathrm{Im}(S(j)) + \pi j + \cdots\right] \ . \qquad (8.3.3)$$

Although the subleading corrections to $\mathrm{Re}(S(j))$ will not affect our studies below, the corrections to $\mathrm{Im}(S(j))$ will be somewhat important since they will make a finite phase shift of the oscillation. The corresponding entropy (8.1.11) improving the black curve of Fig. 8.1 is shown in Fig. 8.2.

Firstly, Fig. 8.2 clearly shows that the signs of $(-1)^j \Omega_j$ are equal to the sign of $\cos\left[\mathrm{Im}(S(j)) + \pi j + \eta\right]$. As mentioned in the previous paragraph, we empirically fitted the possible subleading correction η by an $\mathcal{O}(1)$ constant. Although η is in principle a function of j, N^2 such as $\eta(\frac{j}{N^2})$, constant η seems to be reasonably good within the relatively short ranges of charges in Fig. 8.2.[1] The agreements in Fig. 8.2 justify our interpretation that the oscillation caused

---

[1]We also note that, upon including the 1-loop determinant factor of the Legendre transformation (8.2.6) in this framework, one obtains much better agreements than those in Fig. 8.2. However, we do not show these results here since they do not seem to be based on a systematic calculus of the subleading terms.
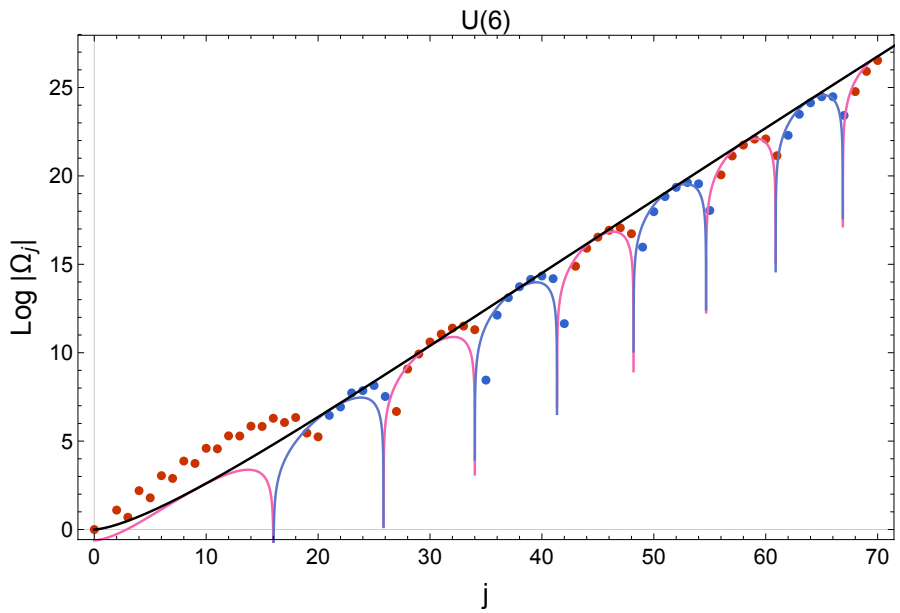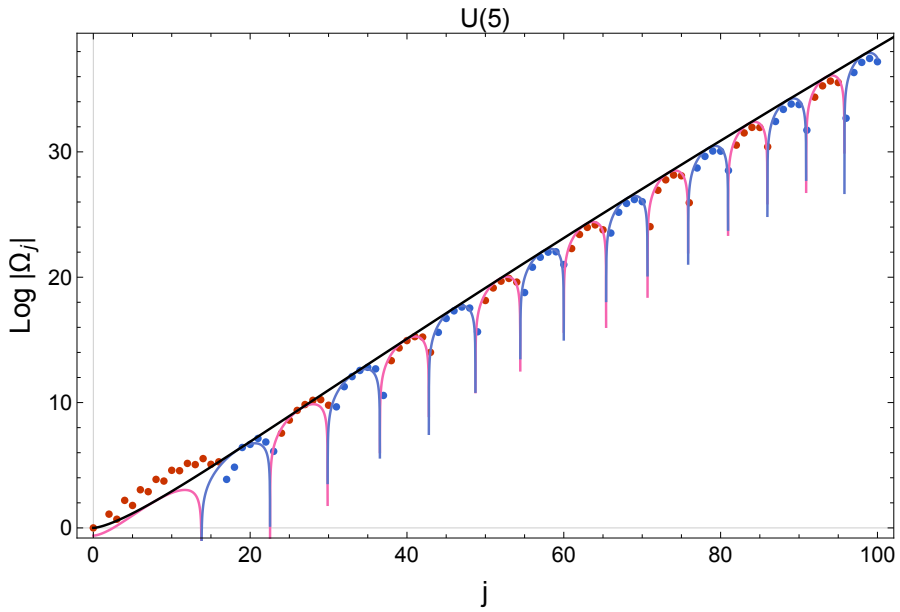
(a) $N = 5$

(b) $N = 6$

Figure 8.2: Same plots as Fig. 8.1, with the extra red/blue curves for $\mathrm{Re}(S(j)) + \log|\cos[\mathrm{Im}(S(j)) + \pi j + \eta]|$. A subleading constant η is empirically tuned to $\eta \approx -1$ to minimize the overall off-phase behaviors. The red and blue colors of the curves denote $\cos[\mathrm{Im}(S(j)) + \pi j + \eta] \gtrless 0$, respectively.

by the complex saddle point accounts for the sign oscillations of Ω_j. Moreover, Fig. 8.2 shows that the oscillation of $|\cos[\text{Im}(S(j)) + \pi j + \eta]|$ accounts for the subleading oscillations of our numerically computed $\log |\Omega_j|$. Therefore, we find that our finite N numerical data strongly supports the detailed structures of the macroscopic entropy computed at the complex saddle points of Legendre transformation.

As mentioned in the introduction, it seems that our interpretation for the complex saddle point is very universal. To confirm this expectation, it will be helpful to study other index-like generating functions which are simpler than the large N index of the $\mathcal{N} = 4$ Yang-Mills theory. In particular, for the Yang-Mills index, note that the analytic form of $S(j)$ is known only to the leading order in large N and j. Due to this limitation, we added an empirical constant η at a subleading order to see if the structures of $S(j)$ and Ω_j are compatible with each other. So it will be desirable to study simpler examples in which we can easily compute the subleading corrections for the precision tests.

As a simple example, consider the inverse of the MacMahon function,

$$f(x) = \prod_{n=1}^{\infty}(1 - x^n)^n = \exp\left[-\sum_{n=1}^{\infty}\frac{1}{n}\frac{x^n}{(1-x^n)^2}\right] \equiv \sum_{j=0}^{\infty}\Omega_j x^j . \qquad (8.3.4)$$

Numerically, one can easily expand $f(x)$ in power series of x with a computer to very high orders. At large charge j, one can see that the resulting Ω_j's become macroscopic with sign oscillations. We shall now make an analytic evaluation of the asymptotic entropy at $j \gg 1$, with necessary subleading corrections in $\frac{1}{j}$ included. We would like to compute

$$\Omega_j = \frac{1}{2\pi i}\oint\frac{dx}{x}x^{-j}f(x) = \frac{1}{2\pi i}\oint\frac{dx}{x}\exp\left[j\beta - \sum_{n=1}^{\infty}\frac{1}{n}\frac{e^{-n\beta}}{(1-e^{-n\beta})^2}\right] \qquad (8.3.5)$$

where $x \equiv e^{-\beta}$. The saddle point values β_* of β will be small complex numbers

with $\text{Re}(\beta_*) > 0$. At small β, one can use

$$-\sum_{n=1}^{\infty} \frac{1}{n} \frac{e^{-n\beta}}{(1-e^{-n\beta})^2} = -\frac{\zeta(3)}{\beta^2} - \frac{1}{12}\log\beta - \zeta'(-1,0) + \frac{\beta^2}{2880} + \frac{\beta^4}{725760} + \frac{\beta^6}{43545600} + \cdots \; ,$$
(8.3.6)

where $\zeta(s)$ is the Riemann zeta function, and $\zeta'(-1,0) \approx -0.165421$ is the derivative $\zeta'(s,q) \equiv \frac{\partial \zeta(s,q)}{\partial s}$ of the Hurwitz zeta function. Using this formula with higher order corrections in small β, one can approximate the integral (8.3.5) with subleading corrections in $\frac{1}{j}$ included. One finds that the following mutually complex conjugate pair of saddle points are dominant:

$$\beta_*^{\pm} = e^{\pm\frac{\pi i}{3}}\left(\frac{2\zeta(3)}{j}\right)^{\frac{1}{3}} + \frac{1}{36j} + \frac{e^{\mp\frac{\pi i}{3}}}{1296(2\zeta(3)j^5)^{\frac{1}{3}}} + \cdots \; .$$
(8.3.7)

Performing the Gaussian approximations at these two saddle points (with some subleading terms included) and adding the two contributions, one obtains

$$\Omega_j \sim \frac{1}{(2\pi)^{\frac{1}{2}}} \sum_{\pm} \exp\left[\frac{3}{2}e^{\pm\frac{\pi i}{3}}(2\zeta(3)j^2)^{\frac{1}{3}} + \frac{1}{36}\log j - \zeta'(-1,0) - \frac{\log(2\zeta(3))}{36} \mp \frac{\pi i}{36} + \cdots\right]$$

$$\times \left[3e^{\mp\frac{\pi i}{3}}\left(\frac{j^4}{2\zeta(3)}\right)^{\frac{1}{3}} + \frac{1}{4}e^{\pm\frac{\pi i}{3}}\left(\frac{j}{2\zeta(3)}\right)^{\frac{2}{3}} - \frac{1}{216\zeta(3)} + \cdots\right]^{-\frac{1}{2}} \cdot \left[1 + \cdots\right] \; . \; (8.3.8)$$

Here, the three factors on the right hand side come from the saddle point action, the 1-loop determinant, and possible higher loop corrections, respectively. We plot this asymptotic $\log|\Omega_j|$ in Fig. 8.3, together with the dotted plot obtained from the series expansion up to $\mathcal{O}(x^{200})$ order.
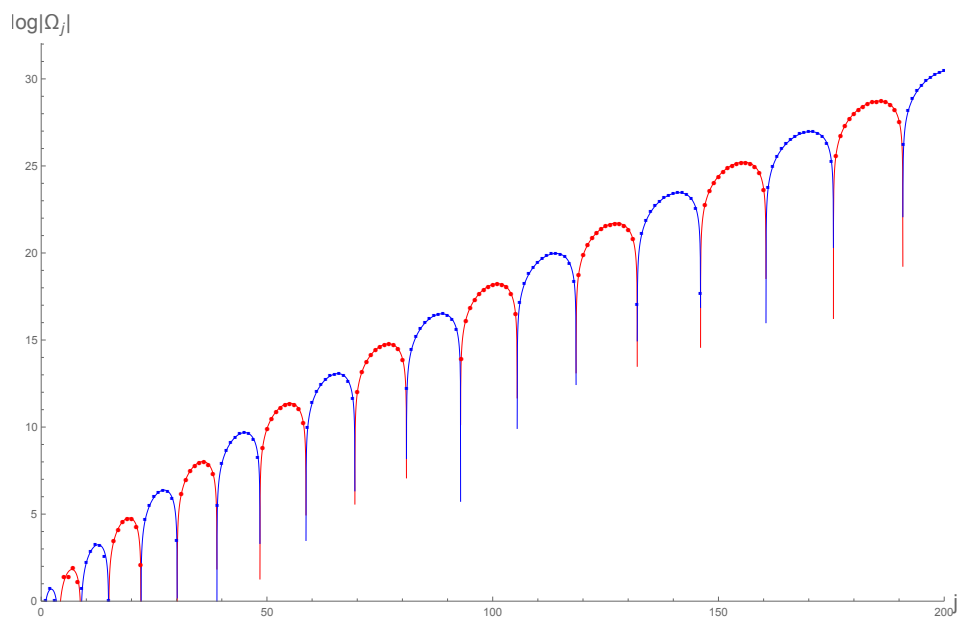
Figure 8.3: Two plots of $\log |\Omega_j|$ for the MacMahon function. Red/blue colors denote the positive/negative signs of Ω_j.

Chapter 9

Comments on deconfinement in AdS/CFT

In this chapter, we study the index of $\mathcal{N} = 4$ Yang-Mills theory on $S^3 \times \mathbb{R}$. We argue that the index should undergo a large N deconfinement phase transition, by computing an upper bound of its 'temperature.' We compute this bound by optimizing the phases of fugacities. The bound we find has some features analogous to the Hagedorn temperature.

9.1 Introduction

In this chapter, we make a small extension of [69] to probe the deconfinement transition from the index. More precisely, we find an upper bound of the transition temperature by studying the local instability of the confining saddle point. Some aspects of this bound is similar to the so-called the Hagedorn temperature [57,59,60]. The similarity arises from the fact that a tachyon condensation instability appears to the confining saddle point [57]. The bound we find is

indeed order 1 in the unit of S^3 radius, obtained by optimizing the phases of fugacities.

We further sketch a possible scenario on how a first order deconfinement transition may happen below our bound. Note that in the partition function of [57], without $(-1)^F$ insertion, there is a plenty of room for this to happen because the partition function depends on the coupling constant. Indeed, studying the interaction effects, [57] suggested a mechanism in which a first order deconfinement transition can happen below the Hagedorn temperature. In the index, this mechanism cannot be realized since one should trust the free QFT calculus. We suggest a new mechanism (without any quantitative studies) of how a deconfinement transition may be realized below our bound in the index.

The remaining part of this chapter is organized as follows. After developing the basic setup at the beginning of section 2, we compute an upper bound of the deconfinement transition temperature from the index in section 2.1, by optimally tuning the phases of fugacities in the index. In section 2.2, we revisit the high temperature Cardy-like behavior studied in [75]. Section 3 concludes with some discussions and remarks.

9.2   The large N index at complex fugacities

The index of 4d $\mathcal{N} = 4$ Yang-Mills theory was found in [68,69]. Its definition is given by

$$Z(\Delta_I, \omega_i) = \mathrm{Tr}\left[(-1)^F e^{-\sum_{I=1}^3 \Delta_I Q_I - \sum_{i=1}^2 \omega_i J_i}\right] , \qquad (9.2.1)$$

with the constraint

$$\Delta_1 + \Delta_2 + \Delta_3 - \omega_1 - \omega_2 = 0 \qquad (9.2.2)$$

on the chemical potentials. Q_I with $I = 1, 2, 3$ are three $U(1)^3 \subset SO(6)$ R-charges, and J_i with $i = 1, 2$ are two $U(1)^2 \subset SO(4)$ angular momentum on

spatial S^3. They are all normalized so that fermionic fields assume $\pm\frac{1}{2}$ eigenvalues. This index counts states whose energy is given by $E = Q_1+Q_2+Q_3+J_1+J_2$, when the S^3 radius is multiplied to E to make it dimensionless. See, e.g. [75] for more explanation on our notation. The free QFT calculus with the $U(N)$ gauge group yields the following unitary matrix integral form of the index [69]:

$$Z = \frac{1}{N!} \int \prod_{a=1}^{N} \frac{d\alpha_a}{2\pi} \cdot \prod_{a<b} \left(2\sin\frac{\alpha_{ab}}{2}\right)^2 \exp\left[\sum_{a,b=1}^{N} \sum_{n=1}^{\infty} \frac{1}{n}\left(1 - \frac{\prod_{I=1}^{3} 2\sinh\frac{n\Delta_I}{2}}{2\sinh\frac{n\omega_1}{2} \cdot 2\sinh\frac{n\omega_2}{2}}\right) e^{in\alpha_{ab}}\right]$$

$$(9.2.3)$$

where $\alpha_{ab} \equiv \alpha_a - \alpha_b$. α_a's are the $U(1)^N \subset U(N)$ gauge holonomies along the temporal circle, if one interprets this as a partition function of a Euclidean QFT on $S^3 \times S^1$.

As pointed out in [75], we shall give nonzero imaginary parts of Δ_I, ω_i compatible with (9.2.2). This will turn out to yield phase factors of fugacities, obstructing 'cancelations' between bosonic/fermionic states at nearby charges. This schematic idea was already explained in the introduction. Making a macroscopic saddle point approximation of the inverse Laplace transformation of the index at charges $\sim N^2$, one wishes to see if one captures macroscopic entropies. Macroscopic charges are insensitive to whether they are integers or half-integers. In particular, it is unclear whether the saddle point approximation computes $+$(degeneracy) or $-$(degeneracy). Due to a rapid oscillation between $\pm$ signs in the index as one changes charges by 'indistinguishable' units, the apparent degeneracy captured by the index may look much smaller than it actually is. Our suggestion is to try to maximally improve this situation by inserting extra phase factors for fugacities, making the rapid oscillation milder, or hopefully absent in favorable cases. A priori, we merely try an optimal obstruction of rapid oscillation, hoping to provide a better lower bound on the true BPS entropy from the index. In case the lower bound saturates the entropy of known

black holes, as in [75], this approach would count them. However, still we modestly have the general possibilities in mind: we seek for possible lower bounds for entropies, which probably will mean upper bounds on various transition temperatures. Conservatively, most of the results in this chapter in principle has to be interpreted this way. However, such bounds will lead to interesting predictions on the gravity duals.

Once we complexify the chemical potentials Δ_I, ω_i, the effective potential for α_a appearing in (9.2.3) (minus log of the integrand) will be complexified. Then the large N saddle points for α_a may deviate from real α_a, i.e. away from the unit circle in the space of $e^{i\alpha_a}$. Finding the large N saddle points in this complex plane appears to be a difficult problem. Here, we first review the large N analysis of the index at real fugacities [69], where the saddle points for $e^{i\alpha_a}$ all stay on the unit circle, and slightly improve it in the following section to see a tachyon instability from the index.

[57, 69] replaces the integrals over a large number of variables α_a by a functional integral over the distribution function $\rho(\theta)$ of N particles on a circle. Here, $\theta \sim \theta + 2\pi$. The exact, or fine-grained, distribution for N particles would have been

$$\rho(\theta) = \frac{1}{N} \sum_{a=1}^{N} \delta(\theta - \alpha_a) = \frac{1}{2\pi N} \sum_{n=-\infty}^{\infty} \sum_{a=1}^{N} e^{in(\theta - \alpha_a)} \ , \qquad (9.2.4)$$

with the normalization $\int_0^{2\pi} d\theta \rho(\theta) = 1$. At large N, with a dense distribution of eigenvalues along the circle, we coarse-grain $\rho(\theta)$ to generic functions. One may Fourier expand $\rho(\theta)$ as

$$\rho(\theta) = \frac{1}{2\pi} + \frac{1}{2\pi} \sum_{n=1}^{\infty} \left[\rho_n e^{in\theta} + \rho_{-n} e^{-in\theta} \right] \quad , \quad \rho_{-n} = \rho_n^* \ . \qquad (9.2.5)$$

This function is subject to the local constraint $\rho(\theta) \geq 0$. The global constraint

$\int_0^{2\pi} d\theta \rho(\theta) = 1$ is already solved in the above expression. In the exact fine-grained expression (9.2.4), the n'th Fourier coefficient ρ_n is given by

$$\rho_n = \frac{1}{N} \sum_{a=1}^{N} e^{-in\alpha_a} \ . \tag{9.2.6}$$

The functional integral form of Z in the large N limit is given by [69]

$$Z = \int \prod_{n=1}^{\infty} [d\rho_n d\rho_{-n}] \exp\left[-N^2 \sum_{n=1}^{\infty} \frac{1}{n} \rho_n \rho_{-n} \frac{\prod_I (1 - e^{-n\Delta_I})}{\prod_i (1 - e^{-n\omega_i})} \right] \ . \tag{9.2.7}$$

Here, in the manipulation, we used $\sum_I \Delta_I = \sum_i \omega_i$.

For simplicity, from now on, let us consider the case with equal charges, $Q_1 = Q_2 = Q_3 \equiv Q$, $J_1 = J_2 \equiv J$. Then one sets $\Delta_1 = \Delta_2 = \Delta_3 \equiv \Delta$, $\omega_1 = \omega_2 \equiv \omega$, satisfying $3\Delta = 2\omega$. We label $e^{-\omega} = x^3$, $e^{-\Delta} = x^2$. Then one finds

$$Z = \int \prod_{n=1}^{\infty} [d\rho_n d\rho_{-n}] \exp\left[-N^2 \sum_{n=1}^{\infty} \frac{f(x^n)}{n} \rho_n \rho_{-n} \right] \tag{9.2.8}$$

with

$$f(x) = \frac{(1 - x^2)^3}{(1 - x^3)^2} \ . \tag{9.2.9}$$

At real fugacity in the physical range $0 < x < 1$, f is positive. This implies that all the mode integrals over ρ_n can be approximated by a Gaussian integral around $\rho_n = 0$. Since the large N saddle point is a uniform distribution $\rho(\theta) = \frac{1}{2\pi}$, one does not have to worry about the positivity constraint $\rho(\theta) \geq 0$. The resulting partition function is given by

$$Z \sim \prod_{n=1}^{\infty} f(x^n)^{-1} = \prod_{n=1}^{\infty} \frac{(1 - x^{3n})^2}{(1 - x^{2n})^3} \ , \tag{9.2.10}$$

and agrees with the index over gravitons in $AdS_5 \times S^5$ [69]. (This analysis was done in [69] with all 4 fugacities kept.) Since the free energy is independent of N, the index does not see deconfinement at arbitrary high 'temperature' (meaning x close to 1, or ω close to 0).

On the other hand, in the partition function without $(-1)^F$ at weak coupling, the term $f(x^n)$ appearing in (9.2.8) is replaced by [57]

$$1 - z_{\mathrm{B}}(x^n) - (-1)^{n-1} z_F(x^n) \ . \tag{9.2.11}$$

z_B and z_F are bosonic and fermionic parts of the 'letter partition function' respectively. This expression turns negative beyond certain values of x, say at $x > x_H$ for $n = 1$. It turns out that the coefficient for $n = 1$ becomes negative first, driving ρ_1 to condense. As discussed in [57], this implies that the low temperature saddle point with $\rho_n = 0$, preserving the 'winding number symmetry' in the Euclidean picture, seize to exist. So one identifies $T_H \equiv -\log x_H$ as the Hagedorn temperature of this system. The actual phase transition to the high temperature deconfining phase may happen below this temperature, and various scenarios at weak but nonzero coupling are discussed in [57]. In any scenarios, T_H is the upper bound for the temperature for which the free energy of the dominant saddle point can be at $\mathcal{O}(N^0)$ order. This allows us to identify T_H as an upper bound for the deconfinement transition temperature.

9.2.1 Instability of the confining saddle point

Now we introduce a phase for x, shifting $x \to xe^{i\phi}$ with real x, $\phi \sim \phi + 2\pi$, and redo the analysis starting from (9.2.8). Now with the complexified effective action, one should allow $e^{i\alpha_a}$'s away from the unit circle at the saddle points. This would mean that one will have to generalize the ansatz from the unit circle to a more general curve on the complex plane. This apparently complicated task will not be discussed here.

We restrict our interest to the fate of the graviton saddle point, focussing on the local fluctuations. In (9.2.8), we are simply asking whether the effective
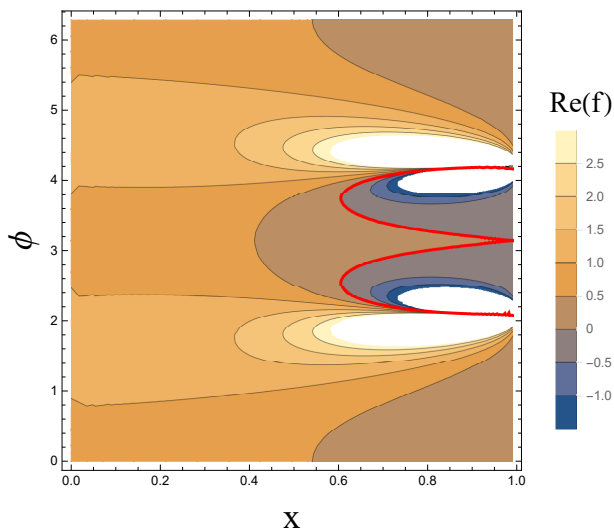
Figure 9.1: Contour plot of $\mathrm{Re}(f)$ on the x-ϕ space. The red line shows the curve $\mathrm{Re}(f) = 0$.

action

$$S_{\mathrm{eff}} = N^2 \sum_{n=1}^{\infty} \frac{f(x^n)}{n} \rho_n \rho_{-n} \tag{9.2.12}$$

is locally stable or not around $\rho_n = 0$. Clearly, even with complex $f(x^n)$, $\rho_n = 0$ will continue to be an extremum under their small variations. One simply has to make sure if the real part of S_{eff} is at its local minimum, and if the imaginary part of it is stationary. If both of these conditions are met, the Gaussian integration of the virtually unconstrained small fluctuations $\delta\rho_n$ (around $\rho_n = 0$) clearly yields the known graviton index on $AdS_5 \times S^5$ [69], simply with complexified fugacities.

The above analysis will hold if $\mathrm{Re}(f(x^n e^{in\phi})) > 0$. If this can go negative at finite $x < 1$, at optimally tuned ϕ, this will imply the disappearance of the graviton saddle point. One should tune ϕ so that $\mathrm{Re}(f)$ becomes 0 at lowest possible x. This is because, with boson/fermion cancelation, we see less spectrum

and the phase transitions apparently look delayed or even become invisible in the index. With minimized boson/fermion cancelations, we can probably see a transition with minimized delay. So we identify the lowest x with $\mathrm{Re}(f) = 0$ as the 'temperature' where tachyon condensation starts. We call this value x_H.

One finds that $\mathrm{Re}(f(xe^{i\phi}))$ as a function of x, ϕ is given by

$$\frac{(1 - x^2)(1 + x^2 - 2x\cos\phi)^2 \left(2x(2 + 5x^2 + 2x^4)\cos\phi + (1 + x^2)(1 + 4x^2 + x^4 + 3x^2\cos(2\phi))\right)}{(1 + x^6 - 2x^3\cos(3\phi))^2} .$$
(9.2.13)

All other factors are positive except the last factor on the numerator. The vanishing condition

$$2x(2 + 5x^2 + 2x^4)\cos\phi + (1 + x^2)(1 + 4x^2 + x^4 + 3x^2\cos(2\phi)) = 0 \quad (9.2.14)$$

is solved by

$$\cos\phi = \frac{-2 - 5x^2 - 2x^4 \pm \sqrt{-2 + 2x^2 + 9x^4 + 2x^6 - 2x^8}}{6x(1 + x^2)} . \quad (9.2.15)$$

This line on the x-ϕ plane is shown in by Fig. 9.1 by the red curve. On the right sides of this curve, one finds $\mathrm{Re}(f) < 0$. In the remaining region, $\mathrm{Re}(f) > 0$.

On the red curve, the minimal value of x (maximal value of chemical potential ω, meaning minimal 'temperature') is obtained when the two solutions for ϕ get degenerate, i.e. when

$$-2 + 2x^2 + 9x^4 + 2x^6 - 2x^8 = 0 . \quad (9.2.16)$$

The relevant solutions is $x_H = \sqrt{\frac{\sqrt{3}-1}{2}} \approx 0.605$. This is the point at which one can optimally tune ϕ to trigger the tachyon condensation at lowest x. The tuned value of ϕ is given by $\cos\phi = -\frac{1}{2x_H}$, i.e. $\phi \approx 0.81\pi$ or $\approx (2 - 0.81)\pi$. The two values of ϕ's are symmetric around $\phi = \pi$, as is manifest from Fig. 9.1. They are at the top of the two dome regions for $\mathrm{Re}(f) \leq 0$. This will set

the upper bound on the actual deconfinement transition temperature. At these points, one finds

$$\omega_H = -3 \log x_H \approx 1.508. \tag{9.2.17}$$

This is higher than the Hawking-Page transition point

$$\omega_{\mathrm{HP}}^{\mathrm{known}} = \frac{\pi}{16} \sqrt{414 - 66\sqrt{33}} \approx 1.159 \tag{9.2.18}$$

of the known black holes, computed in section 2.3 of [75]. See also our section 2.3 below for a review and summary. Our upper bound ω_H^{-1} is lower than the Hawking-Page temperature of known black holes, $\omega_H^{-1} < (\omega_{\mathrm{HP}}^{\mathrm{known}})^{-1}$.

The tachyon instability of ρ_1 has some similarities with the Hagedorn behavior in the partition function of [57]. In particular, as one approaches $x \to x_H$ from below, the density of states exhibits an exponential growth [57]. However, in the index, this feature is not visible in the graviton index (9.2.10). Namely, due to nonzero $\mathrm{Im}(f)$ at x_H, $\cos\theta = -\frac{1}{2x_H}$, the index remains finite even at $x = x_H$.

For $x > x_H$, ρ_1 should condense. The free energy is expected to be of order N^2. In this regime, $\omega < \omega_H$, there seem to be no reason to expect that the true saddle point for $e^{i\alpha_a}$'s be on the unit circle. So it seems that we cannot apply the studies made in [57], beyond the transition.

At $x < x_H$, whether the saddle point with $\rho_n = 0$ is a global one or not is of course unclear. To this end, one should make a more global study, again at more general contour on the space of $e^{i\alpha_a}$.

9.2.2 Cardy limit revisited

Despite the complication stated at the end of section 2.1, due to complex effective action, one can still make a quantitative analysis at $\omega = -3 \log x \ll 1$.

(Here, x means the real modulus of the complex fugacity $xe^{i\phi}$.) This is the so-called 'Cardy limit' studied in [75]. To see this, consider the following 2-body potential

$$
\begin{aligned}
V_{\text{eff}}(\theta) &= -\log\left(2\sin\frac{\theta}{2}\right)^2 + \sum_{n=1}^{\infty}\frac{1}{n}\left(f(x^n e^{in\phi}) - 1\right)\left(e^{in\theta} + e^{-in\theta}\right) \quad (9.2.19) \\
&= -\log\left(2\sin\frac{\theta}{2}\right)^2 + \sum_{n=1}^{\infty}\frac{1}{n}\left(\frac{(1 - x^{2n}e^{2in\phi})^3}{(1 - x^{3n}e^{3in\phi})^2} - 1\right)\left(e^{in\theta} + e^{-in\theta}\right)
\end{aligned}
$$

between two eigenvalues α_a, α_b, where $\theta = \alpha_{ab}$. This leads to a 'force' on the complex θ plane, which is in fact a cylinder with $\theta \sim \theta + 2\pi$, given by

$$
-\frac{\partial V_{\text{eff}}}{\partial \theta} = \cot\frac{\theta}{2} + 2\sum_{n=1}^{\infty}\left(\frac{(1 - x^{2n}e^{2in\phi})^3}{(1 - x^{3n}e^{3in\phi})^2} - 1\right)\sin(n\theta) \ . \qquad (9.2.20)
$$

The first term coming from the Haar measure behaves like $\sim \frac{2}{\theta}$ at small θ, which is repulsive at real θ. Had θ been real and nonzero (even if small), one could have rearranged part of the second term in V_{eff} as

$$
-\sum_{n=1}^{\infty}\frac{1}{n}(e^{in\theta} + e^{-in\theta}) = \log(1 - e^{i\theta})(1 - e^{-i\theta}) = \log\left(2\sin\frac{\theta}{2}\right)^2 \ , \qquad (9.2.21)
$$

canceling the first term of V_{eff}. However, for complex θ, separating terms in the sum over n could be dangerous.

Now let us consider the second term of V_{eff} in the 'high temperature limit' $\omega \to 0^+$. In the index, this limit may or may not be nontrivial, depending on the value of ϕ. For instance, at $\phi = 0$ and $0 < x < 1$, the index will never exhibit a macroscopic entropy as shown in [69]. The crucial reason for this was that $\text{Re}(f(x^n))$ remained positive, as shown in Fig. 9.1 along the x-axis. However, note that beyond $x > x_H = \sqrt{\frac{\sqrt{3}-1}{2}}$, there is a region in the x-ϕ plane which has $\text{Re}(f) < 0$, providing chances for a macroscopic entropy. Even though the analysis of section 2.1 was limited to the situation where $e^{i\alpha_a}$'s sit on the unit circle, it is still an important question whether $\text{Re}(f(x^n e^{in\phi}))$ can go negative,

291

since this will allow $V_{\text{eff}}(\theta)$ to have negative real part even at (small) complex θ. So we carefully re-investigate the results of section 2.1 on the behaviors of $\text{Re}(f(x^n e^{in\phi}))$.

We first study the term with $n = 1$, i.e. $\text{Re}(f(xe^{i\phi}))$. It will turn out that understanding this term will be most important even in the Cardy limit. The region with $\text{Re}(f(xe^{i\phi})) < 0$ is on the right side of the red curve shown in Fig. 9.1, consisting of the 'dome' regions. Therefore, if one wishes to take the Cardy limit $x \to 1^-$, one should again keep ϕ at an optimal value in this region, to maximally obstruct cancelations of nearby bosons/fermions. For the term with $n = 1$, it is easy to see from Fig. 9.1 how to set ϕ, as $x \to 1^-$. This is easily noticed by following the valley of lowest $\text{Re}(f)$ inside the dome. At $x = x_H$, the optimal value was shown to be $\phi = \cos^{-1}\left(-\frac{1}{2x_H}\right) \approx 0.81\pi$. From here, we only consider the lower dome, $\phi \le \pi$. As one further increases x, the value of ϕ which minimizes $\text{Re}(f(xe^{i\phi}))$ will decrease, towards $\phi \searrow \frac{2\pi}{3}$ as $x \to 1^-$. Namely, setting $\phi = \frac{2\pi}{3}$, $\text{Re}(f(xe^{i\phi}))$ will maximally diverge to $-\infty$ as $x \to 1^-$.

We would like to see this behavior more quantitatively, including all other terms at higher n's in V_{eff}. Let us take $x = e^{-\frac{\omega}{3}}$ with $\omega \ll 1$ and $\phi \approx \frac{2\pi}{3}$. Then one finds

$$\frac{(1 - x^{2n}e^{2in\phi})^3}{(1 - x^{3n}e^{3in\phi})^2} \approx \frac{(1 - x^{2n}e^{\frac{4\pi ni}{3}})^3}{(1 - x^{3n})^2} \approx \frac{1}{n^2\omega^2}(1 - e^{\frac{4\pi ni}{3}})^3 . \qquad (9.2.22)$$

At $n \ne 1$, the real part of this term will oscillate in its sign. Therefore, it may not be clear at this stage whether setting $\phi = \frac{2\pi}{3}$ is an ideal one or not. A more general study can be made by setting ϕ to be an arbitrary real number between 0 and 2π, and maximize $\log Z$ or the entropy after all the calculus. This was in fact done in [75] (with maximally deconfining distribution, to be addressed shortly below), which indeed confirms that $\phi = \frac{2\pi}{3}$ is the optimal one. So with this understood, we shall set $\phi = \frac{2\pi}{3}$ in this chapter for the simplicity

of presentation.

Since this term (9.2.22) is dominant in (9.2.20) due to the diverging factor $\frac{1}{\omega^2}$, the vanishing force condition at the leading order requires $\sum_{n=1}^{\infty} \frac{(1-e^{\frac{4\pi in}{3}})^3}{n^2\omega^2} \sin(n\theta) \approx$ $0.$[1] So the leading order solution at small ω is $\theta \approx 0$ for all pairs α_a, α_b, i.e. the maximally deconfining configuration. Since all matters are in the adjoint representation, it does not matter in the leading order in ω whether $e^{i\alpha_a}$'s stay on the unit circle or not. These are precisely the Cardy saddle points considered in [75]. As in [75], we assume the global dominance of this saddle point.

With the discussions in the previous paragraph, we can regard the eigenvalues as asymptotically living on the unit circle. Thus we can use the formula (9.2.12), where ρ_n are Fourier coefficients of the distribution on unit circle. Just like the studies made in section 5.3 of [57] for the maximally deconfining saddle point, we set $\rho_n = 1$ for $\rho(\theta) = \delta(\theta)$. One thus obtains

$$\log Z \sim -S_{\text{eff}} = -N^2 \sum_{n=1}^{\infty} \frac{f(x^n)}{n} \rho_n \rho_{-n} \approx -\frac{N^2}{\omega^2} \sum_{n=1}^{\infty} \frac{(1-e^{\frac{4\pi in}{3}})^3}{n^3} = \frac{3N^2}{\omega^2} \left(\text{Li}_3(e^{\frac{4\pi i}{3}}) - \text{Li}_3(e^{\frac{8\pi i}{3}}) \right) .$$
(9.2.23)

$\text{Li}_3(z) = \sum_{n=1}^{\infty} \frac{z^n}{n^3}$ converges for $|z| < 1$, and also at $|z| = 1$ if $z \neq 1$ (i.e. not at the branch point of this function). Here, note that

$$\text{Li}_3(e^{\frac{4\pi i}{3}}) - \text{Li}_3(e^{\frac{8\pi i}{3}}) = \frac{1}{6} \left(\frac{2\pi i}{3} \right)^3 .$$
(9.2.24)

This can be proved by using an identity of Li_3 and the Bernoulli polynomial B_3, as in [75]. Alternatively, one can confirm this simply by performing the infinite sums on the left hand side. For instance, as a brutal but clearest check, we reconfirmed it numerically by computing the infinite sum till $n = 1000$, finding that both sides are $\approx -1.53117i$. So one obtains

$$\log Z \sim \frac{N^2 \left(\frac{2\pi i}{3} \right)^3}{2\omega^2} ,$$
(9.2.25)

---

[1]A more careful treatment of the sum over n, separating $n \lesssim |\omega|^{-1}$ and $n \gtrsim |\omega|^{-1}$, was presented in [75].

at $\omega \ll 1$. This is the specialization of the Cardy-like formula found in [75, 90],

$$\log Z \sim \frac{N^2 \Delta_1 \Delta_2 \Delta_3}{2\omega_1 \omega_2} \quad , \quad \Delta_1 + \Delta_2 + \Delta_3 - \omega_1 - \omega_2 = 2\pi i \ . \tag{9.2.26}$$

Restricting to the case $\Delta_1 = \Delta_2 = \Delta_3 \equiv \Delta$ and $\omega_1 = \omega_2 \equiv \omega \ll 1$, one obtains $\Delta \approx \frac{2\pi i}{3}$. So (9.2.26) indeed reduces to (9.2.25) in the setting of this subsection.

9.3   Discussions

In this chapter, we pointed out that the index of $\mathcal{N} = 4$ Yang-Mills theory on $S^3 \times \mathbb{R}$ should undergo a large N phase transition. A key idea is to turn on the finite phases of BPS fugacities, to optimally obstruct boson/fermion cancelations of nearby BPS states at macroscopic charges. We compute a temperature which sets an upper bound of the confinement-deconfinement transition of the gauge theory in the BPS sector. Recently, in [249], it was shown that when the action is complex as in our model, due to destructive interference, tachyonic modes do not immediately condense and the deconfinement transition is delayed.

One would hope to better understand the actual transition from the index. We think our calculations and arguments clearly indicate the existence of such a transition, visible in the index. Unfortunately, the large N saddle point analysis of the index appears technically tricky, and we leave this interesting question for future studies. However, the studies of this chapter and of [75] shed concrete lights on the BPS black holes in $AdS_5 \times S^5$.

Turning the logic around, one would also like to find (perhaps unstable) saddle points of the large N index at small charges, to study small AdS black holes in the microcanonical ensemble [250]. For instance, it will be interesting to see if the non-interacting mix picture [116] between the small black hole and the hair can be confirmed from the QFT side. See also [117].

More generally, it will be desirable to further study how rich the landscape of BPS black holes is in $AdS_5 \times S^5$. It is almost certain to us that BPS hairy black holes will be playing prominent roles. The mildly singular nature of BPS hairy black holes, studied in [111,112], might be a clue for better understanding their differences from the previous analytic solutions of [83–86]. It may be helpful to get a better notion on the near-horizon distinction of these two classes of black holes. From the QFT dual side, it will be nice to develop a sharper criterion for the hairiness of the deconfining saddle points. The condensations of certain modes in the bulk force their dual operators to assume expectation values at nonzero BPS chemical potentials. Within the simple consistent truncation of [116], further studied in [111,112,117], the dual operator is easy to identify. With no guarantee that the deconfining saddle points of this chapter and of [75] will be within this truncation ansatz, one should figure out what kind of operators should be considered. Technically, it is also interesting to see whether one can find supersymmetric operators that can be inserted in the index.

It has been found in [75] that the large charge limits of non-hairy black holes [83–86] are counted by the index. This presumably means that they are likely to be the dominant saddle points in the large charge limit. It will be interesting to clarify how this happens: for instance, whether there are further phase transitions to non-hairy black holes, or whether hairy black holes asymptotically become indistinguishable with non-hairy ones. For instance, we find some studies on large rotating AdS black holes [251], which can be made hairy only at very low Hawking temperature. Although these are non-BPS black holes, they may give lessons to large BPS black holes.

Appendix A

Asymptotic behavior and identities of special functions

The q-Pochhammer symbol $(|q| < 1)$ is defined as

$$
(a;q)_n := \prod_{i=0}^{n-1}(1 - aq^i), \quad n > 0,
$$
$$
(a;q)_0 := 1,
$$
$$
(a;q)_n := \frac{1}{(aq^n;q)_{-n}}, \quad n < 0.
$$

(A.0.1)

The Cardy limit $(q \to 1^-)$ of the infinite q-Pochhammer symbol is given by

$$
(aq^m;q^2) \equiv (aq^m;q^2)_\infty = \prod_{i=0}^{\infty}(1 - aq^{m+2i}) , \quad q = e^{-\beta} ,
$$
$$
\lim_{\beta \to 0^+} (aq^m;q^2)_\infty = (1 - aq^m)^{1/2} \exp\left[-\frac{1}{2\beta}\mathrm{Li}_2(aq^m)\right]\left(1 + \mathcal{O}(\beta)\right)
$$
$$
= \exp\left[-\frac{1}{2\beta}\mathrm{Li}_2(aq^{m-1})\right]\left(1 + \mathcal{O}(\beta)\right) , \quad a \in \mathbb{C} \,\&\, a \notin [1,\infty) ,
$$
$$
\lim_{\beta \to 0^+} (q^m;q^2)_\infty = \frac{\sqrt{2\pi}}{\Gamma(m/2)}(2\beta)^{-(m-1)/2} \exp\left[-\frac{1}{2\beta}\mathrm{Li}_2(1)\right]\left(1 + \mathcal{O}(\beta)\right) .
$$

(A.0.2)

These asymptotic formulae (A.0.2) are well-known for $|a| \leq 1$ [252]. To extend it to whole complex plane $\mathbb{C}$, we used the modular property of the Jacobi theta function and the Dedekind eta function. Also note that these asymptotic formulae (A.0.2) have a branch cut along $(1, +\infty)$. For further details, refer to appendix A of [79].

We can extend the definition of the infinite q-Pochhammer symbol to $|q| > 1$ region using the plethystic exponential function as following:

$$(a; q^2)_\infty = \text{PE}\left[-\frac{a}{1-q^2}\right] = \text{PE}\left[\frac{aq^{-2}}{1-q^{-2}}\right] = \text{PE}\left[-\frac{aq^{-2}}{1-q^{-2}}\right]^{-1} = \frac{1}{(aq^{-2}; q^{-2})_\infty} \, .$$
(A.0.3)

Using this formula, one can easily check that the $q \to 1^+$ limit of the infinite q-Pochhammer symbol is given by

$$\lim_{\beta \to 0^-} (aq^m; q^2)_\infty = \exp\left[-\frac{1}{2\beta}\text{Li}_2(aq^{m-1})\right]\left(1 + \mathcal{O}(\beta)\right) , \quad a \in \mathbb{C} \ \& \ a \notin [1, \infty) ,$$
(A.0.4)

i.e. the same as the $q \to 1^-$ limit.

In addition, q-Pochhammer symbol satisfies the following infinite q-binomial theorem;

$$\sum_{n=0}^{\infty} \frac{(a; q^2)_n}{(q^2; q^2)_n} x^n = \frac{(ax; q^2)_\infty}{(x; q^2)_\infty}.$$
(A.0.5)

The polylogarithm function is defined by a power series in a when $|a| < 1$ as

$$\text{Li}_n(a) = \sum_{k=1}^{\infty} \frac{a^k}{k^n} ,$$
(A.0.6)

and can be extended to $|a| \geq 1$ by the process of analytic continuation. Note that the polylogarithm function is multi-valued. It has a branch point at $a = 1$, and we take the principal branch with a branch cut along $(1, +\infty)$ and the principal value range $[0, 2\pi)$. Accordingly, we set the branch cut of the logarithm function as $(0, -\infty)$, i.e. its principal value range is $(-\pi, +\pi]$.

The polylogarithm function satisfies the following inversion formula involving Bernoulli polynomials $B_n(x)$ $(n \in \mathbb{Z})$:

$$\text{Li}_n(a) + (-1)^n \text{Li}_n(1/a) = -\frac{(2\pi i)^n}{n!} B_n\left(\frac{\log a}{2\pi i} - p\right), \quad 2\pi p \leq \text{Im}(\log a) < 2\pi(p+1) \ \& \ |a| \leq 1,$$

$$B_1(x) = x - \frac{1}{2}, \quad B_2(x) = x^2 - x + \frac{1}{6}, \quad B_3(x) = x^3 - \frac{3}{2}x^2 + \frac{1}{2}x, \ \cdots.$$

$$\text{(A.0.7)}$$

Also, the polylogarithm function exhibits the following limiting behavior:

$$\lim_{|a| \to 0} \text{Li}_n(a) = a, \tag{A.0.8}$$

which gives the asymptotic formula of the polylogarithm function when $|a| \to \infty$ from A.0.7.

We also use the theta function defined as following:

$$\theta(a; q^2) \equiv (a; q^2)_\infty (a^{-1} q^2; q^2)_\infty, \tag{A.0.9}$$

whose Cardy limit $\beta \to 0$ is given by

$$\lim_{\beta \to 0} \theta(aq^m; q^2) = \exp\left[-\frac{1}{2\beta}\left(-\frac{1}{2}\log^2(\hat{a}q^{m-1}) + \pi i \log(\hat{a}q^{m-1}) + \frac{\pi^2}{3}\right)\right](1 + \mathcal{O}(\beta)),$$

$$\text{(A.0.10)}$$

where

$$\hat{a} \equiv a e^{-2\pi i p} \quad \Rightarrow \quad \log \hat{a} = \log a - 2\pi i p. \tag{A.0.11}$$

Here, we used (A.0.2) and (A.0.7).

Bibliography

[1] S. Weinberg and E. Witten, *Limits on Massless Particles*, *Phys. Lett. B* **96** (1980) 59.

[2] S. R. Coleman and J. Mandula, *All Possible Symmetries of the S Matrix*, *Phys. Rev.* **159** (1967) 1251.

[3] J. M. Bardeen, B. Carter and S. W. Hawking, *The Four laws of black hole mechanics*, *Commun. Math. Phys.* **31** (1973) 161.

[4] S. W. Hawking, *Gravitational radiation from colliding black holes*, *Phys. Rev. Lett.* **26** (1971) 1344.

[5] J. D. Bekenstein, *Black holes and the second law*, *Lett. Nuovo Cim.* **4** (1972) 737.

[6] S. W. Hawking, *Black hole explosions*, *Nature* **248** (1974) 30.

[7] J. D. Bekenstein, *Generalized second law of thermodynamics in black hole physics*, *Phys. Rev. D* **9** (1974) 3292.

[8] S.-F. Wu, B. Wang, G.-H. Yang and P.-M. Zhang, *The Generalized second law of thermodynamics in generalized gravity theories*, *Class. Quant. Grav.* **25** (2008) 235018 [0801.2688].

[9] D. Lovelock, *The Einstein tensor and its generalizations*, J. Math. Phys. **12** (1971) 498.

[10] S. W. Hawking, *Breakdown of Predictability in Gravitational Collapse*, Phys. Rev. D **14** (1976) 2460.

[11] A. Strominger and C. Vafa, *Microscopic origin of the Bekenstein-Hawking entropy*, Phys. Lett. B **379** (1996) 99 [hep-th/9601029].

[12] J. L. Cardy, *Operator Content of Two-Dimensional Conformally Invariant Theories*, Nucl. Phys. B **270** (1986) 186.

[13] J. Breckenridge, R. C. Myers, A. Peet and C. Vafa, *D-branes and spinning black holes*, Phys. Lett. B **391** (1997) 93 [hep-th/9602065].

[14] J. M. Maldacena and A. Strominger, *Statistical entropy of four-dimensional extremal black holes*, Phys. Rev. Lett. **77** (1996) 428 [hep-th/9603060].

[15] C. V. Johnson, R. R. Khuri and R. C. Myers, *Entropy of 4-D extremal black holes*, Phys. Lett. B **378** (1996) 78 [hep-th/9603061].

[16] R. Emparan and H. S. Reall, *A Rotating black ring solution in five-dimensions*, Phys. Rev. Lett. **88** (2002) 101101 [hep-th/0110260].

[17] H. Elvang, *A Charged rotating black ring*, Phys. Rev. D **68** (2003) 124016 [hep-th/0305247].

[18] H. Elvang and R. Emparan, *Black rings, supertubes, and a stringy resolution of black hole nonuniqueness*, JHEP **11** (2003) 035 [hep-th/0310008].

[19] R. Emparan, *Rotating circular strings, and infinite nonuniqueness of black rings*, *JHEP* **03** (2004) 064 [`hep-th/0402149`].

[20] H. Elvang, R. Emparan, D. Mateos and H. S. Reall, *A Supersymmetric black ring*, *Phys. Rev. Lett.* **93** (2004) 211302 [`hep-th/0407065`].

[21] H. Elvang, R. Emparan, D. Mateos and H. S. Reall, *Supersymmetric black rings and three-charge supertubes*, *Phys. Rev. D* **71** (2005) 024033 [`hep-th/0408120`].

[22] I. Bena and N. P. Warner, *One ring to rule them all ... and in the darkness bind them?*, *Adv. Theor. Math. Phys.* **9** (2005) 667 [`hep-th/0408106`].

[23] M. Cyrier, M. Guica, D. Mateos and A. Strominger, *Microscopic entropy of the black ring*, *Phys. Rev. Lett.* **94** (2005) 191601 [`hep-th/0411187`].

[24] J. M. Maldacena, A. Strominger and E. Witten, *Black hole entropy in M theory*, *JHEP* **12** (1997) 002 [`hep-th/9711053`].

[25] J. D. Bekenstein, *A Universal Upper Bound on the Entropy to Energy Ratio for Bounded Systems*, *Phys. Rev. D* **23** (1981) 287.

[26] G. 't Hooft, *Dimensional reduction in quantum gravity*, *Conf. Proc. C* **930308** (1993) 284 [`gr-qc/9310026`].

[27] L. Susskind, *The World as a hologram*, *J. Math. Phys.* **36** (1995) 6377 [`hep-th/9409089`].

[28] S. Hawking and S. F. Ross, *Duality between electric and magnetic black holes*, *Phys. Rev. D* **52** (1995) 5865 [`hep-th/9504019`].

[29] E. Witten, *SL(2,Z) action on three-dimensional conformal field theories with Abelian symmetry*, in *From Fields to Strings: Circumnavigating Theoretical Physics: A Conference in Tribute to Ian Kogan*, pp. 1173–1200, 7, 2003, `hep-th/0307041`.

[30] D. Marolf and S. F. Ross, *Boundary Conditions and New Dualities: Vector Fields in AdS/CFT*, *JHEP* **11** (2006) 085 [`hep-th/0606113`].

[31] O. Aharony, M. Berkooz, D. Tong and S. Yankielowicz, *Confinement in Anti-de Sitter Space*, *JHEP* **02** (2013) 076 [`1210.5195`].

[32] J. de Boer, E. P. Verlinde and H. L. Verlinde, *On the holographic renormalization group*, *JHEP* **08** (2000) 003 [`hep-th/9912012`].

[33] J. de Boer, *The Holographic renormalization group*, *Fortsch. Phys.* **49** (2001) 339 [`hep-th/0101026`].

[34] G. 't Hooft, *A Planar Diagram Theory for Strong Interactions*, *Nucl. Phys. B* **72** (1974) 461.

[35] O. Aharony, S. S. Gubser, J. M. Maldacena, H. Ooguri and Y. Oz, *Large N field theories, string theory and gravity*, *Phys. Rept.* **323** (2000) 183 [`hep-th/9905111`].

[36] J. M. Maldacena, *The Large N limit of superconformal field theories and supergravity*, *Int. J. Theor. Phys.* **38** (1999) 1113 [`hep-th/9711200`].

[37] S. S. Gubser, I. R. Klebanov and A. M. Polyakov, *Gauge theory correlators from noncritical string theory*, *Phys. Lett. B* **428** (1998) 105 [`hep-th/9802109`].

[38] E. Witten, *Anti-de Sitter space and holography*, *Adv. Theor. Math. Phys.* **2** (1998) 253 [`hep-th/9802150`].

[39] J. Kaplan, *Lectures on AdS/CFT from the Bottom Up*, .

[40] J. McGreevy, *Holographic duality with a view toward many-body physics*, *Adv. High Energy Phys.* **2010** (2010) 723105 [`0909.0518`].

[41] J. Polchinski, *Introduction to Gauge/Gravity Duality*, in *Theoretical Advanced Study Institute in Elementary Particle Physics: String theory and its Applications: From meV to the Planck Scale*, pp. 3–46, 10, 2010, `1010.6134`, DOI.

[42] J. Penedones, *TASI lectures on AdS/CFT*, in *Theoretical Advanced Study Institute in Elementary Particle Physics: New Frontiers in Fields and Strings*, pp. 75–136, 2017, `1608.04948`, DOI.

[43] R. Bousso, *The Holographic principle*, *Rev. Mod. Phys.* **74** (2002) 825 [`hep-th/0203101`].

[44] O. Aharony, O. Bergman, D. L. Jafferis and J. Maldacena, *N=6 superconformal Chern-Simons-matter theories, M2-branes and their gravity duals*, *JHEP* **10** (2008) 091 [`0806.1218`].

[45] E. Witten, *Some comments on string dynamics*, in *STRINGS 95: Future Perspectives in String Theory*, pp. 501–523, 7, 1995, `hep-th/9507121`.

[46] A. Strominger, *Open p-branes*, *Phys. Lett. B* **383** (1996) 44 [`hep-th/9512059`].

[47] N. Seiberg, *Five-dimensional SUSY field theories, nontrivial fixed points and string dynamics*, *Phys. Lett. B* **388** (1996) 753 [`hep-th/9608111`].

[48] K. A. Intriligator, D. R. Morrison and N. Seiberg, *Five-dimensional supersymmetric gauge theories and degenerations of Calabi-Yau spaces*, *Nucl. Phys. B* **497** (1997) 56 [`hep-th/9702198`].

[49] A. Brandhuber and Y. Oz, *The D-4 - D-8 brane system and five-dimensional fixed points, Phys. Lett. B* **460** (1999) 307 [`hep-th/9905148`].

[50] O. Bergman and D. Rodriguez-Gomez, *5d quivers and their AdS(6) duals, JHEP* **07** (2012) 171 [`1206.3503`].

[51] O. Bergman, D. Rodríguez-Gómez and G. Zafrir, *5d superconformal indices at large N and holography, JHEP* **08** (2013) 081 [`1305.6870`].

[52] I. Klebanov and A. Polyakov, *AdS dual of the critical O(N) vector model, Phys. Lett. B* **550** (2002) 213 [`hep-th/0210114`].

[53] S. Giombi and X. Yin, *Higher Spin Gauge Theory and Holography: The Three-Point Functions, JHEP* **09** (2010) 115 [`0912.3462`].

[54] T. Hartman, C. A. Keller and B. Stoica, *Universal Spectrum of 2d Conformal Field Theory in the Large c Limit, JHEP* **09** (2014) 118 [`1405.5137`].

[55] S. Hawking and D. N. Page, *Thermodynamics of Black Holes in anti-De Sitter Space, Commun. Math. Phys.* **87** (1983) 577.

[56] E. Witten, *Anti-de Sitter space, thermal phase transition, and confinement in gauge theories, Adv. Theor. Math. Phys.* **2** (1998) 505 [`hep-th/9803131`].

[57] O. Aharony, J. Marsano, S. Minwalla, K. Papadodimas and M. Van Raamsdonk, *The Hagedorn - deconfinement phase transition in weakly coupled large N gauge theories, Adv. Theor. Math. Phys.* **8** (2004) 603 [`hep-th/0310285`].

[58] D. J. Gross and E. Witten, *Possible Third Order Phase Transition in the Large N Lattice Gauge Theory*, Phys. Rev. D **21** (1980) 446.

[59] R. Hagedorn, *Statistical thermodynamics of strong interactions at high-energies*, Nuovo Cim. Suppl. **3** (1965) 147.

[60] J. J. Atick and E. Witten, *The Hagedorn Transition and the Number of Degrees of Freedom of String Theory*, Nucl. Phys. B **310** (1988) 291.

[61] A. M. Polyakov, *Thermal Properties of Gauge Fields and Quark Liberation*, Phys. Lett. B **72** (1978) 477.

[62] L. Susskind, *Lattice Models of Quark Confinement at High Temperature*, Phys. Rev. D **20** (1979) 2610.

[63] G. 't Hooft, *On the Phase Transition Towards Permanent Quark Confinement*, Nucl. Phys. B **138** (1978) 1.

[64] I. R. Klebanov and A. A. Tseytlin, *Entropy of near extremal black p-branes*, Nucl. Phys. B **475** (1996) 164 [`hep-th/9604089`].

[65] N. Drukker, M. Marino and P. Putrov, *From weak to strong coupling in ABJM theory*, Commun. Math. Phys. **306** (2011) 511 [`1007.3837`].

[66] C. P. Herzog, I. R. Klebanov, S. S. Pufu and T. Tesileanu, *Multi-Matrix Models and Tri-Sasaki Einstein Spaces*, Phys. Rev. D **83** (2011) 046001 [`1011.5487`].

[67] D. L. Jafferis and S. S. Pufu, *Exact results for five-dimensional superconformal field theories with gravity duals*, JHEP **05** (2014) 032 [`1207.4359`].

[68] C. Romelsberger, *Counting chiral primaries in N = 1, d=4 superconformal field theories*, *Nucl. Phys. B* **747** (2006) 329 [hep-th/0510060].

[69] J. Kinney, J. M. Maldacena, S. Minwalla and S. Raju, *An Index for 4 dimensional super conformal theories*, *Commun. Math. Phys.* **275** (2007) 209 [hep-th/0510251].

[70] J. Bhattacharya, S. Bhattacharyya, S. Minwalla and S. Raju, *Indices for Superconformal Field Theories in 3,5 and 6 Dimensions*, *JHEP* **02** (2008) 064 [0801.1435].

[71] E. Witten, *Constraints on Supersymmetry Breaking*, *Nucl. Phys. B* **202** (1982) 253.

[72] V. Pestun et al., *Localization techniques in quantum field theories*, *J. Phys. A* **50** (2017) 440301 [1608.02952].

[73] L. Di Pietro and Z. Komargodski, *Cardy formulae for SUSY theories in d = 4 and d = 6*, *JHEP* **12** (2014) 031 [1407.6061].

[74] S. Choi, C. Hwang, S. Kim and J. Nahmgoong, *Entropy Functions of BPS Black Holes in AdS$_4$ and AdS$_6$*, *J. Korean Phys. Soc.* **76** (2020) 101 [1811.02158].

[75] S. Choi, J. Kim, S. Kim and J. Nahmgoong, *Large AdS black holes from QFT*, 1810.12067.

[76] S. Choi, J. Kim, S. Kim and J. Nahmgoong, *Comments on deconfinement in AdS/CFT*, 1811.08646.

[77] S. Choi and C. Hwang, *Universal 3d Cardy Block and Black Hole Entropy*, *JHEP* **03** (2020) 068 [1911.01448].

[78] S. Choi and S. Kim, *Large AdS$_6$ black holes from CFT$_5$*, 1904.01164.

[79] S. Choi, C. Hwang and S. Kim, *Quantum vortices, M2-branes and black holes*, 1908.02470.

[80] P. Agarwal, S. Choi, J. Kim, S. Kim and J. Nahmgoong, *AdS black holes and finite N indices*, 2005.11240.

[81] V. Kostelecky and M. J. Perry, *Solitonic black holes in gauged N=2 supergravity*, *Phys. Lett. B* **371** (1996) 191 [hep-th/9512222].

[82] M. Cvetic, G. Gibbons, H. Lu and C. Pope, *Rotating black holes in gauged supergravities: Thermodynamics, supersymmetric limits, topological solitons and time machines*, hep-th/0504080.

[83] J. B. Gutowski and H. S. Reall, *Supersymmetric AdS(5) black holes*, *JHEP* **02** (2004) 006 [hep-th/0401042].

[84] J. B. Gutowski and H. S. Reall, *General supersymmetric AdS(5) black holes*, *JHEP* **04** (2004) 048 [hep-th/0401129].

[85] Z. Chong, M. Cvetic, H. Lu and C. Pope, *Five-dimensional gauged supergravity black holes with independent rotation parameters*, *Phys. Rev. D* **72** (2005) 041901 [hep-th/0505112].

[86] H. K. Kunduri, J. Lucietti and H. S. Reall, *Supersymmetric multi-charge AdS(5) black holes*, *JHEP* **04** (2006) 036 [hep-th/0601156].

[87] D. D. Chow, *Charged rotating black holes in six-dimensional gauged supergravity*, *Class. Quant. Grav.* **27** (2010) 065004 [0808.2728].

[88] Z.-W. Chong, M. Cvetic, H. Lu and C. Pope, *Non-extremal charged rotating black holes in seven-dimensional gauged supergravity*, *Phys. Lett. B* **626** (2005) 215 [`hep-th/0412094`].

[89] D. D. Chow, *Equal charge black holes and seven dimensional gauged supergravity*, *Class. Quant. Grav.* **25** (2008) 175010 [`0711.1975`].

[90] S. M. Hosseini, K. Hristov and A. Zaffaroni, *An extremization principle for the entropy of rotating BPS black holes in AdS$_5$*, *JHEP* **07** (2017) 106 [`1705.05383`].

[91] S. M. Hosseini, K. Hristov and A. Zaffaroni, *A note on the entropy of rotating BPS AdS$_7 \times S^4$ black holes*, *JHEP* **05** (2018) 121 [`1803.07568`].

[92] A. Cabo-Bizet, D. Cassani, D. Martelli and S. Murthy, *Microscopic origin of the Bekenstein-Hawking entropy of supersymmetric AdS$_5$ black holes*, *JHEP* **10** (2019) 062 [`1810.11442`].

[93] D. Cassani and L. Papini, *The BPS limit of rotating AdS black hole thermodynamics*, *JHEP* **09** (2019) 079 [`1906.10148`].

[94] Z.-W. Chong, M. Cvetic, H. Lu and C. Pope, *Charged rotating black holes in four-dimensional gauged and ungauged supergravities*, *Nucl. Phys. B* **717** (2005) 246 [`hep-th/0411045`].

[95] D. D. K. Chow and G. Compère, *Dyonic AdS black holes in maximal gauged supergravity*, *Phys. Rev. D* **89** (2014) 065003 [`1311.1204`].

[96] S. Choi, D. Gang and N. Kim, *Black holes and Large N complex saddles in 3D-3D correspondence*, `2012.10944`.

[97] K. Hristov, S. Katmadas and C. Toldo, *Matter-coupled supersymmetric Kerr-Newman-AdS$_4$ black holes*, *Phys. Rev. D* **100** (2019) 066016 [1907.05192].

[98] M. Cvetic, M. Duff, P. Hoxha, J. T. Liu, H. Lu, J. Lu et al., *Embedding AdS black holes in ten-dimensions and eleven-dimensions*, *Nucl. Phys. B* **558** (1999) 96 [hep-th/9903214].

[99] J. P. Gauntlett, S. Kim, O. Varela and D. Waldram, *Consistent supersymmetric Kaluza-Klein truncations with massive modes*, *JHEP* **04** (2009) 102 [0901.0676].

[100] S. Lee and D. Yokoyama, *Geometric free energy of toric AdS$_4$/CFT$_3$ models*, *JHEP* **03** (2015) 103 [1412.8703].

[101] E. D'Hoker, M. Gutperle, A. Karch and C. F. Uhlemann, *Warped AdS$_6 \times S^2$ in Type IIB supergravity I: Local solutions*, *JHEP* **08** (2016) 046 [1606.01254].

[102] E. D'Hoker, M. Gutperle and C. F. Uhlemann, *Warped AdS$_6 \times S^2$ in Type IIB supergravity II: Global solutions and five-brane webs*, *JHEP* **05** (2017) 131 [1703.08186].

[103] E. D'Hoker, M. Gutperle and C. F. Uhlemann, *Warped AdS$_6 \times S^2$ in Type IIB supergravity III: Global solutions with seven-branes*, *JHEP* **11** (2017) 200 [1706.00433].

[104] F. Apruzzi, M. Fazzi, A. Passias, D. Rosa and A. Tomasiello, *AdS$_6$ solutions of type II supergravity*, *JHEP* **11** (2014) 099 [1406.0852].

[105] H. Kim, N. Kim and M. Suh, *Supersymmetric AdS$_6$ Solutions of Type IIB Supergravity*, *Eur. Phys. J. C* **75** (2015) 484 [1506.05480].

[106] M. Cvetic, H. Lu and C. Pope, *Gauged six-dimensional supergravity from massive type IIA*, *Phys. Rev. Lett.* **83** (1999) 5226 [hep-th/9906221].

[107] M. Berkooz, D. Reichmann and J. Simon, *A Fermi Surface Model for Large Supersymmetric AdS(5) Black Holes*, *JHEP* **01** (2007) 048 [hep-th/0604023].

[108] M. Berkooz and D. Reichmann, *Weakly Renormalized Near 1/16 SUSY Fermi Liquid Operators in N=4 SYM*, *JHEP* **10** (2008) 084 [0807.0559].

[109] L. Grant, P. A. Grassi, S. Kim and S. Minwalla, *Comments on 1/16 BPS Quantum States and Classical Configurations*, *JHEP* **05** (2008) 049 [0803.4183].

[110] C.-M. Chang and X. Yin, *1/16 BPS states in $\mathcal{N} = 4$ super-Yang-Mills theory*, *Phys. Rev. D* **88** (2013) 106005 [1305.6314].

[111] J. Markeviciute, *Rotating Hairy Black Holes in $AdS_5 \times S^5$*, *JHEP* **03** (2019) 110 [1809.04084].

[112] J. Markeviciute and J. E. Santos, *Evidence for the existence of a novel class of supersymmetric black holes with $AdS_5 \times S^5$ asymptotics*, *Class. Quant. Grav.* **36** (2019) 02LT01 [1806.01849].

[113] A. Gadde, L. Rastelli, S. S. Razamat and W. Yan, *Gauge Theories and Macdonald Polynomials*, *Commun. Math. Phys.* **319** (2013) 147 [1110.3740].

[114] A. Arabi Ardehali, *High-temperature asymptotics of supersymmetric partition functions*, *JHEP* **07** (2016) 025 [1512.03376].

[115] J. Bourdier, N. Drukker and J. Felix, *The exact Schur index of $\mathcal{N} = 4$ SYM*, *JHEP* **11** (2015) 210 [1507.08659].

[116] S. Bhattacharyya, S. Minwalla and K. Papadodimas, *Small Hairy Black Holes in $AdS_5 x S^5$*, *JHEP* **11** (2011) 035 [`1005.1287`].

[117] J. Markeviciute and J. E. Santos, *Hairy black holes in $AdS_5 \times S^5$*, *JHEP* **06** (2016) 096 [`1602.03893`].

[118] S. Ferrara, R. Kalosh and A. Strominger, *N=2 extremal black holes*, *Phys. Rev. D* **52** (1995) 5412 [`hep-th/9508072`].

[119] F. Denef, *Supergravity flows and D-brane stability*, *JHEP* **08** (2000) 050 [`hep-th/0005049`].

[120] J. P. Gauntlett and J. B. Gutowski, *Concentric black rings*, *Phys. Rev. D* **71** (2005) 025013 [`hep-th/0408010`].

[121] J. P. Gauntlett and J. B. Gutowski, *General concentric black rings*, *Phys. Rev. D* **71** (2005) 045002 [`hep-th/0408122`].

[122] D. Berenstein, *A Toy model for the AdS / CFT correspondence*, *JHEP* **07** (2004) 018 [`hep-th/0403110`].

[123] H. Lin, O. Lunin and J. M. Maldacena, *Bubbling AdS space and 1/2 BPS geometries*, *JHEP* **10** (2004) 025 [`hep-th/0409174`].

[124] H.-C. Kim, S.-S. Kim and K. Lee, *5-dim Superconformal Index with Enhanced En Global Symmetry*, *JHEP* **10** (2012) 142 [`1206.6781`].

[125] N. A. Nekrasov, *Seiberg-Witten prepotential from instanton counting*, *Adv. Theor. Math. Phys.* **7** (2003) 831 [`hep-th/0206161`].

[126] S. M. Hosseini, I. Yaakov and A. Zaffaroni, *Topologically twisted indices in five dimensions and holography*, *JHEP* **11** (2018) 119 [`1808.06626`].

[127] S. M. Hosseini, K. Hristov, A. Passias and A. Zaffaroni, *6D attractors and black hole microstates*, *JHEP* **12** (2018) 001 [1809.10685].

[128] D. R. Morrison and N. Seiberg, *Extremal transitions and five-dimensional supersymmetric field theories*, *Nucl. Phys. B* **483** (1997) 229 [hep-th/9609070].

[129] M. R. Douglas, S. H. Katz and C. Vafa, *Small instantons, Del Pezzo surfaces and type I-prime theory*, *Nucl. Phys. B* **497** (1997) 155 [hep-th/9609071].

[130] O. J. Ganor, D. R. Morrison and N. Seiberg, *Branes, Calabi-Yau spaces, and toroidal compactification of the N=1 six-dimensional E(8) theory*, *Nucl. Phys. B* **487** (1997) 93 [hep-th/9610251].

[131] U. H. Danielsson, G. Ferretti, J. Kalkkinen and P. Stjernberg, *Notes on supersymmetric gauge theories in five-dimensions and six-dimensions*, *Phys. Lett. B* **405** (1997) 265 [hep-th/9703098].

[132] C. Hwang, J. Kim, S. Kim and J. Park, *General instanton counting and 5d SCFT*, *JHEP* **07** (2015) 063 [1406.6793].

[133] N. Nekrasov and S. Shadchin, *ABCD of instantons*, *Commun. Math. Phys.* **252** (2004) 359 [hep-th/0404225].

[134] S. Shadchin, *On certain aspects of string theory/gauge theory correspondence*, other thesis, 2, 2005.

[135] F. Benini and P. Milan, *Black Holes in 4D $\mathcal{N}$=4 Super-Yang-Mills Field Theory*, *Phys. Rev. X* **10** (2020) 021037 [1812.09613].

[136] M. Honda, *Quantum Black Hole Entropy from 4d Supersymmetric Cardy formula*, *Phys. Rev. D* **100** (2019) 026008 [1901.08091].

[137] A. Arabi Ardehali, *Cardy-like asymptotics of the 4d $\mathcal{N} = 4$ index and AdS$_5$ blackholes*, *JHEP* **06** (2019) 134 [1902.06619].

[138] J. Kim, S. Kim and J. Song, *A 4d N=1 Cardy Formula*, 1904.03455.

[139] S. R. Wadia, *N = Infinity Phase Transition in a Class of Exactly Soluble Model Lattice Gauge Theories*, *Phys. Lett. B* **93** (1980) 403.

[140] M. Marino, *Spectral Theory and Mirror Symmetry*, *Proc. Symp. Pure Math.* **98** (2018) 259 [1506.07757].

[141] B. Collie and D. Tong, *The Partonic Nature of Instantons*, *JHEP* **08** (2009) 006 [0905.2267].

[142] S. Bolognesi and K. Lee, *Instanton Partons in 5-dim SU(N) Gauge Theory*, *Phys. Rev. D* **84** (2011) 106001 [1106.3664].

[143] P. Jefferson, H.-C. Kim, C. Vafa and G. Zafrir, *Towards Classification of 5d SCFTs: Single Gauge Node*, 1705.05836.

[144] P. Jefferson, S. Katz, H.-C. Kim and C. Vafa, *On Geometric Classification of 5d SCFTs*, *JHEP* **04** (2018) 103 [1801.04036].

[145] H. Hayashi, S.-S. Kim, K. Lee and F. Yagi, *5-brane webs for 5d $\mathcal{N} = 1$ G_2 gauge theories*, *JHEP* **03** (2018) 125 [1801.03916].

[146] H. Hayashi, S.-S. Kim, K. Lee and F. Yagi, *Dualities and 5-brane webs for 5d rank 2 SCFTs*, *JHEP* **12** (2018) 016 [1806.10569].

[147] H. Hayashi, S.-S. Kim, K. Lee and F. Yagi, *Rank-3 antisymmetric matter on 5-brane webs*, *JHEP* **05** (2019) 133 [1902.04754].

[148] M. Fluder and C. F. Uhlemann, *Precision Test of AdS$_6$/CFT$_5$ in Type IIB String Theory*, *Phys. Rev. Lett.* **121** (2018) 171603 [1806.08374].

[149] M. Fluder, S. M. Hosseini and C. F. Uhlemann, *Black hole microstate counting in Type IIB from 5d SCFTs*, JHEP **05** (2019) 134 [1902.05074].

[150] H.-C. Kim and S. Kim, *M5-branes from gauge theories on the 5-sphere*, JHEP **05** (2013) 144 [1206.6339].

[151] J. Kallen, J. Minahan, A. Nedelin and M. Zabzine, N^3-*behavior from 5D Yang-Mills theory*, JHEP **10** (2012) 184 [1207.3763].

[152] G. Lockhart and C. Vafa, *Superconformal Partition Functions and Non-perturbative Topological Strings*, JHEP **10** (2018) 051 [1210.5909].

[153] H.-C. Kim, J. Kim and S. Kim, *Instantons on the 5-sphere and M5-branes*, 1211.0144.

[154] J. A. Minahan, A. Nedelin and M. Zabzine, *5D super Yang-Mills theory and the correspondence to AdS_7/CFT_6*, J. Phys. A **46** (2013) 355401 [1304.1016].

[155] H.-C. Kim, S. Kim, S.-S. Kim and K. Lee, *The general M5-brane superconformal index*, 1307.7660.

[156] J. A. Harvey, R. Minasian and G. W. Moore, *NonAbelian tensor multiplet anomalies*, JHEP **09** (1998) 004 [hep-th/9808060].

[157] T. Maxfield and S. Sethi, *The Conformal Anomaly of M5-Branes*, JHEP **06** (2012) 075 [1204.2002].

[158] S. Kim and J. Nahmgoong, *Asymptotic M5-brane entropy from S-duality*, JHEP **12** (2017) 120 [1702.04058].

[159] J. Nahmgoong, *6d superconformal Cardy formulas*, 1907.12582.

[160] F. Benini, K. Hristov and A. Zaffaroni, *Black hole microstates in AdS$_4$ from supersymmetric localization*, JHEP **05** (2016) 054 [1511.04085].

[161] F. Benini, K. Hristov and A. Zaffaroni, *Exact microstate counting for dyonic black holes in AdS4*, Phys. Lett. B **771** (2017) 462 [1608.07294].

[162] A. Kapustin, B. Willett and I. Yaakov, *Nonperturbative Tests of Three-Dimensional Dualities*, JHEP **10** (2010) 013 [1003.5694].

[163] D. Gang, E. Koh, K. Lee and J. Park, *ABCD of 3d $\mathcal{N} = 8$ and 4 Superconformal Field Theories*, 1108.3647.

[164] J. Bhattacharya and S. Minwalla, *Superconformal Indices for N = 6 Chern Simons Theories*, JHEP **01** (2009) 014 [0806.3251].

[165] S. Kim, *The Complete superconformal index for N=6 Chern-Simons theory*, Nucl. Phys. B **821** (2009) 241 [0903.4172].

[166] O. Aharony, S. Giombi, G. Gur-Ari, J. Maldacena and R. Yacoby, *The Thermal Free Energy in Large N Chern-Simons-Matter Theories*, JHEP **03** (2013) 121 [1211.4843].

[167] S. Jain, S. Minwalla, T. Sharma, T. Takimi, S. R. Wadia and S. Yokoyama, *Phases of large N vector Chern-Simons theories on $S^2 \times S^1$*, JHEP **09** (2013) 009 [1301.6169].

[168] J. Bagger and N. Lambert, *Modeling Multiple M2's*, Phys. Rev. D **75** (2007) 045020 [hep-th/0611108].

[169] J. Bagger and N. Lambert, *Gauge symmetry and supersymmetry of multiple M2-branes*, Phys. Rev. D **77** (2008) 065008 [0711.0955].

[170] A. Gustavsson, *Algebraic structures on parallel M2-branes*, *Nucl. Phys. B* **811** (2009) 66 [`0709.1260`].

[171] Y. Yoshida and K. Sugiyama, *Localization of 3d $\mathcal{N} = 2$ Supersymmetric Theories on $S^1 \times D^2$*, `1409.6713`.

[172] D. Gaiotto, L. Rastelli and S. S. Razamat, *Bootstrapping the superconformal index with surface defects*, *JHEP* **01** (2013) 022 [`1207.3577`].

[173] D. Gaiotto and E. Witten, *S-Duality of Boundary Conditions In N=4 Super Yang-Mills Theory*, *Adv. Theor. Math. Phys.* **13** (2009) 721 [`0807.3720`].

[174] H.-C. Kim, J. Kim, S. Kim and K. Lee, *Vortices and 3 dimensional dualities*, `1204.3895`.

[175] S. Pasquetti, *Factorisation of N = 2 Theories on the Squashed 3-Sphere*, *JHEP* **04** (2012) 120 [`1111.6905`].

[176] C. Beem, T. Dimofte and S. Pasquetti, *Holomorphic Blocks in Three Dimensions*, *JHEP* **12** (2014) 177 [`1211.1986`].

[177] C. Hwang, H.-C. Kim and J. Park, *Factorization of the 3d superconformal index*, *JHEP* **08** (2014) 018 [`1211.6023`].

[178] M. Taki, *Holomorphic Blocks for 3d Non-abelian Partition Functions*, `1303.5915`.

[179] M. Fujitsuka, M. Honda and Y. Yoshida, *Higgs branch localization of 3d $\mathcal{N} = 2$ theories*, *PTEP* **2014** (2014) 123B02 [`1312.3627`].

[180] F. Benini and W. Peelaers, *Higgs branch localization in three dimensions*, *JHEP* **05** (2014) 030 [1312.6078].

[181] F. Benini and A. Zaffaroni, *A topologically twisted index for three-dimensional supersymmetric theories*, *JHEP* **07** (2015) 127 [1504.03698].

[182] C. Hwang and J. Park, *Factorization of the 3d superconformal index with an adjoint matter*, *JHEP* **11** (2015) 028 [1506.03951].

[183] C. Hwang, H. Kim and J. Park, *On 3d Seiberg-Like Dualities with Two Adjoints*, *Fortsch. Phys.* **66** (2018) 1800064 [1807.06198].

[184] Y. Imamura and S. Yokoyama, *Index for three dimensional superconformal field theories with general R-charge assignments*, *JHEP* **04** (2011) 007 [1101.0557].

[185] T. Dimofte, D. Gaiotto and S. Gukov, *3-Manifolds and 3d Indices*, *Adv. Theor. Math. Phys.* **17** (2013) 975 [1112.5179].

[186] S. Pasquetti and M. Sacchi, *From 3d dualities to 2d free field correlators and back*, *JHEP* **11** (2019) 081 [1903.10817].

[187] F. Nieri and S. Pasquetti, *Factorisation and holomorphic blocks in 4d*, *JHEP* **11** (2015) 155 [1507.00261].

[188] L. F. Alday, D. Gaiotto and Y. Tachikawa, *Liouville Correlation Functions from Four-dimensional Gauge Theories*, *Lett. Math. Phys.* **91** (2010) 167 [0906.3219].

[189] M. Aganagic, N. Haouzi, C. Kozcaz and S. Shakirov, *Gauge/Liouville Triality*, 1309.1687.

[190] M. Aganagic, N. Haouzi and S. Shakirov, A_n-*Triality*, 1403.3657.

[191] C. Hwang, P. Yi and Y. Yoshida, *Fundamental Vortices, Wall-Crossing, and Particle-Vortex Duality*, *JHEP* **05** (2017) 099 [1703.00213].

[192] F. Benini and A. Zaffaroni, *Supersymmetric partition functions on Riemann surfaces*, *Proc. Symp. Pure Math.* **96** (2017) 13 [1605.06120].

[193] C. Closset and H. Kim, *Comments on twisted indices in 3d supersymmetric gauge theories*, *JHEP* **08** (2016) 059 [1605.06531].

[194] D. Martelli, A. Passias and J. Sparks, *The gravity dual of supersymmetric gauge theories on a squashed three-sphere*, *Nucl. Phys. B* **864** (2012) 840 [1110.6400].

[195] K. Hristov, C. Toldo and S. Vandoren, *On BPS bounds in D=4 N=2 gauged supergravity*, *JHEP* **12** (2011) 014 [1110.2688].

[196] T. Nishioka and I. Yaakov, *Supersymmetric Renyi Entropy*, *JHEP* **10** (2013) 155 [1306.2958].

[197] X. Huang, S.-J. Rey and Y. Zhou, *Three-dimensional SCFT on conic space as hologram of charged topological black hole*, *JHEP* **03** (2014) 127 [1401.5421].

[198] T. Nishioka, *The Gravity Dual of Supersymmetric Renyi Entropy*, *JHEP* **07** (2014) 061 [1401.6764].

[199] J. Dowker, *Entanglement entropy for odd spheres*, 1012.1548.

[200] H. Casini, M. Huerta and R. C. Myers, *Towards a derivation of holographic entanglement entropy*, *JHEP* **05** (2011) 036 [1102.0440].

[201] S. M. Hosseini, K. Hristov and A. Zaffaroni, *Gluing gravitational blocks for AdS black holes*, *JHEP* **12** (2019) 168 [1909.10550].

[202] D. L. Jafferis, *The Exact Superconformal R-Symmetry Extremizes Z*, *JHEP* **05** (2012) 159 [1012.3210].

[203] N. Bobev and P. M. Crichigno, *Universal spinning black holes and theories of class $\mathcal{R}$*, *JHEP* **12** (2019) 054 [1909.05873].

[204] F. Benini, D. Gang and L. A. Pando Zayas, *Rotating Black Hole Entropy from M5 Branes*, *JHEP* **03** (2020) 057 [1909.11612].

[205] S. M. Hosseini and A. Zaffaroni, *Large N matrix models for 3d $\mathcal{N} = 2$ theories: twisted index, free energy and black holes*, *JHEP* **08** (2016) 064 [1604.03122].

[206] F. Azzurli, N. Bobev, P. M. Crichigno, V. S. Min and A. Zaffaroni, *A universal counting of black hole microstates in AdS_4*, *JHEP* **02** (2018) 054 [1707.04257].

[207] N. Bobev and P. M. Crichigno, *Universal RG Flows Across Dimensions and Holography*, *JHEP* **12** (2017) 065 [1708.05052].

[208] A. Kapustin and B. Willett, *Generalized Superconformal Index for Three Dimensional Field Theories*, 1106.2484.

[209] C. Closset, H. Kim and B. Willett, *Supersymmetric partition functions and the three-dimensional A-twist*, *JHEP* **03** (2017) 074 [1701.03171].

[210] C. Closset, H. Kim and B. Willett, *Seifert fibering operators in 3d $\mathcal{N} = 2$ theories*, *JHEP* **11** (2018) 004 [1807.02328].

[211] A. Kapustin, B. Willett and I. Yaakov, *Exact Results for Wilson Loops in Superconformal Chern-Simons Theories with Matter*, *JHEP* **03** (2010) 089 [0909.4559].

[212] N. Hama, K. Hosomichi and S. Lee, *Notes on SUSY Gauge Theories on Three-Sphere*, *JHEP* **03** (2011) 127 [1012.3512].

[213] N. Hama, K. Hosomichi and S. Lee, *SUSY Gauge Theories on Squashed Three-Spheres*, *JHEP* **05** (2011) 014 [1102.4716].

[214] S. M. Hosseini and N. Mekareeya, *Large N topologically twisted index: necklace quivers, dualities, and Sasaki-Einstein spaces*, *JHEP* **08** (2016) 089 [1604.03397].

[215] S. M. Hosseini, K. Hristov and A. Passias, *Holographic microstate counting for AdS_4 black holes in massive IIA supergravity*, *JHEP* **10** (2017) 190 [1707.06884].

[216] F. Benini, H. Khachatryan and P. Milan, *Black hole entropy in massive Type IIA*, *Class. Quant. Grav.* **35** (2018) 035004 [1707.06886].

[217] S. Ryu and T. Takayanagi, *Holographic derivation of entanglement entropy from AdS/CFT*, *Phys. Rev. Lett.* **96** (2006) 181602 [hep-th/0603001].

[218] K. Hristov, I. Lodato and V. Reys, *On the quantum entropy function in 4d gauged supergravity*, *JHEP* **07** (2018) 072 [1803.05920].

[219] K. Hristov, I. Lodato and V. Reys, *One-loop determinants for black holes in 4d gauged supergravity*, *JHEP* **11** (2019) 105 [1908.05696].

[220] B. Mukhametzhanov and A. Zhiboedov, *Modular invariance, tauberian theorems and microcanonical entropy*, *JHEP* **10** (2019) 261 [1904.06359].

[221] S. Pal and Z. Sun, *Tauberian-Cardy formula with spin*, *JHEP* **01** (2020) 135 [1910.07727].

[222] F. Benini, N. Bobev and P. M. Crichigno, *Two-dimensional SCFTs from D3-branes*, *JHEP* **07** (2016) 020 [1511.09462].

[223] S. L. Cacciatori and D. Klemm, *Supersymmetric AdS(4) black holes and attractors*, *JHEP* **01** (2010) 085 [0911.4926].

[224] S. Katmadas, *Static BPS black holes in U(1) gauged supergravity*, *JHEP* **09** (2014) 027 [1405.4901].

[225] N. Halmagyi, *Static BPS black holes in AdS_4 with general dyonic charges*, *JHEP* **03** (2015) 032 [1408.2831].

[226] K. Hristov, S. Katmadas and C. Toldo, *Rotating attractors and BPS black holes in AdS_4*, *JHEP* **01** (2019) 199 [1811.00292].

[227] R. Emparan, C. V. Johnson and R. C. Myers, *Surface terms as counterterms in the AdS / CFT correspondence*, *Phys. Rev. D* **60** (1999) 104001 [hep-th/9903238].

[228] D. L. Jafferis, I. R. Klebanov, S. S. Pufu and B. R. Safdi, *Towards the F-Theorem: N=2 Field Theories on the Three-Sphere*, *JHEP* **06** (2011) 102 [1103.1181].

[229] D. Z. Freedman and S. S. Pufu, *The holography of F-maximization*, *JHEP* **03** (2014) 135 [1302.7310].

[230] M. Fluder and J. Sparks, *D2-brane Chern-Simons theories: F-maximization = a-maximization*, *JHEP* **01** (2016) 048 [1507.05817].

[231] L. A. Pando Zayas and Y. Xin, *Topologically twisted index in the 't Hooft limit and the dual AdS$_4$ black hole entropy*, *Phys. Rev. D* **100** (2019) 126019 [1908.01194].

[232] K. A. Intriligator and N. Seiberg, *Mirror symmetry in three-dimensional gauge theories*, *Phys. Lett. B* **387** (1996) 513 [hep-th/9607207].

[233] O. Aharony and A. Hanany, *Branes, superpotentials and superconformal fixed points*, *Nucl. Phys. B* **504** (1997) 239 [hep-th/9704170].

[234] A. Guarino, D. L. Jafferis and O. Varela, *String Theory Origin of Dyonic N=8 Supergravity and Its Chern-Simons Duals*, *Phys. Rev. Lett.* **115** (2015) 091601 [1504.08009].

[235] T. Dimofte, D. Gaiotto and S. Gukov, *Gauge Theories Labelled by Three-Manifolds*, *Commun. Math. Phys.* **325** (2014) 367 [1108.4389].

[236] S. Cecotti, C. Cordova and C. Vafa, *Braids, Walls, and Mirrors*, 1110.2115.

[237] P. M. Crichigno, D. Jain and B. Willett, *5d Partition Functions with A Twist*, *JHEP* **11** (2018) 058 [1808.06744].

[238] N. Banerjee, J. Bhattacharya, S. Bhattacharyya, S. Jain, S. Minwalla and T. Sharma, *Constraints on Fluid Dynamics from Equilibrium Partition Functions*, *JHEP* **09** (2012) 046 [1203.3544].

[239] B. Assel, D. Cassani and D. Martelli, *Localization on Hopf surfaces*, *JHEP* **08** (2014) 123 [1405.5144].

[240] A. Arabi Ardehali, J. T. Liu and P. Szepietowski, *High-Temperature Expansion of Supersymmetric Partition Functions*, *JHEP* **07** (2015) 113 [1502.07737].

[241] B. Assel, D. Cassani, L. Di Pietro, Z. Komargodski, J. Lorenzen and D. Martelli, *The Casimir Energy in Curved Space and its Supersymmetric Counterpart*, *JHEP* **07** (2015) 043 [1503.05537].

[242] N. Bobev, M. Bullimore and H.-C. Kim, *Supersymmetric Casimir Energy and the Anomaly Polynomial*, *JHEP* **09** (2015) 142 [1507.08553].

[243] D. Cassani and D. Martelli, *The gravity dual of supersymmetric gauge theories on a squashed S^1 x S^3*, *JHEP* **08** (2014) 044 [1402.2278].

[244] Y. Tachikawa, *On S-duality of 5d super Yang-Mills on S^1*, *JHEP* **11** (2011) 123 [1110.0531].

[245] Y. Hwang, J. Kim and S. Kim, *M5-branes, orientifolds, and S-duality*, *JHEP* **12** (2016) 148 [1607.08557].

[246] J. Zanelli, *Chern-Simons Forms in Gravitation Theories*, *Class. Quant. Grav.* **29** (2012) 133001 [1208.3353].

[247] S. Bhattacharyya, S. Lahiri, R. Loganayagam and S. Minwalla, *Large rotating AdS black holes from fluid mechanics*, *JHEP* **09** (2008) 054 [0708.1770].

[248] A. Hanany, N. Mekareeya and G. Torri, *The Hilbert Series of Adjoint SQCD*, *Nucl. Phys. B* **825** (2010) 52 [0812.2315].

[249] C. Copetti, A. Grassi, Z. Komargodski and L. Tizzano, *Delayed Deconfinement and the Hawking-Page Transition*, 2008.04950.

[250] S. Choi, S. Jeong and S. Kim, *The Yang-Mills duals of small AdS black holes*, to appear.

[251] O. J. Dias, R. Monteiro, H. S. Reall and J. E. Santos, *A Scalar field condensation instability of rotating anti-de Sitter black holes*, *JHEP* **11** (2010) 036 [1007.3745].

[252] S. Fredenhagen and V. Schomerus, *Boundary Liouville theory at c = 1*, *JHEP* **05** (2005) 025 [hep-th/0409256].

초록

이 논문은 안티 드 지터 시공간의 블랙홀을 등각장론을 이용한 홀로그래피 방식으로 연구하는 것에 목표를 둔다. 먼저, 3,4,5,6차원 초등각장론의 초등각지표가 Cardy 그리고 large N 극한에서 탈속박을 나타냄을 보인다. 이의 엔트로피는 4,5,6,7차원 안티 드 지터 시공간 블랙홀의 Bekenstein-Hawking 엔트로피와 정확하게 일치한다. 즉, 블랙홀의 미시상태를 탈속박된 쿼크-글루온 플라즈마를 통해 홀로그래피 방식으로 설명한 것이다.

또한, 3차원, 5차원 게이지 이론의 높은 온도에서의 독특한 형태의 탈속박에 관해서 연구한다. 먼저, M2-막 위의 초등각장론의 $N^{3/2}$ 탈속박 자유도를 자기홀극의 응축을 통해 명확하게 설명한다. 5차원 초등각장론의 $N^{5/2}$ 탈속박 자유도와 이에 대한 인스탄톤 솔리톤의 역할도 논의될 것이다.

더하여, 4차원 $\mathcal{N} = 4$ 초대칭-양-밀스 이론의 초등각지표를 수치적으로 연구하여, 이 지표의 빠른 진동이 Legendre 변환의 복소 화학 퍼텐셜 극점을 통해 구현됨을 보인다. 마지막으로, 초등각지표에서의 탈속박 상전이에 관해 논의할 것이다.

이 논문은 안디 드 지터 시공간의 블랙홀 및 양자중력에 대한 미시적인 연구에 체계적이고 보편적인 체계를 제공하였다는 점에도 그 의의가 있다.